



**UNIVERSITY OF
KWAZULU-NATAL**

**INYUVESI
YAKWAZULU-NATALI**

**METAL COMPLEXES WITH PHOSPHOR-1, 1-DITHIOLATO LIGANDS:
GREEN SYNTHESIS, STRUCTURES, ANTIMICROBIAL STUDIES AND
DYE-SENSITIZED SOLAR CELL APPLICATION**

2016

TOMILOLA JOSEPH AJAYI

**METAL COMPLEXES WITH PHOSPHOR-1, 1-DITHIOLATO LIGANDS:
GREEN SYNTHESIS, STRUCTURES, ANTIMICROBIAL STUDIES AND
DYE-SENSITIZED SOLAR CELL APPLICATION.**

TOMILOLA JOSEPH AJAYI

2016

A thesis submitted to the School of Chemistry & Physics, College of Agriculture, Engineering and Science (CAES), University of KwaZulu-Natal, Westville Campus, for the degree of Doctor of Philosophy.

This is a thesis in which the chapters are written in full dissertation format.

As the candidate's supervisor, I have approved this thesis for submission:

Supervisor:

WERNER E. VAN ZYL

Signed:



.Name ...WERNER E. VAN ZYL...Date...19 JANUARY 2017...

DECLARATIONS

DECLARATION 1 - PLAGIARISM

I, TOMILOLA JOSEPH AJAYI, declare that:

1. The research reported in this thesis, except where otherwise indicated, is my original research.
2. This thesis has not been submitted for any degree or examination at any other University.
3. This thesis does not contain other persons' data, pictures, graphs or other information unless specifically acknowledged as being sourced from other persons.
4. This thesis does not contain other persons' writing unless specifically acknowledged as being sourced from other researchers. Where other written sources have been quoted, then:
 - a. Their words have been re-written but the general information attributed to them has been referenced
 - b. Where their exact words have been used, then their writing has been placed in italics and inside quotation marks and referenced.
5. This thesis does not contain text, graphics or tables copied and pasted from the internet, unless specifically acknowledged, and the source being detailed in the thesis and in the References sections.

Signed.....

DECLARATION 2 - PUBLICATIONS

DETAILS OF CONTRIBUTION TO PUBLICATIONS that form part and/or include research presented in this thesis (include publications in preparation, submitted, *in press* and published and give details of the contributions of each author to the experimental work and writing of each publication)

Publication 1 (manuscript in preparation)

Tomilola J. Ajayi, Michael N. Pillay, and Werner E. van Zyl. **Solvent-free mechanochemical synthesis of dithiophosphonic acids and corresponding nickel (II) complexes and anti-bacterial studies**

Contributions: I synthesized, characterized and wrote the initial draft of the manuscript and carried out subsequent modifications towards publication of the paper. Michael N. Pillay solved the crystal structure.

Publication 2 (manuscript in preparation)

Tomilola J. Ajayi, Moses Ollengo, and Werner E. van Zyl. **Multimetallic and multiferrocenyl dithiophosphonate transition-metal complexes as potential high-efficiency co-sensitizer in dye-sensitized solar cells.**

Contributions: I synthesized, characterized and wrote the initial draft of the manuscript and carried out subsequent modifications towards publication of the paper. Moses Ollengo assisted in analyzing the optical properties.

Publication 3 (manuscript in preparation)

Tomilola J. Ajayi, Moses Ollengo, and Werner E. van Zyl. **Transition metal complexes of zwitterionic dithiophosphonate: theoretical, optical, and antibacterial studies.**

Contributions: I synthesized, characterized and wrote the initial draft of the manuscript and carried out subsequent modifications towards publication of the paper. Moses Ollengo assisted in analyzing the optical properties.

Signed:.....

DECLARATION 3 - CONFERENCE PROCEEDINGS

1. Tomilola J. Ajayi, Werner E. van Zyl. Green Route to Synthesis of (4-Methoxy-Phenyl) - Phosphonodithioic Acid and Its Ni & Co Complexes. (Paper presented at 2nd International Conference on Past and Present Research Systems of Green Chemistry, September 14-16, 2015 Orlando, USA)
2. Tomilola J. Ajayi, Werner E. van Zyl. Multimetallic And Multiferrocenyl Assemblies Of Ferrocenyl -Based Dithiophosphate And Their Electrochemical Properties. (Paper presented at 18th International Conference on coordination chemistry and applications, March 14-15, 2016, Paris, France.)
3. Tomilola J. Ajayi, Werner E. van Zyl. Multi-Ferrocenyl Dithiophosphate Transition-Metal Complexes as Potential High Efficiency Co-Sensitizer in Dye-Sensitized Solar Cells (paper presented at 6th EuCheMS Chemistry, 15th, September 2016, Seville, Spain.).

DEDICATION

THIS WORK IS DEDICATED TO MY TO MY LATE MOTHER

ACKNOWLEDGEMENT

My sincere gratitude goes to my supervisor, Professor W.E. van Zyl for initiating this project, his knowledge sharing, invaluable support, constructive criticism and input to the project.

My appreciation also goes to my wife, Oluwakemi Ajayi and my kids, Greatness and Eminence Ajayi for their love, understanding, encouragement, supports and prayers during the course of this research. I owe you a lot for denying you most of the time we are supposed to spend together as a family and investing it in this research work.

I also appreciate my laboratory mates, Sicelo Sithole, Michael Pillay, Fezile Potwana, Vashen Moodley, Eric Ayom; you guys are terrific! You made the laboratory conducive and encouraging for research and your contributions are highly appreciated.

My gratitude also goes to my father, for setting me up on a good foundation in life, and of course, I will not forget my late mother for her love which still keeps me going even while she is no more. I also appreciate my siblings for being there always.

I acknowledge the University of KwaZulu-Natal and the Eskom TESP initiative for financial support of this project.

Finally, I am immensely grateful to God Almighty who has been everything to me.

LIST OF FIGURES

Figure 1.1: Dithiadiphosphetane disulfide dimers based on the Lawesson's Reagent (B) motif.....	3
Figure 1.2: Classes: (I) dithiophosphato; (II) dithiophosphonato; (III) dithiophosphinato.....	5
Figure 1.3: Typical resonance structures of the dithiophosphonate anion.....	9
Figure 1.4: Typical binding modes to form metal-dithiophosphonate complexes.....	10
Figure 1.5: (a) A 4-coordinate Nickel(II) complex. (b) A 6-coordinate Ni(II) polymeric complex containing a pyridyl-trisulfide linker.....	12
Figure 1.6: Example of a neutral Ni(II) complex containing both a chelating and monoconnective S bound dithiophosphonato ligand.....	13
Figure 1.7: A tetranuclear Ni(II) complex containing 4- and 6-coordination around the metal center.....	15
Figure 1.8: A typical 4-coordinate Zn(II) dithiophosphonate complex.....	16
Figure 1.9: Typical applications of phosphorus and phosphorus-based compound in our society.....	18
Figure 1.10: The ideal synthesis.....	20
Figure 2.1: Different types of the most common phosphor-1, 1,-dithiolates.....	42
Figure 2.2: Photographs demonstrating the progress of the green synthesis of dithiophosphonic acids.....	45
Figure 2.3: Photographs demonstrating the immediate colorimetric change by reacting neat viscous dithiophosphonic acid with solid NiCl ₂ ·6H ₂ O.....	47
Figure 2.4. The products formed are a racemic mixture of S and R chiral enantiomers of dithiophosphonic acids.	50
Figure 2.5: The ³¹ P NMR spectrums of [Ni{S ₂ P(OH)(4-MeOC ₆ H ₄) ₂ } ₂] 5 and [Ni{S ₂ P(OCH ₃)(4-MeOC ₆ H ₄) ₂ } ₂] 6	52

Figure 2.6. ORTEP molecular structure of Ni(II) complex 5 . Notice the two hydrated water molecules.....	54
Figure 3.1: ORTEP molecular structure of complex 18	75
Figure 3.2: ORTEP molecular structure of Ni(II) complex 19	76
Figure 3.3: (a) ORTEP molecular structure of oxidized Cd(II) complex 23 . (b) ORTEP molecular structure of polymeric expansion of oxidized Cd(II) complex 23	80
Figure 4.1: UV-VIS spectra of the ligands and complexes.....	97
Figure 4.2. Electronic absorption spectra of 24, 26, 27 & 28	98
Figure 4.3: Electronic absorption spectra of 25, 29, 30, & 31	100
Figure 4.4: Photoluminescent spectra of 30 & 31	101
Figure 4.5: ORTEP molecular structure of 24	102
Figure 4.6: ORTEP molecular structure of 25	104
Figure 4.7: ORTEP molecular structure of 29	105
Figure 5.1. Electronic absorption spectra of the co-sensitizers.....	127
Figure 5.2: Typical schematic energy diagram of HOMO and LUMO levels for the co-sensitizers compared to the energy levels calculated for TiO ₂	128
Figure 5.3. J–V curves for DSCs based on N719- co-sensitized with different ferrocenyl dithiophosphate complexes and N719-sensitized photoelectrodes under irradiation.....	130
Figure 5.4: Electrochemical impedance measurement fitted data for all complexes.....	132
Figure 5.5. Photograph showing the Sciencetech SF-150 Solar Simulator.....	136
Figure 5.6. Photograph of the electrochemical (impedance and cyclic voltammetry) spectrophotometer..	137

Figure 6.1: Graphs showing the comparative result of antibacterial activity of the compounds on <i>Bacillus subtilis</i>	144
Figure 6.2: Graphs showing the comparative result of antibacterial activity of our compounds on <i>Klebsiella oxytoca</i>	145
Figure 6.3: Graph showing the comparative result of antibacterial activity for compounds on <i>Salmonella sp</i>	146
Figure 6.4: Graph showing the comparative result of antibacterial activity of the compounds on <i>Methicillin-Resistant Staphylococcus aureus (MRSA)</i>	149
Figure 6.5: Graph showing the comparative result of antibacterial activity of the compounds on <i>Escherichia coli</i>	149
Figure 6.6: Graph showing the comparative result of antibacterial activity of the compounds on <i>Staphylococcus aureus</i>	150
Figure 6.7: Graph showing the comparative result of antibacterial activity of the compounds on <i>Klebsiella pneumoniae</i>	150
Figure 6.8: Graph showing the comparative result of antibacterial activity of the compounds on <i>Shigella dysentery</i>	151
Figure 6.9: Graph showing the comparative result of antibacterial activity of the compounds on <i>Bacillus subtilis</i>	151
Figure 6.10: The incubated plates showing the diameter of zones of inhibition of the compound against the test isolates.....	154
Figure 6.11: The incubated plates showing the diameter of zones of inhibition of the compound against the test isolates.....	155

LIST OF SCHEMES

Scheme 1.1: Reaction scheme for synthesis of dimer $[\text{PhP}(\mu\text{-S})\text{S}]_2$ A and Lawesson's reagent (B).....	2
Scheme 1.2: Synthetic route to ammonium dithiophosphonate salt related to this study.....	8
Scheme 1.3: Interconversion between cis/trans isomers in a square planar Ni(II) complex.....	14
Scheme 2.1: Synthesis of the dimer $[\text{PhP}(\mu\text{-S})\text{S}]_2$ and below the greener version in Lawesson's Reagent.....	43
Scheme 2.2: Comparison between the Traditional and Green chemistry method for the formation of dithiophosphonic acids.....	45
Scheme 2.3.A synthesis method for the formation of Ni(II) complexes.....	47
Scheme 3.1: Synthesis of ferrocenyl dithiophosphonate metal complexes in different mole ratios.....	73
Scheme 4.1: Synthesis of transition-metal complexes from zwitterionic dithiophosphonate ligand.....	96
Scheme 8.1. Possible future dithiophosphonate work.....	159
Scheme 8.1. Possible future reactions of zwitterions forming a dual functional dithiophosphonate/dithiocarbamate ligand.....	160

LIST OF TABLES

Table 2.1: Yield, melting points, EI-MS, 31P NMR and elemental analyses data for 1-16	51
Table 2.2: Selected bond lengths (Å) and angles (°).....	54
Table 2.3: Crystal data and structure refinement of 5	55
Table 2.4: Solubility data for Compounds 1-16	56
Table 3.1: Selected bond lengths (Å) and angles (°) for 18	75
Table 3.2: Selected bond lengths (Å) and angles (°) for 19	77
Table 3.3: Crystal data and structure refinement for 18 and 19	78
Table 3.4: Selected bond lengths (Å) and angles (°) for 23	81
Table 3.5: Crystal data and structure refinement for 23	82
Table 3.6: Solubility Data for Compounds 17-23	83
Table 4.1: Selected bond lengths (Å) and angles (°) for 24	103
Table 4.2: Selected bond lengths (Å) and angles (°) for 25	104
Table 4.3: Selected bond lengths (Å) and angles (°) for 29	106
Table 4.4: Details of X-ray data collection and refinement.....	107
Table 4.5: Solubility Data for Compounds 24-31	108
Table 5.1: Experimental data and electrochemical properties of Ni, Zn, and Cd complexes.....	128
Table 5.2: Photovoltaic parameters for the DSSCs based on different Photoelectrodes.....	130
Table 6.1: Diameter of Zones of Inhibition (mm) of the Compound against the test Isolates.....	144
Table 6.2: Diameter of Zones of Inhibition (mm) of the Compound against the test Isolates.....	148

ABSTRACT

This study describes the isolation, characterization, and applications of new dithiophosphonate salts and their ability to facilitate metal complex formation. A variety of dithiophosphonate salts, including zwitterionic compounds, was obtained from the reaction of 2,4-bis(4-methoxyphenyl)- and 2,4-diferrocenyl -1,3-dithiadiphosphetane disulfide precursors, $(RP(S)S)_2$ ($R = 4-C_6H_4OMe$ or $FeC_{10}H_9$).

A green (solventless) and mechanochemical synthetic approach to the formation of dithiophosphonic acids and their corresponding Ni(II), Zn(II), Cd(II) complexes is described. The new green synthetic approach was applied in the formation of a series of known compounds in order to compare the new green approach with traditional methods. In total, 4 ligands and 12 complexes were prepared in a green manner. This study found that the green method was far more advantageous for the following reasons: i) it is a simple and facile process, ii) reaction time is short, taking less than 5 minutes to reach completion, iii) solvents and thus waste are eliminated, and iv) heating steps are avoided. Combined, this process led to less time, cost and energy to be expended, all with a high yield of product formation. It was found that in select cases, metal chloride precursors could be added directly to the acid, leading to product formation, with the formation of HCl, either driven off as a gas or dissolved in small amount of water, filtration and separation steps are thus not needed. All new ligand acids- or salts and corresponding metal complexes were characterized by 1H , ^{31}P NMR, and FTIR. Bulk purity was confirmed by either ESI-MS or elemental analysis and crystal structures were obtained in select cases using single crystal X-ray crystallography.

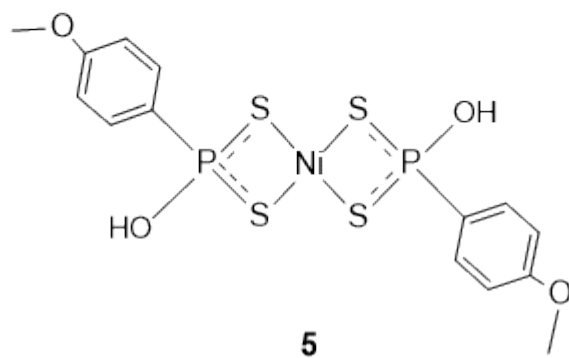
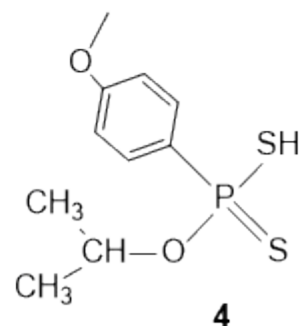
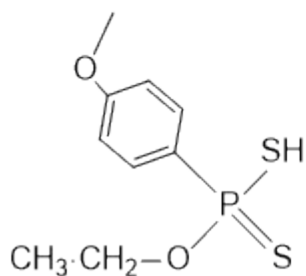
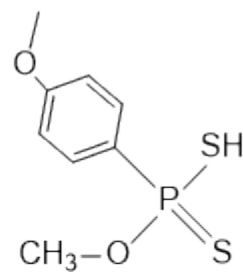
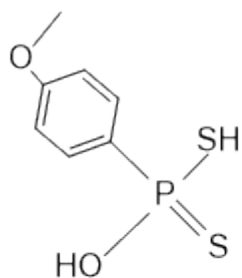
The formation, characterization, and dye sensitized solar cell application of new ferrocenyl dithiophosphonate salts and their complexes were also investigated. The ligand was synthesized by the reaction of water and ferrocenyl Lawesson's reagent (FcLR) in a stoichiometric ratio leading to a multidentate ligand with possibilities of employing its S, S' and O donor atoms in coordination. Nickel(II), cadmium(II), and zinc(II) complexes were formed from the ligand in different metal-to-ligand ratios leading to a multiferrocenyl and multimetallic assemblies. The application of ferrocenyl dithiophosphonate

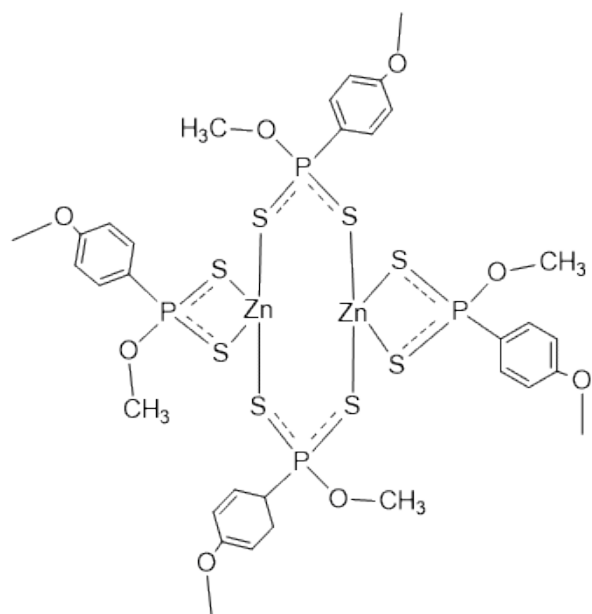
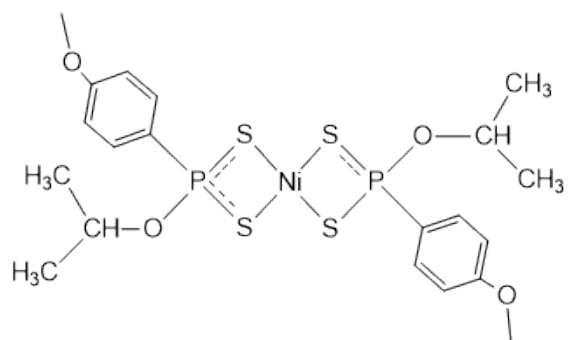
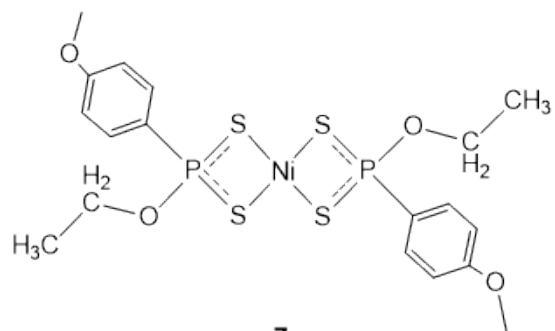
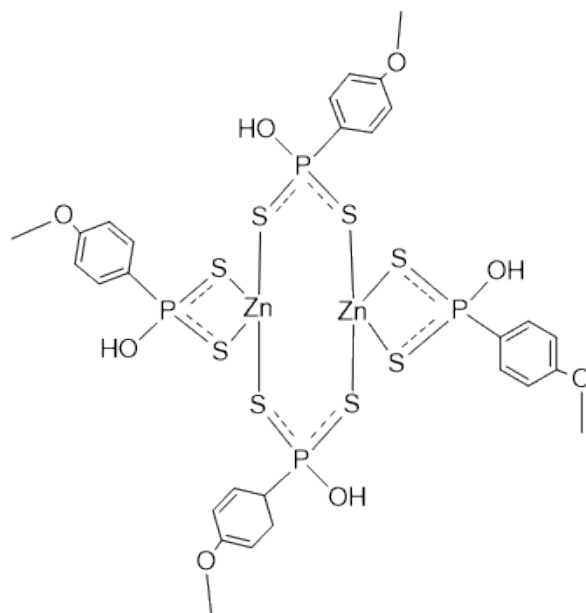
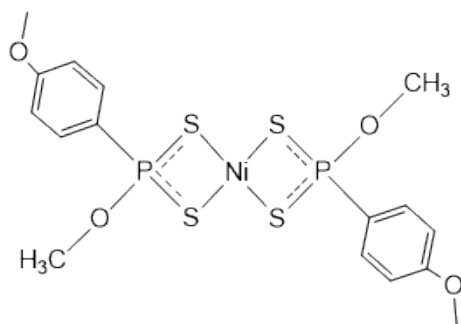
complexes in this work promises to be potentially high efficiency co-sensitizer in dye-sensitized solar cells. After overall co-sensitization of the state-of-the-art ruthenium dye, N719, the overall conversion efficiency of the cell co-sensitized with Zn(II) complex/N719 dye ($\eta=8.30\%$) and Cd(II) complex/N719 dye ($\eta=7.78\%$) were compared to that of ordinary N719 dye ($\eta=7.14\%$) under the same experimental conditions. The cells containing N719 co-sensitized with zinc(II) and cadmium(II) ferrocenyl dithiophosphonate complexes showed improved performance above the efficiency of free N719 dye. The DSSC were characterized using UV-Vis, cyclic voltammetry, electrochemical impedance spectroscopy, and photovoltaic measurements (*I-V curves*)

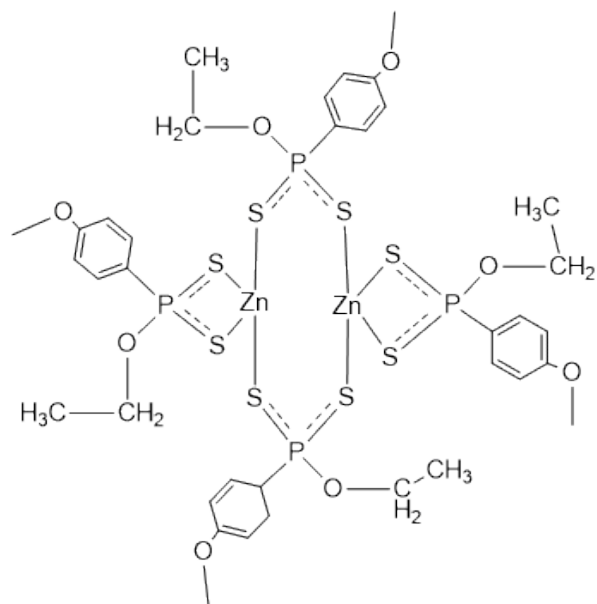
The synthesis, characterization, optical properties, and antimicrobial studies of *zwitterionic* dithiophosphonate salts and their Ni(II), Zn(II) and Cd(II) complexes were also investigated. This type of zwitterion-dithiophosphonate ligand was obtained from the reaction between Lawesson's reagent and amino alcohols (instead of the conventional alcohols) leading to a ligand having space-separated opposite charges on the same compound (zwitterion), with notably a negative charge localized on a S atom, and a positive charge on the quaternary N atom. Optical (UV-Vis and photoluminescence) properties of structurally characterized complexes were investigated with two of the complexes showing luminescence properties.

Finally, antibacterial susceptibility tests showed the bacteria *Methicillin-Resistant Staphylococcus aureus* (MRSA), *Escherichia coli*, *Staphylococcus aureus*, *Klebsiella pneumoniae*, *Bacillus subtilis*, *Shigella dysenteriae*, *Pseudomonas aeruginosa*, *Klebsiella oxytoca*, and *Salmonella sp* are susceptible to most of the compounds studied at various concentrations.

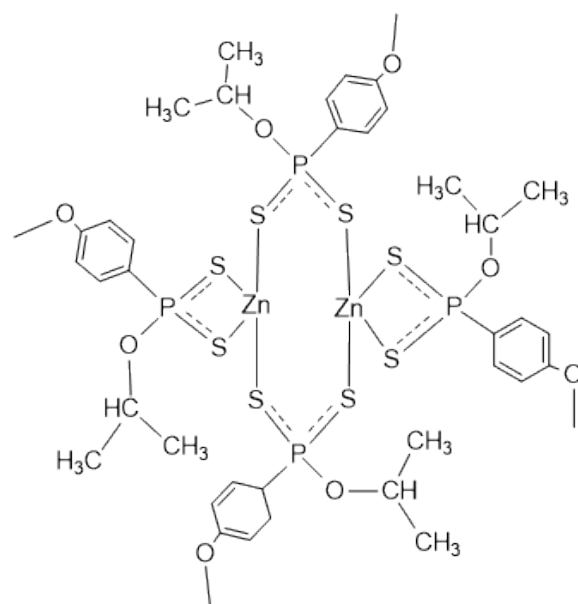
LIST OF LIGANDS AND COMPLEXES



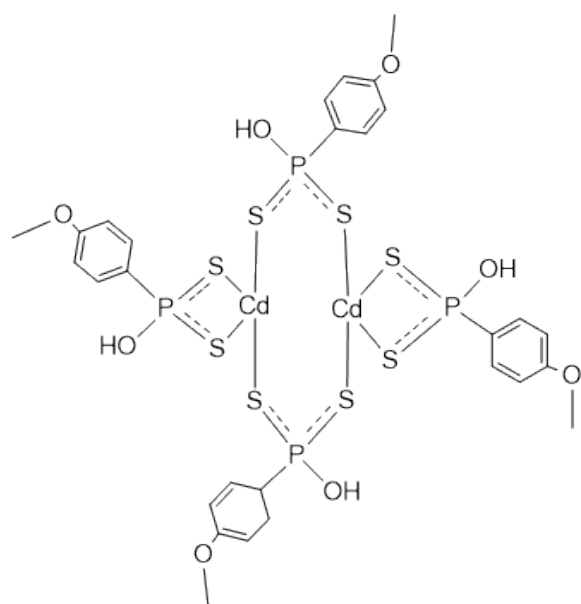




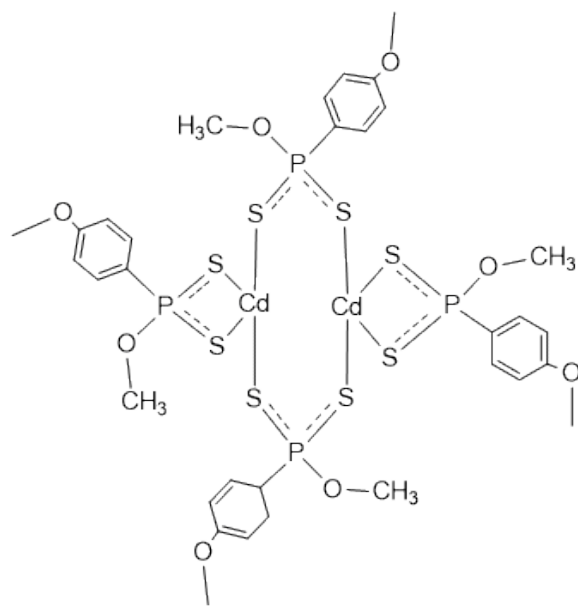
11



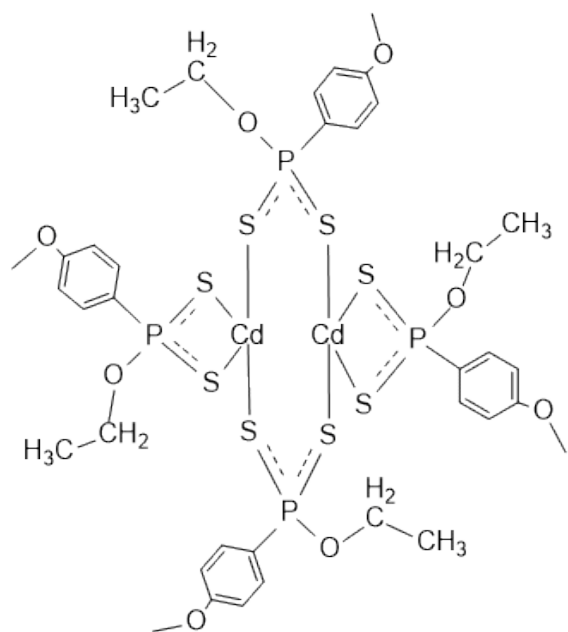
12



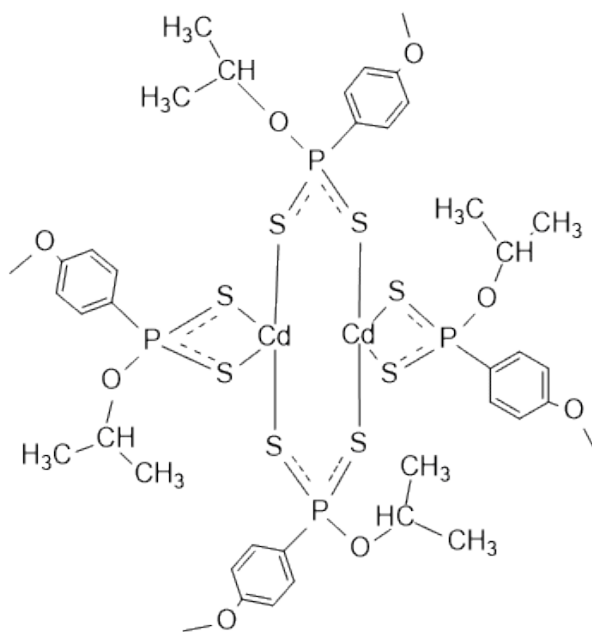
13



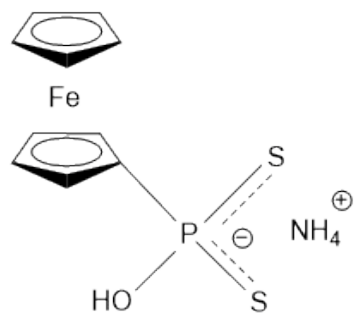
14



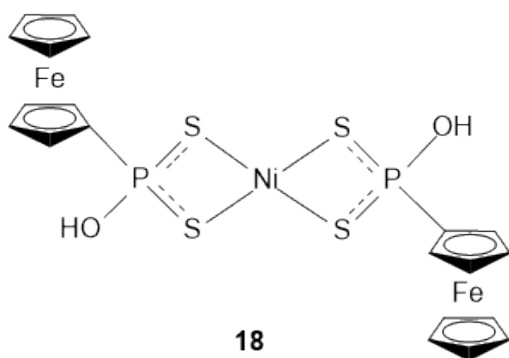
15



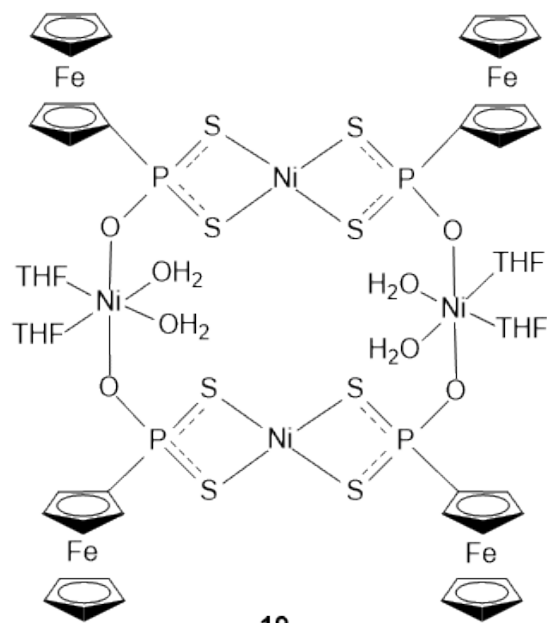
16



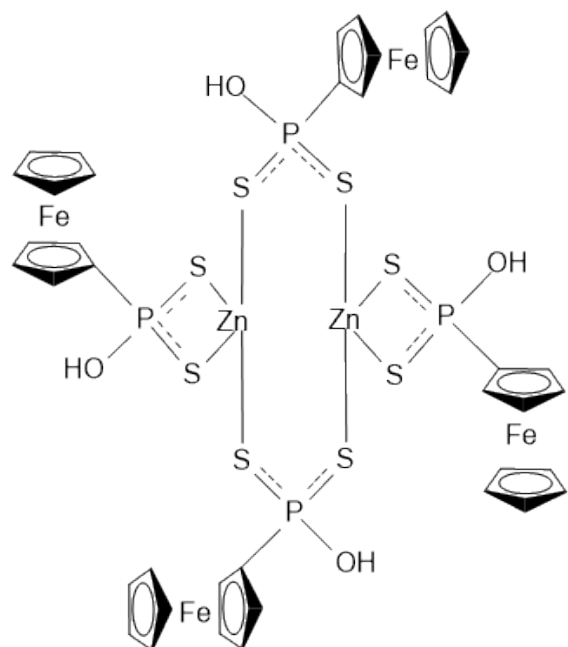
17



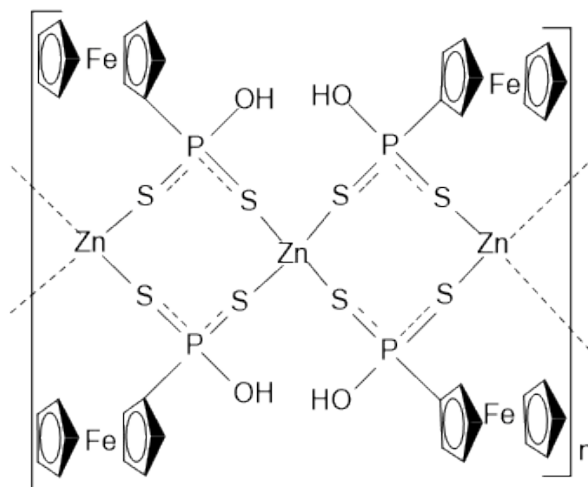
18



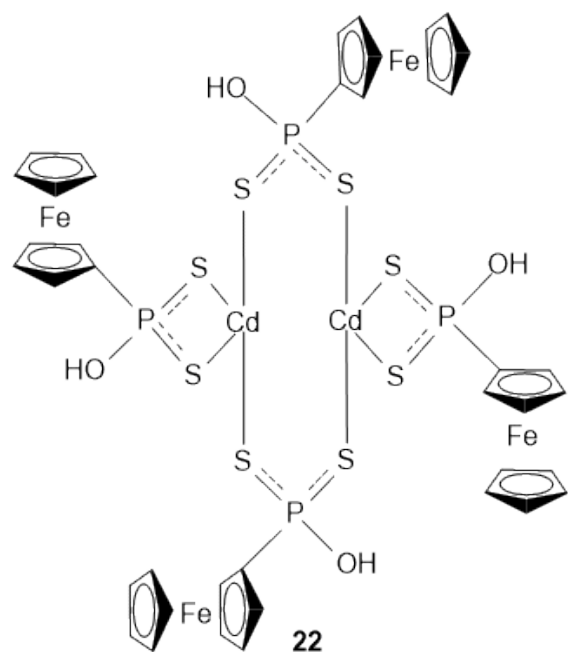
19



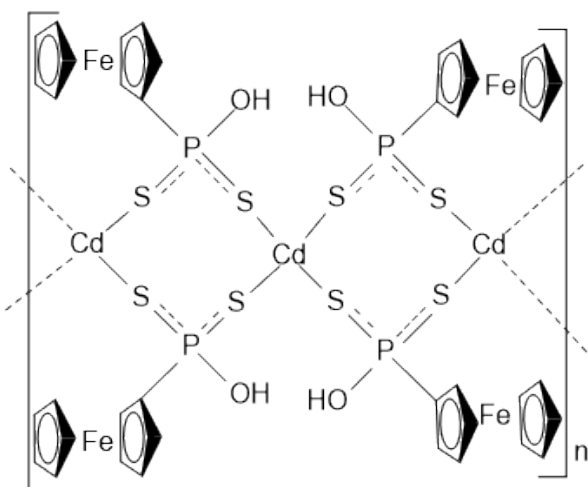
20



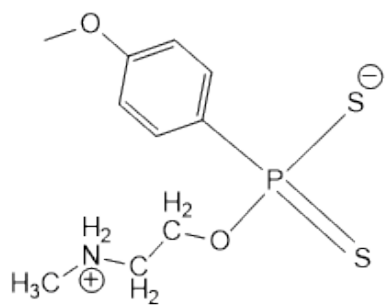
21



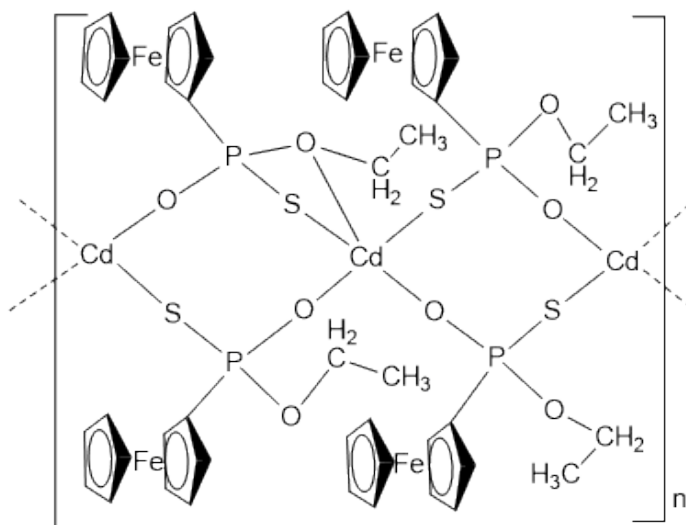
22



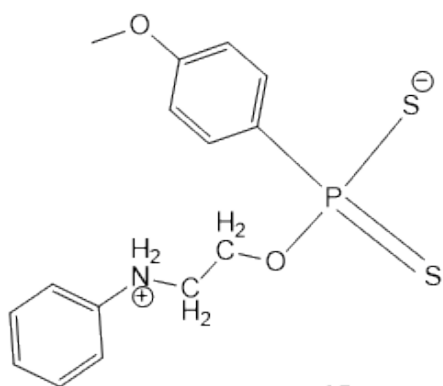
23



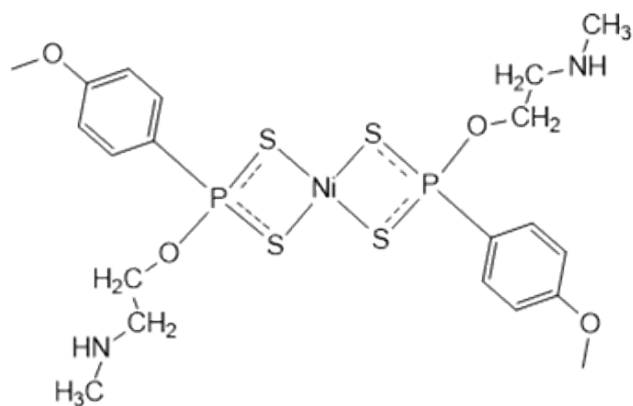
24



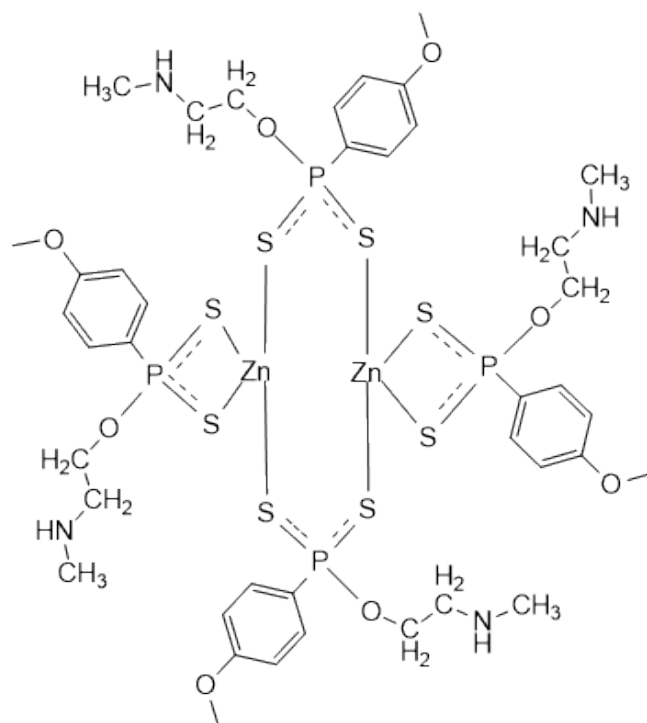
23b



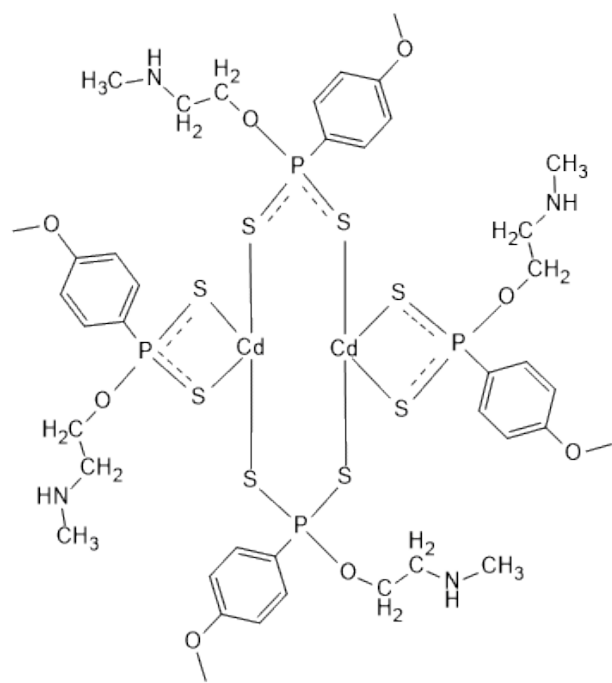
25



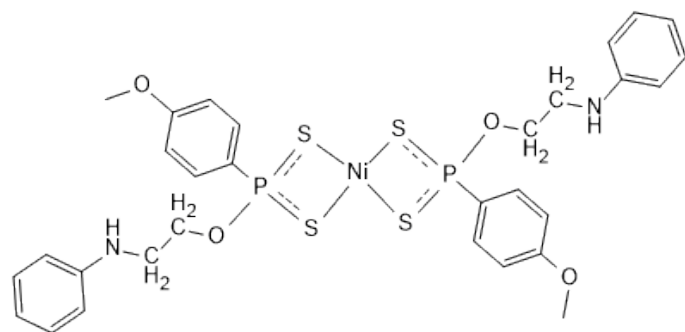
26



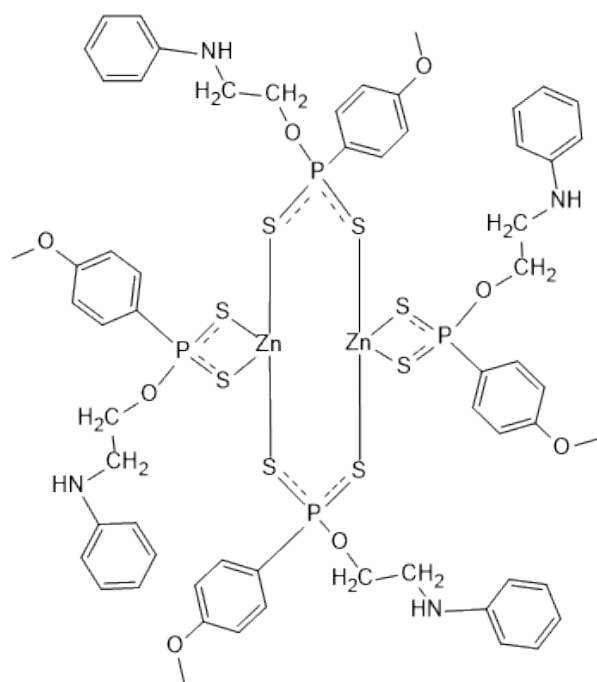
27



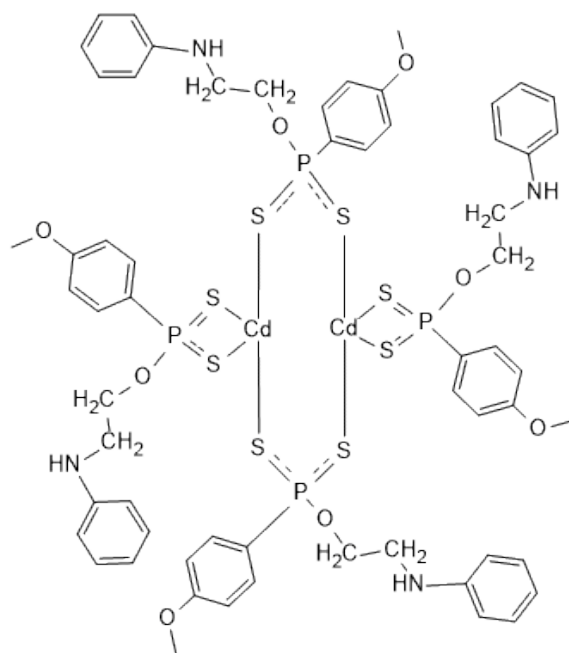
28



29



30



31

ABBREVIATIONS AND SYMBOLS

°C	Degrees Celsius
Å	Ångstrom
MHz	Mega Hertz
cm ⁻¹	Wavenumbers
λ	Wavelength
ppm	Parts Per Million
DCM	Dichloromethane (CH ₂ Cl ₂)
THF	Tetrahydrofuran
CH ₃ CN	Acetonitrile
CDCl ₃	Deuterated Chloroform
NMR	Nuclear Magnetic Resonance
▪ ¹ H	Proton Nuclei
▪ ¹³ C	Carbon-13 Nuclei
▪ ³¹ P	Phosphorus-31 Nuclei
▪ s	Singlet
▪ d	Doublet
▪ t	Triplet
▪ quart	Quartet
▪ dd	Doublet Of Doublets
▪ d quart	Doublet Of Quartets
▪ m	Multiplet
FTIR	Fourier Transform Infrared
IR	Infrared
▪ s	Strong
▪ m	Medium
▪ w	Weak

IUPAC	International Union of Pure and Applied Chemistry
PIN	Preferred IUPAC Name
HSAB	Hard and Soft Acid-Base
ORTEP	Oak Ridge Thermal Ellipsoid Plot
DSC	Dye-sensitized Solar Cells
LR	Lawesson's Reagent
FcLR	Ferrocenyl Lawesson

Table of Contents

Title Page.....	i
Declaration 1: Plagiarism	ii
Declaration 2: Publications	iii
Declaration 3: Conference Proceedings.....	iv
Dedication.....	v
Acknowledgments.....	vi
List of Figures.....	vii
List of Schemes.....	x
List of Tables.....	xi
Abstract.....	xii
List of precursors, ligands, and complexes.....	xiv
Abbreviations and Symbols.....	xxi
Table of Content	xxiii
Chapter 1: Introduction.....	1
1.1 Background.....	1
1.2 Phosphorus-Sulfur Heterocycles.....	1
1.3 Lawesson's Reagent.....	3
1.4 Phosphor-1, 1-Dithiolato Ligands.....	5
1.4.1 Classes of Phosphor-1, 1-Dithiolato Ligands.....	5

1.4.2	Resonance and Co-Ordination Modes of Phosphor-1, 1-Dithiolato Ligands.....	8
1.5	Complexes Relevant To This Study.....	11
1.5.1	Group 10: Nickel.....	11
1.5.2	Group 12: Zinc and Cadmium.....	15
1.6	Green Synthesis Approach to Phosphor-1, 1-Dithiolato Ligands and Complexes.....	17
1.7	Applications Related To This Study.....	21
1.7.1	Dye-sensitized Solar Cell (DSC) Application of Ferrocenyl Dithiophosphonate Complexes	21
1.7.2	Antibacterial Studies of New Phosphor-1, 1-Dithiolato Ligands, and Complexes.....	24
1.8	Aims And Objectives of the Study.....	26
1.9	Overview	27
1.10	References.....	29
Chapter 2:	Solvent-Free Mechanochemical Synthesis of Dithiophosphonic Acids and Corresponding Transition Metal Complexes.....	41
2.1	Background.....	41
2.2	Results and Discussion.....	44
2.2.1	Synthesis of Dithiophosphonic Acids.....	44
2.2.2	Synthesis of Ni(II), Cd(II) and Zn(II) Dithiophosphonate Complexes.....	46
2.2.3	Characterization.....	48
	2.2.3.1 Crystal Structure.....	52
	2.2.3.2 Solubility.....	56
2.3	Conclusions.....	57
2.4	Experimental.....	58
2.4.1	Method.....	58
2.4.2	Materials.....	58

2.4.3	Characterization Methods.....	58
2.4.4	Crystallography.....	59
2.4.5	Ligand synthesis.....	60
2.4.6	Metal Complex Synthesis.....	62
2.5	References.....	68

Chapter 3: Synthesis of New Ferrocenyl Dithiophosphonate Ligand and its Transition-Metal

Complexes.....	71
3.1 Background.....	71
3.2 Results And Discussion.....	72
3.2.1 Synthesis of Ligand and the Corresponding Complexes	72
3.2.2 Characterization.....	73
3.2.2.1 Crystal structures.....	74
3.2.2.2 Solubility	83
3.3 Conclusions.....	84
3.4 Experimental.....	85
3.4.1 Method.....	85
3.4.2 Materials.....	85
3.4.3 Characterization Methods.....	85
3.4.4 Crystallography.....	86
3.4.5 Synthesis of Hydroxyl Derivative of Ferrocenyl Dithiophosphonate Ligand.....	87
3.4.6 Synthesis of Ni(II), Cd(II), Zn(II) Complexes.....	88
3.5 References.....	92

Chapter 4: Synthesis of New Zwitterionic Dithiophosphonate Ligand and Corresponding Transition Metal Complexes.....	94
4.1 Background.....	94
4.2 Result and Discussion.....	95
4.2.1 Synthesis of Zwitterionic Ligand and the Corresponding Complexes.....	95
4.2.2 Characterization.....	96
4.2.2.1 UV-VIS and Photoluminescence Studies.....	97
4.2.2.2 Crystal Structure.....	101
4.2.2.3 Solubility.....	108
4.3 Conclusions.....	108
4.4 Experimental.....	110
4.4.1 Methods.....	110
4.4.2 Materials.....	110
4.4.3 Characterization Methods.....	110
4.4.4 Crystallography.....	111
4.4.5 Synthesis of Zwitterionic Ligands.....	112
4.4.6 Synthesis of Ni(II), Cd(II) and Zn(II) Complexes of Zwitterionic Ligands.....	114
4.5 References.....	120
Chapter 5: Dye Sensitized Solar Cell Application of Ferrocenyl Dithiophosphonate Transition Metal Complexes	124
5.1 Background.....	124
5.2 Result And Discussions.....	125
5.2.1 Optical Properties of the Co-Sensitizers.....	125
5.2.2 Electrochemical Properties of Co-Sensitizers.....	128
5.2.3 Photovoltaic Properties.....	129

5.2.4	Electrochemical Impedance Spectra Analysis	131
5.3	Conclusion.....	133
5.4	Experimental.....	134
5.4.1	Material.....	134
5.4.2	Method.....	134
5.4.3	DSSC Fabrication.....	135
5.4.4	Characterization.....	136
5.4.4.1	Solar Cell Efficiency.....	136
5.4.4.2	Electrochemical Impedance Spectroscopy.....	137
5.5	References.....	138
Chapter 6: Antibacterial Studies of the New Dithiophosphonate Ligands and Their Complexes.....		142
6.1	Background.....	142
6.2	Result and Discussions.....	143
6.2.1	Dithiophosphonate Complexes Synthesized Via Green Route.....	143
6.2.2	Zwitterionic Dithiophosphonate Ligand and Their Complexes.....	146
6.3	Conclusion.....	152
6.4	Experimental.....	153
6.4.1	Antibacterial susceptibility test of Dithiophosphonate Complexes Synthesized Via Green Route.....	153
6.4.2	Antibacterial Susceptibility Test of Zwitterionic Dithiophosphonate Ligand and Their Complexes	154
6.5	References.....	156
Chapter 7: Conclusions and Future Work.....		158
7.1	Conclusion.....	158

7.2 Future Works.....159

Appendix.....162

CHAPTER 1

INTRODUCTION

1.1 BACKGROUND

There has been an upsurge of knowledge in the chemistry of transition metal complexes containing sulfur-based ligands. This is reflected in the recent increase of publications on novel complex syntheses, especially in the field of bioinorganic chemistry and on the formation of interesting organometallics, such as sulfur containing carbene ligands. The present research work is centered on dithio-organophosphorus which are also a major class of sulfur-containing ligands.

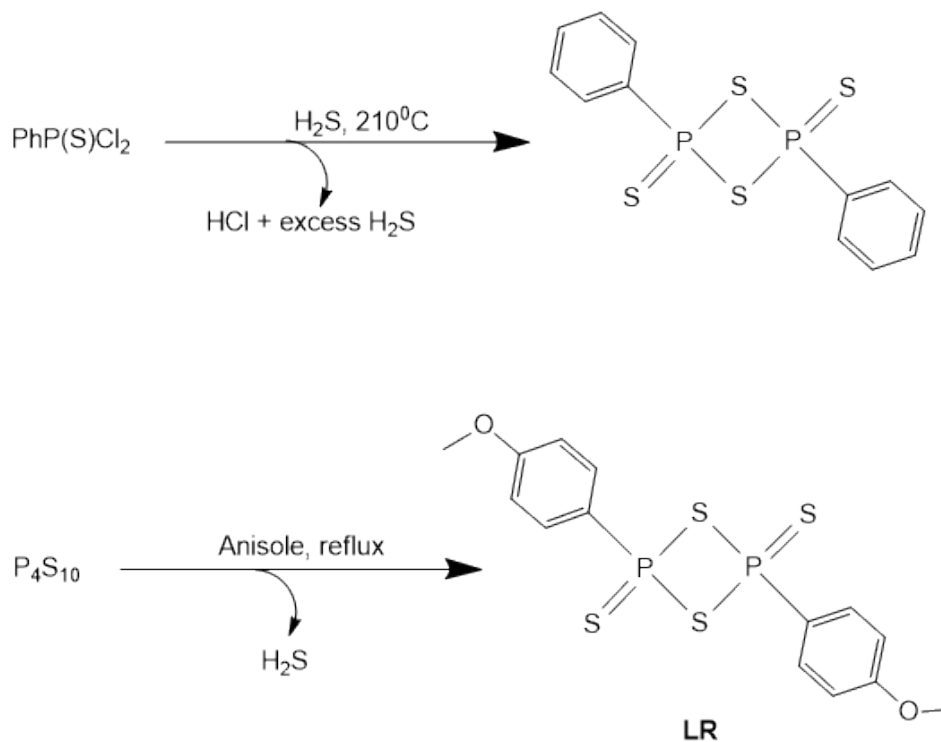
Dithio-organophosphorus chemistry has been investigated for more than a century and has a long history in inorganic chemistry. Dithio-organophosphorus, including dithiophosphates and -phosphinates, dithioimidodiphosphinates, and mixed thio-oxo analogs, as well as dithioarsinates, have been at the center of inorganic and organometallic research interest for decades. These are versatile ligands, yielding a great diversity of molecular and supramolecular structures and showing a variety of coordination patterns when complexed with metals. The phosphor-1,1-dithiolate ligands are an important example of dithio-organophosphorus compounds and provide the basis for the present study. Lawesson's reagent and its precursor phosphorus pentasulfide (Berzelius reagent), have both proven important starting materials in the synthesis of phosphor-1, 1-dithiolato ligands.^{1,2}

1.2 PHOSPHORUS-SULFUR HETEROCYCLES

The reaction of alcohols, alkenes, and cycloalkenes with phosphorus pentasulfide has been reported since 1943 in US patents.^{3,4} The products of these reactions have interesting properties as oil additives. Following this,⁵ investigations into similar reactions of cyclohexene prompted Lecher *et al*⁶ to channel their interests into aromatic compounds including benzene, *o*-xylene, and anisole, to name a few. Each of these products showed the dithiadiphosphetane structure, a four-membered ring with alternating phosphorus and sulfur

atoms. This class of compounds was first reported in 1952 by Fay and Lankelma,⁵ who investigated the reaction of phosphorus pentasulfide (structurally: P_4S_{10}) with cyclohexene, forming a dimer (**A**) (**Figure 1.1**). The synthetic procedure and characterization of dimer **A**, however, was not reported until 1962 by Newallis *et al*⁷ which entailed bubbling H_2S gas into $PhP(S)Cl_2$ at a temperature of $210\text{ }^\circ\text{C}$ and resulted in the desired product formation along with large amounts of corrosive HCl by-product.

A significant improvement came in 1978 when Lawesson and co-workers reported⁸ the reaction between the electron-rich aromatic anisole and P_4S_{10} which led directly to the formation of dimer 2,4-bis(4-methoxyphenyl)-1,3-dithiadiphosphetane-2,4-disulfide,⁹ albeit with the release of stoichiometric amounts of H_2S gas, but without the release of HCl (**Scheme 1.1**). Anisole serves as both the solvent and reactant and this dimer has become known as Lawesson's Reagent (**B**) in the vernacular of dithiophosphonates, it is commercially available and its general chemistry has been extensively reviewed.¹⁰ It was noted that the reaction between anisole and P_4S_{10} could be performed easily and a high yield product could be obtained.



Scheme 1.1: Reaction scheme for synthesis of dimer **A** and **B**

1.3 LAWESSON'S REAGENT

Lawesson's reagent and its analogs (**Figure 1.1**) are all cyclic dimers commonly known as diphosphetane disulfides.¹¹ The reaction of P_4S_{10} with differing aryl substrates yield a wealth of diphosphetane disulfides, *via* a convenient and relatively simple synthesis.⁸ These reaction products are high yielding and can be used as a thionation agent in a variety of reactions. The most commonly known member of this class of compounds known as Lawesson's Reagent (**LR**).¹²⁻¹³ Lawesson's reagent (**B**) and the generally more soluble phenetole analogue (**C**) are both readily prepared by the reflux of P_4S_{10} in anisole for (**B**) or phenetole for (**C**) (**Figure 1.1**). The synthesis of a ferrocenyl derivative (**D**) requires the reflux of P_4S_{10} in a suspension of ferrocene and xylene. This ferrocenyl Lawesson's reagent (FcLR) was first reported by Woollins and co-workers and was of great interest due to the incorporation of an organometallic moiety into the ligand.¹⁴

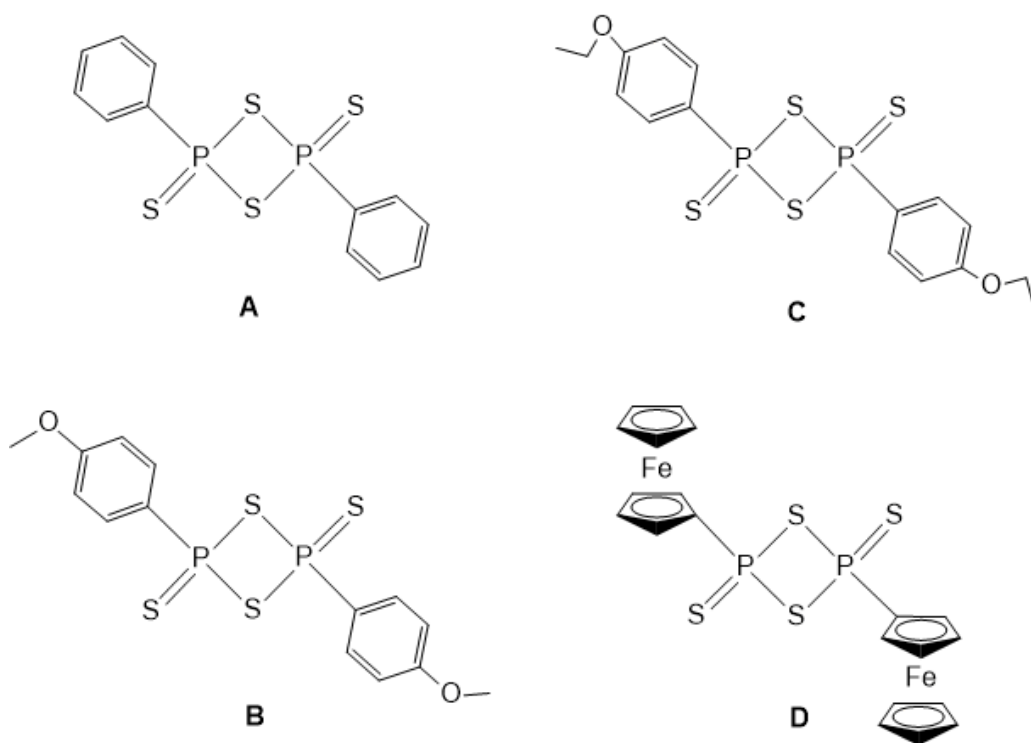


Figure 1.1. Dithiadiphosphetane disulfide dimers based on the Lawesson's Reagent (**B**) motif.

Since 1978, Lawesson's Reagent has become one of the thionating reagents of choice because it gives high yields, is easy to handle, simple to synthesize and only decomposes in solution at temperatures in excess of 110°C.¹⁵ As with all sulfur-based phosphorus compounds, it gradually hydrolyses and/or becomes oxidized in the presence of either moisture or air (oxygen), replacing S atoms for O atoms. In that sense, the final fate of all P/S compounds reported in this thesis, including the metal complexes, is the formation of phosphoric acid, H₃PO₄ as the main (thermodynamic) product. Reactions with transition metal complexes, transformations of alcohols to thiols and the synthesis of thiacege compounds confirm that **LR** is an all-purpose reagent for novel sulfur-containing compounds. Lawesson's reagent has a long history of application in organic chemistry but has only fairly recently shown great promise in the reaction between Lawesson's reagent and alcohols (especially primary and secondary alcohols) to yield the dithiophosphonate class ligands, and to be investigated in coordination chemistry with transition metals.² Although the conversion of ketones into thiones still occupy the largest share of **LR**'s utility, alcoholysis of dithiadiphosphetane dimers, including **LR**, yields the corresponding dithiophosphonic acid.¹⁶ A wide variety of alcohols are now known to be utilized in this manner, including unsaturated (allyl), sterically demanding (adamantyl), and quasi-strained (cyclopentyl), in addition to the reaction of **LR** with silanols and trialkyl silanols.² Although the release of H₂S is not usually recommended in chemical synthesis, it is noteworthy to point out that reactions which slowly release H₂S are now actively pursued in medicinal chemistry. For example, the generation of H₂S from the phosphinodithioates slow-release donor GYY4137 has been investigated and the key decomposition products formed during hydrolysis have been identified, as well as the mechanism by which H₂S is generated.¹⁷

1.4 PHOSPHOR-1,1-DITHIOLATE LIGANDS

1.4.1 Classes of Phosphor-1,1-dithiolate Ligand

This class of compounds is subdivided into three subclasses: the dithiophosphates, dithiophosphinates and the dithiophosphonates and are characterized by having the S_2P functionality. A preference for IUPAC names is usually avoided due to cumbersome systematic nomenclature when referring to ligands in this class. Mostly in literature, two naming systems are frequently used in the case of phosphor-1,1-dithiolate ligands. The preferred IUPAC name (PIN) for phosphor-1,1-dithiolate compounds (**Figure 1.2**) are phosphorodithioates, phosphonodithioates and phosphinodithioates which correspond to the commonly used dithiophosphates (**I**), dithiophosphonates (**II**) and dithiophosphinates (**III**) respectively. The latter naming system has been used consistently throughout this study¹⁸.

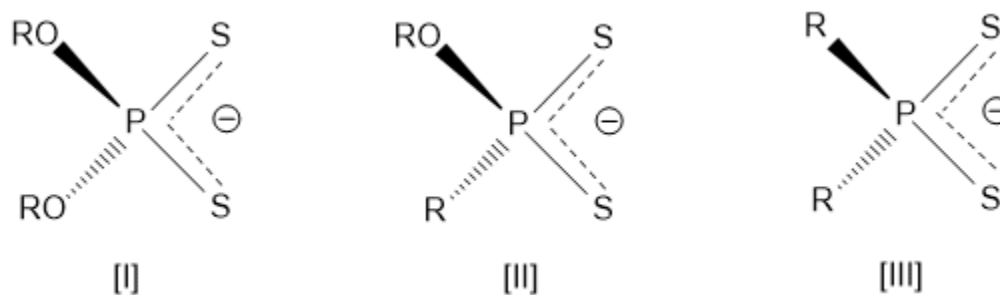


Figure 1.2. Classes: (I) dithiophosphato; (II) dithiophosphonato; (III) dithiophosphinato

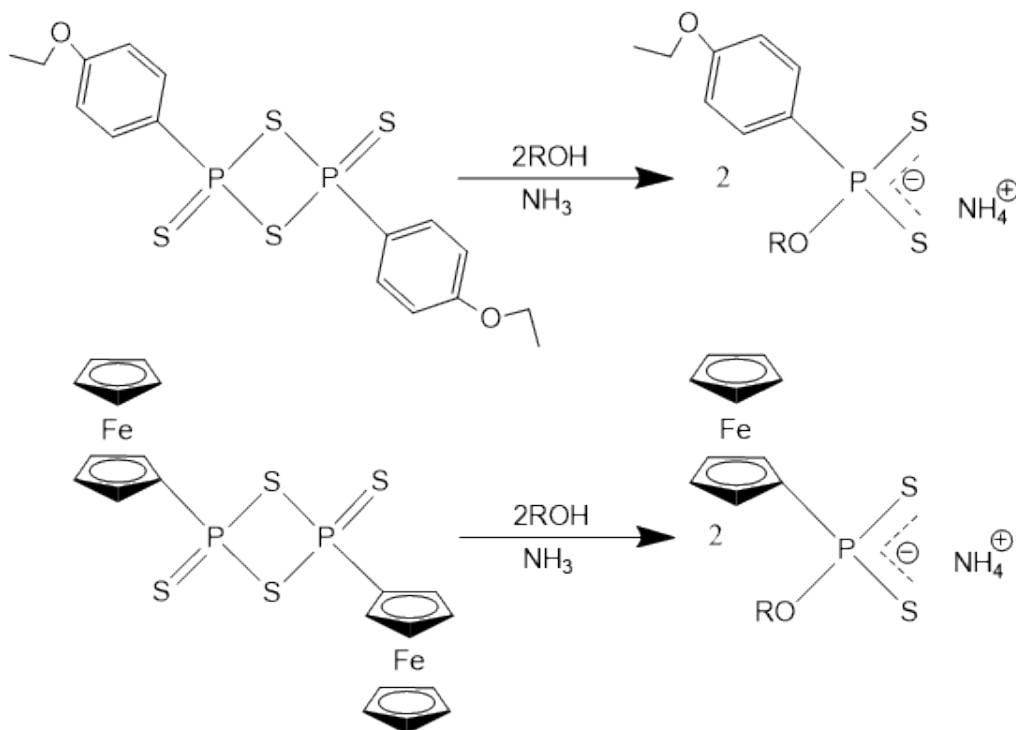
The dithiophosphates and dithiophosphinates have been studied extensively with complexes of the main group and transition metals being far more abundant in literature than those of the dithiophosphonates probably due to the comparative convenience of ligand preparation.^{19,20} However, the literature showed a distinct scarcity of metal dithiophosphonate complexes compared to other phosphor-1,1-dithiolate ligands.¹⁹ The dithiophosphonato ligand, **III**, may be described as a hybrid of ligand **I** and **II** and represents the major ligand type that is the basis of this work.¹ For various reasons, the dithiophosphonato ligand,¹⁸ is the main focus in the present study. The following are possible reasons why the ligand $[S_2PR(OR)]^-$, is worthy of investigation: a) it can still be considered relatively new in the chemical literature and indeed

for the majority of main- and transition metals simply non-existent; b) from the reaction between a common precursor (usually Lawesson's Reagent or a derivative thereof), and any compound that contains a 1° or 2° alcohol functionality, a tremendous number of new and varied derivatives can be obtained in a facile manner; c) the ligand design could be controlled through the synthetic methodology (with respect to solubility and materials properties, and steric effects, etc.) to perform reactions and yield new products in both organic (and potentially aqueous) phases; d) the asymmetric nature of the ligand allows for an additional challenge in that complex isomers can be formed, a feature not possible for the symmetrical dithiophosphinates, $[S_2PR_2]^-$ or dithiophosphates, $[S_2P(OR)_2]^-$ and e) solution and solid state ^{31}P NMR spectroscopy is a valuable tool to obtain mechanistic and structural information.²¹ The dithiophosphonates can coordinate to virtually all main group and transition metals, giving rise to a wide variety of coordination patterns, with the closely related dithiophosphates providing a good precedent.¹⁹

There has been inconsistency for several decades in the application of nomenclature for metal dithiophosphonates. In this regard phosphonic acid, $HPO(OH)_2$, is the parent acid of the phosphonate anion, $[HPO_3]^{2-}$ from which all title ligands in the thesis are derived. The IUPAC systematic name for commonly known phosphonic acid $HPO(OH)_2$ is Dihydroxyphosphine oxide, and these systematic names are thus rarely used, but "preferred IUPAC names" (PIN) are used instead. A PIN is a name that is preferred among two or more IUPAC names, but "the existence of preferred IUPAC names does not prevent the use of other names".¹⁸ This implies since no single correct form currently exists and as long as there is no ambiguity, the reader being addressed must be considered in the type of nomenclature that is used. In addition, there was no guidance as to the naming of a phosphonate derivative containing a P-C bond and thio infix according to 1990, 2001, and 2005 IUPAC recommendations of Nomenclature of Inorganic Chemistry (Red Book).²²⁻²³ According to another recommendation in Nomenclature of Organic Chemistry (Blue Book), published in 1979, 1993 and 2004 draft Recommendations, the acid $R(OR')P(S)(SH)$ is named a phosphonodithioic acid, and anions are named by changing the 'ic acid' ending to 'ate', i.e.

phosphonodithioate and neutral salts and esters are both named using the name of the anion derived from the name of the acid.^{18, 24}

In this thesis, usually in the context of the deprotonated acid, dithiophosphonato will be used when describing a ligand as a formal coordination entity, and dithiophosphonate when referring to an anion. The symmetric cleavage of diphosphetane disulfide dimers, such as Lawesson's reagent [(4-MeOC₆H₄P(S)S)₂] or its ferrocenyl analogue [(4-EtOC₁₀H₉P(S)S)₂], by two stoichiometric equivalents of primary or secondary alcohol, produces dithiophosphonic acids [HS₂PR(OR')]. Similarly attempted reactions with tertiary alcohols have been shown to result in an elimination reaction rather than the formation of the desired dithiophosphonic acid. Deprotonation of the acid by a weak base such as ammonia yields the dithiophosphonate salt NH₄[S₂PR(OR')] which is shown in **Scheme 1.2**. A variation of this procedure using sodium alkoxide salts to circumvent the use of ammonia has been reported.¹⁷ Variation in the alcohol, as well as the phosphetane dimer used, offers a wide scope for an investigation into a multitude of new dithiophosphonate derivatives, and selective variation of either reactant, delivers control in ligand design with respect to steric and electronic properties. In this thesis, we investigated new dithiophosphonate ligand derivatives by varying the alcohol to using water as a protic source, the latter is ironically hardly ever used in this context. The study also looked into the design of a green and sustainable synthetic route to the new and existing dithiophosphonate ligands.



Scheme 1.2. Synthetic route to ammonium dithiophosphonate salt related to this study (R=Aryl/alkyl group)

1.4.2 Resonance and Coordination Modes Phosphor-1,1-Dithiolate Ligands

Dithiophosphonate ligands have displayed a variety of coordination patterns towards metal atoms during complexation. This is as a result of variation in resonance (**Figure 1.3**) structures which the S_2P moiety may adopt. The ligand may coordinate by either monodentate binding or bidentate binding. When the negative charge resides exclusively on either sulfur atom on the ligand, monodentate coordination will possibly result. Bidentate coordination is more common when delocalization of the charge is across the S-P-S atoms of the ligand, and when steric effects around the metal centre allow for it. Resonance also accounts for the different binding modes in mononuclear or multinuclear complexes depending on the nature of the metal centre to which it is bonded. Typical binding modes common to this class of ligand are shown in **Figure 1.4**.

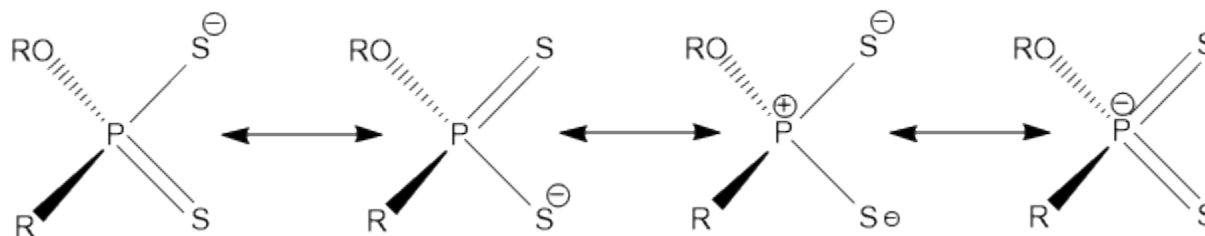


Figure 1.3. Typical resonance structures of the dithiophosphonate anion

The ligand resonance is best explained with the understanding of Hard and Soft acid-base (HSAB) theory which refers to Lewis acids and bases species as “Hard” because they have a small atomic radius, high charge states and are not easily polarized²⁵ while the reverse is the case for species termed “Soft”. In general, hard acids react, though not exclusively but preferentially with hard bases and soft species tend to share a similar affinity for one another.²⁵ Hard or soft properties depend on the system in which they are placed and the relative hardness or softness of other species within the same system. The dithiophosphonate ligand class are Lewis bases and are largely classified as soft species but are flexible in their behaviour as either soft or hard species. This is largely dependent on the Lewis acid (the metal ion) to which they are bound. The co-ordination system shown in **Figure 1.4** have all been observed for P/S type ligands.^{19,18}

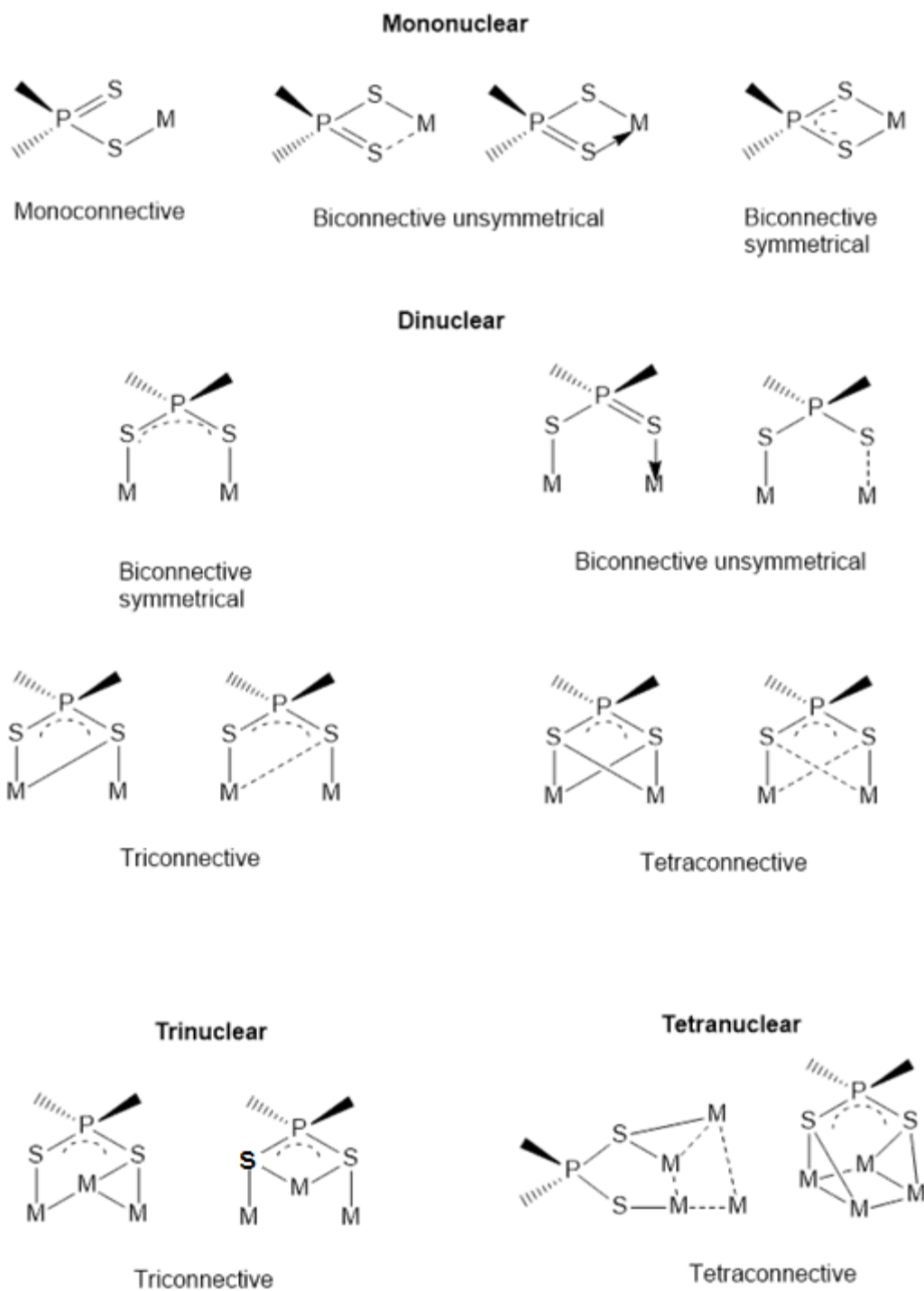


Figure 1.4: Typical binding modes to form metal-dithiophosphonate complexes

1.5 COMPLEXES RELEVANT TO THIS STUDY

Woollins and co-workers²⁶⁻²⁷ have previously reported similar metal complexes of interest in this study but we present new derivatives and more importantly, for the first time, a green solventless and mechanochemical approach to the synthesis of dithiophosphonate acids and complexes. The conventional reaction steps reported to date for the complexation reactions are relatively simple but not green and sustainable as it involves the use of hazardous solvents (waste). Traditionally, stoichiometric equivalents of both ligand and metal were stirred together in a solvent and the formation of a precipitate showed successful complexation, followed by filtration to isolate the solid product, heating of the reaction was conducted when deemed necessary. Woollins and co-workers also reported studies where metal salts are reacted stoichiometrically and directly with sodium alkoxides of the appropriate alcohol, leading to direct complex formation. But the disadvantage is that it still required heating for the duration of the reaction, followed by filtration steps and the alcohol need to be in liquid state (ie simple alcohols). In this study we present a synthesis of ligand and complexes without solvents, filtration steps, or heating, thus improving yields and reducing waste.

1.5.1 Group 10: Nickel

Nickel(II) complexes are by far the most widely reported²⁶⁻³⁰ dithiophosphonate complexes amongst all metals in this ligand class, however, a few other group 10 metals Pd(II) and Pt(II) have also been reported.³¹⁻³² The synthesis of first Ni(II) dithiophosphonate complex $[\text{Ni}\{\text{S}_2\text{PPh}(\text{OEt})\}_2]$, and the crystal structure was reported in 1967.²⁸ Typical Ni(II) complexes of this class is mononuclear and neutral and generally, adopts a square planar geometry (**Figure 1.5a**). It usually exhibits an isobidentate binding mode, which is proved by equal P-S bond lengths in the solid state.^{30, 33} The use of diols of the type $\text{HO}(\text{CH}_2)_n\text{OH}$ ($n = 2-4$) has shown to become a popular alternative and has displayed the formation of dinuclear metal complexes.³⁴ Formation of ferrocenyl moieties has been described by replacing aromatics in complexes of the type $[\text{Ni}\{\text{S}_2\text{PFc}(\text{OR}')\}_2]$ where $\text{R}' = \text{Et}, \text{iPr}, \text{etc.}$ ^{27, 35} The demonstration of neutral Ni(II) complexes linked together with a variety of N-donor ligands such as pyridinyl-alkyne and pyridyl tetrazine and bipyridine or

pyridinyl-1,4 diamine combinations³⁶ resulting in the formation of 6-coordinate Ni(II) polymeric type complexes was reported by Aragoni et al.³⁷ as shown in **Figure 1.5b**

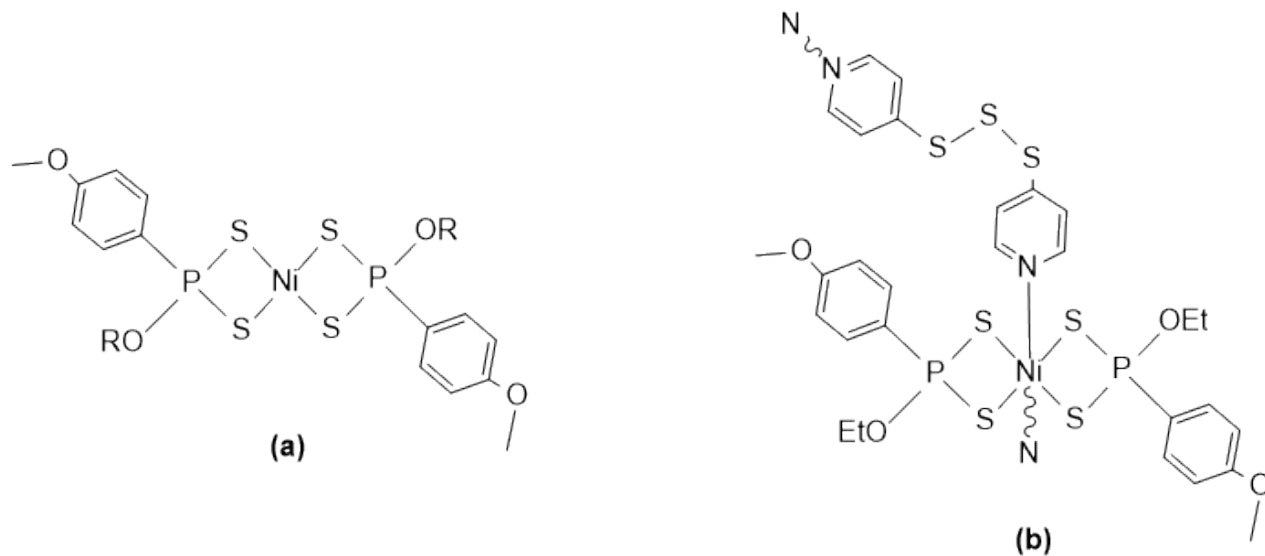


Figure 1.5: (a) A 4-coordinate Ni(II) complex. (b) A 6-coordinate Ni(II) polymeric complex containing a pyridyl-trisulfide linker

Cationic Ni(II) complexes with one dithiophosphonate ligand and a neutral triaza macrocycle were reported by Lopez and co-workers.³⁸ Monoanionic Ni(II) complexes of the type $[\text{Ni}\{\text{S}_2\text{PAr}(\text{OMe})\}\{\text{C}_6\text{F}_5\}_2]^-$ has also been reported³⁹ using an anionic pentafluorophenylate ligand. Likewise, dianionic complexes of the type $[\text{Ni}\{\text{S}_2\text{P}(\text{O})(\text{Et})\}_2]^{2-}$, $[\text{Ni}\{\text{S}_2\text{P}(\text{O})(\text{Ar})\}_2]^{2-}$ and the Fc derivative $[\text{Ni}\{\text{S}_2\text{P}(\text{O})(\text{Fc})\}_2]^{2-}$ are found in the literature.⁴⁰⁻⁴² Formation of a neutral Ni(II) dithiophosphonate complex (**Figure 1.6**) containing both a chelating and monoconnective S donor atom is known, with further coordination by a 2,4,6-tris(2-pyridyl)-1,3,5-triazine-N, N,N ligand.⁴³

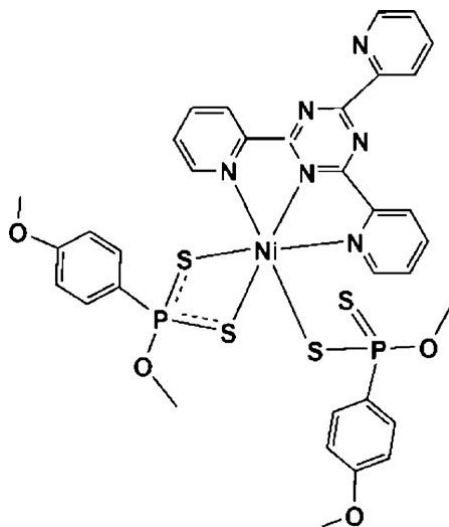
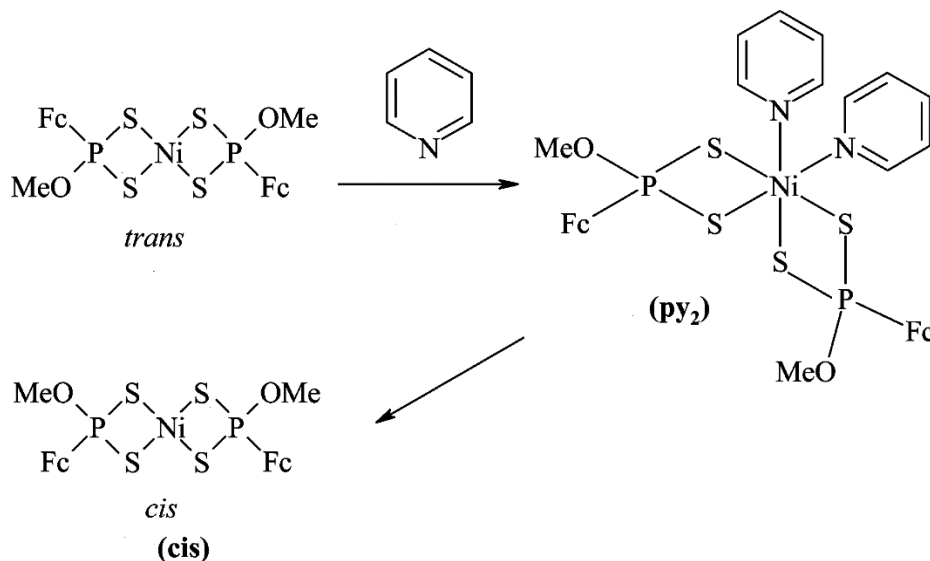


Figure 1.6. Example of a neutral Ni(II) complex containing both a chelating and monoconnective S bound dithiophosphonato ligand

The asymmetric nature of the dithiophosphonato ligand has given rise to its formation of isomers. Generally, the formation of *trans* isomer is the exclusive isomer (in solid state) to dithiophosphonate complexes but only for Ni(II) exceptions has been observed with the occurrence of a *cis* isomer, commonly under rare circumstances, such as extensive hydrogen bonding.⁴⁴ The Ni(II) complexes with square planar geometry has shown to take on two different isomeric configurations, *trans* with the ferrocenyl groups on the opposite side of the square plane and *cis* with the ferrocenyl groups on the same side of the square plane²⁷; there is a proof to show that the isomerization takes place *via* a *cis*-ML₂(solv)₂ intermediate, see **Scheme. 1.3.** Formation of 6-coordinate Ni(II) complexes of the type [Ni{S₂PAr(OMe)}₂(py)₂] with py ligands opposite (*trans*) to each other in a virtual octahedral geometry has been described by adding pyridine to *trans*-[Ni{S₂PAr(OMe)}₂].⁴⁵⁻⁴⁶



Scheme 1.3. Interconversion between *cis/trans* isomers in a square planar Ni(II) complex

There has been reports on structures with a hydroxyl group in the complex, of the type $[\text{Ni}\{\text{S}_2\text{PAr}(\text{OH})\}_2]^{47}$. The first related structure with a hydroxyl/ferrocenyl moiety is reported in this thesis (**Chapter 3**). A phenol derivative in a complex of the type $[\text{Ni}\{\text{S}_2\text{PAr}(\text{O}-2,4-\text{C}_6\text{H}_3(\text{tBu})_2)\}_2]^{48}$ and an alkyl group bound directly to the P atom in type $[\text{Ni}\{\text{S}_2\text{PEt}(\text{OCH}(\text{CH}_3)_2)\}_2]^{49}$ are also known. Generally, the majority of Ni(II) complexes are mononuclear but an exception of an interesting tetranuclear complex (**Figure 1.7**) was reported by Rothenberger et.al. and the first such complex with the corresponding ferrocenyl moiety is reported in this thesis (**Chapter 3**).

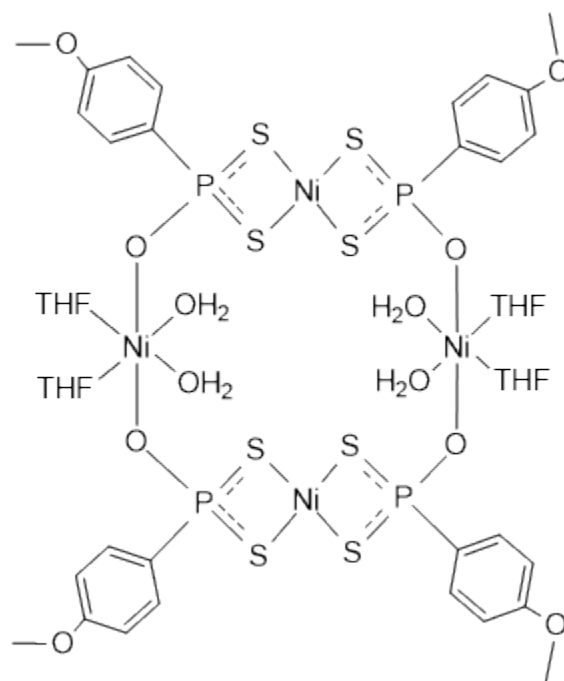


Figure 1.7. A tetranuclear Ni(II) complex containing 4- and 6-coordination around the metal center

A variety of new nickel(II) complexes are described in this work and they are all in agreement with binding modes that have all been observed for P/S type ligands. All our nickel complexes from the traditional route are conformable to those synthesized *via* a green route where there are less expended cost and time together with the elimination of hazardous waste.

1.5.2 Group 12: Zinc and Cadmium

The reported dithiophosphonate complexes of Zn(II) (**Figure 1.8**) are typically seen with similar coordination mode,^{34,50-52} and mostly embrace a 4-coordinate pattern with both a chelating and bridging mode, simultaneously. They all exhibit 4-coordinate geometry and are dinuclear in nature with an anisobidentate bonding mode in all cases. The only exception to these complexes are two monoconnective S-bound moieties as well as derivatized bipyridine ligands that formed complexes with zinc(II) and led to the formation of a mononuclear coordination polymer.⁵³

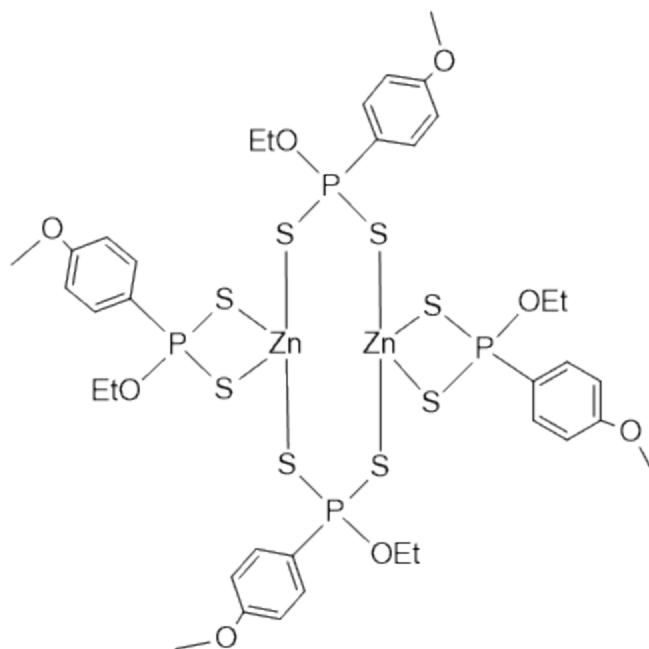


Figure 1.8. A typical 4-coordinate Zn(II) dithiophosphonate complex

The cadmium(II) complexes are very similar to zinc(II) in terms of coordination and structural geometry. Both cadmium(II) and zinc(II) complexes are generally dinuclear, but because cadmium contains a larger atom size, the metal can accommodate larger coordination numbers. Few dinuclear 4-coordinate complexes of cadmium(II) has been reported⁵⁴ however, the majority are 5-coordinate aniso- bidentate binding of Cd(II) containing two S-P-S chelates and a triconnective mode with an S-atom bridging two metal centers.⁵⁵⁻⁵⁷ Limited examples where two S-P-S chelating bipyridine derivatives led to the formation of mononuclear 6-coordinate coordination polymers has also been described.⁵⁸⁻⁵⁹ The general difference in their coordination mode may largely be due to Cd(II) being a soft Lewis acids, while Zn(II) is an intermediate Lewis acid/base and the dinuclear characteristics of the complexes generally result in the formation of an eight-membered ring comprising of two metal atoms, two phosphorus atoms, and four sulfur atoms.

We report the synthesis of series of group 12 metal (zinc and cadmium) complexes in this work and they all conform to coordination modes that have all been observed for P/S type ligands. There is a deviation in the case where ligand to metal ratio was changed and coordination polymers resulted. All our zinc and

cadmium products from the traditional route are in agreement with those synthesized via a green route leading to less expended cost and time and also the elimination of hazardous waste.

1.6 GREEN SYNTHESIS APPROACH TO PHOSPHOR-1, 1-DITHIOLATO LIGANDS, AND COMPLEXES

Green chemistry is the design of chemical products and processes that lower or eradicate the generation of hazardous substances and waste.⁶⁰ This concept of Green Chemistry was first developed at early 1990s⁶¹ and the Environmental Protection Agency's (EPA) efforts to speed the adoption of this revolutionary and diverse discipline have led to significant environmental benefits, innovation, and a strengthened economy.⁶² The term Green Chemistry was first used by the EPA in the USA during the early 1990s.^{63,64} Since then, the methodology to pursue 'environmentally friendly chemistry' has greatly increased and green chemists are now investigating environmentally benign chemical processes that are simple, economical and able to reduce or eliminate risk to the environment.⁶⁵

Today, almost all manufacturing, research and processing industries—automotive, electronics, pulp and paper, chemical, mining, food, and cleaning depend on the extensive use of solvents. To satisfy this dependency, almost 15 billion kilograms of organic and halogenated solvents are produced worldwide each year.⁶⁷ The solvents are used as process aids, cleaning agents, dispersants and as a solvent during synthesis, and these solvents inevitably end up leaching into our ecosystems⁶⁸. In global efforts to reduce generated hazardous waste, "green" chemistry and chemical processes are continuously being integrated with modern developments in science and industry⁶⁹.

Dithio-organophosphorus compounds, used extensively in this study, are phosphorus-based and phosphorus is a critical element for our food production systems, manufacturing industries, and general economic growth. The current phosphorus (P) consumption rate is over 20×10^{12} g phosphorus per year⁷⁰ while future demand is anticipated to be very high as illustrated in **Figure 1.9**. Therefore increasing use and demand for

dithio-organophosphorus compounds which are multiplying daily must be accompanied by green synthetic methods for it to be sustainable.

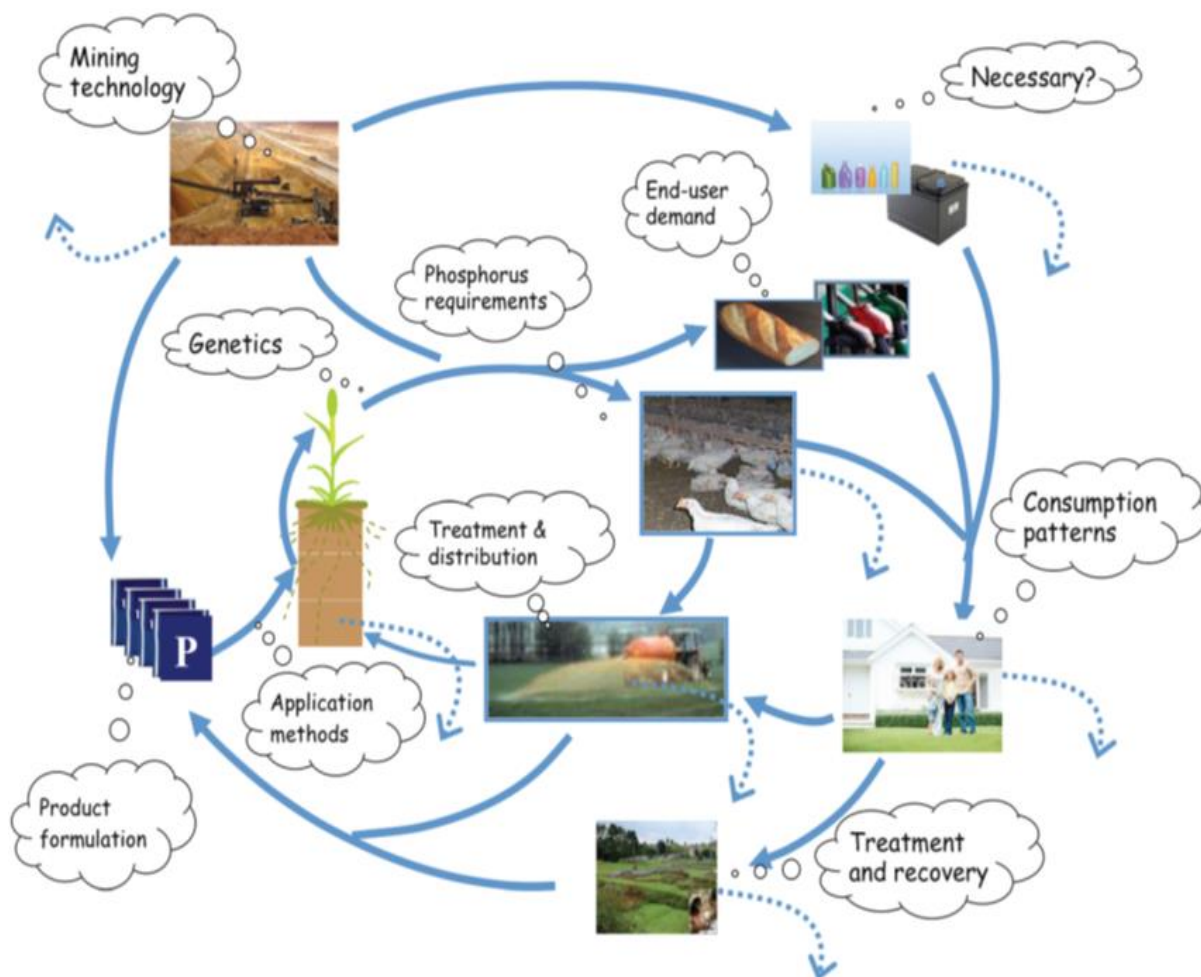


Figure 1.9: Typical applications of phosphorus and phosphorus-based compound in our society⁷¹

Unfortunately, a more immediate environmental problem is the widespread leakage of P to water bodies where it causes algal blooms, loss of aquatic biodiversity, and increased risk to human health.⁷² Phosphorus is therefore both a critical element and a pollutant and must be produced and used more efficiently and sustainably.⁷³ Achieving long-term sustainability of phosphorus production and use in society will require insights from a variety of emerging approaches, including “green chemistry”.

The most vital aspect of green chemistry is the idea of design and all about the careful planning of chemical formation and molecular design to reduce the adverse effect on the environment. The twelve principles of green chemistry are “design rules” to assist green chemists to realize their goal of sustainability.⁷⁴ The Twelve Principles of Green Chemistry were first advocated by Anastas and Warner⁶⁵ and are a globally accepted general set of criteria for assessment of the environmental acceptability of processes for the synthesis of chemical products. These principles are stated below:⁶⁵

- It is better to prevent waste than to treat or clean up waste after it is formed.
- Synthetic methods should be designed to maximize the incorporation of all materials used in the process into the final product.
- Wherever practicable, synthetic methodologies should be designed to use and generate substances that possess little or no toxicity to human health and the environment.
- Chemical products should be designed to preserve the efficiency of the function while reducing toxicity.
- The use of auxiliary substances (e.g. solvents, separation agents, etc.) should be made unnecessary wherever possible and, innocuous when used.
- Energy requirements should be recognized for their environmental and economic impacts and should be minimized. Synthetic methods should be conducted at ambient temperature and pressure.
- A raw material or feedstock should be renewable rather depleting wherever technically and economically practicable.
- Unnecessary derivatization (blocking group, protection/deprotection, and temporary modification of physical/chemical processes) should be avoided whenever possible.
- Catalytic reagents (as selective as possible) are superior to stoichiometric reagents.
- Chemical products should be designed so that at the end of their function they do not persist in the environment and break down into innocuous degradation products.

- Analytical methodologies need to be further developed to allow for real-time, in-process monitoring and control prior to the formation of hazardous substances.
- Substances and the form of a substance used in a chemical process should be chosen so as to minimize the potential for chemical accidents, including releases, explosions, and fires.

Clark report in 1999 that in chemical synthesis,⁷⁵ the ideal concept will be a combination of a number of environmental, health and safety, and economic goals which are illustrated in **Figure 1.10**.

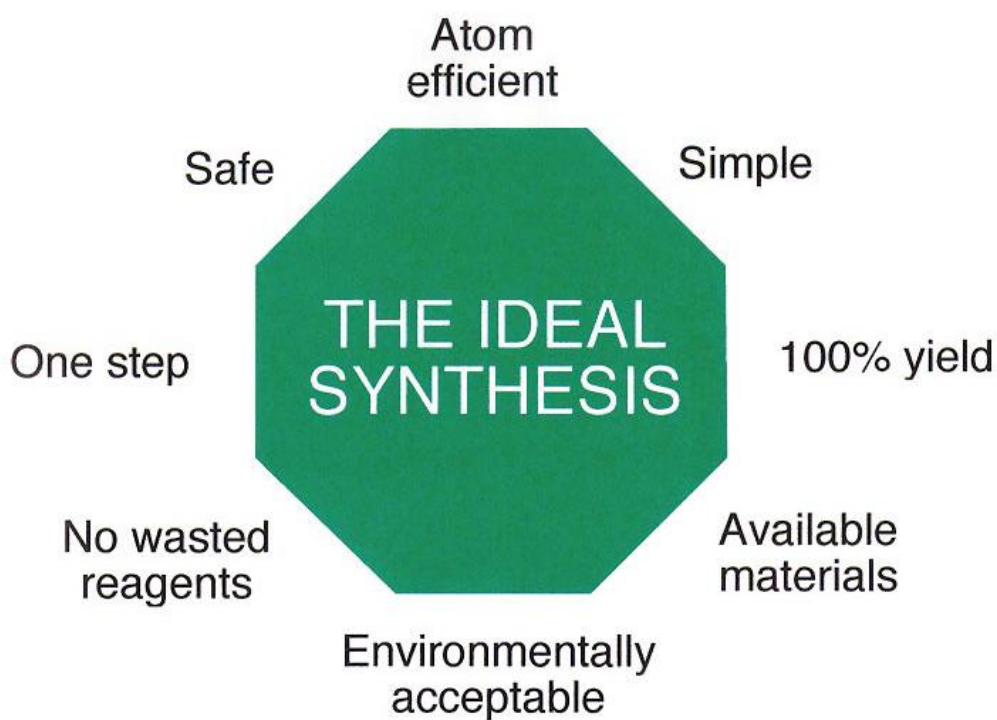


Figure 1.10 The ideal synthesis⁷⁵

It has recently been shown that while conventional synthesis methods have been greatly successful, they are inherently wasteful and make use of organic solvents which are toxic to the environment. As raw materials become more limited, it is essential that we strive to make synthetic chemistry more efficient.⁶⁶ Therefore, **Chapter 2** of this thesis reports the green synthesis of dithio-organophosphorus ligand and complexes which are also based on the above principles of green chemistry. The aim was to ensure

prevention of waste, achieved full atom efficiency, achieved a one-step and faster synthetic route and eliminate solvent usage by grinding two reactants to obtain our product. Also, minimization of expended thermal energy, reduction of derivatives, and safer chemistry for accident prevention were all achieved.

1.7 APPLICATIONS RELATED TO THIS STUDY

Dithiophosphonate applications include, but are not limited to anti-wear additives in lubricant oils,⁷⁶⁻⁷⁸ flotation reagents in the mining industry,⁷⁸ and pesticides in agriculture.⁷⁹ Research have also been channeled into the use of dithiophosphonates in making thin layers by chemical vapour deposition (CVD). In this study, we report a dye-sensitized solar cell application of dithiophosphonate complexes of interest as well as their biological application as an anti-bacterial. Optical and theoretical studies on the new dithiophosphonate and complexes are also reported in this study.

1.7.1 A Dye-Sensitized Solar Cell (DSC) Application of Ferrocenyl Dithiophosphonate Complexes

The world's demand for energy is expected to double by the year 2050 and triple by the end of the century.⁸⁰ A supply of inexhaustible energy is unavoidable for global political, economic and environmental stability. Global warming and environmental pollution caused by high consumption rate of fossil fuels have led to a greater focus on renewable energy sources and sustainable development. The development of carbon-free sources of energy that are scalable to meet increasing societal demands is, therefore, one of the major scientific challenges of this century. Hence, to replace fast depleting fossil fuels and its hazards arising from increasing global energy demands, the search for clean alternative energy sources is required. Solving this problem has placed solar cells, also called photovoltaic cells, at the centre of an ongoing research effort to utilize and exploit clean and renewable energy.⁸¹⁻⁸⁷

The development of dye-sensitized solar cells (DSC) based on nanocrystalline TiO₂ thin films pioneered by O'Regan, Grätzel, and co-workers have gathered tremendous attention in the field of photovoltaics.^{86, 88-}

⁸⁹. This interest emanated from the capacity of these devices to convert sunlight into electricity and this has proven to come with low fabrication cost, unlike traditional silicon-based solar cells.⁸⁶ The major challenge scientists are facing in order to completely replace the conventional Si-based solar cells is in the area of cell efficiency improvements. Numerous approaches have been employed to enhance the photovoltaic performance of DSC in order to tackle the problems of efficiency. These include, but are not limited to, the replacement of the commonly used liquid electrolyte with a solid or quasi-solid electrolyte,⁹⁰⁻⁹¹ use of nanocellulose-based electrolyte which can enhance the photocurrent by multiplanar scattering,⁹⁰ the use of scattering photoanodes as described by Lu and co-workers.⁹² Turri and co-workers described the deployment of a luminescent external polymeric coating material,⁹³ and finally co-sensitization, which may, in turn, be the most effective of all approaches to enhance DSC device performance. Co-sensitization is a way of employing a combination of two or more dyes on the same semiconducting film (usually titania), which can, as a result, extend the light-harvesting spectrum of the device and in turn enhance the photocurrent of the DSC. Records of high cell efficiency as result of co-sensitization are found in the literature. For example, up to 14.7% cell efficiency have been described by using the carbazole/alkyl-functionalized oligothiophene/alkoxysilyl-anchor ADEKA-1 as a photosensitizer co-sensitized with the carboxy-anchor dye LEG-4.⁹⁴ Also, cell efficiency of about 7% was achieved by employing NIR dyes as co-sensitizers as reported by Nazeeruddin.⁹⁵⁻⁹⁷ Porphyrin dyes was also mentioned in a few reports as co-sensitizers for increasing the efficiency of individual cells.⁹⁸⁻⁹⁹ Organic dyes as co-sensitizers has also been found to enhance the performance of the ruthenium-based state-of-the-art dye abbreviated N719.¹⁰⁰⁻¹⁰⁶

Investigations have shown that the majority of the research on improving DSC performance have been generally focussed on the selection of appropriate co-sensitizer and sensitizer combinations that can maximize the light-harvesting spectrum in order to enhance the photovoltaic efficiency of the device. In recent time, some d^{10} metal-organic complexes were developed into DSCs as co-sensitizers and were described to show promising cell performance.¹⁰⁷⁻¹¹³ However, researchers are still confronted with the challenges of competitive light absorption which can affect the performance of DSC,¹¹⁴ such as the

conventional redox mediator, Γ/I_3^- ,¹¹⁵⁻¹¹⁶ the dyes' aggregation,¹¹⁷⁻¹¹⁸ and the recombination of charge.¹¹⁹ Therefore, it is necessary to not only look into maximizing the spectral absorption of the dye mixture but also to model co-sensitizers that can deal with the challenge of competitive light absorption by the Γ/I_3^- redox couple, hence, the elimination of dye aggregation.

Kumar and co-worker have shown that ferrocene can be utilized as an antenna in DSC¹²⁰ and have described the light-harvesting properties of the homo- and heteroleptic complexes of ferrocenyl dithiocarbamates,¹²¹⁻¹²⁴ π -conjugated derivatives of ferrocene with different anchors, like hydroxyl, carboxyl and aldehyde, as well as quinoxaline derivatives of the biferrocenyl moiety with different anchors.¹²⁵ They recently reported results of an investigation related to ferrocenyl dithiocarbamates as a possible co-sensitizer to be implemented in DSCs.^{104, 120} Ferrocenyl-substituted triphenylamine-based donor-acceptor dyes for use in dye-sensitized solar cells was also recently reported by Misra et al.¹²⁶ The electronic absorption band of ferrocenyl systems at around 450 nm¹²⁷⁻¹²⁸ has demonstrated their capability to compensate for weak absorbance of the state-of-the-art-dye, N719, which is found at a lower wavelength region. It has also been reported that N719 is capable of accepting the photoluminescent energy of ferrocenyl complexes and expanding its spectral output as a result of d^{10} transition metal complexes of ferrocenyl ligand having excitation at around 450 nm exhibiting photoluminescence that overlaps with the absorption spectrum of N719.¹²⁹

Taking this into consideration, we report in **Chapter 5** of this thesis the first co-sensitization applications of transition-metal ferrocenyl dithiophosphonates in dye-sensitized solar cell. Ni(II), Zn(II) and Cd(II) ferrocenyl dithiophosphonate complexes were co-sensitized with a state-of-the-art-dye (N719) and great improvement in the DSC performance resulted.

1.7.1 Antibacterial Studies of New Phosphor-1, 1-Dithiolate Ligands, and Complexes

Microorganisms have existed on the earth for more than 3.8 billion years and exhibit the greatest genetic and metabolic diversity amongst all species¹⁴⁷. In the 1670s, Antoni van Leeuwenhoek identified bacteria for the first time with the aid of the microscope he invented for the observations of muscle fibres, bacteria, spermatozoa, and blood flow in capillaries.¹⁴⁸⁻¹⁴⁹ But the connection of these bacteria with the disease was not discovered until the nineteenth century. Robert Koch, a scientist in 1880's discovered the microorganisms that are responsible for diseases such as tuberculosis, cholera, and typhoid.¹⁴⁹⁻¹⁵⁰ In 1904, Paul Ehrlich, a Nobel Prize winner, developed a field which he defined as chemotherapy—the use of chemicals against infection, meaning chemicals at concentrations permitted by the host could interfere with the proliferation of microorganisms.¹⁴⁹ A purely synthetic antimicrobial drug, known as salvarsan, an arsenic-containing compound, demonstrated to be viable against the protozoal malady dozing disorder (*trypanosomiasis*), and the spirochaete ailment of *syphilis* was developed by Ehrlich in 1910.¹⁵¹ Until the discovery of penicillin in the 1940s by Florey and Chain, an outstanding agent in terms of safety and efficacy which saved several lives of infected soldiers during World War II.^{149, 152-153} Disease-causing types of microorganisms have put up resistance to constant bombardments which sought to deprive them of their host using antimicrobial agents.¹⁵⁴ Many antibacterial agents have been developed to combat bacterial diseases such as syphilis, tuberculosis, bubonic epidemic, diphtheria, typhoid, gas gangrene, tetanus, gonorrhea, and leprosy.¹⁴⁹ Presently, resistance to antimicrobial agents among bacteria, parasites, viruses and other disease-causing organisms has become public health challenges worldwide.¹⁵³ A major setback in the development of antibiotics and their application to clinical medicine has been the enhancement of bacterial resistance towards antibacterial drugs. This may be largely due to constant use of antibiotics which in turn increases selective pressure in the bacteria population, thereby permitting the survival of the resistant bacteria and eradication of the susceptible ones.¹⁵⁵ The mechanisms, as well as the chemical nature of the antimicrobial agents, play a key role in bacterial resistance development.¹⁵⁴ Mechanisms by which

antibacterial agents act can be categorized based on the bacterial structure or the function that is affected by the chemotherapeutic agents,^{154, 156} includes:

- Inhibition of cell metabolism
- Inhibition of nucleic acid transcription and replication.
- Inhibition of the bacterial cell divider amalgamation.
- Inhibition of ribosome function.
- Inhibition of folate metabolism.

Because antimicrobial resistance is fast becoming a global concern with the rapid increase in multidrug-resistant bacteria,¹⁵⁷ this has led to a continuing search for new antimicrobial compounds, including coordination complexes of biologically important molecules.¹⁵⁸⁻¹⁵⁹ This makes the activity of dithiophosphonate complexes of great interest.¹⁶⁰ Although there are many dithiophosphonate derivatives, only a few antibacterial activity studies relative to this class of compounds are present in literature.¹⁶¹⁻¹⁶³

In **Chapter 6** of this thesis, we report antibacterial susceptibility tests on the following bacteria: *Methicillin-Resistant Staphylococcus aureus (MRSA)*, *Escherichia coli*, *Staphylococcus aureus*, *Klebsiella pneumoniae*, *Bacillus subtilis*, and *Shigella dysenteriae*, *Pseudomonas aeruginosa*, *Klebsiella oxytoca*, and *Salmonella sp* using our new dithiophosphonate compounds at various concentrations.

1.8 AIMS AND OBJECTIVES OF THE STUDY

The main aims of the study are as follows:

Synthesis and characterization of new dithiophosphonate acids and salts to be used as ligands.

Synthesis and characterization of new Ni(II), Cd(II) and Zn(II) dithiophosphonate complexes.

The investigation into the dye sensitized solar cell and antibacterial applications of selected complexes.

The research objectives are as follows:

- The design of a green and sustainable (solventless) route to the synthesis of new dithiophosphonate ligand and metal complexes and comparing the advantages of such with traditional methods.
- Synthesis and characterization of new dithiophosphonate ligand systems based on Lawesson's reagent and ferrocenyl derivative of Lawesson's reagent (FcLR) using water, aliphatic alcohols, and amino alcohols.
- Synthesis and characterization of new metal (Zn, Cd, Ni) complexes of water, aliphatic alcohols and amino alcohols derivatives of dithiophosphonate ligand.
- Full characterization of all new compounds isolated using NMR spectroscopy (^1H , ^{31}P , ^{13}C), FTIR spectroscopy and mass spectrometry.
- Investigate representative X-ray crystallographic studies of new ligands and complexes.
- Investigate novel optical (solid-state luminescence and UV) studies on dithiophosphonate complexes derived from this work.
- Perform computational/theoretical studies on crystallographic structures of dithiophosphonate complexes obtained in this work.
- Carry out dye sensitized solar cell (DSC) investigations of new ferrocenyl dithiophosphonate complexes.
- Carry out antibacterial studies on selected metal complexes of dithiophosphonate ligands.

1.9 OVERVIEW

This thesis is divided into 8 chapters and below is a summary of the contents of each chapter.

Chapter 1: The present chapter gives a broad literature overview of the main topics touched upon in this thesis. It starts with a general introduction to the phosphor-1,1-dithiolate class of ligands, and the dithiophosphonate ligand class in particular, as well as the role of diphosphetane disulfide dimers as important starting materials for ligand synthesis. The major synthetic routes to dithiophosphonates and the need for green and sustainable synthetic routes. The DSC application is outlined with respect to the improvement of the device's efficiency. The antibacterial application is summarized with respect to solving antibacterial agent resistant challenges. The chapter also contains the main aims, objectives, and overview by a chapter of the thesis.

Chapter 2: This chapter describes green and modified conventional route to the synthesis of new dithiophosphonate ligand systems and Ni(II), Cd(II), and Zn(II) complexes. It also presents characterization and experimental data pertaining to the new ligands and complexes which are synthesized in this study. A summary of the discussion on characterization data result contained in this chapter include, NMR (^{31}P , ^{13}C , ^1H) spectroscopic data, selected IR bands, mass spectroscopic result, crystallographic data percentage yield and melting points.

Chapter 3: This chapter contains a synthesis of new ferrocenyldithiophosphonate ligand and transition metal complexes. It also contains characterization and experimental data pertaining to the new synthesized ligand and complexes. A summary of the discussion on characterization data result contained in this chapter include, NMR (^{31}P , ^{13}C , ^1H) spectroscopic data, selected IR bands, mass spectroscopic result, UV, crystallographic data, percentage yield and melting points.

Chapter 4: This chapter contains a synthesis of new zwitterionic dithiophosphonate ligands and their Ni(II), Cd(II), and Zn(II) complexes. It also contains characterization and experimental data associated with the new synthesized ligands and complexes. A summary of the discussion on characterization data result contained in this chapter include, NMR (^{31}P , ^{13}C , ^1H) spectroscopic data, selected IR bands, mass spectroscopic result, UV, crystallographic data, percentage yield and melting points.

Chapter 5: Contains a dye sensitized solar cell application of new ferrocenyl dithiophosphonate complexes studied in this work. The discussion of data results contained in this chapter centers around the photovoltaic parameters of the cells, electrochemical impedance spectroscopic data, and cyclic voltammetry data. Comparison of solar efficiency measurement of the state-of-the-art dye (N719) with those sensitized with ferrocenyl dithiophosphonate complexes from this work is reported in this chapter.

Chapter 6: This chapter contains antibacterial susceptibility testing on new dithiophosphonate ligands and complexes investigated in this work. The susceptibility test against Gram-negative and Gram-positive human pathogenic bacteria are reported in this chapter.

Chapter 7: This chapter conclude by summarizing the main findings of the study contained in this thesis and highlight potential future works along the same topic

1.10 REFERENCES

1. Van Zyl, W. E., *Comm. Inorg. Chem.* **2010**, 31 (1-2), 13-45.
2. Van Zyl, W. E.; Fackler, J. P., *Phosphorus, Sulfur, Silicon, Relat. Elem.* **2000**, 167 (1), 117-132.
3. Angel H. S., US Patent 2381377. **1943**, 97.
4. May R. L., US Patent 2356073, **August 15, 1944**.
5. Fay, P.; Lankelma, H. P., *J. Am. Chem. Soc.* **1952**, 74 (19), 4933-4935.
6. Lecher, H. Z.; Greenwood, R. A.; Whitehouse, K. C.; Chao, T. H., *J. Am. Chem. Soc.* **1956**, 78 (19), 5018-5022.
7. Newallis, P. E.; Chupp, J. P.; Groenweghe, L. C. D. *J. Org. Chem.* **1962**, 27 (11), 3829-3831.
8. Pederson B. S., Nilsson N. H. and Lawesson S.-O., *Bull. Soc. Chim. Belg.* **1978**, 87, 223-225.
9. Mohammad, A.; Varshney, C.; Nami, S. A. A., *Spectrochim. Acta, Part A*: **2009**, 73 (1), 20-24.,
11. Haiduc, I.; Mezei, G.; Micu-Semeniuc, R.; Edelmann, F. T.; Fischer, A., *Z. Anorg. Allg. Chem* **2006**, 632 (2), 295-300.
12. Abbotto, A.; Manfredi, N., *J. Chem. Soc., Dalton Trans* **2011**, 40 (46), 12421-12438.
13. Rathore, H. S.; Varshney, G.; Mojumdar, S. C.; Saleh, M. T.; *J. Therm. Anal. Calorim.* **2007**, 90 (3), 681-686.
14. Foreman, M. R. S. J.; Slawin, A. M. Z.; Woollins, J. D., *J. Chem. Soc., Dalton Trans.* **1996**, (18), 3653-3657.
15. Jesberger M., T. P. D., Barner L., *Synth.* **2003** 13, 1929-1933.
16. Navech J., M. R. a. S. M., *Phosphorus, Sulfur, Silicon Relat. Elem.* **1988**, 107, 306-310.

17. Alexander B.E., Khan S. J. C., T.F., Maliszewski J., A. Perry, M.P. Pitak, M. Whiteman and M.E. Wood, *Nitric Oxide* **2015**, *47*, S52.
18. Van Zyl, W. E.; Woollins, J. D., *Coord.Chem. Rev.* **2013**, *257* (3–4), 718-731.
19. Haiduc, I.; Sowerby, D. B.; Lu, S.-F., *Polyhedron* **1995**, *14* (23–24), 3389-3472.
20. Haiduc, I.; Sowerby, D. B., *Polyhedron* **1996**, *15* (15), 2469-2521.
21. Casas, J. S.; Castiñeiras, A.; Rodríguez-Argüelles, M. a. C.; Sánchez, A. n.; Sordo, J.; Vázquez López, A.; Pinelli, S.; Lunghi, P.; Ciancianaini, P.; Bonati, A.; Dall’Aglia, P.; Albertini, R.; *J.Inorg. Biochem.* **1999**, *76* (3–4), 277-284.
22. Connelly N.G., J. A. M., *RSC Publishing* **2001**, *Recommendations 2000*.
23. Connelly N.G., T. D., Hartshorn R.M, Hutton A.T., *RSC Publishing* **2005**, 224-227
24. Panico R, W. H. P, Richter J.C. *Appl. Chem.* **1999**, *71*, 1327-1333.
25. Pearson, R. G., *J.Am.Chem.Soc.* **1963**, *85* (22), 3533-3539.
26. Gray, I. P Slawin, A. M. Z, Woollins, J. D, *Dalton Trans.* **2004**, (16), 2477-2486.
27. Gray, I. P.; Milton, H. L.; Slawin, A. M. Z.; Woollins, J. D., *Dalton Trans.s* **2003**, (17), 3450-3457.
28. Hartung, H., *Z. Chem.*, **1967**, (7), 241-241.
29. Ouml; Zcan, Y.; Ide, S.; Karakus, M.; Yilmaz, H., *Anal. Sci.* **2002**, *18* (11), 1285-1286.
30. Arca, M.; Cornia, A.; Devillanova, F. A.; Fabretti, A. C.; Isaia, F.; Lippolis, V.; Verani, G., *Inorg Chim Acta* **1997**, *262* (1), 81-84.
31. Fackler Jr, J. P.; Thompson Jr, L. D., *Inorg Chim Acta* **1981**, *48*, 45-52.
32. Aragoni, M. C.; Arca, M.; Demartin, F.; Devillanova, Francesco A.; Graiff, C.; Isaia, F.; Lippolis, V.; Tiripicchio, A.; Verani, G., *Euro.J.Inorg.Chem.* **2000**, *2000* (10), 2239-2244.

33. Gataulina, A. R.; Safin, D. A.; Gimadiev, T. R.; Pinus, M. V., *Transition Met. Chem* **2008**, *33* (7), 921-921.
34. Karakus, M.; Yilmaz, H., *Russian Journal of Coordination Chemistry* **2006**, *32* (6), 437-443.
35. Karakus, M.; Lönnecke, P.; Yakhvarov, D.; Hey-Hawkins, E., *Z. Anorg. Allg. Chem* **2004**, *630* (10), 1444-1450.
37. Aragoni, M. C.; Arca, M.; Champness, N. R.; De Pasquale, M.; Devillanova, F. A.; Isaia, F.; Lippolis, V.; Oxtoby, N. S.; Wilson, C., *CrystEngComm* **2005**, *7* (60), 363-369.
38. Santana M.D., Navarro G. G., C.M., Lozano A.A., Perez J., Garcia L., Lopez G., *Polyhedron* **2002**, *21* 1935.
39. Sanchez G., J. G., Meseguer D.J., Serrano J.L., Perez J., Molins E., Lopez G., *Inorg. Chim. Acta* . **2004**, *357*, 677-682,.
40. Alberti E., G. A. A., Brenna S., Castelli F., Galli S., Maspero A, *Polyhedron* **2007**, *26*, 958.
41. Arora S.K., D. M. H., Fernando Q., *Acta Crystallogr* **1978**, *B 34*, 3355.
42. Thomas C.M., A. N., Stoeckli-Evans H., Suss-Fink G., *J. Organomet. Chem.* **2001**, *633*, 85-90.
43. Aragoni, M. C.; Arca, M.; Devillanova, F. A.; Hursthouse, M. B.; Huth, S. L.; Isaia, F.; Lippolis, V.; Mancini, A.; Soddu, S.; Verani, G., *Dalton Trans* **2007**, (21), 2127-2134.
44. Albano, V. G.; Aragoni, M. C.; Arca, M.; Castellari, C.; Demartin, F.; Devillanova, F. A.; Isaia, F.; Lippolis, V.; Loddo, L.; Verani, G., *Chem. Commun.* **2002**, (11), 1170-1171.
45. Aragoni M.C., M. A., Demartin F., Devillanova F.A., Graiff C., Isaia F., Lippolis V., Tiripicchio A., Verani, *J. Chem. Soc. Dalton Trans.* **2001**, 2671-2677
46. Karakus, M.; Lönnecke, P.; Hey-Hawkins, E., *Z. Anorg. Allg. Chem* **2004**, *630* (8-9), 1249-1252.

47. Shi, W.; Kelting, R.; Shafaei-Fallah, M.; Rothenberger, A., *J.Organomet. Chem.* **2007**, 692 (13), 2678-2682.
48. Ozcan Y., Karakus M., Yilmaz H., *Acta Crystallogr.* **2002**, C 58, m388.
49. Bone S.P., Constantinescu R., Haiduc I., *J. Chem. Res.* **1979**, 69, 933.
50. Blaurock, S.; Edelmann, F. T.; Haiduc, I.; Mezei, G.; Poremba, P., *Inorg.Chim. Acta* **2008**, 361 (1), 407-410.
51. Karakus, M.; Yilmaz, H.; Bulak, E., *Russian Journal of Coordination Chemistry* **2005**, 31 (5), 316-321.
52. Karakus, M.; Yilmaz, H.; Bulak, E.; Lönnecke, P., Crystallographic report: *App. Organomet. Chem.* **2005**, 19 (3), 396-397.
53. F. Devillanova, C. A., M. Arca, M.B. Hursthouse, S.L. Huth, *Univ. of Southampton, Crystal Structure Report Archive* **2006**, 238-.
54. Gray, I. P.; Milton, H. L.; Slawin, A. M. Z.; Woollins, J. D., *Dalton Trans* **2003**, 17.
55. Shi, W.; Shafaei-Fallah, M.; Anson, C. E.; Rothenberger, A., *Dalton Trans.* **2006**, (26), 3257-3262.
56. Gray, I. P.; Milton, H. L.; Slawin, A. M. Z.; Woollins, J. D., *Dalton Trans* **2004**, 16.
57. Karakus, M.; Yilmaz, H.; Bulak, E.; Lönnecke, P., *Appl Organomet Chem* **2005**, 19.
58. Devillanova F., Arca M., Hursthouse M.B., Huth S.L., *Univ. of Southampton, Crystal Structure Report Archive* **2006**, 248.
59. Devillanova F., Arca M., Hursthouse M.B., Huth S.L., *Univ. of Southampton, Crystal Structure Report Archive* **2006**, 235.
60. Anastas, P. T., *Chem.Rev.* **2007**, 107 (6), 2167-2168.

61. Collins T. J, in *Green Chemistry, Macmillan Encyclopedia of Chemistry, Simon, and Schuster Macmillan New York*. **1997**, 2, 691–697
62. US Environmental Protection Agency (EPA),. <https://www.epa.gov/greenchemistry>.
63. Lancaster, M., *Royal Society of Chemistry, Cambridge 2002*, pp 3-7.
64. Trost, B. M., *Science* **1991**, 254, 1471-1477.
65. Anastas, P. T. W., J. C., *Oxford University Press, Oxford* **1998**, pp 12-30.
66. Mason, B. P.; Price, K. E.; Steinbacher, J. L.; Bogdan, A. R.; McQuade, D. T., *Chem. Rev.* **2007**, 107 (6), 2300-2318.
67. A, W. K., *Chemical week* **1996**, 158 (38), 14.
68. DeSimone, J. M., *Science* **2002**, 297 (5582), 799-803.
69. Sharma, V. K.; Yngard, R. A.; Lin, Y., *Adv. Colloid Interface Sci.* **2009**, 145 (1–2), 83-96.
70. Reijnders, L., *Resources, Conservation and Recycling* **2014**, 93, 32-49.
71. Withers, P. J. A.; Elser, J. J.; Hilton, J.; Ohtake, H.; Schipper, W. J.; van Dijk, K. C., *Green Chem.* **2015**, 17 (4), 2087-2099.
72. Smith, V. H.; Schindler, D. W., *Trends in Ecology & Evolution* **2009**, 24 (4), 201-207.
73. Elser, J.; Bennett, E., Phosphorus cycle: A broken biogeochemical cycle. *Nature* **2011**, 478 (7367), 29-31.
74. Anastas, P.; Eghbali, N., *Chem. Soc. Rev.* **2010**, 39 (1), 301-312.
75. Clark H., *Green Chem.* **1999**, 1 (1), 1-8.
76. Lawton, S. L.; Kokotailo, G. T., *Inorg. Chem.* **1969**, 8 (11), 2410-2421.

77. Harrison, P. G.; Begley, M. J.; Kikabhai, T.; Killer, F., *J.Chem.Soc., Dalton Trans.* **1986**, (5), 925-928.
78. Alimarin, I. P.; Tat'yana, V. R.; Vadim, M. I., *Russ.Chem.Rev.* **1989**, 58 (9), 863.
79. Edmundson, R. S., *Chapman, and Hall, London* **1988**.
80. In Basic Research Needs for Solar Energy Utilization, *U.S. Department of Energy*,
81. Pil J. Yoo, Ki Tae Nam, Jifa Qi, Soo-Kwan Lee, Juhyun Park, Angela M. Belcher and Paula T. Hammond., *Nat Mater* **2006**, 5 (3), 159-159.
82. Bartlett, A. A., *Am. J.Phys.* **1986**, 54 (5), 398-402.
83. Hubbert, M. K., *Am. J.Phys.* **1981**, 49 (11), 1007-1029.
84. Hubbert, M. K., Energy from Fossil Fuels. *Science* **1949**, 109 (2823), 103-109.
85. Chandrasekharam, M.; Srinivasarao, C.; Suresh, T.; Reddy, M. A.; Raghavender, M.; Rajkumar, G.; Srinivasu, M.; Reddy, P. Y., *J.Chem.Sci.* **2011**, 123 (1), 37-46.
86. O'Regan, B.; Gratzel, M., A low-cost, high-efficiency solar cell based on dye-sensitized colloidal TiO₂ films. *Nature* **1991**, 353 (6346), 737-740.
87. Campbell, C. J., *Population and Environment* 24 (2), 193-207.
88. Gratzel, M., Photoelectrochemical cells. *Nature* **2001**, 414 (6861), 338-344.
89. Grätzel, M., *J.Photochem. Photobio.C* **2003**, 4 (2), 145-153.
90. Bella F., Nair J. R, Meligrana G., Gerbaldi C., *Chem. Eng.Trans.* **2014**, 41, 211-217.
91. Bella F., Gerbaldi C., *RSC Advances* **2013**, 3, 15993-15999.
92. Zhao P., Liu D., Sun P., Liu F., Lu G., *Electrochim. Acta* **2015**, 182, 257-264.

93. Griffini G., Nisic F., Dragonetti C., Roberto D., Levi M., Bongiovanni R., Turri S., *Adv. Energy Mater.* **2015**, *5*, 1401312-1401319.
94. Kakiage K., Yano T., Oya K., Fujisawa J.-I., Hanaya M., *Chem. Commun* **2015**, *51*, 15894-15901.
95. Yum J. H., Walter P., Geiger T., Nüesch S, Ko K. J., Grätzel M., Nazeeruddin M. K. *Chem. Commun.* **2007**, 4680-4689.
96. Cid J. J., Jang S. R., Nazeeruddin M. K., Ferrero E. M., Palomares E., Ko J. J., Grätzel M., Torres T.; *Angew. Chem* **2007**, *119*, 8510-8517.
97. Cid J. J., Jang S. R., Nazeeruddin M. K., Ferrero E. M., Palomares E., Ko J. J., Grätzel M., Torres T.; *Angew. Chem. Int. Ed.* **2007**, *334*, 8358-8365.
98. Lan C. M., Pan, T. Y., Chang C. W., Chao W. S., Chen C. T., Wang C. L., Lin C. Y., Diau W. G, *Energy Environ. Sci.* **2012**, *5*, 6460-6467.
99. Mojiri-Foroushani M., Salehi-Vanani N., *Electrochim. Acta* **2013**, *92*, 315-330.
100. Ogura R. Y., Morooka M., Orihashi M., Suzuki Y., Noda K., *Appl. Phys. Lett* **2009**, 24-30.
101. Han L., Chen H., C. Malapaka, Zhang S., Yang X., Yanagida M., Chiranjeevi B., *Energy Environ. Sci.* **2012**, *5*, 6057-6062.
102. Ozawa H., Arakawa H. *RSC Advances* **2012**, *2*, 3198-3203.
103. Lin R. Y. Y., Cheng Y. T, Lee C. P., Hsu Y. C, hou H. H. C, Hsu C. Y., Chen Y. C., Ho K. C., Lin J. T., Tsai C. T., *Org. Lett.* **2012**, *14*, 3612-3619.
104. Magne C., M. U., Pauporté T., *RSC Adv.* 2013, *3*, 6318; b) J. Chang, C. P. Lee, D. Kumar, P. W. Chen, Lin L. Y., Thomas K. R. J., Ho K. C., *J. Power Sources* **2013**, *240*, 779-785.
105. Wei L., Yang Y. N., Y., Fan R., Wang P., Li L., *Phys. Chem. Chem. Phys.* **2015**, *17*, 1273-1280.

106. Yum J.-H., Wenger E. B., S., Nazeeruddin M. K., Grätzel M., *Energy Environ. Sci.* **2011**, *4*, 842-8
107. Wang X., Li L., Fan R. Q., Cao W. W., Yang B., Wang H., Liu J. Y. *Dalton Trans* **2012**, *41*, 10619.
108. Wei, L.; Yang, Y.; Fan, R.; Na, Y.; Wang, P.; Dong, Y.; Yang, B.; Cao, W., *Dalton Trans.* **2014**, *43* (29), 11361-11370.
109. Gao, S.; Fan, R. Q.; Wang, X. M.; Qiang, L. S.; Wei, L. G.; Wang, P.; Zhang, H. J.; Yang, Y. L.; Wang, Y. L., *J.Mat.Chem. A* **2015**, *3* (11), 6053-6063.
110. Wang, X.-M.; Wang, P.; Fan, R.-Q.; Xu, M.-Y.; Qiang, L.-S.; Wei, L.-G.; Yang, Y.-L.; Wang, Y.-L., *Dalton Trans.* **2015**, *44* (11), 5179-5190.
111. Gao, S.; Fan, R. Q.; Wang, X. M.; Qiang, L. S.; Wei, L. G.; Wang, P.; Yang, Y. L.; Wang, Y. L.; Luan, T. Z., *RSC Advances* **2015**, *5* (54), 43705-43716.
112. Dong, Y.-W.; Fan, R.-Q.; Wang, P.; Wei, L.-G.; Wang, X.-M.; Gao, S.; Zhang, H.-J.; Yang, Y.-L.; Wang, Y.-L., *Inorganic Chem.* **2015**, *54* (16), 7742-7752.
113. Zervaki, G. E.; Papastamatakis, E.; Angaridis, P. A.; Nikolaou, V.; Singh, M.; Kurchania, R.; Kitsopoulos, T. N.; Sharma, G. D.; Coutsolelos, A. G., *Eur. J. Inorg.Chem.* **2014**, *2014* (6), 1020-1033.
114. Han, L.; Islam, A.; Chen, H.; Malapaka, C.; Chiranjeevi, B.; Zhang, S.; Yang, X.; Yanagida, M., *Energy & Environ.Sci.* **2012**, *5* (3), 6057-6060.
115. Wang, M.; Chamberland, N.; Breau, L.; Moser, J.-E.; Humphry-Baker, R.; Marsan, B.; Zakeeruddin, S. M.; Grätzel, M., *Nat Chem* **2010**, *2* (5), 385-389.
116. Tian, H.; Sun, L., *J.Mat.Chem.* **2011**, *21* (29), 10592-10601.
117. Song, B. J.; Song, H. M.; Choi, I. T.; Kim, S. K.; Seo, K. D.; Kang, M. S.; Lee, M. J.; Cho, D. W.; Ju, M. J.; Kim, H. K., *Chemistry – A Eur.J.* **2011**, *17* (40), 11115-11121.

118. Bessho, T.; Zakeeruddin, S. M.; Yeh, C.-Y.; Diau, E. W.-G.; Grätzel, M., *Angew.Chem.Int.Ed.* **2010**, *49* (37), 6646-6649.
119. Wang, H.; Liu, M.; Zhang, M.; Wang, P.; Miura, H.; Cheng, Y.; Bell, J., *Phys. Chem.Chem.Phys.* **2011**, *13* (38), 17359-17366.
120. Yadav, R.; Trivedi, M.; Kociok-Köhn, G.; Chauhan, R.; Kumar, A.; Gosavi, S. W., *Eur..J.Inorg.Chem.* **2016**, *2016* (7), 1013-1021.
121. Kumar, A.; Chauhan, R.; Molloy, K. C.; Kociok-Köhn, G.; Bahadur, L.; Singh, N., *Chem. – A Eur. J.* **2010**, *16* (14), 4307-4314.
122. Singh, V.; Chauhan, R.; Gupta, A. N.; Kumar, V.; Drew, M. G. B.; Bahadur, L.; Singh, N., *Dalton Trans.* **2014**, *43* (12), 4752-4761.
123. Singh, S. K.; Chauhan, R.; Diwan, K.; Drew, M. G. B.; Bahadur, L.; Singh, N., *J. Organomet.Chem.* **2013**, *745–746*, 190-200.
124. Singh, S. K.; Chauhan, R.; Singh, B.; Diwan, K.; Kociok-Kohn, G.; Bahadur, L.; Singh, N., *Dalton Trans.* **2012**, *41* (4), 1373-1380.
125. Chauhan, R.; Shahid, M.; Trivedi, M.; Amalnerkar, D. P.; Kumar, A., *Eur.J.Inorg.Chem.* **2015**, *2015* (22), 3700-3707.
126. Misra, R.; Maragani, R.; Patel, K. R.; Sharma, G. D., *RSC Advances* **2014**, *4* (66), 34904-34911.
127. Gray, H. B.; Sohn, Y. S.; Hendrickson, N., *Am.Chem.Soc.* **1971**, *93*(15), 3603-3612.
128. Smith, J. J.; Meyer, B., *J.Chem.Phys.* **1968**, *48* (12), 5436-5439.
129. Singh, N.; Kumar, A.; Prasad, R.; Molloy, K. C.; Mahon, M. F., *Dalton Tran.* **2010**, *39* (10), 2667-2675.
130. Bethe, H., Termaufspaltung in Kristallen. *Annalen der Physik* **1929**, *395* (2), 133-208.

131. Hoffmann, R., *The Journal of Chemical Physics* **1963**, 39 (6), 1397-1412.
132. Hoffmann, R.; Lipscomb, W. N., *The Journal of Chemical Physics* **1962**, 36 (8), 2179-2189.
133. Burdett, J. K., *Progress in Solid State Chemistry* **1984**, 15 (3), 173-255.
134. Ziegler, T., *Chemical Reviews* **1991**, 91 (5), 651-667.
135. Becke, A. D., Density- functional thermochemistry. I. *J.Chem.Phys.* **1992**, 96 (3), 2155-2160.
136. Perdew, J. P.; Chevary, J. A.; Vosko, S. H.; Jackson, K. A.; Pederson, M. R.; Singh, D. J.; Fiolhais, C., *Phys.Rev. B* **1992**, 46 (11), 6671-6687.
137. Chermette, H., *Coord.Chem.Rev.***1998**, 178–180, Part 1, 699-721.
138. Johnson, K. H.; Smith, F. C., *Chem.Phys.Lett.* **1971**, 10 (2), 219-223.
139. Belanzoni, P.; Baerends, E. J.; van Asselt, S.; Langewen, P. B., *J.Phys.Chem.***1995**, 99 (35), 13094-13102.
140. Bureau, C.; Lécayon, G., *J ChemPhys.* **1997**, 106 (21), 8821-8829.
141. Snijders, J. G.; Meer, W. v. d.; Baerends, E. J.; Lange, C. A. d., *J.Chem.Phys.* **1983**, 79 (6), 2970-2974.
142. Ravenek, W.; Jacobs, J. W. M.; van der Avoird, A. *Chem.Phys.* **1983**, 78 (3), 391-404.
143. Eriksson, L. A.; Malkina, O. L.; Malkin, V. G.; Salahub, D. R., *Int.J.Quantum Chem.***1997**, 63 (2), 575-583.
144. Karakus, M.; Solak, S.; Hökelek, T.; Dal, H.; Bayrakdar, A.; Özdemir Kart, S.; Karabacak, M.; Kart, H. H., *Spectrochim Acta A Mol Biomol Spectrosc* **2014**, 122, 582-590.
145. Kart, H. H.; Özdemir Kart, S.; Karakuş, M.; Kurt, M., *Spectrochim Acta A Mol Biomol Spectrosc* **2014**, 129, 421-428.

146. Aydemir, C.; Karakus, M.; Kara, I.; Kiraz, A. Ö.; Kolsuz, N., *J Mol.Struct.* **2016**, *1111*, 61-68.
147. Dun, E., *J. Biol. Med.*, **1999**, *72* 281–285.
148. <https://explorable.com/discovery-of-bacteria>. access December 6, 2016
149. Patrick, G. L. *Oxford University Press, Oxford* **1995**, 154-204.
150. Gest, H., *Notes Rec. R. Soc. Lond.* **2004**, *58*, , 187-201.
151. Heynick, F., *Brit. J. Psychiat.* **2009**, *195*, 456-476.
152. Mahoney, J. F. A., R.C.; Harris, A., *Am. J. Public Health Nations Health* **1943**, *33*, 1387-1391.
153. Saga, T. Y., K., *JMAJ* **2009**, *52*, , 103-108.
154. Yousif, E.; Majeed, A.; Al-Sammarrae, K.; Salih, N.; Salimon, J.; Abdullah, B., *Arab.J.Chem.*
155. Yanling, J. X., L.; Zhiyuan, L., The antibacterial drug discovery. *InTech.* **2013**, 289-308.
156. Fluit, A. C. V., M.R.; Schmitz, F-J. *Clin. Microbiol. Rev* **2001**, *14*, , 836-871.
157. Saha, S., Dhanasekaran, D., Chandraleka, S., Thajuddin, N. and Panneerselvam, A., *Adv.Biol.Res.* **(2010)** *4*,224-229.
158. Farrell, N., *Compr.Coord.Chem.* **2003**, *9*, 809-840.
159. Johari, R., Kumar, G., Kumar, D., and Singh, S., *J.Indi.Chem. Council* **2009**, *26*, 23-27.
160. Chauhan, H. P. S.; Singh, U. P.; Shaik, N. M.; Mathur, S.; Huch, V., *Polyhedron* **2006**, *25* (15), 2841-2847.
161. Cherkasov, R. A.; Nizamov, I. S.; Gabdullina, G. T.; Almetkina, L. A.; Shamilov, R. R.; Sofronov, A. V., *Phosphorus, Sulfur, Silicon Relat. Elem.* **2013**, *188* (1-3), 33-35.

162. Aydemir, C.; Solak, S.; Acar Doganlı, G.; Sensoy, T.; Arar, D.; Bozbeyoglu, N.; Mercan Dogan, N.; Lönnecke, P.; Hey-Hawkins, E.; Sekerci, M.; Karakus, M., *Phosphorus, Sulfur, Silicon Relat. Elem.* **2015**, *190* (3), 300-309.
163. Karakus, M.; Ikiz, Y.; Kaya, H. I.; Simsek, O., *Chem.Centr.J.* **2014**, *8* (1), 18.

CHAPTER 2

SOLVENT-FREE MECHANOCHEMICAL SYNTHESIS OF DITHIOPHOSPHONIC ACIDS AND CORRESPONDING TRANSITION METAL COMPLEXES

2.1 BACKGROUND

Dithio-organophosphorus compounds are used in diverse and important areas of the chemical and allied industries. Applications range from anti-oxidant additives in the oil- and petroleum industry,¹ zinc dithiophosphates, in particular, have been used as a lubricant additive (antioxidant) for the past 60 years.² There has also been a drive toward so-called green lubricants,³ agricultural pesticide derivatives,⁴ and metal ore extraction reagents as well as flotation agents in the mining industry.⁵ Within the realm of green chemistry, Anastas and co-workers recently suggested a structural modification in organophosphorus compounds to reduce toxicity could be achieved by replacing the present oxono analogues as acetylcholinesterase (AChE) inhibitors by the less reactive thiono analogues.⁶ Additionally, there has been a call to observe the sustainability of global phosphorus (P) use, which is emerging as a major societal goal to secure future food, energy, and water security for a growing population – the so-called greening of the phosphorus cycle.⁷ While there is an initiative to become more aware of solvents from nature,⁸ conventional synthesis methods still greatly rely on inherently wasteful organic solvents which are toxic to the environment. Solvent-free methods are therefore considered more beneficial.⁶ Solvents are commonly used as process aids, cleaning agents, dispersants and in R&D synthesis which typically ends up leaching into surrounding ecosystems.⁹ The phosphor-1, 1 dithiolate class of compounds is varied and include, amongst others, the dithiophosphates **A**, dithiophosphinates **B**, and dithiophosphonates **C**, shown in delocalized form across the S-P-S bonds in **Figure 2. 1**. The dithiophosphonato ligand, **C**, which is the focus of the present study, may be described as a *hybrid* of **A** and **B**.¹⁰ The literature reveals that¹¹ type **C** acids were slow to

develop compared to the better established $[\text{HS}_2\text{PR}_2]$ and especially $[\text{HS}_2\text{P}(\text{OR})_2]$ counterparts. A reason for this may be the unavailability of key starting materials, but this impediment changed with the development of dimers of the type $[\text{RP}(\mu\text{-S})_2]$ ($\text{R} = \text{aryl}$) which have traditionally been used by organic chemists to convert ketones into thiones.¹²

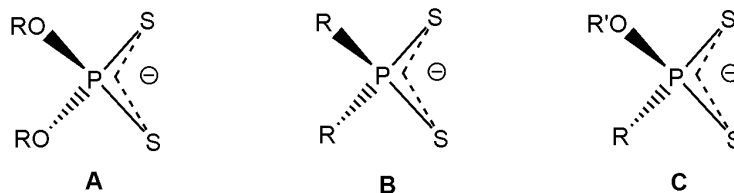
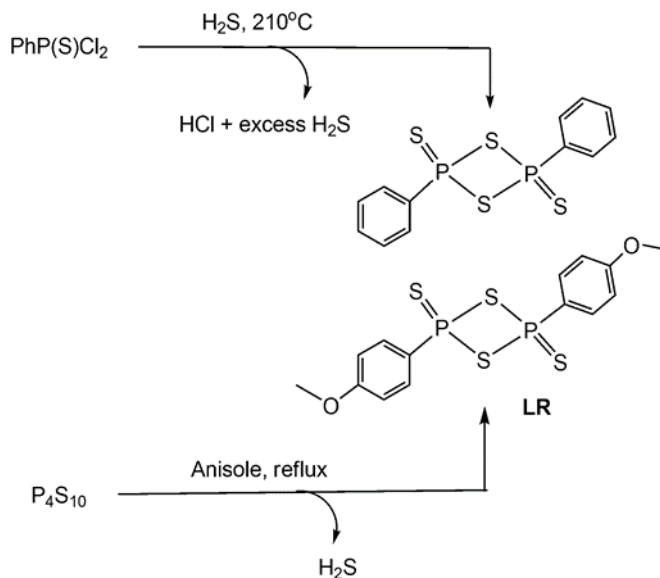


Figure 2.1: Different types of the most common phosphor-1, 1,-dithiolates

The preparation and characterization of the phenyl-derived dimer $[\text{PhP}(\mu\text{-S})_2]$ was first described in 1962 but the procedure is decidedly the very antithesis of a green chemistry methodology and requires the use of wasteful excess and toxic H_2S gas introduced sub-surface at elevated temperature ($>210^\circ\text{C}$) with the release of copious amounts of corrosive HCl as by-product.¹³⁻¹⁴ A significant improvement came in 1978 when Lawesson and co-workers reported¹⁵ the reaction between the electron-rich aromatic anisole and P_4S_{10} which leads directly to the formation of dimer 2,4-bis(4-methoxyphenyl)-1,3-dithiadiphosphetane-2,4-disulfide, $[(4\text{-MeOC}_6\text{H}_4)\text{P}(\mu\text{-S})_2]$, albeit with the release of stoichiometric amounts of H_2S gas, but without the release of HCl , **Scheme 2.1**. Anisole serves as both the solvent and reactant and this dimer has become known as Lawesson's Reagent (**LR**) in the vernacular of dithiophosphonates, it is commercially available and its general chemistry has been comprehensively reviewed.¹⁶



Scheme 2.1: Synthesis of the dimer $[\text{PhP}(\mu\text{-S})\text{S}]_2$ (above) and below the greener version in Lawesson's Reagent (**LR**).

Although the conversion of ketones into thiones still occupy the largest share of **LR**'s utility, alcoholysis of dithiadiphosphetane dimers, including **LR**, yields the corresponding dithiophosphonic acid.¹⁷ A wide variety of alcohols are now known to be utilized in this manner, including unsaturated (allyl), sterically demanding (adamantyl), and quasi-strained (cyclopentyl), in addition to the reaction of **LR** with silanols and trialkyl silanols. Although the release of H_2S is typically discouraged in chemical synthesis, it is noteworthy to point out that reactions which slowly release H_2S are now actively pursued in medicinal chemistry. For example, the generation of H_2S from the phosphinodithioate slow-release donor GYY4137 has been investigated and the key decomposition products formed during hydrolysis have been identified as well as the mechanism by which H_2S is generated.¹⁸

This thesis investigated phosphor-1,1-dichalcogenates of the late-transition metals (Groups 10 & 12),¹⁹ and report i) an entirely green and solvent-free synthesis method for dithiophosphonic acids at 100% atom economy and ii) using the unmodified acid ligands directly in the formation nickel and zinc (II) complexes.

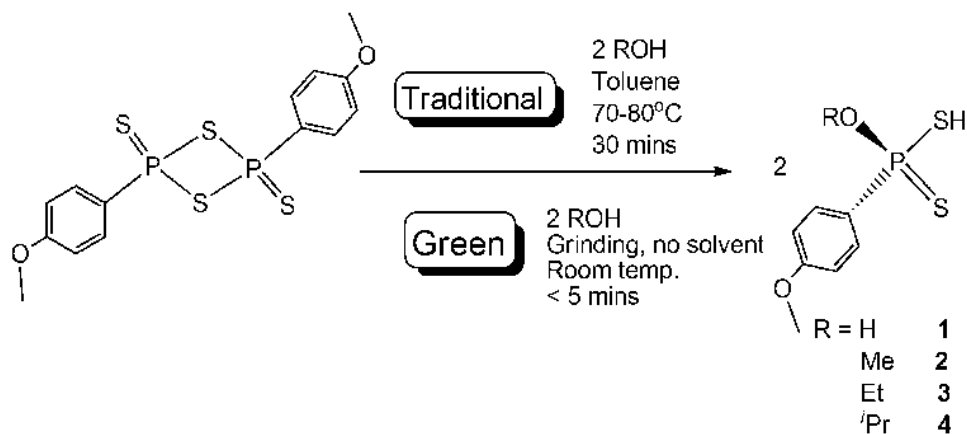
2.2 RESULTS AND DISCUSSION

2.2.1 Synthesis of Dithiophosphonic Acids

The *conventional synthesis methodology* used to form dithiophosphonic acids, $\text{HS}_2\text{PR}(\text{OR}')$, typically starts with the anisoyl derived Lawesson's Reagent (**LR**), although the phenetolyl¹¹ and even ferrocenyl²⁰ versions of the dimer have also been successfully utilized. **LR** is placed in a Schlenk tube and heated to $\sim 80^\circ\text{C}$ using an oil bath followed by the slow addition of the appropriate alcohol. A small amount of inert solvent such as toluene is added to give the magnetic stirrer bar mobility. The addition of solvent immediately leads to a dilution effect, which in turn results in more time needed for the reaction to proceed to completion. Afterward, the acid needs to be separated from the solvent, which requires further heating for distillation, and loss of yield is inevitable. The acid is generally very viscous and difficult to manipulate but can be precipitated as an ammonium salt by bubbling ammonia through the solution in an ice bath at 0°C which turns it into a free-flowing powder upon drying.

By contrast, the *green synthesis methodology* described in the present study circumvents many of these obstacles. **LR** is placed in a Schlenk tube and is covered under a blanket of nitrogen to avoid hydrolysis, *vide infra*. At room temperature, 2 molar equivalents of mono-hydroxy alcohols (ie simple alcohols such as MeOH, EtOH, etc.) are dripped directly onto **LR**; higher alcohols such as diols (ethylene glycol), pentaerythritol, etc. would require different molar ratios, see **Figure 2.2**. Mechanochemical synthesis in general terms refers to reactions induced by the input of mechanical energy, usually grinding.²¹⁻²² Once the alcohol is added, the mixture is gently ground, **Scheme 2.2**. This process appears very deceptive because initially, it seems that no reaction is taking place. It is suggested that it is for this reason that previous attempts at mechanochemical synthesis for this system had been prematurely abandoned. But the reaction dynamics changes quite dramatically in less than 5 minutes when the mixture turns viscous, subsequently identified as the acid product. This highlights another advantage of the green method, namely the reaction both starts and finishes at room temperature, giving no opportunity for any alcohol to evaporate through

extensive heating during the reaction. By contrast, conventional methods require much longer (>30 min.) reaction times.



Scheme 2.2. Comparison between the Traditional and Green chemistry method for the formation of dithiophosphonic acids.

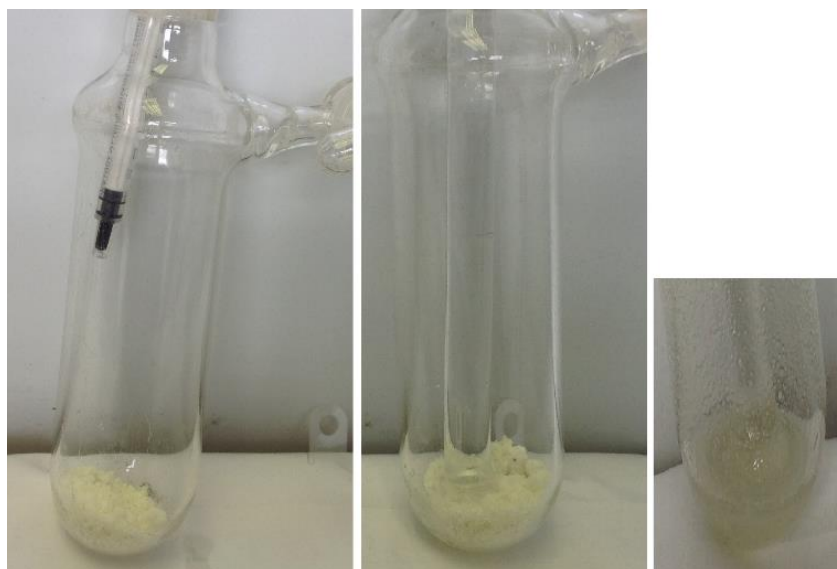


Figure 2.2. Photographs demonstrating the progress of the green synthesis of dithiophosphonic acids. (Left): In a ~2 cm diameter Schlenk tube, under a blanket of nitrogen, two molar equivalents of water or simple alcohols are dripped slowly via a disposable syringe onto yellow Coloured solid Lawesson's Reagent. (Middle): After addition of liquid, the mixture is gently ground with a glass rod at room temperature. (Right): In less than 15 minutes for 1, and less than 5 minutes for 2-4 the dithiophosphonic acid forms (shown in close-up) as a viscous liquid.

Theories to comprehensively explain the reaction chemistry at the solid-liquid interface during solvent-free mechanochemical processes are lacking. Following from work by Paul and Curtin²³ Bala and Coville reviewed different scenarios for melt reactions²⁴ (a sub-class of solvent-free reactions) most commonly observed for solid-solid and solid-gas reactions that can be described as binary systems with a minimum eutectic temperature. In this study, the focus is on a solid-liquid interface system which appears to be a rare example to both starts and finish at room temperature. We focused on alcohols in liquid form as one reagent which was all very efficient for this particular transformation; we also attempted materials with alcohol functionalities in solid forms, such as cholesterol etc., but they were less efficient and require further optimization.

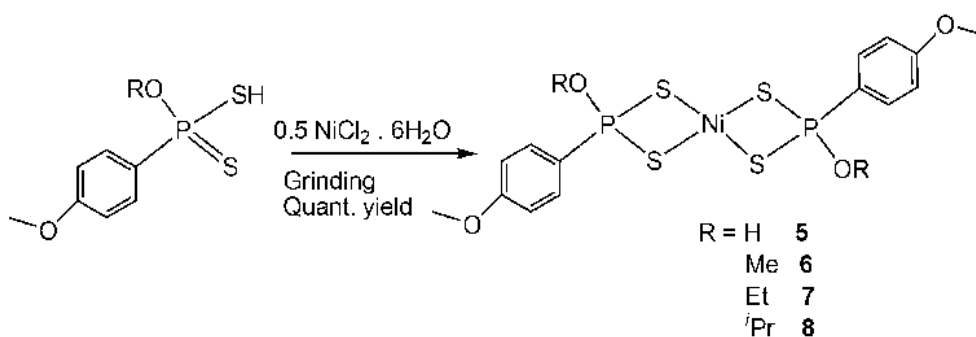
2.2.2 Preparation of Ni(II), Cd(II) and Zn (II) Dithiophosphonate Complexes

Once the dithiophosphonic acids **1-4** could be routinely formed, the investigation moved to their use as ligands to form metal complexes. Here the goal was not to produce new metal complexes through conventional solvent-based methods, but instead to show a new green and sustainable synthesis methodology. We started from the hexahydrate $\text{NiCl}_2 \cdot 6\text{H}_2\text{O}$ (distinct green colour) and formed Ni(II) dithiophosphonates which have a distinctly purple colour, allowing for simple colorimetric means to detect product formation. The most abundant metal complexes reported containing the dithiophosphonate ligand is that of Ni(II) yet to date they were all formed by traditional means. Zn(II) and Cd(II) dithiophosphonate complexes were subsequently formed in a similar manner. This new methodology departs from the conventional methods in a number of ways: i) we found no need to first convert the ligands to their respective ammonium or sodium salts, but used the ligands in acid form directly, ii) this had the advantage that no filtration step (to remove NH_4Cl and/or NaCl) was later needed, iii) the reaction proceeded without solvent and at room temperature, and iv) there was no need to first isolate the ligand before commencing to complex formation, since the ligand formed in >98% yield in step 1, without unwanted side-products, complex formation was immediate by adding the Ni(II), Cd(II) and Zn(II) precursor. The yields for the acids were all exceptionally high that we attribute to i) the 100% concentration of the reactants in intimate

contact with each other (no solvents, no dilution effects) and ii) the oxophilic nature of the P atom which would always prefer P-O binding to P-S binding, the former providing a continuous driving force for the reaction to reach completion. The yields for the nickel, cadmium, and zinc(II) complexes were slightly lower but still much higher than could be achieved by synthesis through conventional means, which we ascribe to the absence of salt formation as a by-product, negating extraction and filtration steps. The reaction is shown below in **Figure 2.3** and **Scheme 2.3**.



Figure 2.3. Photographs demonstrating the immediate colorimetric change by reacting neat viscous dithiophosphonic acid (left) with solid $\text{NiCl}_2 \cdot 6\text{H}_2\text{O}$ (green, not shown), followed by gentle grinding resulting in the distinct purple coloured $[\text{Ni}\{\text{S}_2\text{P}(\text{OR})(4\text{-MeOC}_6\text{H}_4)\}_2]$ complexes forming within seconds (right).



Scheme 2.3. A synthetic method for the formation of Ni(II) complexes (representative scheme).

Again, as is the case for the acids, we propose mechanochemical synthesis for this system had been overlooked due to the preconceived notion that the reaction always requires a solvent. For example in 1997, Verani and co-workers reported²⁵ a number of $[\text{Ni}\{\text{S}_2\text{P}(\text{OR})(4\text{-MeOC}_6\text{H}_4)\}_2]$ ($\text{R} = \text{Me}, \text{Et}, \text{}^i\text{Pr}$) complexes similar to those in the present study. A typical synthesis started in a favorable green manner by adding equivalent amounts of nickel(II) chloride and **LR** but then turned conventional by suspending the solids in a huge excess (100 mL) of the appropriate alcohol, ROH. The stirred reaction mixture was refluxed for 1–3 h, then filtered and the solvent was removed under vacuum. In the present study, we hope to demonstrate the excess alcohol is not required, thus negating additional reflux, filtration, and solvent and waste removal steps.

We are aware of only two examples where Ni(II) had previously been used in a solvent-free system for any ligand, the one was obtained by mechanochemical and the other by thermochemical means. The use of dimethylglyoxime (H_2dmg) as a chelating agent for the gravimetric analysis of Ni(II) was discovered by Tschugaeff in 1905.²⁶ Yet the mechanochemical preparation of $[\text{Ni}(\text{Hdmg})_2]$ and $[\text{Ni}(\text{H}_2\text{dmg})_2]^{2+}$ from nickel halides and H_2dmg was only reported a century later.²⁷ Thermochemical work by Fabrizzi and co-workers focused²⁸ on a nickel(II) bis(diamine) complex having a pink-red nitro isomer and a blue coloured nitrito isomer. The facile reversible thermally induced nitro–nitrito interconversion for the design of thermochromic devices was studied.

2.2.3 Characterization

This study reports the first series of characterized dithiophosphonic acids by green methods. Due to the viscous nature of the acids, we did not attempt to measure the boiling points. The melting points for the Ni(II), Cd(II) and Zn(II) complexes were determined and complexes **7** and **8** were within 1°C from identical complexes previously reported.²⁵ Together with satisfactory elemental analysis (see **Table 2.1**) bulk purity was satisfactory. The melting point for complex **6** differed substantially from the literature value,²⁵ but bulk purity was established based on elemental analysis and NMR results which negated the possibility of

solvated molecules present in the as-prepared crystal structure. Complex **5** has no precedent with 2 water hydrate molecules; there are related complexes reported with THF solvates, and with much higher melting points. Electrospray ionization (negative) mass spectrometry (EI-MS) results were obtained for the acids. The EI- mass spectrum for acid **1** showed a peak at m/z 218 corresponding to $[(1-H)^+]$, 15%. For acid **2** a peak at m/z 232 corresponded to $[(2-H)^+]$, 100%. Acid **3** is the only product that did not show an $(M-H)^+$ peak at expected m/z 246, but instead a peak at m/z 232 corresponding to the replacement of an S by an O atom either before or during the experiment, $[(3-H-S+O)^+]$ or $[(3-H-O)^+]$ while for acid **4** there was a peak at m/z 261 corresponding to $[(4-H)^+]$, 65%. It was further noted that all acids **1-4** showed a peak at m/z 232.98 of significant intensity, including **1**, which has a formula weight below 232. This peak could not be assigned with accuracy but presumably, derives from a hydrolysis or oxidation (or both) event either before or during the experiment, see NMR results for further discussion. In the 1H NMR, the S-H peaks for the acids **1-4** are the only peculiarity to point out. There are other reports where the S-H proton for acids of the related dithiophosphates are not observed or recorded.²⁹ The S-H proton was observed for **1** at δ (ppm) = 1.76 and for **2** at δ (ppm) = 3.41 whilst no S-H peaks were observed for **3** and **4**. Note the distinct upfield shift for **1** compared to **2**; a similar effect was observed for the corresponding complexes **5** and **6** in the ^{31}P NMR, see below. We nevertheless substituted H_2O for D_2O (**1**) and MeOH for CD_3OD (**2**) and noted the previously observed S-H protons have now both disappeared. The ^{31}P NMR spectra of all the acids show singlet peaks in the range 74 to 89 ppm, but this requires a cautionary note. Initially, we made no attempt to keep the reaction in an inert environment because it was reasoned that the product forms rapidly and there is not sufficient time for side-products to form. But the ^{31}P NMR spectrum for each acid we obtained, under those circumstances, showed two singlet peaks *ca.* >10 ppm apart, with the upfield peak of lesser intensity but growing more intense over time, and with further peaks also developing upfield over time. The formed acids are racemic mixtures of (*R*) and (*S*) chiral enantiomers, and as such, they cannot be differentiated by NMR, **Figure 2.4**. No attempt was made to separate the enantiomers of the racemic mixture. It became clear that additional by-products formed. The appearance of the by-products (see below)

could be explained, but it should be pointed out the by-products can easily be avoided by keeping the whole system continuously under an inert atmosphere.

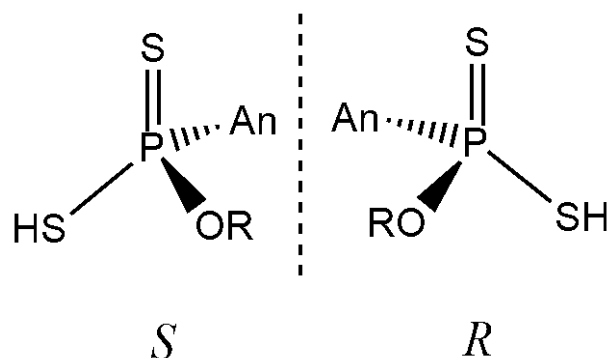


Figure 2.4. The products formed are a racemic mixture of S and R chiral enantiomers of dithiophosphonic acids. An = anisoyl

What was observed with regards to by-product formation was akin to a reported series of elegant hydrolysis studies performed by Burn et al.³⁰⁻³² more than 2 decades ago. They followed the mechanistic and kinetic hydrolysis pathway (by ³¹P NMR) of the zinc(II) dithiophosphate [Zn{S₂P(OEt)₂}]₂ in 10-fold water excess and at 85°C, and could monitor the replacement of S atoms by O atoms, as well as C-O bond cleavage, giving rise to sequential higher upfield shifts, right to the final hydrolysis product, H₃PO₄, at 0 ppm. It is clear from those studies that the ultimate fate of possibly all phosphor-1,1-dithiolate acids, salts, and complexes, in the presence of moisture (hydrolysis) and oxygen (oxidation), is phosphoric acid, but this can be well avoided by excluding both H₂O and O₂ from the system. The ³¹P NMR of the Ni(II) complexes showed singlet peaks for both [Ni{S₂P(OH)(4-MeOC₆H₄)}]₂ **5** at 58.12 ppm and for [Ni{S₂P(OCH₃)(4-MeOC₆H₄)}]₂ **6** at 104.40 ppm; a remarkable difference of 46 ppm between seemingly closely related complexes, see **Figure 2.5**. The resonance peak for **5** is in close agreement to the complex [Ni{S₂P(OH)(4-MeOC₆H₄)}]₂(THF)₂ reported by Rothenberger and co-workers, but in their case they found two resonance peaks at δ (ppm) = 42.3 and 56.9 that they assign to partial decomposition, this study only found one peak. It should also be pointed out that the heavily solvated tetranuclear Ni(II) complex [Ni₂{AnP(O)S₂}]₂(THF)₂(H₂O)₂ had a ³¹P NMR resonance peak at 56.1 ppm.³³

Table 2.1. Yield, melting points, EI-MS, ^{31}P NMR and elemental analyses data for **1-16**.

Entry	% Yield	m.p.(°C)	EI-MS	^{31}P NMR	Elem. anal. /%	
					H	C
1 ^a	98	liquid	218 [(M-H)+ 5%]	74.1	N/O	N/O
2	98	liquid	232 [(M-H)+100%]	89.5	N/O	N/O
3	99	liquid	232 [(M-H-O)+ 100%]	86.4(102.9) ^h	N/O	N/O
4	98	liquid	261 [(M-H)+ 65%]	84.2 / 84.3 ^c	N/O	N/O
5 ^b	96	125 (N/A) ^d	N/O	58.1 (56.1) ^e	3.55 (3.24)	32.91(33.82)
6	96	160 (184) ^f	N/O	104.4(105.7) ^g	3.77 (3.84)	36.65 (36.59)
7	97	130 (131) ^f	N/O	101.9(102.2) ^g	4.29 (4.37)	39.12 (39.08)
8	97	167 (168) ^f	N/O	97.7 (99.1) ^g	4.82 (4.85)	41.39 (41.32)
9	97	131 (N/A)	N/O	57.1	3.67(3.20)	33.12 (33.37)
10	98	169 (N/A)	N/O	103.04(105.1) ^h	3.85 (3.79)	35.99 (36.13)
11	94	176 (N/A)	N/O	99.7(101.3) ^h	4.21 (4.32)	38.52 (38.61)
12	93	171 (N/A)	N/O	98.8. (98.5) ^h	4.72 (4.80)	39.98 (40.85)
13	95	166(N/A)	N/O	59.7	3.03 (2.93)	30.12 (30.52)
14	97	156(N/A)	N/O	86.9(109.8) ^h	3.29 (3.48)	33.02 (33.19)
15	96	162(N/A)	N/O	84.3(106.5) ^h	4.02 (3.99)	36.12 (35.62)
16	95	156(N/A)	N/O	86.5(104.0) ^h	4.28 (4.44)	38.01 (37.83)

Key to table: N/O = not obtained. a = all four acids (**1-4**) are viscous colourless liquids; b = all four Ni complexes (**5-8**) are purple solids; c = in *d*₆-DMSO; d = m.p. for related THF solvated $[\text{Ni}\{\text{S}_2\text{P}(\text{OH})(4\text{-MeOC}_6\text{H}_4)\}_2(\text{THF})_2]$ and $[\text{Ni}\{\text{S}_2\text{P}(\text{OH})(4\text{-MeOC}_6\text{H}_4)\}_2(\text{THF})_4]$ is 195 (decomp.) and 250°C (decomp.), respectively, after ref. 38; e = $[\text{Ni}_2\{\text{AnP}(\text{O})\text{S}_2\}_2(\text{THF})_2(\text{H}_2\text{O})_2]_2 = 56.1$ ppm (An = anisoyl), after ref. 43 ; f = after ref. 34; g = after ref. 44; h = after ref. 35

The ^{31}P NMR of the Zn(II) complexes share a very close chemical shift with reported values by Woollins and co-workers³⁵ though the ^{31}P NMR for Cd(II) complexes were not very close, their other properties are similar to what is found in the literature.

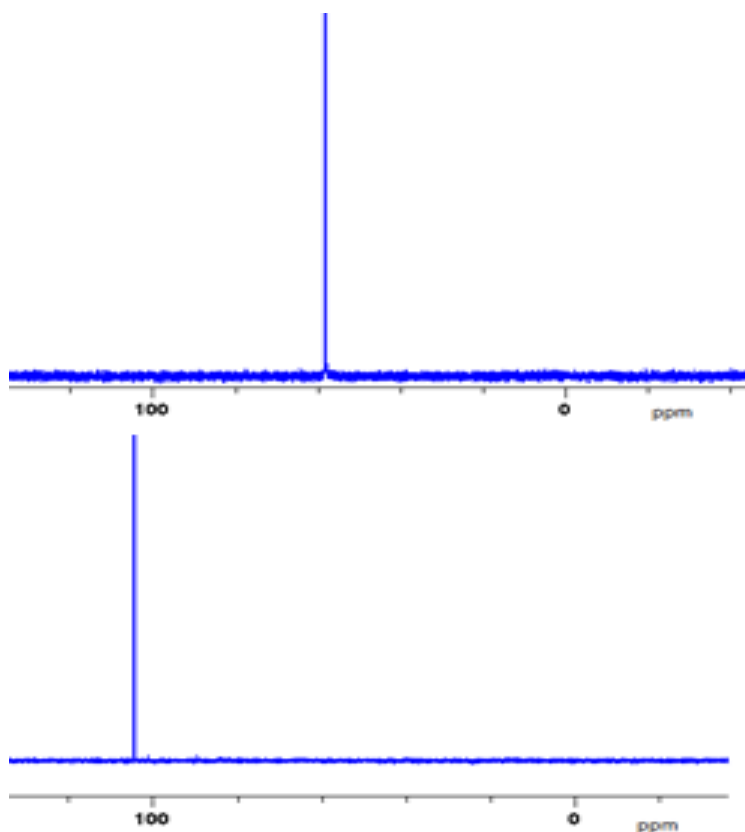


Figure 2.5. The ^{31}P NMR spectrums of $[\text{Ni}\{\text{S}_2\text{P}(\text{OH})(4\text{-MeOC}_6\text{H}_4)\}_2]$ **5** and $[\text{Ni}\{\text{S}_2\text{P}(\text{OCH}_3)(4\text{-MeOC}_6\text{H}_4)\}_2]$ **6** showing singlet peaks at 58.12 and 104.40 ppm, respectively. Note the large shift of 46 ppm for two closely related derivatives.

2.2.3.1 Crystal structure

Although complex **5** was obtained in high yield and had a singlet ^{31}P NMR peak closely related to similar compounds (above), the as-prepared material had an unsatisfactory elemental analysis, and we suspected the presence of solvate, **Table 2.1**. This was indeed confirmed through X-ray studies of the complex. The starting $\text{NiCl}_2 \cdot 6\text{H}_2\text{O}$ (0.5 g) leads to 12.62 mmol of free water (*ca.* 0.23 mL) upon reaction with the acid ligand. This is a sufficient volume to already wet all generated powder of the product, and only requires a few additional drops of water to partly solubilize the complex. Amongst all the complexes **5-16** formed,

complex **5**, **9** and **13** were by far the most soluble in water. X-ray quality single crystals of **5** grew from the solution upon slow evaporation of the solvent. This is the first example of a decidedly ‘green structure’ for any Ni(II) dithiophosphonate complex reported to date, containing only hydrated waters, all others solvated structures contain organic molecules, especially THF. The structure is shown in **Figure 2.6**, together with 2 hydrated water molecules. The molecular structure is unsurprising, containing a 4-coordinate, slightly distorted square-planar geometry around the Ni(II) center with water solvate. The bond lengths and angles are comparable with related structures and the P-OH groups are in a trans orientation with respect to each other, generated by the Ni atom that acts as a crystallographic inversion center. Details of the X-ray data is shown in **Table 2.2**.

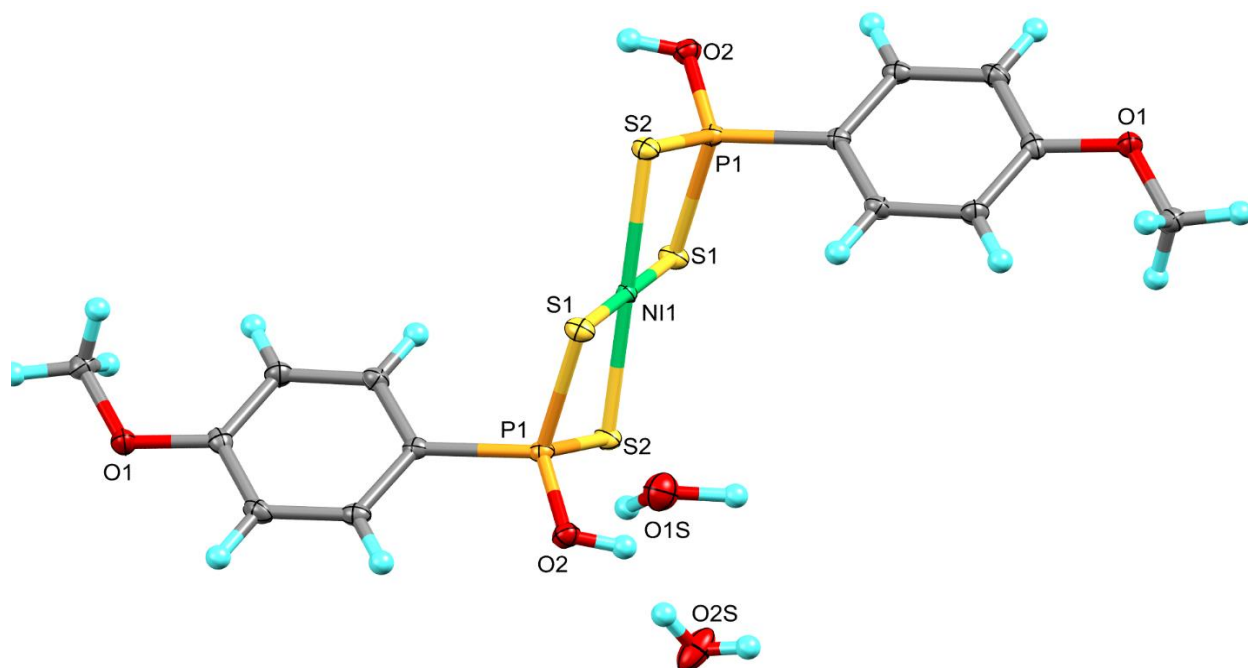


Figure 2.6. ORTEP molecular structure of Ni(II) complex **5**. Notice the two hydrated water molecules

Table 2.2: Selected bond lengths (Å) and angles (°)

Bond lengths (Å)		Bond angles (°)	
O(2)-P(1)	1.511(3)	C(1)-P(1)-S(2)	107.63(11)
P(1)-S(1)	2.0434(11)	O(2)-P(1)-C(1)	109.88(15)
P(1)-S(2)	2.0429(11)	O(2)-P(1)-S(1)	115.62(11)
S(1)-Ni(1)	2.2134(8)	O(2)-P(1)-S(2)	116.33(11)
S(2)-Ni(1)	2.2192(8)	S(2)-P(1)-S(1)	98.90(5)
Ni(1)-S(2a)	2.2192(8)	P(1)-S(1)-Ni(1)	85.05(4)
C(1)-P(1)	1.802(3)	S(1)-Ni(1)-S(1a)	180
		S(1)-Ni(1)-S(2)	88.93(3)

Table 2.3. Crystal data and structure refinement of **5**.

Empirical formula	C ₁₄ H ₁₆ NiO ₄ P ₂ S ₄ ·2H ₂ O
Formula weight	533.21
Temperature/K	100(2)
Crystal system	Monoclinic
Space group	C2/c
a/Å	23.7087(15)
b/Å	7.4340(4)
c/Å	13.4003(7)
α/°	90
β/°	105.507(4)
γ/°	90
Volume/Å ³	2275.8(2)
Z	4
μ/mm ¹	1.398
F(000)	1168.0
Crystal size/mm ³	0.432 × 0.256 × 0.106
Radiation	MoKα (λ = 0.71073)
2θ range for data collection/°	3.566 to 57.028
Index ranges	-31 ≤ h ≤ 31, -9 ≤ k ≤ 9, -17 ≤ l ≤ 17
Reflections collected	21960
Independent reflections	2888 [Rint = 0.029]
Data/restraints/parameters	2888/2/150
Goodness-of-fit on F ²	1.031
Final R indexes [I ≥ 2σ (I)]	R1 = 0.0506, wR2 = 0.1349
Final R indexes [all data]	R1 = 0.0524, wR2 = 0.1365
Largest diff. peak/hole / e Å ⁻³	1.71/-0.78

2.2.3.2 Solubility

Although this thesis describes solvent-free methods to form acids and corresponding complexes, knowledge about the solubility of compounds, especially to choose the appropriate solvent for spectroscopic measurements, or generally where mechanochemical methods are not possible, is often useful. To this end, a series of qualitative solubility tests were performed on all the compounds, **1-16**. Results are shown in

Table 2.4

Table 2.4. Solubility Data for Compounds **1-16**

Entry	Acetone	CH ₃ CN	EtOH	Hexane	Ether	CH ₂ Cl ₂	Water	THF
1	I	S	VS	I	PS	PS	VS	S
2	I	S	VS	I	PS	PS	S	S
3	I	I	VS	I	PS	PS	VS	S
4	I	S	VS	I	PS	PS	S	S
5	PS	I	PS	I	PS	S	S	VS
6	PS	I	PS	I	PS	VS	I	VS
7	PS	I	PS	I	PS	VS	I	VS
8	PS	I	PS	I	PS	VS	I	VS
9	PS	I	PS	I	PS	VS	S	VS
10	PS	I	PS	I	PS	VS	I	VS
11	PS	I	PS	I	PS	VS	I	VS
12	PS	I	PS	I	PS	VS	I	VS
13	PS	I	PS	I	PS	VS	S	VS
14	PS	I	PS	I	PS	VS	I	VS
15	PS	I	PS	I	PS	VS	I	VS
16	PS	I	PS	I	PS	VS	I	VS

Key to table: I = Insoluble (the material was quantitatively recovered after filtration); PS = Partly Soluble (10% of the material dissolved); S = Soluble (80% of the material dissolved); VS = Very Soluble (a clear solution emerged immediately). The solubility data is based on the following experimental criteria: 0.02 g of the compound was dissolved in 1.0 mL of the appropriate solvent and was hard shaken for 5-10 seconds at 23°C

A variety of solvents were tested over a wide range of dielectric constants, including protic/aprotic and polar/non-polar solvents. Noteworthy is for example how the acids are soluble in protic solvents such as water and ethanol, but the corresponding complexes are insoluble in those solvents.

2.3 CONCLUSIONS

The first mechanochemical synthesis procedure is described for the formation of dithiophosphonic acid derivatives by using green chemistry methods with 100% atom economy and essentially 100% atom efficiency. The procedure circumvented tedious consecutive steps such as heating, reflux, filtration, and solvent removal. In a proof-of-concept experiment, the acids were then used *in situ* to form Ni(II) dithiophosphonate complexes in high yield. The present study focuses on common alcohols in the liquid phase under ambient conditions. In future, the more challenging mechanochemical reaction where precursor alcohols are in the solid phase should be investigated.

2.4 EXPERIMENTAL

2.4.1 Method

Mechanochemical grinding was carried out in a dried and clean standard schlenk tube (~2 cm diameter) using a ball head glass rod under a blanket of nitrogen. The Schlenk line is critical for this important reactions because it requires the minimization of contact with air or other airborne contaminants.

2.4.2 Materials

Lawesson's reagent was either purchased from Aldrich or prepared from literature procedures.³⁴ All other reagents were used as purchased from Aldrich and used as received. Distilled water was used for the reaction and in all cases where water is required in this work. All other alcohols were either dried over calcium oxide or molecular sieves.

2.4.3 Characterization Methods

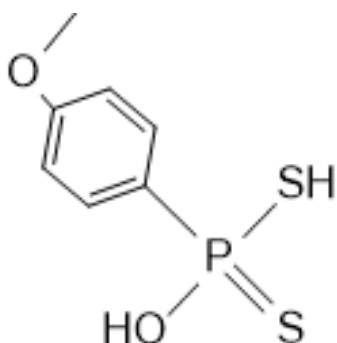
¹H and ³¹P NMR spectra were recorded on a Bruker Avance 400 MHz spectrometer. NMR data are expressed in parts per million (ppm) downfield shift referenced internally to the residual proton impurity in the deuterated solvent and are reported as chemical shift position (δ_{H}), relative integral intensity, multiplicity (s = singlet, d = doublet, t = triplet, sept = septet, and m = multiplet), coupling constant J in Hz, and assignment. ³¹P NMR spectra chemical shifts are reported relative to an 85% H₃PO₄ in D₂O external standard solution, all at 298 K. The yields were determined by performing the reaction in a dry pre-weighed Schlenk tube, weighing the sample after drying. Mass spectra were recorded with a Waters Micromass LCT Premier TOF-MS. The mode of ionization was ESI (electrospray) negative, [M-H]⁻. Samples were prepared to ~2ppm concentration in the desired solvent and infused into the mass spectrometer. Infrared spectra were recorded in the range 4000–380 cm⁻¹ on a Perkin-Elmer Spectrum 100 FT-IR spectrometer.

2.4.4 Crystallography

A crystal of complex **5**, $[\text{Ni}\{\text{S}_2\text{P}(\text{OH})(4\text{-C}_6\text{H}_4\text{-OMe})\}_2]$, with approximate dimensions 0.106 mm x 0.256 mm x 0.432 mm, was mounted on a glass fibre with epoxy resin. All intensity and geometric data were collected on a Bruker APEXII CCD diffractometer equipped with a graphite monochromated Mo-K α radiation ($\lambda = 0.71073 \text{ \AA}$). APEXII software was used for preliminary determination of the unit cell.³⁵ Determination of integrated intensities and unit cell refinement were performed using SAINT.³⁶ The SADABS program was used to apply an empirical absorption correction³⁷. The integration of the data yielded a total of 21960 reflections to a maximum θ angle of 28.51° (0.74 \AA resolution). XPREP determined the space group to be C 2/c, with $Z = 4$ for the formula unit, $\text{C}_{14}\text{H}_{16}\text{NiO}_4\text{P}_2\text{S}_4 \cdot 2\text{H}_2\text{O}$.³⁹ The structure was solved with XS⁴⁰ and subsequent structure refinements were performed with XL.⁴¹ A complete listing of crystallographic data and parameters are reported in **Table 2.3**

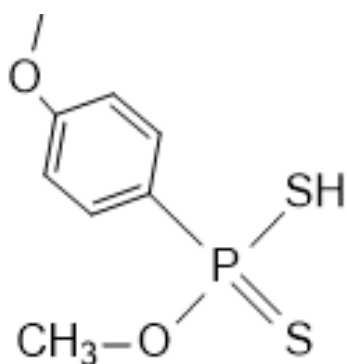
2.4.5 Ligand synthesis

Hydroxy-4-methoxyphenyldithiophosphonic acid (1)

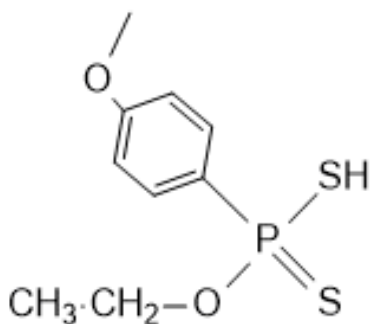


Lawesson's Reagent (1.0 g, 2.48 mmol) was placed in a clean and oven dried Schlenk tube, and distilled water (0.1 mL, 4.90 mmol) was added. The reactants were ground together for 15 minutes under dried inert gas (N_2). This derivative took the longest to complete the reaction compared to other alcohols that took <5 minutes. A viscous liquid formed. (1.06 g, 98.6 %). ^{31}P NMR ($CDCl_3$) δ : 74.13, 1H NMR ($CDCl_3$) δ : 1.76 (1H, s, SH), 3.71 (3H, s, ArOMe), 6.83 (2H, dd, $^4J_{PH}$ 2.62 Hz, $^3J_{HH}$ 9.0 Hz, *m*-ArH), 7.51 (1H, s, OH), 7.78 (2H, dd, $^3J_{PH}$ 13.8 Hz, $^3J_{HH}$ 9.0 Hz, *o*-ArH). Selected FT-IR (4000–350 cm^{-1}): 2945(m), 2305 (b), 1595 (s), 1501 (s), 1256 (s), 1120 (s), 1023(s), 892(b), 803 (w), 612 (w) 526 (m).

(Methoxy)-4-methoxyphenyldithiophosphonic acid (2)

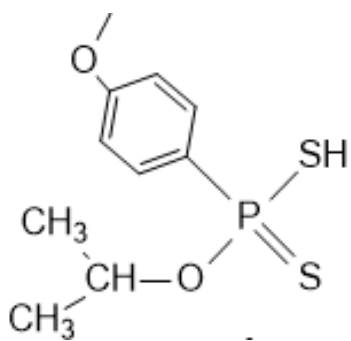


To a clean and oven dried Schlenk tube, Lawesson's Reagent (1.00 g, 2.48 mmol) and methanol (0.2 mL, 4.9 mmol) was added. The reactants were ground together in the dried schlenk tube for about 2 minutes with a pestle-like glass rod. A viscous liquid resulted. (1.14 g, 98.5 %). ^{31}P NMR ($CDCl_3$) δ : 89.54. 1H NMR ($CDCl_3$) δ : 3.41 (1H, s, SH), 3.81 (3H, d, $^2J_{HH}$ 8.7 Hz, CH_3), 3.85 (3H, s, ArOMe), 6.92 (2H, dd, $^4J_{PH}$ 3.51 Hz, $^3J_{HH}$ 9.0 Hz, *m*-ArH), 7.88 (2H, dd, $^3J_{PH}$ 14.4 Hz, $^3J_{HH}$ 9.0 Hz, *o*-ArH). Selected FT-IR (4000-350 cm^{-1}): 2941 (m), 2433 (b), 1593 (s), 1498 (s), 1256 (s), 1114 (s), 827 (w), 679 (s) 530 (m).

(Ethoxy)-4-methoxyphenyldithiophosphonic acid (3)

To Lawesson's Reagent (1.00 g, 2.48mmol) in a clean and dried Schlenk tube, ethanol (0.3 mL, 4.9 mmol) was added. The reactants were ground together for 3 minutes until a viscous liquid formed. (1.21g, 98.90%). ^{31}P NMR (CDCl_3) δ : 86.56. ^1H NMR (CDCl_3) δ : 1.36 (3H, t, $^3J_{\text{HH}}$ 7.1 Hz, CH_3), 3.78 (3H, s, ArOMe), 4.25 (2H, m, $^3J_{\text{HH}}$ 7.2 Hz, CH_2), 6.92 (2H, dd, $^4J_{\text{PH}}$ 3.3 Hz, $^3J_{\text{HH}}$ 9.0

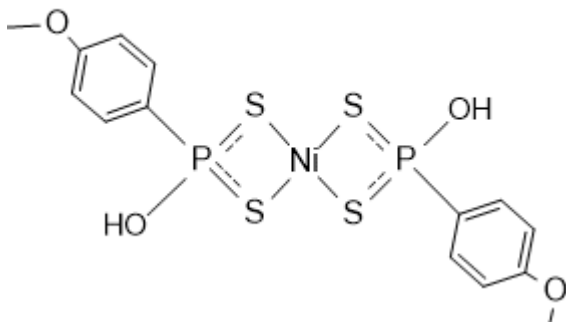
Hz, *m*-ArH), 7.88 (2H, dd, $^3J_{\text{PH}}$ 14.67 Hz, $^3J_{\text{HH}}$ 9.0 Hz, *o*-ArH). Selected FT-IR (4000-350 cm^{-1}):2941 (m), 2433 (b), 1593 (s), 1498.84(s), 1256 (s), 1114 (s), 827 (w), 679 (s) 530.65(m).

Bis (Isopropoxy)-4-methoxyphenyldithiophosphonic acid (4)

To Lawesson's reagent (1.00 g, 2.48 mmol) in a clean and oven dried Schlenk tube with pestle-like glass rod, dried isopropanol (0.4 mL, 4.9 mmol) was added. The reactants were ground together for 3 minutes until viscous liquid formed. (1.27g, 98.7%). ^{31}P NMR (CDCl_3) δ : 84.32. ^1H NMR (CDCl_3) δ : 1.40 (6H, d, $^3J_{\text{HH}}$ 6.0 Hz), 3.82 (3H, s, ArOMe), 5.08 (1H, sept, $^3J_{\text{HH}}$ 6.4 Hz, CH), 6.95 (2H, d, $^3J_{\text{HH}}$

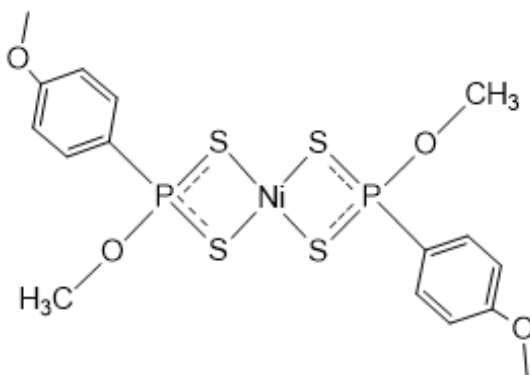
9.0 Hz, *m*-ArH), 7.90 (2H, dd, $^3J_{\text{PH}}$ 14.61 Hz, $^3J_{\text{HH}}$ 9.0 Hz, *o*-ArH). Selected FT-IR (4000–350 cm^{-1}): 2977(m), 2434 (b), 1595 (s), 1499 (s), 1255 (s), 1111 (s), 961(m) , 828(m), 617(s) 530 (m).

2.4.6 Metal Complex Synthesis



Non-green route: Ammonia gas was bubbled into compound **1** (1.00g, 4.54 mmol) and $\text{NiCl}_2 \cdot 6\text{H}_2\text{O}$ (0.45 g, 1.92 mmol) was added and ground together for 5 minutes. The immediate formation of a purple complex resulted.

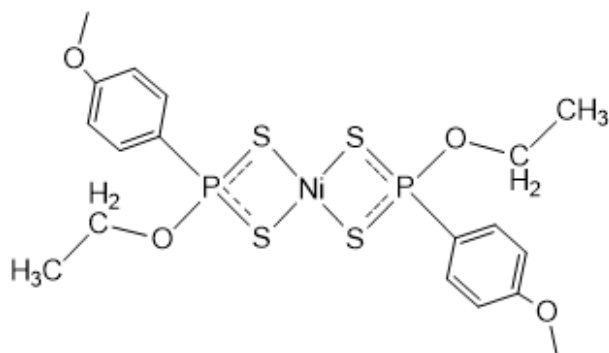
Green route: Solid $\text{NiCl}_2 \cdot 6\text{H}_2\text{O}$ (0.45 g, 1.92 mmol) was added to acid **1** (1.0 g, 4.54 mmol) and ground together for 5 minutes. The complex was dried under vacuum to give a purple solid (1.09 g, 96.3%) which was crystallized by slow evaporation from small amounts of water to give purple colored X-ray quality crystals. ^{31}P NMR (DMSO) δ : 58.12. ^1H -NMR (DMSO) δ : 3.80 (3H, s, ArOMe), 6.95 (1H, d, $J = 8.00, 19.3$ Hz, m-ArH), 8.25 (1H, d, $J=8.00, 17.5$ Hz, o-ArH). Selected FT-IR (4000–350 cm^{-1}): 3109 (m), 2559 (b), 1593 (s), 1499 (s), 1260 (s), 1113 (s), 1028(s), 937(s), 800 (w), 768(s) 619 (s) 546 (s)



A mixture of $\text{NiCl}_2 \cdot 6\text{H}_2\text{O}$ (0.50 g, 2.13 mmol) and viscous acid **2** (1.00g, 4.30 mmol) were ground together and an immediate purple complex resulted. The complex precipitated upon addition of water and was then filtered under vacuum to give a dry purple solid (1.08 g, 96.8 %). ^{31}P NMR (CDCl_3) δ : 104.4. ^1H

NMR (CDCl_3) δ : 3.87 (3H, s, ArOMe), 3.99 (3H, d, $J = 14.77$ Hz, CH_3), 7.00 (2H, d, $J=5.92$ Hz, m-ArH), 7.99 (2H, d, $J=5.92$ Hz, o-ArH). Selected FT-IR (4000-350 cm^{-1}): 2968 (m), 2292 (b), 1593 (s), 1501 (s), 1259 (s), 1116 (s), 962.38(b), 827 (w), 616 (s) 549 (s).

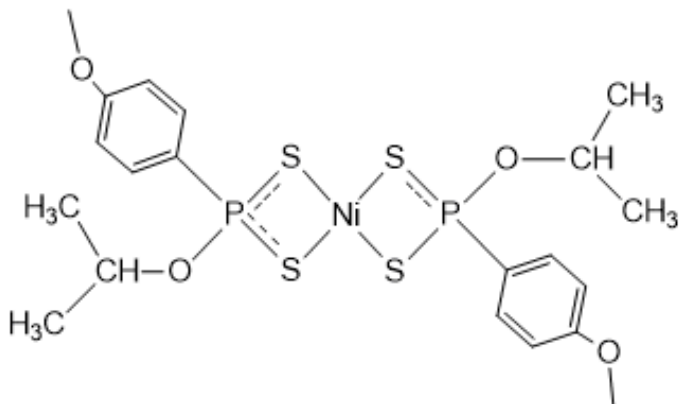
[Ni {S₂P(OEt)(4-C₆H₄-OMe)}₂] (7)



A mixture of NiCl₂ · 6H₂O (0.48 g, 2.02 mmol) and viscous acid **3** (1.00 g, 4.0 mmol) was ground and an immediate purple complex resulted. Workup was performed as for **6** above. Dry purple solid (1.09 g, 97.8 %). ³¹P NMR (CDCl₃) δ: 100.9. ¹H NMR (CDCl₃) δ: 1.35 (3H,

t, J = 7.06 Hz, CH₃), 3.8 (3H, s, ArOMe), 4.29 (2H, d, J = 17.13 Hz, CH₂), 6.97 (1H, d, J = 8.72 Hz, m-ArH), 7.91 (1H, dd, J=8.72, Hz, o-ArH). Selected FT-IR (4000-350cm⁻¹): 2971 (m), 2288 (b), 1593 (s), 1498 (s), 1257 (s), 1112 (s), 1020 (s), 800 (m), 616 (s) 551 (s).

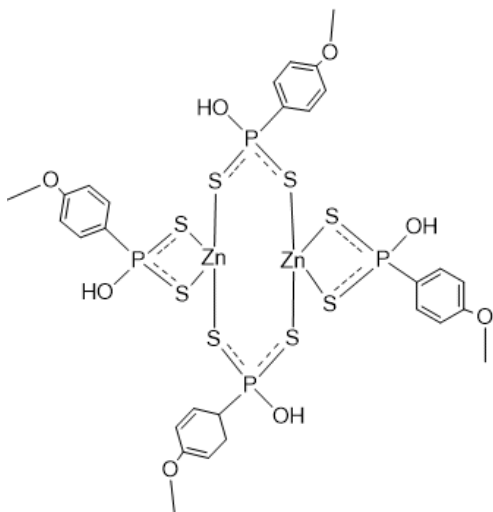
Ni{S₂P(OiPr)(4-C₆H₄-OMe)}₂] (8)



A mixture of NiCl₂ · 6H₂O (0.45 g, 1.92 mmol) and viscous acid **4** (1.00g, 3.8 mmol) were ground together and an immediate purple complex resulted. Workup was performed as for **6** above. Dry purple solid (1.07g, 96.7%). ³¹P NMR

(CDCl₃) δ: 97.8. ¹H NMR (CDCl₃) δ: 1.41 (6H, d, J=6.16 Hz, (CH₃)₂), 3.81(s, 3H, ArOMe), 5.22 (1H, d, J=1.20 Hz, CH), 7.00 (1H, d, J=5.84 Hz, m-ArH), 8.01 (1H, d, J=5.84 Hz, o-ArH). Selected FT-IR (4000–350 cm⁻¹): 2967(m), 2274 (b), 1593 (s), 1501 (s), 1260 (s), 1116 (s), 1023(s), 959(m), 800 (w), 616 (s) 550 (m)

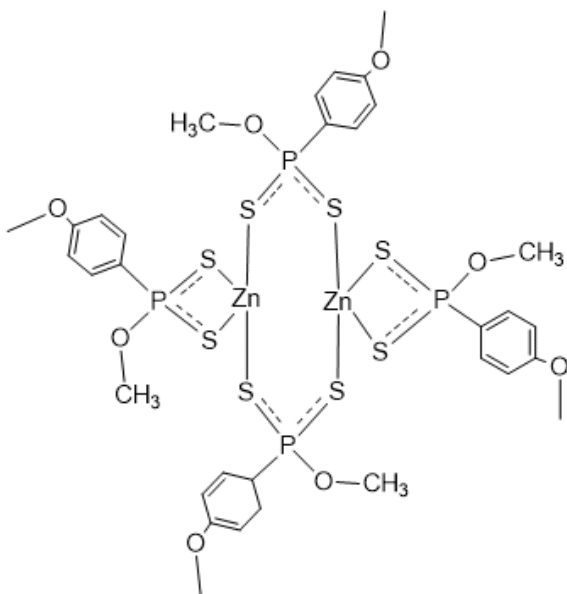
[Zn {S₂P(OH)(4-C₆H₄-OMe)}₂], (9)



3109(m), 2044 (b), 1593 (s), 1499 (s), 1253 (s), 1119 (s), 1080(s), 818(s), 668(s) 559 (s)

Solid Zn (O₂CCH₃).2H₂O (0.50 g, 2.27 mmol) was added to acid **1** (1.00g, 4.54 mmol) and were ground together for few minutes. An immediate white complex resulted. The complex precipitated upon addition of water was dried under vacuum to give a white solid (1.12g, 97.1%).³¹P NMR (DMSO) δ: 56.98, ¹H-NMR (DMSO) δ: 3.79 (s, 3H, ArOMe), 6.95 (1H, d, J=8.58 Hz, m-ArH), 7.67 (1H, d, J=8.58,Hz, o-ArH). Selected FT-IR (4000–350 cm⁻¹):

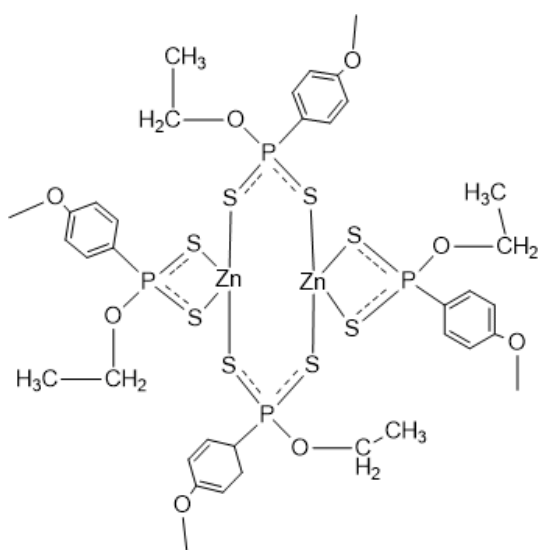
[Zn {S₂P(OMe)(4-C₆H₄-OMe)}₂], (10)



1113 (s), 1017 (b), 827 (w), 651 (s) 537 (s).

A mixture of Zn(OAc)₂.2H₂O (0.47 g, 2.14 mmol) and viscous acid **2** (1.00 g, 4.30 mmol) were ground together and an immediate white complex resulted. Workup was performed as for **6** above. Dry white solid (1.11g, 98.1%).³¹P NMR (CDCl₃) δ: 103.04. ¹H-NMR (CDCl₃) δ: 3.87 (3H, s, ArOMe), 3.94 (3H, d, J=15.57 Hz, CH₃), 6.99 (2H, d, J=8.76 Hz, m-ArH), 7.98 (1H, dd, J=8.76, Hz, o-ArH). Selected FT-IR (4000-350 cm⁻¹):2836 (m), 2563 (b), 1592 (s), 1498 (s), 1255 (s),

[Zn{S₂P(OEt)(4-C₆H₄-OMe)}₂] (11)

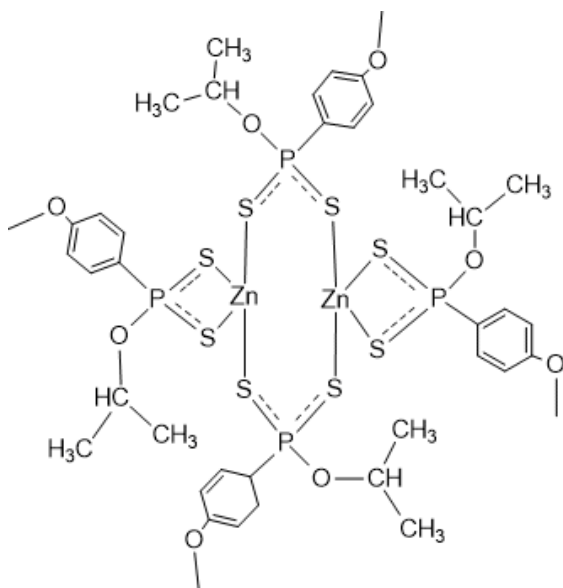


A mixture of Zn(OAc)₂·2H₂O (0.44 g, 2.00 mmol) and viscous acid **3** (1.00 g, 4.00mmol) were ground together and an immediate white complex resulted.

Workup was performed as for **6** above. Dry white solid (1.05g,93.5%). ³¹P NMR (CDCl₃) δ: 99.7. ¹H-NMR (CDCl₃) δ: 1.42 (3H, t, J=7.04 Hz, CH₃), 3.81(s, 3H, ArOMe), 4.35 (1H, d, J=2.60 Hz, CH), 6.98 (1H, d, J= 8.78 Hz, m-ArH), 7.98 (1H, d, J=8.78 Hz, o-ArH). Selected FT-IR (4000-350 cm⁻¹):

2927.28(m), 2561 (b), 1592 (s), 1499 (s), 1256 (s), 1108 (s), 1019 (vs.), 802 (m), 772 (m) 651 (s), 619 (s) 536 (s).

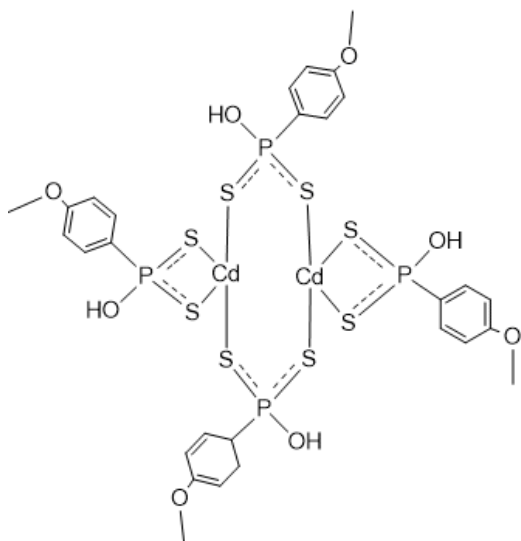
[Zn{S₂P(OiPr)(4-C₆H₄-OMe)}₂] (12)



A mixture of Zn(OAc)₂·2H₂O (0.42 g, 1.92 mmol) and viscous acid **4** (1.00 g, 3.8 mmol) were ground together and an immediate white complex resulted. Workup was performed as for **6** above. Dry white solid (1.01g, 90.4%).³¹P NMR (CDCl₃) δ: 96.6. ¹H-NMR (CDCl₃) δ: 1.45 (1H, d, J=6.16 Hz, (CH₃)₂), 3.81(s, 3H, ArOMe), 5.15 (1H, d, J=2.24 Hz, CH), 6.98 (1H, dd, J=8.76 Hz, m-ArH), 7.97 (1H, dd, J=8.78, Hz, o-ArH). Selected FT-IR (4000–350 cm⁻¹): 2975(m), 2058 (b), 1593 (s), 1498 (s), 1253 (s), 1110 (s), 1099(s), 959(m), 828 (s),

618 (s) 536 (m)

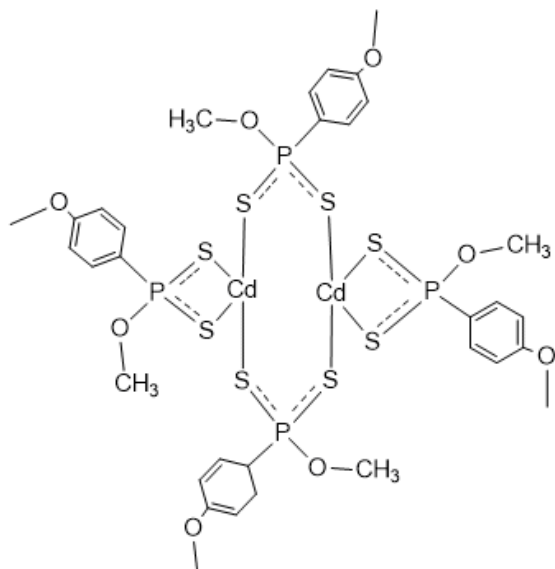
[Cd {S₂P(OH)(4-C₆H₄-OMe)}₂], (13)



(m)

A mixture of CdCl₂·2H₂O (0.50 g, 2.27 mmol) and viscous acid **1** (1.00g, 4.54 mmol) were ground together and an immediate white complex resulted. Workup was performed as for **6** above. Dry white solid (1.18g, 95.1%). ³¹P NMR (CDCl₃) δ: 89.67. ¹H-NMR (CDCl₃) δ: 3.32(s, 3H, ArOMe), 6.37 (1H, dd, J=8.76 Hz, m-ArH), 7.45 (1H, dd, J=8.78, 14.71 Hz, o-ArH). Selected FT-IR (4000–350 cm⁻¹): 2975(m), 2058 (b), 1593 (s), 1498 (s), 1253 (s), 1110 (s), 1099(s), 959(m), 828 (s), 618 (s) 536

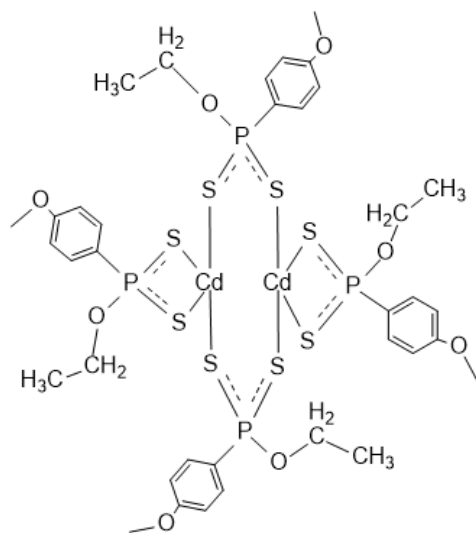
[Cd {S₂P(OMe)(4-C₆H₄-OMe)}₂], (14)



959(m), 828 (s), 618 (s) 536 (m).

A mixture of CdCl₂·2H₂O (0.47 g, 2.22 mmol) and viscous acid **2** (1.00 g, 4.30 mmol) were ground together and an immediate white complex resulted. Workup was performed as for **6** above. Dry white solid (1.20g, 95.1%). ³¹P NMR (CDCl₃) δ: 89.54. ¹H-NMR (CDCl₃) δ: 3.74(s, 3H, ArOMe), 3.92(3H, d, J=15.57 Hz, CH₃), 6.88 (1H, dd, J=8.76 Hz, m-ArH), 7.83 (1H, dd, J=8.78 Hz, o-ArH). Selected FT-IR (4000–350 cm⁻¹): 2975(m), 2058 (b), 1593 (s), 1498 (s), 1253 (s), 1110 (s), 1099(s),

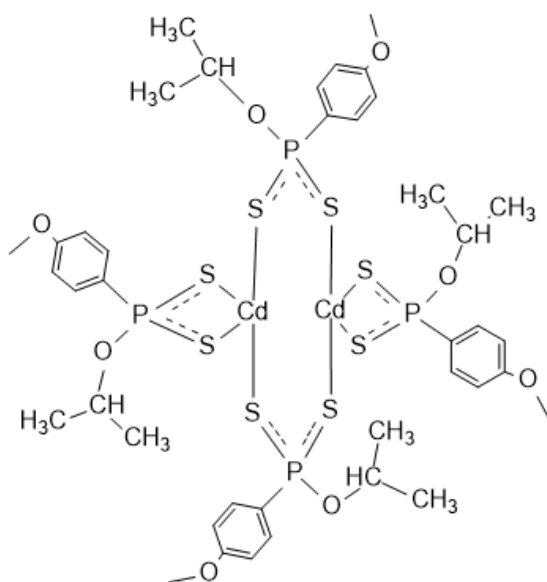
[Cd {S₂P(OEt)(4-C₆H₄-OMe)}₂], (15)



A mixture of CdCl₂·2H₂O (0.44 g, 2.00 mmol) and viscous acid **3** (1.00 g, 4.00 mmol) were ground together and an immediate white complex resulted. Workup was performed as for **6** above. Dry white solid (1.17g, 96%). ³¹P NMR (CDCl₃) δ: 84.26. ¹H-NMR (CDCl₃) δ: 1.37 (3H, m, J=7.04 Hz, CH₃), 3.79(s, 3H, ArOMe), 4.28 (1H, d, J=2.60 Hz, CH), 6.94 (1H, dd, J=8.76 Hz, m-ArH), 7.89 (1H, dd, J=8.78, 12.43 Hz, o-ArH). Selected FT-IR (4000–350 cm-

1): 2975(m), 2058 (b), 1593 (s), 1498 (s), 1253 (s), 1110 (s), 1099(s), 959(m), 828 (s), 618 (s) 536 (m)

[Cd{S₂P(OiPr)(4-C₆H₄-OMe)}₂], (16)



A mixture of CdCl₂·2H₂O (0.42 g, 1.90 mmol) and viscous acid **4** (1.00 g, 3.8 mmol) were ground together and an immediate white complex resulted. Workup was performed as for **6** above. Dry white solid (1.14g, 95%). ³¹P NMR (CDCl₃) δ: 84.28 ¹H-NMR (CDCl₃) δ: 1.37 (1H, d, J=6.16 Hz, (CH₃)₂), 3.78(s, 3H, ArOMe), 5.07 (1H, d, J=2.24 Hz, CH), 6.93 (1H, dd, J=8.76, 14.71 Hz, m-ArH), 7.88 (1H, dd, J=8.78, 15.71 Hz, o-ArH). Selected FT-IR (4000–350 cm-1):

2975(m), 2058 (b), 1593 (s), 1498 (s), 1253 (s), 1110 (s), 1099(s), 959(m), 828 (s), 618 (s) 536 (m)

2.5 REFERENCES

1. Klamann D., *Verlag-Chemie, Weinheim*, **1984**. 35-153
2. Nicholls M.A., Norton P.R., Kasrai M., Bancroft G.M., *Tribology Int.* **2005**, *38*, 15-39
3. Boyde, S., *Green Chem.* **2002**, *4* (4), 293-307.
4. Patnaik P., *A Comprehensive Guide to Hazardous Properties of Chemical Substances. John Wiley & Sons, Hoboken NJ* **2007**, *3rd edition*.
5. Bromberg, L.; Lewin, I.; Warshawsky, A., *Hydrometallurgy* **1993**, *33* (1), 59-71.
6. Martins, M. A. P.; Frizzo, C. P.; Moreira, D. N.; Buriol, L.; Machado, P., *Chem. Rev.* **2009**, *109* (9), 4140-4182.
7. Withers, P. J. A.; Elser, J. J.; Hilton, J.; Ohtake, H.; Schipper, W. J.; van Dijk, K. C., *Green Chem.* **2015**, *17* (4), 2087-2099.
8. Horvath, I. T., *Green Chem.* **2008**, *10* (10), 1024-1028.
9. DeSimone, J. M., *Science* **2002**, *297* (5582), 799-803.
10. van Zyl, W. E.; Woollins, J. D., *Coord Chem Rev* **2013**, *257*, 718-731.
11. Sewpersad, S.; Van Zyl, W. E., *Acta. Crystallogr. E* **2012**, *68* (12), m1457.
12. Haiduc, I.; Sowerby, D. B.; Lu, S.-F. *Polyhedron* **1995**, *14*, 3389-3472
13. Newallis, P. E.; Chupp, J. P.; Groenweghe, L. C. D., *J. Org. Chem.* **1962**, *27* (11), 3829-3831.
14. Chupp, J. P.; Newallis, P. E., *J. Organic Chem.* **1962**, *27* (11), 3832-3835.
15. Pederson B. S., Nilsson N. H., and S.-Lawesson, *Bull. Soc. Chim. Belg.* **1978**, *87*, 223.
16. Ozturk, T.; Ertas, E.; Mert, O., *Chem. Revi.* **2007**, *107* (11), 5210-5278.

17. Navech J., Mathieu S., Phosphorus, Sulfur, Silicon, and Relat. Elem. **1988**, *107*, 306-309.
18. Alexander B.E., Khan T.F., Maliszewski J., Perry A., Pitak M.P., Whiteman M., Wood M.E., *Nitric Oxide* **2015**, *47*, S52.
19. Van Zyl, W. E., *Comments Inorg Chem* **2010**, *31*, 13-45
20. Pillay, M. N.; van der Walt, H.; Staples, R. J.; van Zyl, W. E., *J. Organomet. Chem.* **2015**, *794*, 33-39.
21. James, S. L.; Adams, C. J.; Bolm, C.; Braga, D.; Collier, P.; Friscic, T.; Grepioni, F.; Harris, K. D. M.; Hyett, G.; Jones, W.; Krebs, A.; Mack, J.; Maini, L.; Orpen, A. G.; Parkin, I. P.; Shearouse, W. C.; Steed, J. W.; Waddell, D. C., *Chem. Soc. Rev.* **2012**, *41* (1), 413-447.
22. Friščić, T.; Jones, W., *Cryst. Growth & Design* **2009**, *9* (3), 1621-1637.
23. Paul, I. C.; Curtin, D. Y., *Acc. Chem. Res.* **1973**, *6* (7), 217-225.
24. Bala, M. D.; Coville, N. J., *J. Organomet. Chem.* **2007**, *692* (4), 709-730.
25. Arca, M.; Cornia, A.; Devillanova, F. A.; Fabretti, A. C.; Isaia, F.; Lippolis, V.; Verani, G., *Inorg.Chim.Acta* **1997**, *262* (1), 81-84.
26. Tschugaeff, L., *Ber. Dtsch. Chem. Ges.* **1905**, *38*, 2520-2522
27. Hihara, G.; Satoh, M.; Uchida, T.; Ohtsuki, F.; Miyamae, H., *Solid State Ionics* **2004**, *172* (1-4), 221-223.
28. Ansa Hortalá, M.; Fabbrizzi, L.; Foti, F.; Licchelli, M.; Poggi, A.; Zema, M., *Inorg.Chem.* **2003**, *42* (3), 664-666.
29. Guo, B.; Njardarson, J. T., *Chem. Commun.* **2013**, *49* (92), 10802-10804.

30. Burn, A. J.; Dewan, S. K.; Gosney, I.; Tan, P. S. G., *J. Chem. Society, Perkin Tran. 2* **1990**, (5), 753-758.
31. Burn, A. J.; Dewan, S. K.; Gosney, I.; Tan, P. S. G., *J. Chem. Soc., Perkin Trans. 2* **1990**, (8), 1311-1316.
32. Burn, A. J.; Gosney, I.; Warrens, C. P.; Wastle, J. P., *J. Chem. Soc., Perkin Trans. 2* **1995**, (2), 265-268.
33. Shi, W.; Shafaei-Fallah, M.; Anson, C. E.; Rothenberger, A., *Dalton Trans.* **2005**, (24), 3909-3912.
34. van Zyl, W. E.; Fackler, J. P., *Phosphorus, Sulfur, Silicon Relat Elem* **2000**, 167,117-172
35. Gray, I. P.; Slawin, A. M. Z.; Woollins, J. D., *Dalton Trans.* **2004**, (16), 2477-2486.
36. Bruker Analytical X-ray System, *Bruker AXS Inc. Madison, WI*, **2013**, *APEX2 Version 2013.1*.
37. Software for the CCD Detector System, *Bruker Analytical X-ray System, Madison, WI*, **2013**, *SAINT Version 8.32B*.
38. Sheldrick, G. M., *University of Gottingen, Gottingen, Germany* **2012**, *SADABS Version 2012/1*.
39. Sheldrick, G. M., *Acta Cryst. A64 XL Version 2013/3* **2008**, 112-122.

CHAPTER 3

SYNTHESIS OF A NEW FERROCENYL DITHIOPHOSPHONATE LIGAND AND ITS NICKEL(II), CADMIUM(II), AND ZINC(II) COMPLEXES

3.1 BACKGROUND

The chemistry of P/S heterocyclic systems will continue to attract research interest due to both their vital roles in commercial bulk materials as well as in organic synthesis.¹ Lawesson's Reagent is well known in synthetic chemistry as a thionation reagent²⁻³ and in several other applications in various sectors.⁴⁻⁹ Ferrocene is a member of the metallocene group and its chemical behaviour is similar to that of an electron rich aromatic.¹⁰ Ferrocene's reaction with P_4S_{10} was carried out to establish whether the reaction forming dithiadiphosphetane disulfides is similar to the corresponding reaction of Lawesson's reagent with anisole, i.e. ferrocenyl dithiophosphonate (FcLR).¹ Woollins and co-workers also reported the sodium salt of ferrocenyl dithiophosphonate of the type $Na[S_2P(OR)(Fc)]^{11}$ [Fc = Ferrocene, R = Me, Et and ⁱPr] and their metal complexes.¹² Metal complexes of other alcohols, including amino alcohol derivatives of ferrocenyl dithiophosphonate, has also been reported¹³⁻¹⁴ but no water derivative of ferrocenyl dithiophosphonate of the type $NH_4[S_2P(OH)(Fc)]^{11}$ and their metal complexes has been reported.

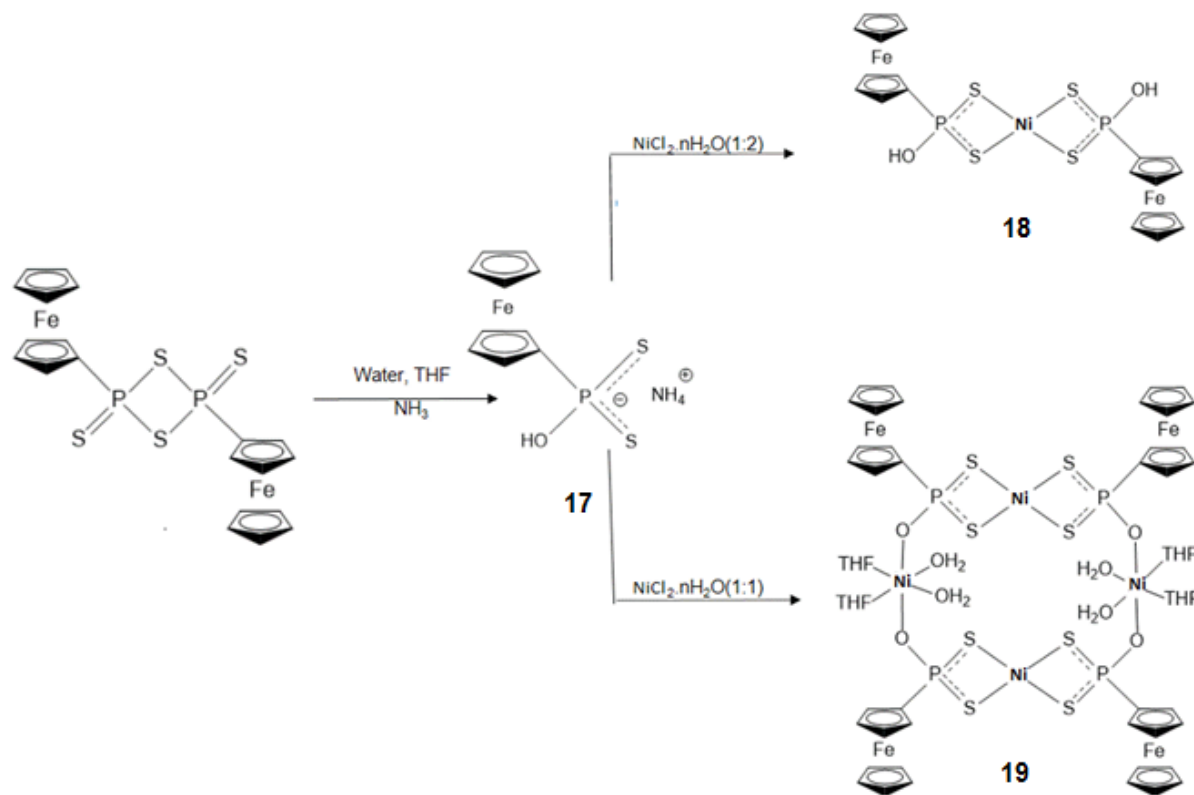
This study reports the synthesis of a new and stable ferrocenyl dithiophosphonate ammonium salt by cleavage of the dimeric structure of FcLR with water. Complexes with multimetallic and multiferrocenyl assemblies were formed with the different ligand to metal ratios and were characterized by different characterization methods including X-ray crystallography.

3.2 RESULTS AND DISCUSSION

3.2.1 Synthesis of Ligand and the Corresponding Complexes

The synthesis of Ni(II) ferrocenyl dithiophosphonate complexes obtained under different Ni:L ratios is shown in **Scheme 3.1**. The ammonium salt of the ferrocenyl dithiophosphonate ligand was prepared by bubbling ammonia into dithiophosphonic acid formed from the reaction between water and ferrocenyl Lawesson's in an equimolar ratio. FcLR undergoes a ring opening reaction allowing cleavage of the dimer and the formed ammonium salt was isolated as a bright yellow powder. Various groups of alcohols had been used for FcLR, including methanol, ethanol, and isopropanol¹² and ring opening by ammonium hydroxide have also been reported.¹⁵ Likewise, amino alcohols,¹³⁻¹⁷ as well as 4-(2, 5-di(thiophen-2-yl)-1H-pyrrol-1-yl) aniline, diacetone-d-glucose, and 2-(3-thienyl) ethanol, have all been used in the nucleophilic ring opening reaction of the FcLR reagent.¹⁸⁻¹⁹

In the present study, water was used to carry out the nucleophilic ring opening without any unwanted oxidation reaction taking place resulting in a stable ligand favourable for metal complexation. The metal complexation chemistry of ferrocenyl dithiophosphonates is scarce, with only a few complexes known.^{12, 15, 18-20}. In this study, we report the synthesis of nickel(II), cadmium(II) and zinc(II) complexes of the new hydroxy ferrocenyl dithiophosphonate ligand. The stoichiometric addition of the corresponding transition-metal salts in 2 different equimolar ratios (1:2 & 1:1) to the THF solution of the FcLR ligand gave the corresponding complexes with multimetallic and multiferrocenyl assemblies. All the compounds are air-stable with good yields, soluble in the polar solvent and partially soluble in dichloromethane, chloroform, and tetrahydrofuran.



Scheme 3.1: Synthesis Nickel(II) complexes as an example of typical ferrocenyl dithiophosphonate metal complexes in different mole ratios.

3.2.2 Characterization.

We report the first nucleophilic ring opening reaction of FcLR with water as a green solvent/reactant and its full characterized dithiophosphonate ammonium salt ligand. The melting point for the ligand occurred at 158°C and it is soluble in polar solvents such as water, methanol, and ethanol. The ^{31}P NMR spectrum of the ligand displayed a sharp singlet at 70.5 ppm. The ^1H NMR and ^{13}C NMR spectra of the compound were, as expected, confirmed by the presence of the ferrocenyl substituent. The IR spectra clearly show strong bands at 1175, 1024, 584 and 488 cm^{-1} for **17**, these can be attributed to $\nu[(\text{P})-\text{O}-\text{C}]$, $\nu[\text{P}-\text{O}-(\text{C})]$, $\nu(\text{PS})_{\text{asym}}$ and $\nu(\text{PS})_{\text{sym}}$ stretching vibrations, respectively. Mass spectrometry showed the parent ions which indicate the bulk purity of the salt and was deemed satisfactory for use in further reactions.

The metal complexes were isolated in varying yields (46–87%) as either brown, orange or yellow powder. All complexes are air stable and partially soluble in dichloromethane, chloroform, and THF and soluble in polar solvents like ethanol, methanol, and water. This seems to be a deviation from what is known for the solubility of these complexes since they usually do not dissolve in polar solvents and we propose this development may likely be due to the presence of the newly introduced hydroxyl groups on our new complexes. The ^{31}P NMR spectra of the complexes display sharp singlets, with shifts away from the corresponding free ligands, confirming complexation. The IR spectra of compounds **18-23** were similar to that of the free ligand, indicating that they were virtually unchanged by complexation and in some cases, mass spectrometry showed fragmented ion of the compounds.

3.2.2.1 Crystal structure

The complexation of metal to ligand in the molar ratio 1:2 and 1:1 gave the X-ray structures of **18** and **19** (**Figures 3.1, 3.2, Table 3.3**). Both structures show square planar geometry about the metal centre with symmetric MS_2P rings where **18** and the asymmetric unit of **19** are isomorphous. The structure of **18** displays typical *trans* arrangement where a ferrocenyl group of the ligand is arranged diagonally opposite on the metal coordination plane while on the other hand the *cis* arrangement is seen on **19** where a ferrocenyl group of each nickel complex unit in the structure are arranged on the same side of the metal coordination plane. The molecular structure of **19** is a tetranuclear Ni(II) complex containing both 4- and 6-coordination around the different Ni(II) centers and it displays multimetallic and multiferrocenyl assemblies. The two geometries are square-planar and octahedral around the nickel(II). The octahedral arrangement for each Ni(II) centre is made up of the P-O portion of the ligand (O donor atom) in the axial position, whilst the equatorial positions are occupied by 2 water molecules (positioned ‘inside’ the macrocycle, presumably due to less steric crowding), and 2 THF molecules on the ‘outside’ of the macrocycle. The water and THF chemical shifts were not detected in the NMR, these solvates presumably leak out of the structure at room temperature after a period of time, leading to a decomposed complex (the X-ray data were collected at cold temperature, 173K, trapping the solvents).

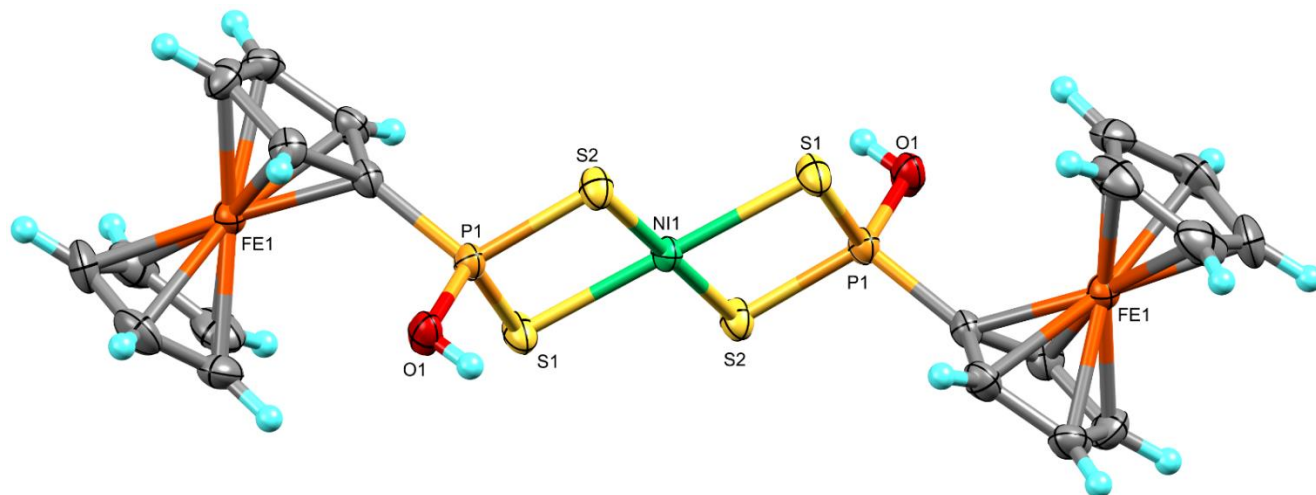


Figure 3.1: ORTEP molecular structure of complex **18**.

Table 3.1: Selected bond lengths (Å) and angles (°) for **18**

Bond lengths (Å)		Bond angles (°)	
O(1)-P(1)	1.569(2)	C(1)-P(1)-S(2)	113.17(10)
P(1)-S(1)	2.0066(11)	O(2)-P(1)-C(1)	102.70(14)
P(1)-S(2)	2.0109(11)	O(2)-P(1)-S(1)	115.46(10)
S(1)-Ni(1)	2.2338(8)	O(2)-P(1)-S(2)	112.55(9)
S(2)-Ni(1)	2.2172(8)	S(2)-P(1)-S(1)	101.05(5)
Ni(1)-S(2a)	2.2172(8)	P(1)-S(1)-Ni(1)	85.11(4)
Ni(1)-S(2b)	2.2172(8)	P(1)-S(2)-Ni(1)	85.45(3)
C(1)-P(1)	1.768(3)	S(1)-Ni(1)-S(2)	88.33(3)
		S(1)-Ni(1)-S(2a)	91.67(3)
		S(1)-Ni(1)-S(1a)	180.0
		C(1)-P(1)-S(1)	112.39(10)

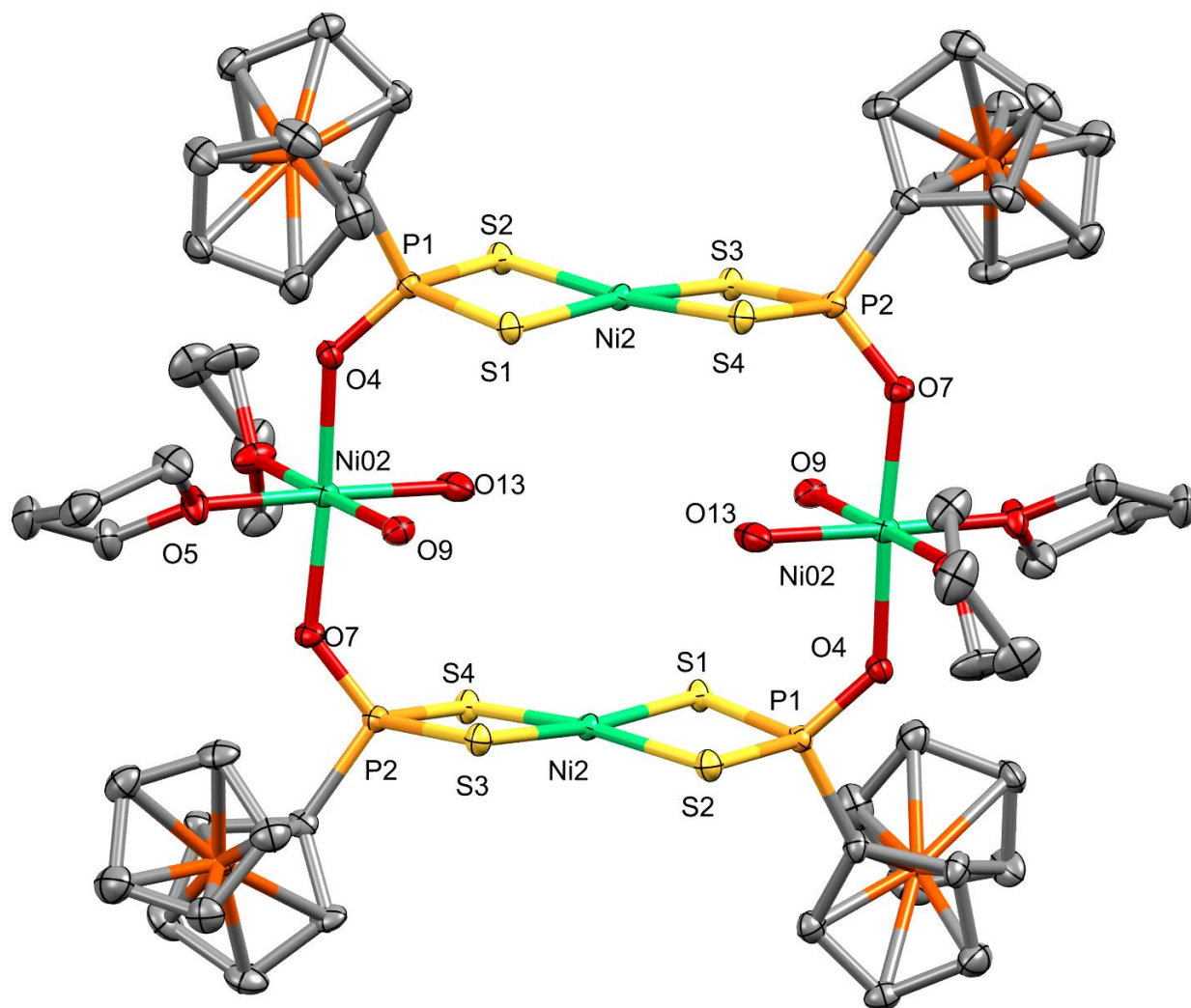


Figure 3.2: ORTEP molecular structure of Ni(II) complex **19**. Hydrogen atoms are omitted for clarity.

Table 3.2: Selected bond lengths (Å) and angles (°) for **19**

Bond lengths (Å)		Bond angles (°)	
O(4)-P(1)	1.511(3)	C(1)-P(1)-S(2)	106.98(16)
O(7)-P(2)	1.518(3)	C(2)-P(2)-S(4)	111.77(18)
P(1)-S(1)	2.0529(15)	O(4)-P(1)-C(1)	107.8(2)
P(1)-S(2)	2.0473(14)	O(7)-P(2)-C(2)	106.88(18)
P(2)-S(3)	2.0400(15)	O(4)-P(1)-S(1)	112.56(17)
P(2)-S(4)	2.2338(8)	O(7)-P(1)-S(2)	108.28(15)
S(1)-Ni(2)	2.2196(11)	O(7)-P(2)-S(3)	117.85(13)
S(2)-Ni(2)	2.2274(11)	O(7)-P(2)-S(4)	114.75(13)
Ni(2)-)-S(3)	2.2172(8)	S(2)-P(1)-S(1)	97.67(6)
Ni(2)-)-S(4)	2.2293(11)	S(4)-P(2)-S(3)	97.43(6)
O(4)-Ni(02)	2.039(3)	P(1)-S(1)-Ni(2)	87.52(5)
O(7)-Ni(02)	2.055(3)	P(1)-S(2)-Ni(2)	87.68(5)
Ni(02)-O(4)	2.008(3)	P(2)-S(3)-Ni(2)	86.88(5)
Ni(02)- O(7)	2.072(3)	P(2)-S(4)-Ni(2)	86.75(5)
		S(1)-Ni(2)-S(2)	88.33(3)
		S(3)-Ni(2)-S(4)	92.89(4)
		C(1)-P(1)-S(1)	109.99(14)
		C(1)-P(2)-S(3)	113.22(14)

Table 3.3. Crystal data and structure refinement for **18** and **19**

Compound	18	19
Formula	[C ₂₈ H ₃₆ Fe ₂ Ni ₂ O ₄ P ₂ S ₄] ₂	C ₂₈ H ₃₆ Fe ₂ NiO ₄ P ₂ S ₄
D _{calc.} / g cm ⁻³	1.644	1.633
μ /mm ⁻¹	2.135	1.847
Formula Weight	1712.32	797.16
Colour	brown	yellow
Shape	chunk	plate
Max Size/mm	0.420	0.198
Mid-Size/mm	0.220	0.180
Min Size/mm	0.140	0.043
T/K	100(2) K	173(2)
Crystal System	Triclinic	monoclinic
Space Group	P -1	P ₂ ₁ /c
a/Å	14.1756(9)	15.0135(17)
b/Å	15.9831(11)	8.0033(9)
c/Å	18.8891(12)	13.1830(3)
α /°	84.280(2)	90
β /°	70.822(2)	115.3950(10)
γ /°	71.957(2)	90
V/Å ³	3843.4(4)	1621.1(3)
Z	6	2
Θ _{min} /°	1.141	3.002
Θ _{max} /°	28.330	50.724
Measured Refl.	60457	16921
Independent Refl.	18715	2955
Completeness to theta	25.242	25.242
R _{int}	0.0206	0.0550
Parameters	855	191
Restraints	0	0
Largest Peak/eÅ ⁻³	5.205	0.69
Deepest Hole/eÅ ⁻³	-2.188	-0.31
GooF	1.086	1.063
wR ₂ (all data)	0.1691	0.0863
wR ₂	0.1597	0.0807
R ₁ (all data)	0.0657	0.0446
R ₁	0.0557	0.0345
F(000)	1942	820.0

The X-ray structure of **23b** shown in (**Figure 3.3**) is the outcome of an unexpected yet new complex resulting from several attempts to obtain a polymeric type structure related to complex **23** that ought to result from a ligand to metal ratio 1:1. Complexes in a ratio of 1:2 is similar to group 12 metal complexes as reported in the literature.²¹ The structure shows one of the sulfur atoms on the ligand $[\text{FcP}(\text{OH})\text{S}_2]^-$ ions was replaced by an ethoxy group as a result of crystal growth in ethanol solvent over 10 days. Though the structure does not represent the expected complex of interest **23**, it does point to the susceptibility of S atoms being replaced by O or OR atoms (see also **Chapter 2**). This implies that for the complex to form, 2 H atoms and 1 S atom had to be removed: an H atom was removed from the EtOH and another from the original P-O-H moiety and the S atoms from P-S. Combined these 3 atoms presumably formed H_2S , which is by far the most common by-product upon hydrolysis or oxidation amongst this class of ligands. The structure of Cd(II) and Zn(II) with a ligand to metal ratio 1:1 will likely result in a coordination polymer as shown in **Figure 3.3** where it will employ the two sulfur atom and one hydroxyl group in coordination. The X-ray structure (**Figure 3.3b**) displayed an exciting polymeric chain with alternating 4- and 5- coordinate Cd(II) metal centres along the chain.

It may thus be necessary to investigate and establish a reaction pathway utilizing different types of alcohols for the formation of similar polymer with multimetallic and multiferrocenyl assemblies shown in (**Figure 3.3b**) which may form new materials with applications.

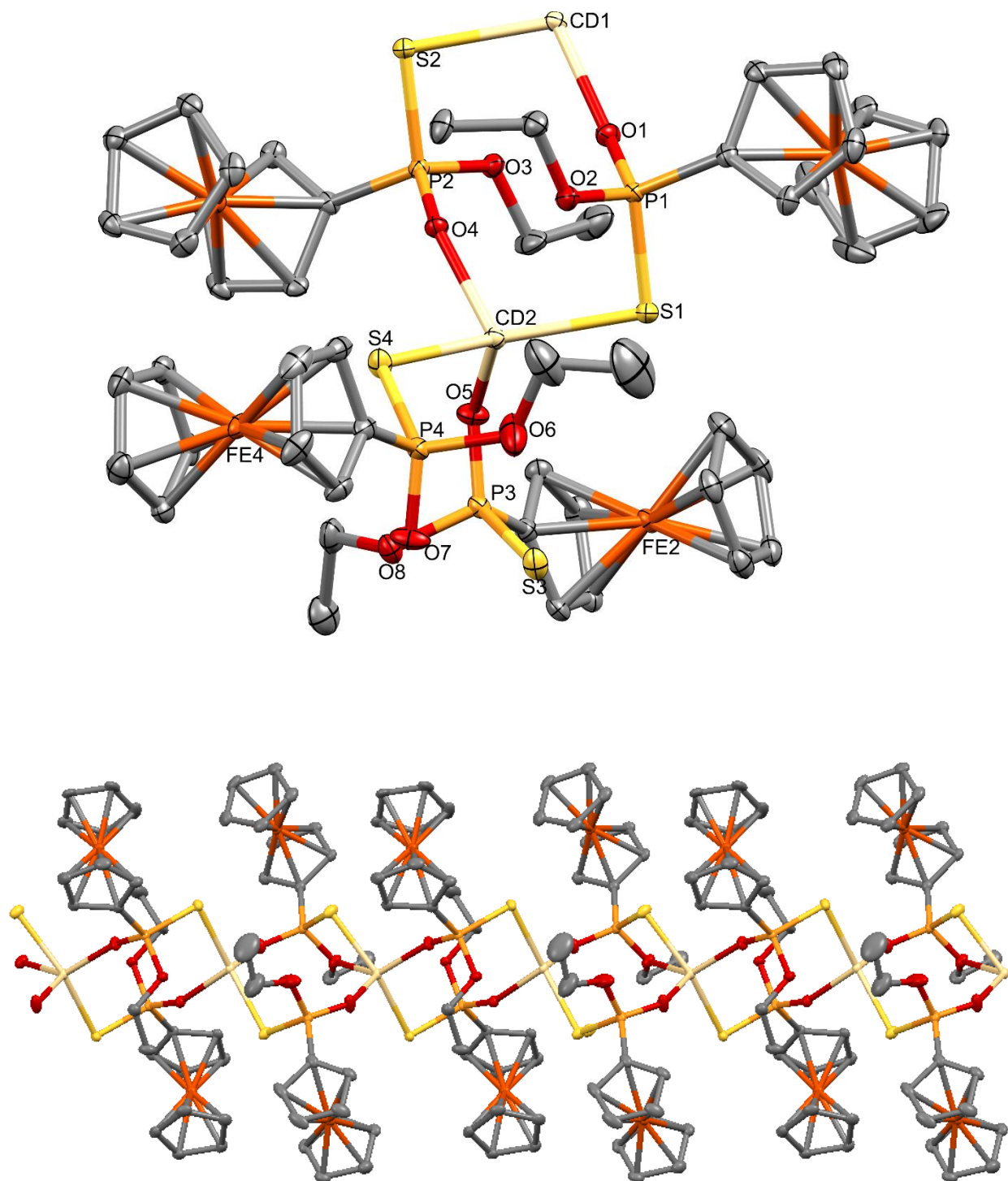


Figure 3.3: (a) ORTEP molecular structure of Cd(II) complex **23b** (b) ORTEP crystal structure of polymeric expansion of new Cd(II) complex **23b**. Hydrogen atoms omitted for clarity.

Table 3.4: Selected bond lengths (Å) and angles (°) for structure in **Fig. 3.3**

Bond lengths (Å)		Bond angles (°)	
O(1)-P(1)	1.49 ⁰⁸ (19)	C(1)-P(1)-S(2)	112.02(9)
P(1)-S(1)	2.0184(9)	C(2)-P(2)-S(4)	105.28(18)
S(2)-Cd(1)	2.4897(7)	O(1)-P(1)-C(1)	119.35(17)
Cd(1)-O(1)	2.2008(18)	O(4)-P(2)-C(2)	121.16(17)
Cd(2)-O(1)	2.2272(19)	O(1)-P(1)-S(1)	116.40(9)
C(1)-P(1)	1.777(3)	O(1)-P(1)-S(2)	101.97(8)
		P(4)-S(4)-Cd(2)	106.97(7)
		P(1)-S(1)-Cd(2)	93.67(3)
		P(2)-S(2)-Cd(1)	93.70(3)
		O(4)-Cd(2)-O(5)	93.43(7)
		S(1)-Cd(2)-S(4)	139.05(18)
		O(1)-Cd(1)-S(2)	104.41(5)
		S(1)-Cd(1)-S(2)	150.22(2)
		C(1)-P(1)-S(1)	109.99(14)
		C(1)-P(2)-S(3)	113.22(14)
		P(1)-C(2)-Fe1	122.73(14)

Table 3.5. Crystal data and structure refinement for **23b**.

Empirical formula	C ₄₈ H ₅₆ Cd ₂ Fe ₄ O ₈ P ₄ S ₄
Formula weight	1461.27
Temperature	100(2) K
Wavelength	0.71073 Å
Crystal system	Monoclinic
Space group	P 21/n
Unit cell dimensions	a = 10.1157(2) Å, b = 22.0569(4) Å, c = 24.2567(4) Å α = 90°. β = 100.7140(10) °. γ = 90°.
Volume	5317.83(17) Å ³
Z	4
Density (calculated)	1.825 Mg/m ³
Absorption coefficient	2.176 mm ⁻¹
F(000)	2928
Crystal size	0.209 x 0.161 x 0.094 mm ³
Theta range for data collection	1.258 to 25.428°.
Index ranges	-12 ≤ h ≤ 8, -22 ≤ k ≤ 26, -27 ≤ l ≤ 29
Reflections collected	23957
Independent reflections	9776 [R(int) = 0.0194]
Completeness to theta = 25.242°	99.7 %
Absorption correction	Semi-empirical from equivalents
Max. and min. transmission	0.834 and 0.646
Refinement method	Full-matrix least-squares on F ²
Data / restraints / parameters	9776 / 0 / 645
Goodness-of-fit on F ²	1.022
Final R indices [I > 2σ(I)]	R1 = 0.0245, wR2 = 0.0544
R indices (all data)	R1 = 0.0313, wR2 = 0.0575
Extinction coefficient	n/a
Largest diff. peak and hole	1.661 and -0.686 e.Å ⁻³

3.2.2.2 Solubility

Knowledge about the solubility of these compounds is useful, especially in choosing the appropriate solvent for spectroscopic measurements, or generally in numerous sectors where their application is needed. To this end, a series of qualitative solubility tests were performed on all the compounds, **17-23**. A variety of solvents were tested over a wide range of dielectric constants, including protic/aprotic and polar/non-polar solvents. Noteworthy is for example how both the ligand and the complexes are soluble in protic solvents such as water and ethanol. Results are shown in **Table 3.6**

Table 3.6. Solubility Data for Compounds **17-23**

Entry	Acetone	CH ₃ CN	EtOH	Hexane	Ether	CH ₂ Cl ₂	Water	THF
17	I	S	VS	I	I	I	VS	I
18	I	S	S	I	I	PS	S	PS
19	I	I	S	I	I	PS	S	PS
20	I	S	S	I	I	PS	S	PS
21	I	I	S	I	I	PS	S	PS
22	I	S	S	I	I	PS	S	PS
23	I	I	S	I	I	PS	S	PS

Key to table: I = Insoluble (the material was quantitatively recovered after filtration); PS = Partly Soluble (10% of the material dissolved); S = Soluble (80% of the material dissolved); VS = Very Soluble (a clear solution emerged immediately). The solubility data is based on the following experimental criteria: 0.02 g of the compound was dissolved in 1.0 mL of the appropriate solvent and was hard shaken for 5-10 seconds at 23°C

3.3 CONCLUSIONS

The first nucleophilic ring opening reaction of ferrocenyl Lawesson with water is described for the formation of dithiophosphonate salt leading complexes with multimetallic and multiferrocenyl assemblies. Our investigations reveal that these new compounds have high potential in dye sensitized solar cells applications and our findings are reported in **Chapter 7** of this thesis. Additional future work on this ligand is discussed in **Chapter 8**.

3.4 EXPERIMENTAL

3.4.1 Method

Synthesis of the ligand and complexes were carried out in a standard Schlenk tube (~2 cm diameter) using standard Schlenk line system under a blanket of nitrogen. The Schlenk line is critical for this important reactions because it requires the minimization of contact with air or other airborne contaminants, otherwise, oxidation and/or hydrolysis may occur.

3.4.2 Materials

Ferrocenyl Lawesson's reagent was prepared from literature procedures.²² All other reagents were used as purchased from Aldrich and used as received. Distilled water was used for the reaction and in all cases where water is required in this work. Dried THF and ether were obtained and used after distillation over sodium wire and benzophenone under a blanket of nitrogen while DCM was collected in the same manner but was distilled over P₂O₅.

3.4.3 Characterization Methods

¹H and ³¹P NMR spectra were recorded using a Bruker Avance 400 MHz spectrometer. NMR data are expressed in parts per million (ppm) downfield shift referenced internally to the residual proton impurity in the deuterated solvent and are reported as chemical shift position (δ_H), relative integral intensity, multiplicity (s = singlet, d = doublet, t = triplet, sept = septet, and m = multiplet), coupling constant J in Hz, and assignment. ³¹P NMR spectra chemical shifts are reported relative to an 85% H₃PO₄ in D₂O external standard solution, all at 298 K. Infrared spectra were recorded in the range 4000–380 cm⁻¹ on a Perkin-Elmer Spectrum 100 FT-IR spectrometer. The yields were determined by performing the reaction in a dry pre-weighed Schlenk tube, weighing the sample after drying. Mass spectra were recorded with a Waters Micromass LCT Premier TOF-

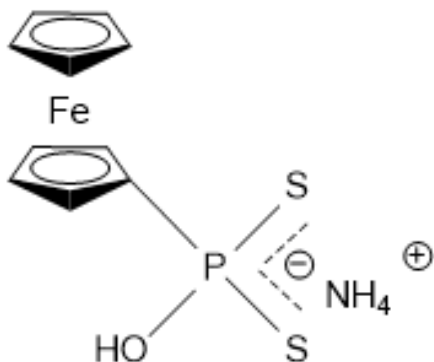
MS. The mode of ionization was ESI (electrospray) negative, $[M-H]^-$. Samples were prepared to ~2 ppm concentration in the desired solvent and infused into the mass spectrometer.

3.4.4 Crystallography

A crystal of complex **18**, $[\text{Ni}(\text{Fc}(\text{OH})\text{PS}_2)_2]$, with approximate dimensions 0.106 x 0.256 x 0.432 mm, and complex **19**, $[\text{Ni}_2(\text{Fc}(\text{OH})\text{PS}_2)_2]_2$, with approximate dimensions 0.198 x 0.18 x 0.043 mm was mounted on a glass fiber with epoxy resin. All intensity and geometric data were collected on a Bruker APEXII CCD diffractometer equipped with a graphite monochromated $\text{Mo-K}\alpha$ radiation ($\lambda = 0.71073 \text{ \AA}$). APEXII software was used for preliminary determination of the unit cell.²³ Determination of integrated intensities and unit cell refinement were performed using SAINT.²⁴ The SADABS program was used to apply an empirical absorption correction.²⁵ The integration of the data yielded a total of 21960 reflections to a maximum θ angle of 28.51° (0.74 \AA resolution). XPREP determined the space group to be P -1 and $\text{P}2_1/c$, with $Z = 6$ and 2 for **18** and **19**.²⁶ The structure was solved with XS²⁷ and subsequent structure refinements were performed with XL.²⁸ A complete listing of crystallographic data and parameters are reported in **Table 3.3** and **3.5**.

3.5.5. Synthesis of Hydroxyl Derivative of Ferrocenyl Dithiophosphate Ligand

Synthesis of $\text{NH}_4[\text{Fc}(\text{OH})\text{PS}_2]$ (17)

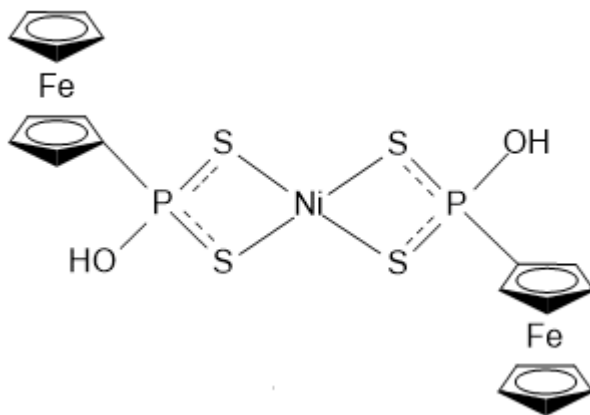


An equivalent molar ratio of distilled water (0.06 g, 3.57 mmol) was added to clean and oven dried Schlenk tube containing about 15 ml THF and ferrocenyl Lawesson's (1 g, 1.78 mmol) was added in one portion stirred overnight under an inert atmosphere at room temperature. After several hours, a clear brown solution resulted and was further stirred to ensure no unreacted precursor in the

reaction. Dry ammonia was bubbled into the resulting clear solution to give a bright yellow precipitate. The solvent was removed by filtration under vacuum and was washed with ether to give a bright orange-brown solid (0.961g, 85.7%). m.p 158 °C, ^{31}P NMR (methanol- d_3) δ : 58.8 ^1H NMR (methanol- d_3) δ : 4.33 (s, 5H, Fc unsubstituted ring), 4.29 (m, 2H, Fc substituted ring), 3.3 (m, 2H, (1H, d, $J=6.40$ Hz Fc substituted ring). Selected FT-IR (4000–350 cm^{-1}): 2768(b), 1163(w), 1404 (m), 937 (s), 812 (s), 594(s), 484 (s). Mass Spec (ESI): $(\text{M}-\text{NH}_4)^+$ 296, $2(\text{M}-\text{NH}_4)^+$ 592

3.4.5 Synthesis of Nickel, Cadmium and Zinc Complexes

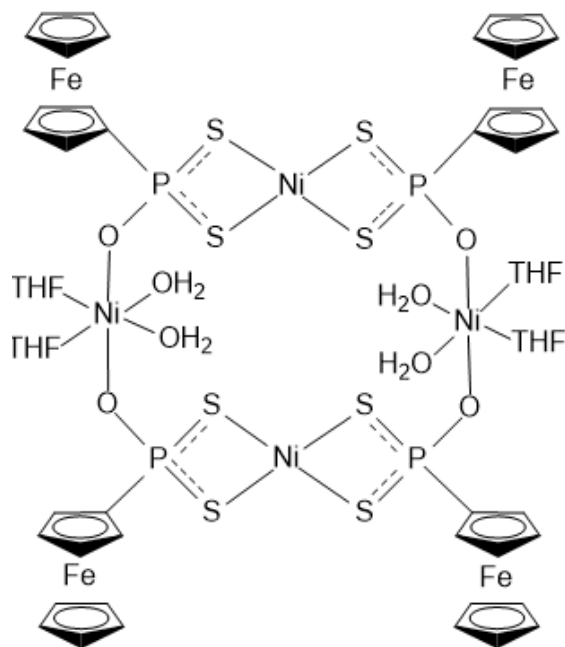
Synthesis of $[\text{Ni}(\text{Fc}(\text{OH})\text{PS}_2)_2]$ (**18**)



A mixture of $\text{NiCl}_2 \cdot 6\text{H}_2\text{O}$ (0.19 g, 0.79 mmol) and salt **17** (0.50 g, 1.59 mmol) in mole ratio 1:2 were stirred together in THF (15 ml) for about 2 hrs. and dark brown colour change was observed. The solvent was pumped down and the resulting dark brown solid was extracted with

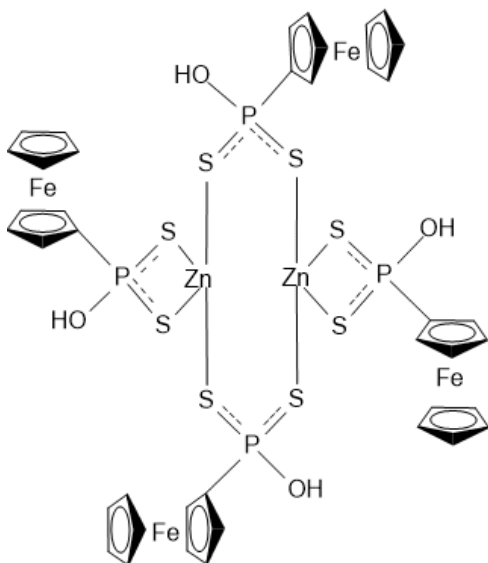
dichloromethane and was filtered under vacuum through Celite. The filtrate was dried under reduced pressure to give a dark brown solid (0.45g, 87%). m.p 162°C . ^{31}P NMR (CDCl_3) δ : 63.5, ^1H NMR (CDCl_3) δ : 4.92 (s, 5H, Fc unsubstituted ring), 4.54 (m, 2H, Fc substituted ring), 3.72 (m, 2H, Fc substituted ring). Selected FT-IR (4000–350 cm^{-1}): 3135(s), 3043(s), 1762(w), 1610(w), 1403 (s), 1101(s) 885(m), 577(s), 497 (m). Mass Spec (ESI): $(\text{M}+\text{THF})^+ 735$.

Synthesis of $[\text{Ni}_2(\text{Fc}(\text{OH})\text{PS}_2)_2]_2$ (**19**)



A mixture of $\text{NiCl}_2 \cdot 6\text{H}_2\text{O}$ (0.38 g, 1.59 mmol) and salt **17** (0.50 g, 1.59 mmol) in ratio 1:1 were stirred together in THF (15 ml) for a few hours. A colour change from orange-brown to dark brown colour was observed. Workup was performed as for **18** above. Brown solid (1.03g, 46%). m.p 168°C ^{31}P NMR (CDCl_3) δ : 83.42, ^1H NMR (CDCl_3) δ : 4.48 (s, 5H, Fc unsubstituted ring), 4.10 (m, 2H, Fc substituted ring), 3.21 (m, 2H, Fc substituted ring). Selected FT-IR (4000–350 cm^{-1}): 3021(b), 1632(w), 1411(s), 1017(s), 812(m), 573(m), 481 (s).

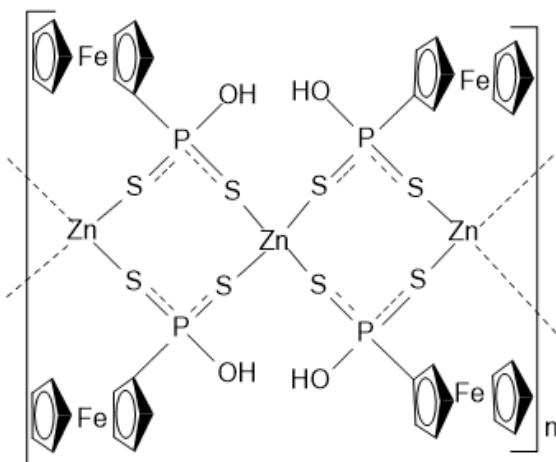
Synthesis of $[\text{Zn}(\text{Fc}(\text{OH})\text{PS}_2)_2]$ (**20**)



A mixture of anhydrous ZnCl_2 (0.11 g, 0.79 mmol) and salt of **17** (0.50 g, 1.59 mmol) were stirred together in THF (15ml) for about 2hrs and yellow complex resulted. Workup was performed as for **18** above. Yellow solid (0.36g, 69%). m.p 166°C . ^{31}P NMR (CDCl_3) δ : 78.2, ^1H NMR (CDCl_3) δ : 4.29 (s, 5H, Fc unsubstituted ring), 3.92 (m, 2H, Fc substituted ring), 3.02 (m, 2H, Fc substituted ring). Selected FT-IR (4000–350 cm^{-1}): 3031(b), 1665(w), 1412(m), 1024(s), 815(m), 534(m), 480 (s). Mass Spec

(ESI): $(1/2\text{M}-\text{Fc})^+$ 488.

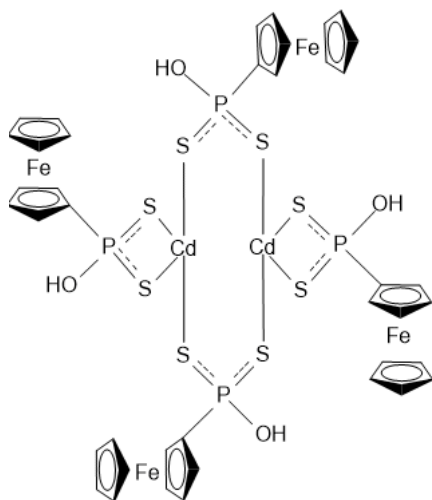
Synthesis of $[\text{Zn}_2(\text{Fc}(\text{OH})\text{PS}_2)_2]_2$ (**21**)



A mixture of anhydrous ZnCl_2 (0.22 g, 0.79 mmol) and salt **17** (0.50g, 1.59 mmol) in ratio 1:1 were stirred together in THF (15ml) for few hours and dark yellow complex resulted. Workup was performed as for **2** above. Brown solid (1.10g, 48%). m.p 168 °C, ^{31}P NMR (CDCl_3) δ : 93.9, ^1H NMR (CDCl_3) δ : 4.59 (s, 5H, Fc unsubstituted ring), 4.27 (m, 2H, Fc substituted ring), 3.32 (m, 2H, Fc

substituted ring). Selected FT-IR (4000–350 cm^{-1}): 3021(b), 1632(w), 1411(s), 1017(s), 812(m), 573(m), 481 (s). Mass Spec (ESI): $(1/2\text{M}-\text{Fc})^+$ 488.

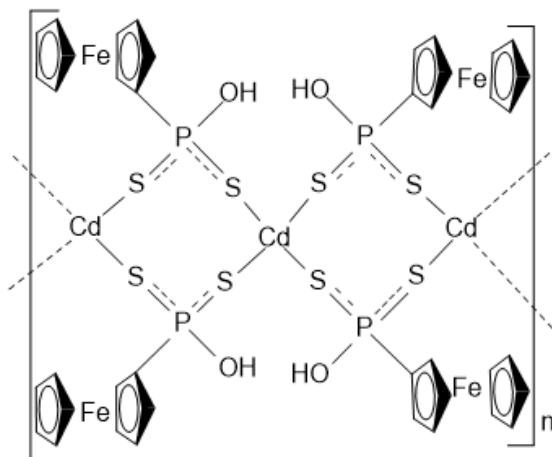
Synthesis of $[\text{Cd}(\text{Fc}(\text{OH})\text{PS}_2)_2]$ (**22**)



$\text{CdCl}_2 \cdot 2\text{H}_2\text{O}$ (0.15 g, 0.796 mmol) and salt **17** (0.50 g, 0.159 mmol) were stirred together in THF (15ml) for about 2hrs and yellow complex resulted. Workup was performed as for **2** above. Yellow solid (0.41g, 73%). m.p 163 °C. ^{31}P NMR (CDCl_3) δ : 93.3 ^1H NMR (CDCl_3) δ : 4.71 (s, 5H, Fc unsubstituted ring), 4.38 (m, 2H, Fc substituted ring), 3.43 (m, 2H, Fc substituted ring). Selected FT-IR (4000–350 cm^{-1}): 3130(s), 3041(s), 1614(w), 1402 (s), 1175(m), 1021(s),

885(m), 817(m), 576(s), 484 (s). Mass Spec (ESI): $(1/2\text{M}-\text{OH})^+$ 690.

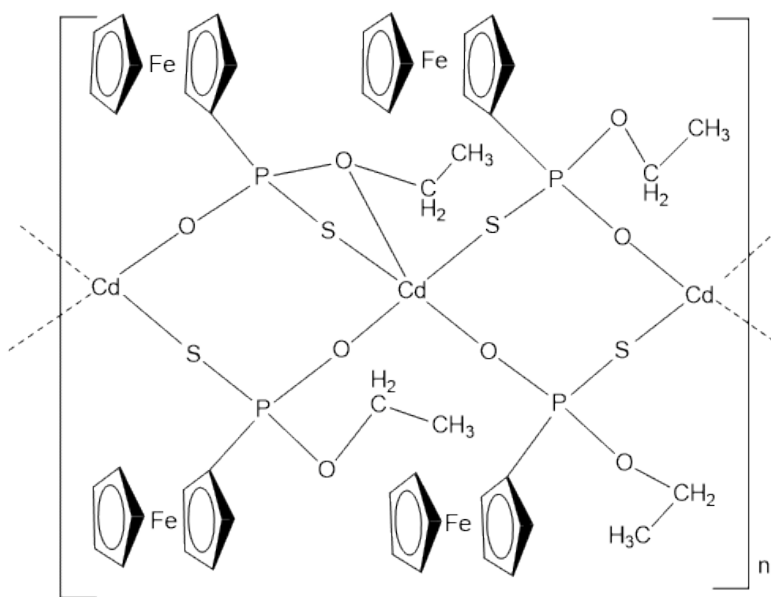
Synthesis of $[\text{Cd}_2(\text{Fc}(\text{OH})\text{PS}_2)_2]_2$ (**23**)



23a: A mixture of CdCl_2 (0.29g, 0.80 mmol) and salt **17** (0.50g, 1.59mmol) in ratio 1:1 were stirred together in THF (15 ml) for few hours and brown complex resulted. Workup was performed as for **2** above. Brown solid (1.12g, 52%). m.p 168 °C. ^{31}P NMR (CDCl_3) δ : 98.9, ^1H NMR (CDCl_3) δ : 4.89 (s, 5H, Fc unsubstituted ring), 4.57 (m, 2H, Fc substituted ring), 3.62 (m, 2H, Fc substituted ring).

Selected FT-IR (4000–350 cm^{-1}): 3021 (b), 1632 (w), 1411 (s), 1017 (s), 812 (m), 573 (m), 481 (s). Mass

Spec (ESI): $(1/2\text{M}-\text{OH})^+$ 690. The introduction of ethanol to the solution of **23a** resulted in the formation



of **23b**(Figure 3.3) ^{31}P NMR (CDCl_3) δ : 83.3, ^1H NMR (CDCl_3) δ : 4.89 (s, 5H, Fc unsubstituted ring), 4.57 (m, 2H, Fc substituted ring), 3.93(m,2H, OCH_2CH_3), 3.62 (m, 2H, Fc substituted ring), 1.22(m,3H, OCH_2CH_3 Selected FT-IR (4000–350 cm^{-1}): 3130(s), 3041(s), 1614(w), 1402 (s), 1175(m), 1021(s), 885(m),817(m),

576(s), 484 (s).

3.5 REFERENCES

1. Foreman, M. R. S. J.; Slawin, A. M. Z.; Woollins, J. D., *J.Chem.Soc., Dalton Trans.* **1996**, (18), 3653-3657.
2. Cava, M. P.; Levinson, M. I., *Tetrahedron* **1985**, *41* (22), 5061-5087.
3. Cherkasov, R. A.; Kuttyrev, G. A.; Pudovik, A. N., *Tetrahedron* **1985**, *41* (13), 2567-2624.
4. van Zyl, W. E.; Woollins, J. D., *Coord Chem Rev* **2013**, *257*, 718-731.
5. D. Klaman, *Verlag-Chemie, Weinheim*, **1984**, 35-153
6. Boyde, S., *Green Chem.* **2002**, *4* (4), 293-307.
7. Nicholls M.A., Norton P.R., Kasrai M., Bancroft G.M., *Tribology Internat* **2005**, *38*, 15-39
8. Patnaik P., *John Wiley & Sons, Hoboken NJ* **2007**, 3rd edition.
9. Bromberg, L.; Lewin, I.; Warshawsky, A., *Hydrometallurgy* **1993**, *33* (1), 59-71.
10. Armstrong, A. T.; Smith, F.; Elder, E.; McGlynn, S. P., *J.Chem.Phys.* **1967**, *46* (11), 4321-4328.
11. Karakus, M.; Lönnecke, P.; Yakhvarov, D.; Hey-Hawkins, E., *Z.Anorg.Allg.Chem* **2004**, *630* (10), 1444-1450.
12. Gray, I. P.; Milton, H. L.; Slawin, A. M. Z.; Woollins, J. D., *Dalton Trans* **2003**, *17*, 3450-3457
13. Karakus, M.; Loennecke, P.; Hildebrand, M.; Hey-Hawkins, E., *Z Anorg Allg Chem* **2011**, *637*, 102-107
14. Karakus, M.; Lönnecke, P.; Hey-Hawkins, E., *Polyhedron* **2004**, *23* (14), 2281-2284.
15. Wang, X.-Y.; Li, Y.; Ma, Q.; Zhang, Q.-F., *Organometallics* **2010**, *29* (12), 2752-2760.
16. Shi, W.; Shafaei-Fallah, M.; Anson, C. E.; Rothenberger, A., *Dalton Trans.* **2005**, (24), 3909-3912.

17. Shi, W.; Kelting, R.; Shafaei-Fallah, M.; Rothenberger, A., *J.Organomet.Chem.***2007**, 692 (13), 2678-2682.
18. Sağlam, E. G.; Erden, S.; Tutsak, Ö.; Eskiköy Bayraktepe, D.; Yazan Durmuş, Z.; Dal, H.; Ebinç, A., *Phosphorus, Sulfur, Silicon Relat.Elem.* **2017**, 119, 322-329.
19. Çılgı, G. K.; Karakuş, M.; AK, M., *Synth. Met.* **2013**, 180, 25-31.
20. Wang X.Y; Shi H.T; Zhang Q.F; *Organometallics* **2011** 30 (3), 380-383
21. Gray, I. P.; Milton, H. L.; Slawin, A. M. Z.; Woollins, J. D., *Dalton Trans.***2003**, (17), 3450-3457.
22. Van Zyl, W. E.; Fackler, J. P., *Phosphorus, Sulfur, Silicon Relat. Elem* **2000**, 167, 117-132
23. Bruker Analytical X-ray System, *Bruker AXS Inc. Madison, WI*, **2013**, *APEX2 Version 2013.1*.
24. Software for the CCD Detector System, *Bruker Analytical X-ray System, Madison, WI*, **2013**, *SAINT Version 8.32B*.
25. Sheldrick, G. M., *University of Gottingen, Gottingen, Germany* **2012**, *SADABS Version 2012/1*.
26. Sheldrick, G. M., *University of Gottingen, Gottingen, Germany* **2013**, *XPREP Version 2013/3*.
27. Sheldrick, G. M., *Acta Cryst. A64* **2008**, *XS Version 2013/1*, , 112-122.
28. Sheldrick, G. M., *Acta Cryst. A64 XL Version 2013/3* **2008**, 112-122.

CHAPTER 4

SYNTHESIS OF A NEW ZWITTERIONIC DITHIOPHOSPHONATE LIGANDS AND SOME LATE-TRANSITION METAL COMPLEXES

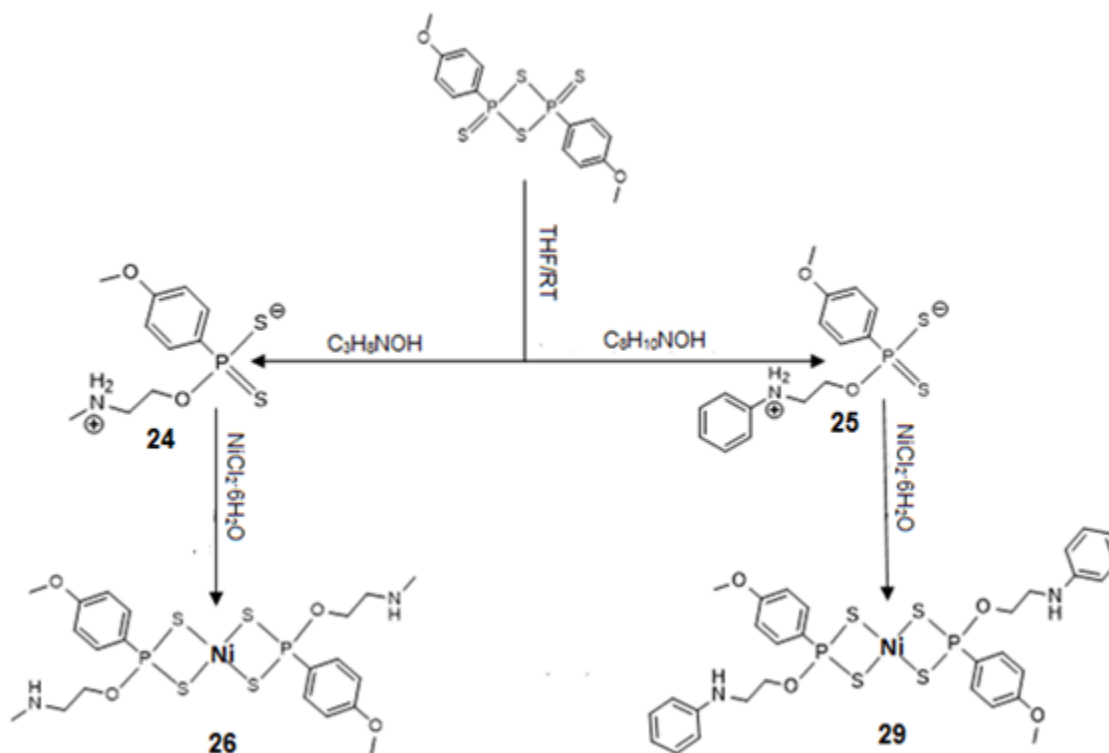
4.1 BACKGROUND

Dithio-organophosphorus, including dithiophosphates, -phosphinates, and -dithiophosphonates, dithioimidodiphosphinates and mixed thio-oxo analogues, as well as dithioarsinates, have been a focus of inorganic and organometallic research for many years.¹⁻⁷ Certain phosphor-1,1-dithiolate ligands are also an important class of dithio-organophosphorus compounds and provide the basis for the present study. Lawesson's reagent and its precursor phosphorus pentasulfide (Berzelius reagent), have both proven important starting materials in the synthesis of these ligands.⁸⁻¹⁰ The literature showed a distinct scarcity of metal dithiophosphonate complexes compared to other phosphor-1,1-dithiolate ligands.¹¹⁻¹² The dithiophosphonates are a well-known class of principally bidentate ligands and a number of its transition-metal (and indeed main group metal) complexes are known.^{10,13-18} However, zwitterionic-based dithiophosphonates show a distinct paucity in the open literature and only a handful of such structurally characterized compounds exist.¹⁹⁻²⁰ Metal complexes from zwitterionic dithiophosphonate ligands have not been reported in the literature. The synthesis of a free ferrocenyl zwitterionic dithiophosphonate was reported in 2004 by Karakus and co-workers, and they described their attempts to prepare the corresponding stable transition metal complexes of the zwitterion but were unsuccessful.²⁰ Nevertheless, we report in this study the synthesis and molecular structure of two new zwitterionic dithiophosphonates ligands, and one crystal structure of a transition metal complex, in addition to other fully characterized complexes. This is to the best of our knowledge the first example of any transition-metal complex derived from a zwitterionic dithiophosphonate ligand to be structurally characterized. Amino alcohols used in this study have industrial and pharmaceutical benefit²¹⁻²² which may be enhanced through complexation to transition metals.

RESULT AND DISCUSSION

4.1.1 Synthesis of Zwitterionic Ligand and the Corresponding Complexes

The transition-metal complexes from zwitterionic dithiophosphonate ligands were prepared as shown in **Scheme 4.1**. The zwitterionic dithiophosphonate ligands were prepared by reacting amino-alcohol and Lawesson's reagent in an equimolar ratio. The dithiophosphonate ligand, as discussed previously, has been prepared from Lawesson's reagent using various alcohols to initiate the ring opening reaction.^{17, 23-29} By comparison, nucleophilic ring-opening of Lawesson's reagent and its derivatives with amino-alcohols have been scarcely investigated, and no complexes have been reported from the zwitterionic dithiophosphonate ligand,^{19, 30} In this study, we present the first complexes that are air stable and are structurally characterized. The addition of the corresponding transition-metal salts in appropriate stoichiometry to the THF solution of the zwitterionic dithiophosphonate ligand gave the corresponding complexes. All the compounds are air-stable and were characterized by ¹H, and ³¹P NMR, infrared, and mass spectroscopy. Their structures were confirmed by single-crystal X-ray diffraction analysis.



Scheme 4.1: Synthesis of Nickel(II) complexes from zwitterionic dithiophosphonate ligand (representative scheme)

4.1.2 Characterization.

The purity and compositions of all the ligands and complexes were examined by NMR spectroscopy. The ligands are white in colour, soluble in the polar solvent and their percentage yields range between 84-87%. All the compounds display well-resolved ^1H NMR signals that integrate to the corresponding hydrogens. A well resolved sharp singlet on the ^{31}P NMR for the ligand and complexes were as expected, to confirm the presence of P atoms. The ^{31}P NMR spectra of both zwitterionic ligands **24** and **25** displayed sharp singlets at δ (P) 108.43 and 110.74 ppm, respectively. In the IR spectra of **24** and **25** characteristic bands are observed for $\nu[\text{P}-\text{O}-(\text{C})]$, (1021 cm^{-1}), and two strong bands about at 643 and 543 cm^{-1} are attributed to $\nu(\text{PS})_{\text{asym}}$ and $\nu(\text{PS})_{\text{sym}}$ stretching vibration, respectively. A medium band signal observed at 3386 cm^{-1} was assigned to the N-H stretching of the amine. The metal complexes from the zwitterionic ligand were isolated in varying yields (59–68%) as either brown or white powder. They are all air stable and soluble in both

dichloromethane and chloroform and THF. The IR spectra of compounds **26-31** are close to that of their corresponding ligand.

4.1.2.1 UV-VIS and Photoluminescence Studies

The maximum wavelength of absorption for the ligands were 244 and 259 nm for **24** and **25**, respectively (**Figure 4.1**). The maximum absorption peaks for the complexes were at 242, 243 and 253 nm for **27**, **28** and **26**, respectively.

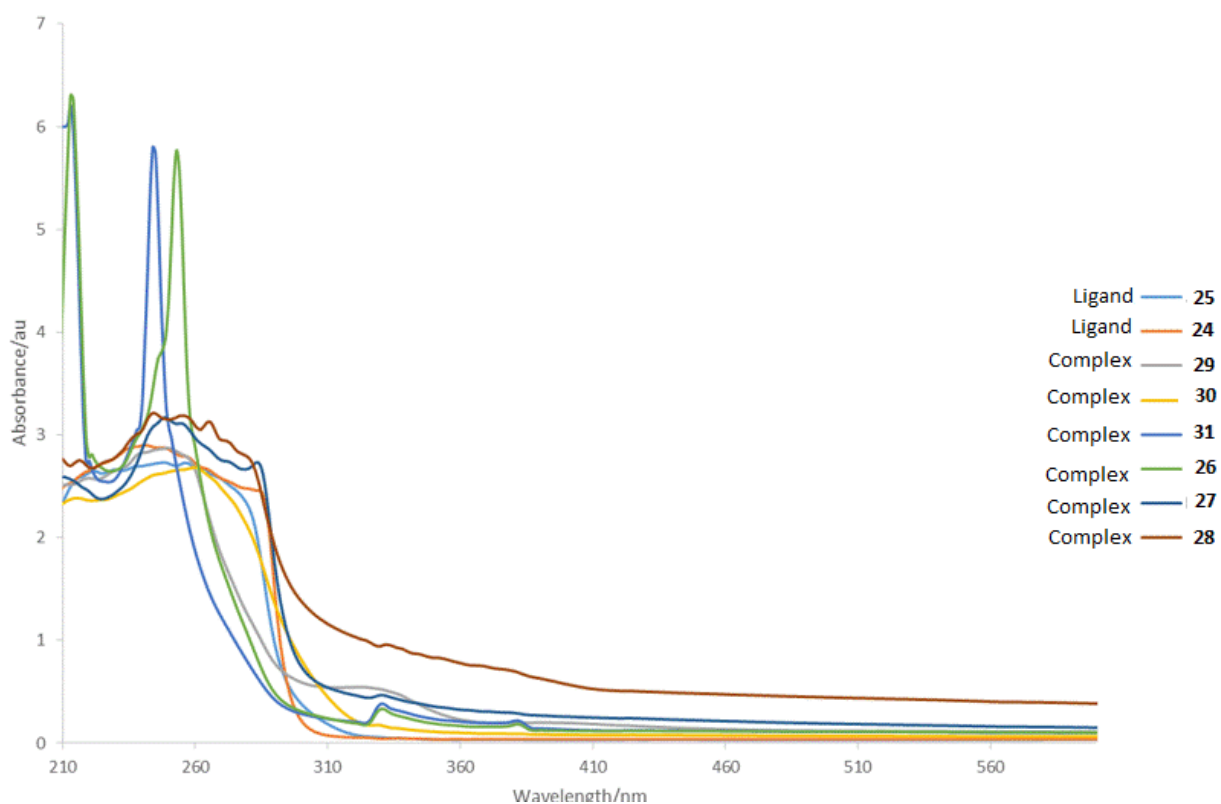


Figure 4.1. UV-VIS spectra of the ligands (**24-25**) and complexes (**26-31**)

The other complexes recorded maximum absorption peaks at 244, 245 and 260 nm for **31**, **29** and **30**, respectively. The band gap energies (E_g) were estimated from the UV-vis spectra by use of Tauc plots considering allowed transitions only. The ligands showed E_g of 4.1 eV and were found to vary depending

on the central metal in their respective complexes. Complex **26** and **27** had a 4.1 eV band gap and **28** showed a much lower band gap of 2.5 eV (**Figure 4.2**).

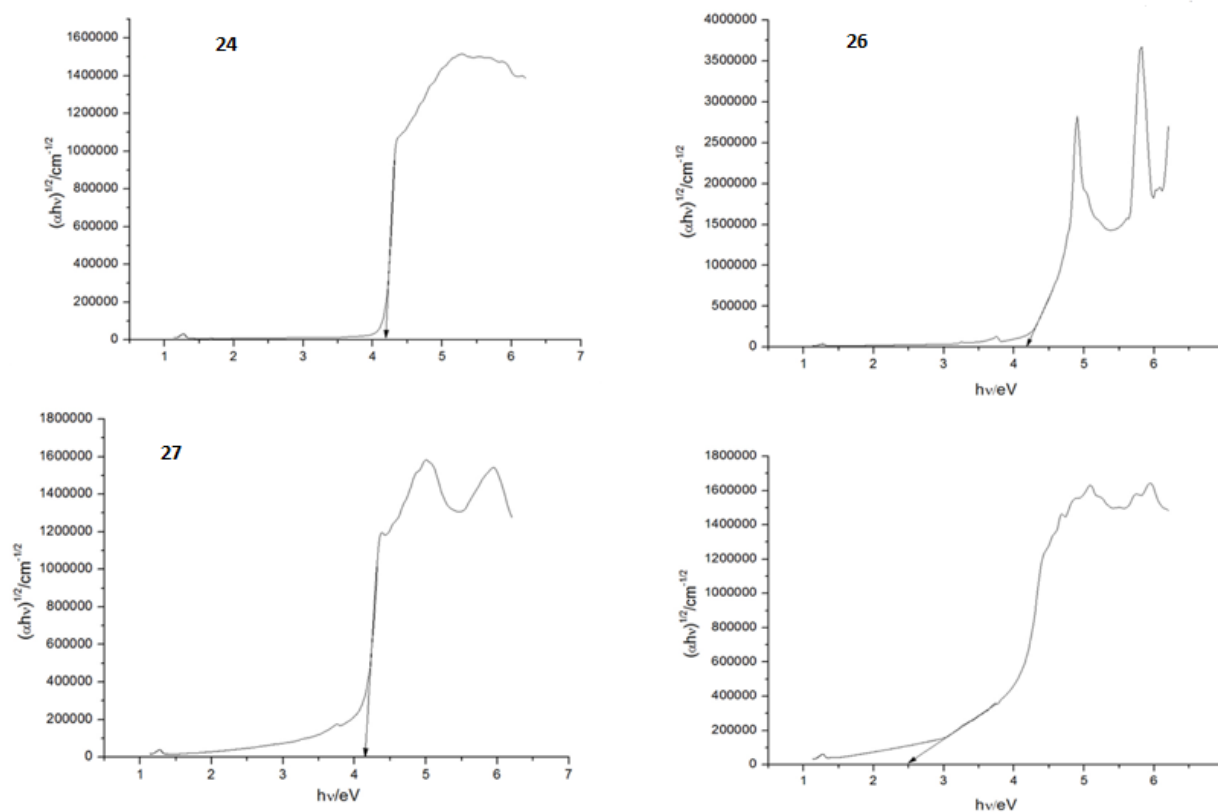


Figure 4.2. Electronic absorption spectra of **24**, **26**, **27** & **28**

Complex **29**, **30** and **31** indicated varied band gaps that can be viewed to depend on occupation of metal d-orbitals as well as size of the metal atom, a d^8 , Ni(II) complex had the lowest E_g of 3.2 eV followed by Zn(II)-complex (d^{10}); 3.9 eV and highest was a Cd(II)-complex (d^{10}) at 4.1 eV (**Figure 4.3**) and the latter had a correspondingly larger atomic radius. The characteristic electron delocalization of electron density across the S-P-S bonds has been shown to be influenced by the nature of the central metal and coordination geometry³¹. The square geometry proposed for these complexes and confirmed from the crystallographic data suggest a predominance of charge accumulation on the bridging sulfur atoms. Consequently, the

electron transition, $n \rightarrow \sigma^*$ predominates as indicated by λ_{\max} ranging from 242 to 253 nm³² and to a lesser degree of covalence in M-S compared to P-S, because P is more electronegative compared to M under investigation. However, the vibrational frequencies of PS₂ depend on the electronic effects of the groups connected to P,³³ because it has a partial positive charge and empty *3d*-orbitals. A net field, therefore, exists in the pseudo-binuclear centers that create intramolecular charge transfer, a phenomenon that modulates absorption bands. For instance, an increase of electron charge on S has a consequence of increasing S-P-S and decrease in the S-M-S dihedral angles³⁴ as result of the reduction of net positive charge on the central metal. In this work, the electron donating methyl group was shown to greatly depopulate Zn and Cd centers as indicated by blue-shifts (242 and 243 nm); both metals have filled d-orbitals, and a red-shifted Ni-complex (d⁸) an effect that can be associated with coulombic attraction. The consequence is the drop-in band gap energy in Cd-complex (2.5 eV) suggesting a lower nuclear charge as the metal reduces its net charge. This indicates the geometry may be distorted from the ideal, and crystallographic data is required to establish the spatial orientation of ligating groups around Cd as S-Cd-S may not be that smaller and Cd-S shorter compared to P-S bond lengths. A lesser electron donating group aromatic ring substituent in **25** showed a drop in band gap energies for smaller radii metals Ni and Zn (3.2 and 3.9 eV) and no change (4.1 eV) for Cd. This could be associated with electron cloud delocalization from Cd to P via S. Out of plane charge transfer may also occur between P and Cd due to an existing electron charge gradient. A red shift observed for Zn(II) complex **30** ($\lambda_{\max} = 260$ nm) could be associated with enhanced out of plane charge transfer given its smaller atomic radius (142 pm) compared to both Ni(II) and Cd(II) (149 and 161 pm, respectively).³⁵⁻³⁶ Both complexes **30** and **31** exhibited considerably large Stokes shifts 3968 and 3217 cm⁻¹ for **30** and **31**, respectively. This could be associated with the dipole moment dependent on metal size, Zn has a smaller radius and correspondingly larger Stokes shifts. This strongly suggests a well-established intramolecular energy transfer that promoted fast relaxation from excited state to the emissive state³⁷ in these two complexes.

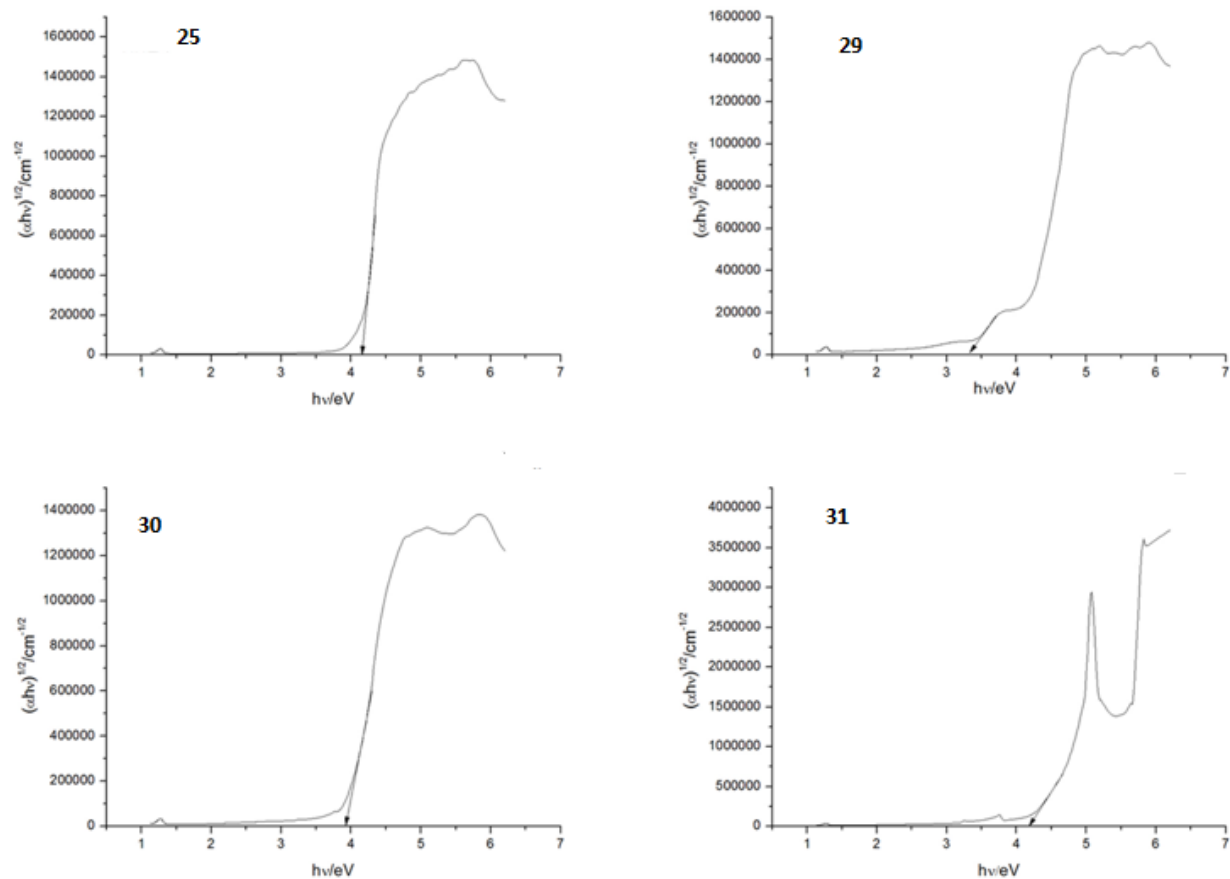


Figure 4.3. Electronic absorption spectra of **25**, **29**, **30**, & **31**,

Following excitation at about 375 nm, it was observed that compound **30** and **31** exhibited strong luminescence in the region of 400–550 nm and these emissions overlap with the excitation spectrum of each compound. The emission and excitation spectra are virtually similar with different peak intensity which may be due to the size of their atomic orbitals. Since they are complexes of metals from the same group (group 12), it can be speculated that size determines relaxation rates, hence, the observed photoluminescence shown in **Figure 4.4**.

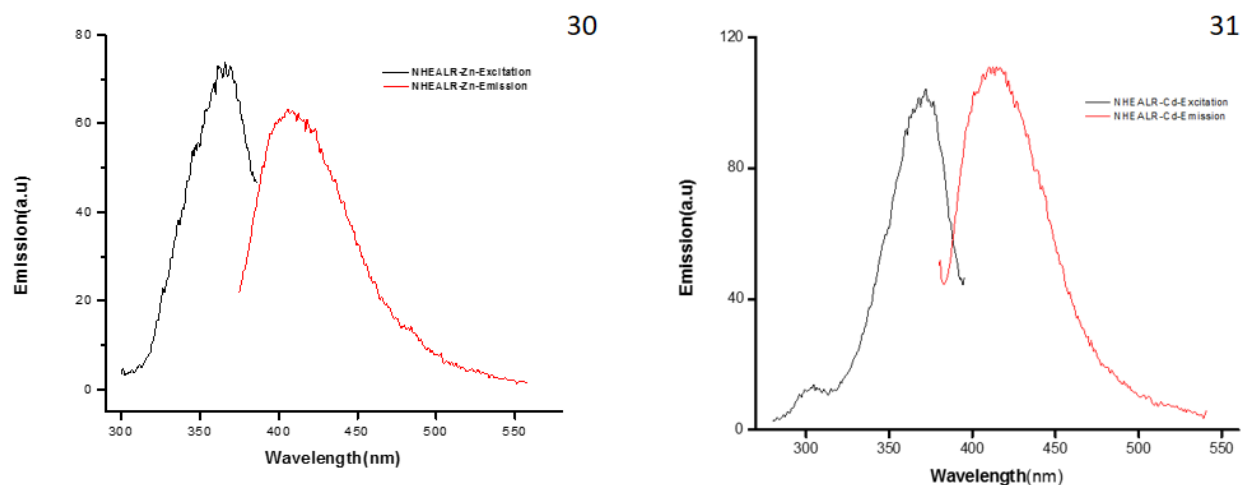


Figure 4.4. Photoluminescent spectra of **30** & **31**

4.1.2.2 Crystal Structure

X-ray structures of compound **24**, **25** and **29** were obtained in this study and XRD quality single crystals were obtained by slow evaporation from THF solution. The molecular structures are shown in **Figure 4.5**, **4.6** and **4.7**. This study reports new crystal structures for zwitterionic ligands having space-separated opposite charges on the same compound (zwitterion), with notably a negative charge on the S atom, and a positive charge on the quaternary N atom. The P–S(1) and P–S(2) bond lengths for **24** ($1.9914(11)^\circ$ and $1.9773(11)^\circ$) and **25** ($1.9789(4)^\circ$ and $1.9902(4)^\circ$) are similar and longer than observed for a P–S double bond (1.94 \AA)³⁸ as would be expected for a delocalized PS₂ fragment. Since the ligand contains both sulfur and nitrogen donor atoms, we proposed that it may employ both N and S for coordination, perhaps forming an octahedral coordination with nickel. But the nickel molecular structure from the zwitterionic ligand showed a close resemblance to the conventional dithiophosphonates' nickel complex coordination mode. The coordination geometry of complex **29** about the Ni(II) center is square planar and is comprised of the four sulfur donor atoms S1, S2, and S3, S4 of the two *N*-ethanol-*N*-methyl dithiophosphonate ligands. This development gave us an indication that other molecular structures of group 12 metal complexes reported in this study with similar ligands will most likely exhibit the traditional dimeric structure as seen in literature.²³

³⁹⁻⁴¹ The ligands **24** and **25** contains both positive and negative charges localised on the N and S atoms, respectively. The anionic S atom portion binds, unsurprisingly, with the metal centre, with the quaternary N cationic portion still intact. But since the final product is neutral and not cationic, as is evident from the crystallographic study, we suggest that the chloride (of the starting Ni(II), Cd(II) and Zn(II)chloride), abstracts one H atom from the N moiety, releasing HCl gas in the process, and leaving a neutral complex.

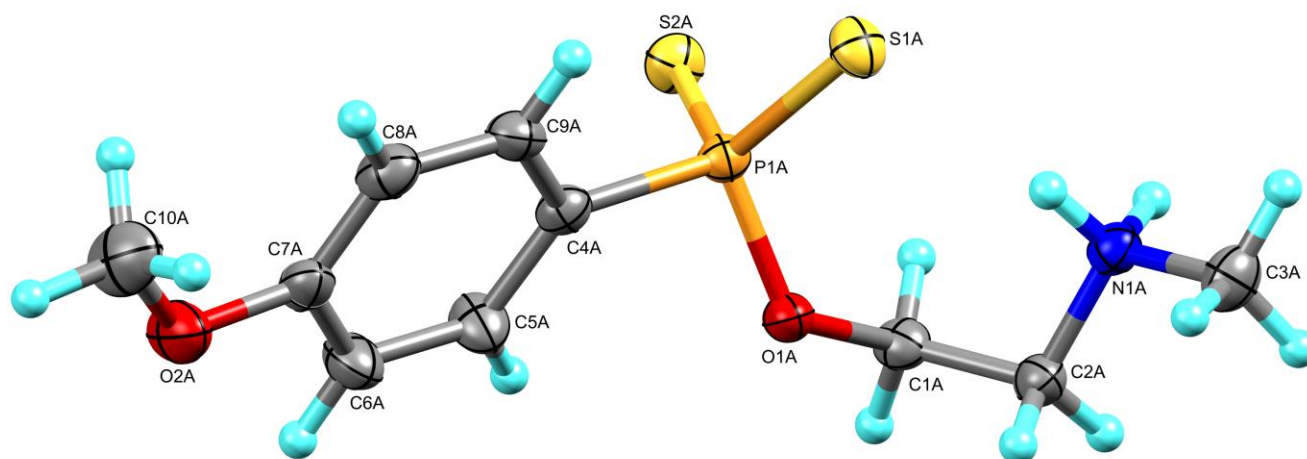


Figure 4.5: ORTEP molecular structure of **24**.

Table 4.1: Selected bond lengths (Å) and angles (°) for **24**

Bond lengths (Å)		Bond angles (°)	
S1A-P1A	1.9914(11)	S2A-P1A-S1A	114.92(5)
S2A-P1A	1.9773(11)	S1A-P1A-O1A	110.05(8)
P1A-O1A	1.6170(19)	C4A-P1A-S1A	110.58(10)
P1A-C4A	1.796(3)	S2A-P1A-C4A	111.47(10)
N1A-C2A	1.488(3)	P1A-O1A-C1A	98.42(11)
N1A-C3A	1.480(3)	P1A-C4A-C5A	120.2(2)
		C2A-N1A-C3A	114.1(2)
		P1A-C4A-C9A	122.1(2)

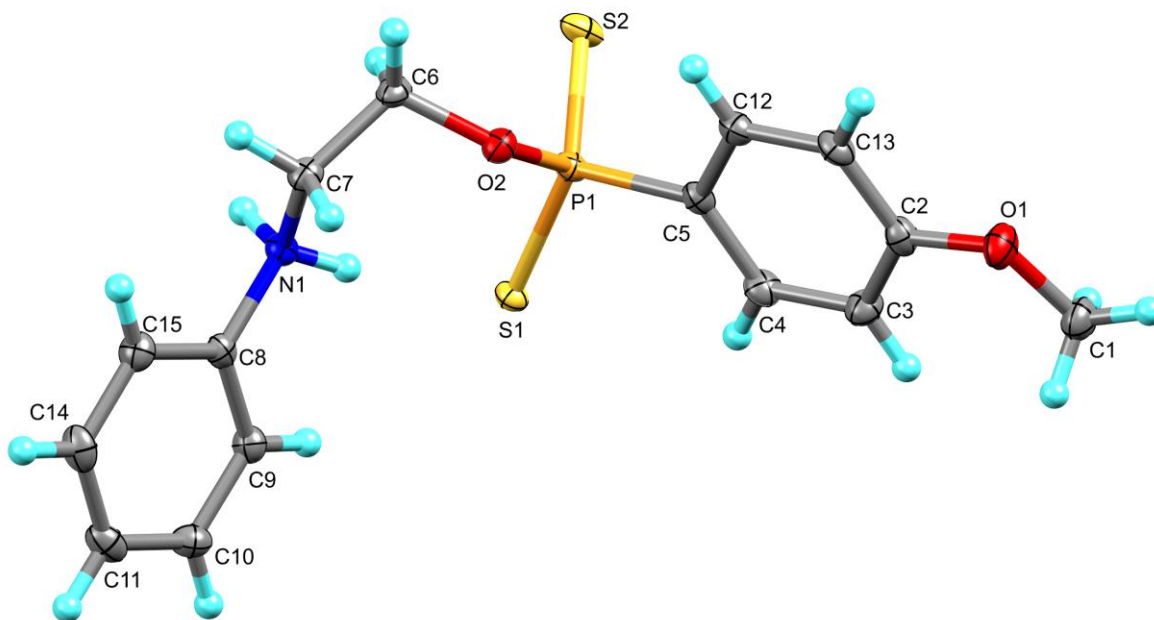


Figure 4.6: ORTEP molecular structure of 25.

Table 4.2: Selected bond lengths (Å) and angles (°) for **25**

Bond lengths (Å)		Bond angles (°)	
P(1)-S(1)	1.9789(4)	S(2)-P(1)-S(1)	114.810(16)
P(1)-S(2)	1.9902(4)	S(1)-P(1)-O(1)	111.15(3)
O(2)-P(1)	1.6223(8)	C(5)-P(1)-S(1)	111.35(4)
P(1)-C(5)	1.8020(11)	S(2)-P(1)-C(5)	112.03(4)
N(1)-C(7)	1.4967(13)	P(1)-O(2)-C(6)	96.85(4)
N(1)-C(8)	1.4719(13)	P(1)-C(5)-C(4)	121.67(8)
		P(1)-C(5)-C(12)	119.32(8)

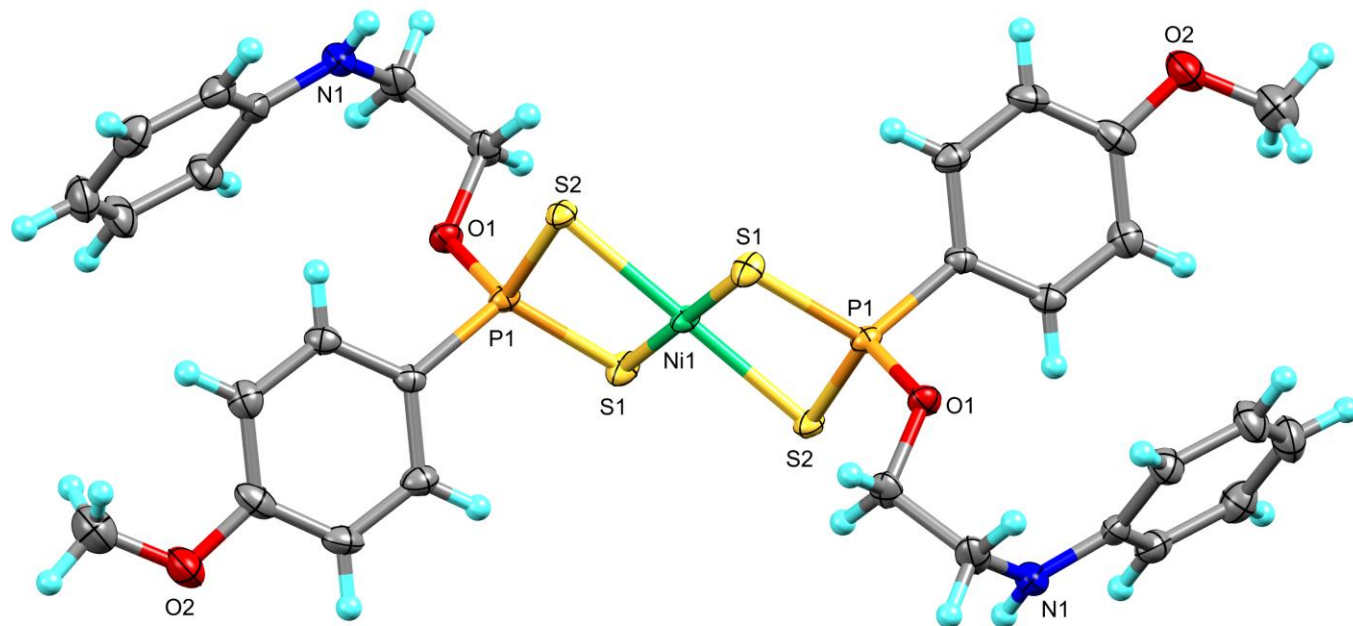


Figure 4.7: ORTEP molecular structure of **29**. Notice the availability of the N-donor atom for further metal coordination.

Table 4.3: Selected bond lengths (Å) and angles (°) for **29**

Bond lengths (Å)		Bond angles (°)	
P(1)-S(1)	2.0030(9)	S(1)-P(1)-S(2)	101.69(4)
P(1)-S(2)	2.0093(8)	O(1)-P(1)-S(2)	112.81(7)
O(1)-P(1)	1.5874(17)	O(1)-P(1)-S(1)	115.32(7)
C(1)-P(1)	1.784(2)	C(1)-P(1)-S(2)	115.15(8)
C(10)-N(1)	1.385(3)	C(1)-P(1)-S(1)	113.37(8)
C(9)-N(1)	1.436(4)	O(1)-P(1)-C(1)	99.19(10)
S(1)-Ni(1)	2.2372(6)	C(8)-O(1)-P(1)	122.47(15)
S(2)-Ni(1)	2.2280(6)	C(2)-C(1)-P(1)	119.14(18)
		N(1)-C(10)-C(15)	123.0(3)
		N(1)-C(9)-C(8)	113.8(2)
		C(6)-C(1)-P(1)	121.2(2)
		S(2)#1-Ni(1)-S(1)	91.66(2)
		S(2)-Ni(1)-S(1)	88.34(2)
		S(1)-Ni(1)-S(1)#1	180.0
		S(2)#1-Ni(1)-P(1)#1	45.325(19)
		S(1)-Ni(1)-P(1)#1	134.87(2)

Table 4.4: Details of X-ray data collection and refinement for compounds **24**, **25** and **29**.

Compound	24	25	29
Formula	C ₁₀ H ₁₆ NO ₂ PS ₂	C ₁₅ H ₁₈ N O ₂ P S ₂	C ₃₀ H ₃₆ NiO ₄ P ₂ S ₄
D _{calc.} / g cm ⁻³	1.400	1.392	1.509
μ/mm ⁻¹	0.512	0.430	0.998
Formula Weight	277.33	339.39	735.507
Colour	yellow	Colorless	clear pale yellow
Shape	chunk	chunk	needle
Max Size/mm	0.20	0.220	0.05
Mid-Size/mm	0.16	0.180	0.120
Min Size/mm	0.13	0.150	0.330
T/K	173(2)	173(2)	173(2)
Crystal System	triclinic	Triclinic	Monoclinic
Space Group	P-1	P -1	P 1 21/c 1
a/Å	8.2940(8)	9.9234(2)	18.7203(5)
b/Å	12.4665(12)	12.7864(3)	11.0739(3)
c/Å	13.9264(14)	13.1830(3)	7.7490(2)
α/°	110.8770(11)	90.2790(10)	90
β/°	99.5892(11)	95.7050(10)	91.4750(10)
γ/°	93.4164(12)	103.2680(10)	90
V/Å ³	1315.5(2)	1619.34(6)	1605.89(7)
Z	4	4	2
Θ _{min} /°	1.598	3.554	2.14
Θ _{max} /°	25.382	28.589°	28.28
Measured Refl.	21421	26838	36020
Independent Refl.	4807	8159	3964
Reflections Used	3498	25.242	3952
R _{int}	0.0597	0.0133	0.0399
Parameters	293	379	201
Restraints	0	0	0
Largest Peak/eÅ ⁻³	0.394	0.404	0.774
Deepest Hole/eÅ ⁻³	-0.293	-0.271	-0.356
GooF	1.047	1.031	1.101
wR ₂ (all data)	0.1003	0.0673	0.0929
wR ₂	0.0894	0.0651	0.0960
R ₁ (all data)	0.0678	0.0262	0.0399
R ₁	0.0414	0.0242,	0.0470
F(000)		712	760

4.1.2.3 Solubility

Information on the solubility of these compounds is essential, especially to choose the applicable solvent for spectroscopic measurements, or generally in various sectors where their application is needed. To this end, a series of qualitative solubility tests were performed on all the compounds **24-31**. A variety of solvents were verified over a wide range of dielectric constants, including protic/aprotic and polar/non-polar solvents. The ligands showed a trend of solubility in protic solvents such as water and ethanol while the complexes showed solubility in nonpolar solvents. The solubility results are shown in **Table 4.5**

Table 4.5. Solubility Data for Compounds **24-31**

Entry	Acetone	CH ₃ CN	EtOH	Hexane	Ether	CH ₂ Cl ₂	Water	THF
24	PS	I	VS	I	I	I	VS	I
25	PS	I	VS	I	I	I	VS	I
26	PS	PS	I	I	PS	S	I	S
27	PS	PS	I	I	PS	S	I	S
28	PS	PS	I	I	PS	S	I	S
29	PS	PS	I	I	PS	S	I	S
30	PS	PS	I	I	PS	S	I	S
31	PS	PS	I	I	PS	S	I	S

Key to table: I = Insoluble (the material was quantitatively recovered after filtration); PS = Partly Soluble (10% of the material dissolved); S = Soluble (80% of the material dissolved); VS = Very Soluble (a clear solution emerged immediately). The solubility data is based on the following experimental criteria: 0.02 g of the compound was dissolved in 1.0 mL of the appropriate solvent and was hard shaken for 5-10 seconds at 23°C

4.2 CONCLUSIONS

The first complexes from new zwitterionic dithiophosphonate ligand are reported. The nucleophilic ring opening reaction of Lawesson's Reagent with amino-alcohols is described for the formation of zwitterionic dithiophosphonate ligand to a leading a variety of new transition metal complexes.

4.3 EXPERIMENTAL

4.3.1 Method

Synthesis of the ligand and complexes were carried out in a standard Schlenk tube (~2 cm diameter) using standard Schlenk line system under a blanket of nitrogen. The Schlenk line is important for these reactions because it requires the minimization of contact with air or other airborne contaminants.

4.3.2 Materials

Lawesson's reagent was prepared from literature procedures.²⁹ All other reagents were used as purchased from Aldrich and used as received. Distilled water was used for the reaction and in all cases where water is required in this work. Dried THF and ether were obtained and used after distillation over sodium wire and benzophenone under a blanket of nitrogen while DCM was collected in the same manner but was distilled over phosphorus (V) pentoxide.

4.3.3 Characterization Methods

¹H and ³¹P NMR spectra were recorded using a Bruker Avance 400 MHz spectrometer. NMR data are expressed in parts per million (ppm) downfield shift referenced internally to the residual proton impurity in the deuterated solvent and are reported as chemical shift position (δ H), relative integral intensity, multiplicity (s = singlet, d = doublet, t = triplet, sept = septet, and m = multiplet), coupling constant J in Hz, and assignment. ³¹P NMR spectra chemical shifts are reported relative to an 85% H₃PO₄ in D₂O external standard solution, all at 298 K. Infrared spectra were recorded in the range 4000–380 cm⁻¹ on a Perkin-Elmer Spectrum 100 FT-IR spectrometer. The yields were determined by performing the reaction in a dry pre-weighed Schlenk tube, weighing the sample after drying. Mass spectra were recorded with a Waters Micromass LCT Premier TOF-MS. The mode of ionization was ESI (electrospray) negative, [M-H]⁻. Samples were prepared to ~2ppm concentration in the desired solvent and infused into the mass spectrometer. The solid-state UV spectra were recorded on a dual beam PerkinElmer Lambda 35 UV-vis spectrophotometer (190-1100 nm) fitted with a Labsphere (RSA-PE-20) integrating sphere in a range of

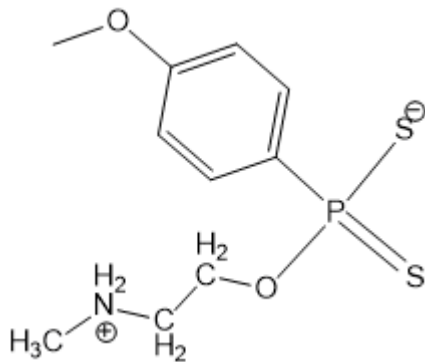
200-800 nm. Solid state luminescence spectra were recorded on a PerkinElmer Ls55 luminescence spectrometer with a front surface accessory.

4.3.4 Crystallography

Single crystal of **24** (yellow chunk-shaped, $0.20 \times 0.16 \times 0.13 \text{ mm}^3$), **25** (colourless, $0.220 \times 0.180 \times 0.150 \text{ mm}^3$) and **29** (was mounted on nylon loop with paratone oil. Data were collected using a Bruker SMART APEX CCD area detector diffractometer equipped with an Oxford Cryosystems low-temperature apparatus operating at $T = 173(2) \text{ K}$. Data were measured using ω and ϕ scans of -0.30° per frame for 10.09 s using MoK α radiation (sealed tube, 50 kV, 40 mA). The total number of runs and images was based on the strategy calculation from the program COSMO. The actually achieved resolution was $\phi = 25.382$. Cell parameters were retrieved using the SAINT⁴² software and refined using SAINT⁴² on 1157 reflections, 5 of the observed reflections. Data reduction was performed using the SAINT⁴² software which corrects for Lorentz polarization. The absorption coefficient (MU) of this material is **24** (0.512), **25** (0.430) and **29** (0.998). The minimum and maximum transmissions are **24**(0.6831 and 0.7452), **25** (0.949 and 0.891) and **29** (0.978 and 0.722). The structure was solved by Charge Flipping using the olex2.solve⁴⁴ structure solution program and refined by Least Squares using version 2014/6 of XL.⁴³ The structure was solved in the space group **24** & **25** (P-1) and **29** (P 1 21/c 1). All non-hydrogen atoms were refined anisotropically. Hydrogen atom positions were calculated geometrically and refined using the riding model. Structure refined by a least squares method on F2, ShellXL-97, incorporated in Olex2⁴⁴. All H-atoms were placed in calculated positions and refined using a riding model.

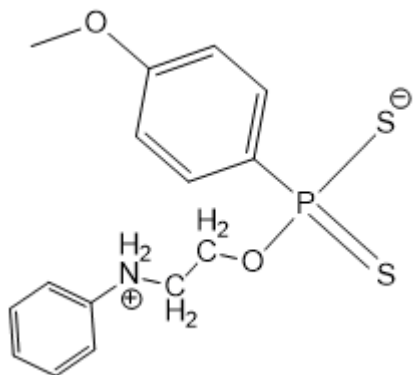
4.3.5 Synthesis of Zwitterionic Ligands

(Methyl-2-aminoethoxy)-4-methoxyphenyl dithiophosphonate Zwitterion (**24**)



Lawesson's Reagent (3.00 g, 7.42 mmol) was treated with N-Methyl-ethanolamine (1.19mL, 14.85 mmol) in a clean and dried Schlenk tube containing dried THF (15ml) at room temperature. The reactants were stirred for half an hour until a clear solution was formed and white precipitate resulted. In a case where precipitates are taking longer to form after a clear solution occurred, the solution was pumped down and hexane was added to precipitate the compound. The precipitate was filtered under vacuum producing a white free flowing powder (3.58 g, 87%). Light-yellow crystals suitable for X-ray analysis were grown by vapour diffusion of diethyl ether into a methanol solution. m.p 176 °C.

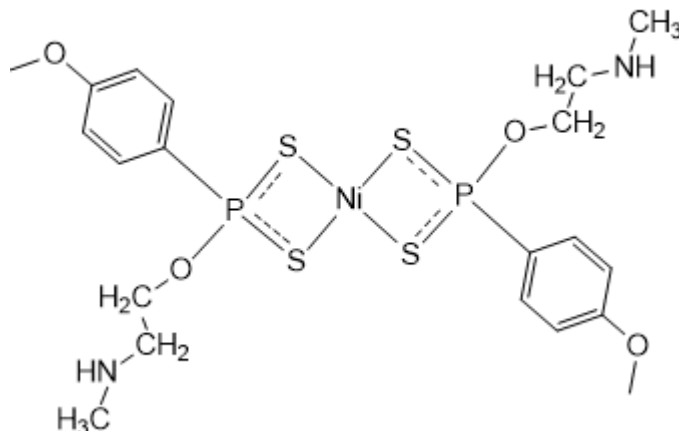
^{31}P -NMR (DMSO):108.43, ^1H -NMR (DMSO) 2.57(3H, s, CH_3N), 3.13 (2H, d, $J=10.49$ Hz, CH_2N), 3.33(2H,br,s,NH), 3.76 (3H, s, ArOMe), 4.00 (2H, d, $J=10.47$ Hz, OCH_2), 6.89 (2H, d, $J=8.88$, 11.17 Hz, *m*-ArH), 7.96 (2H, dd, $J=8.88$, 13.37 Hz, *o*-ArH). ^{13}C -NMR (DMSO) 32.65(1C, s, CH_3N), 48.56 (1C, s, CH_2N), 55.11 (1C, s, ArOCH₃), 57.86(1C, d, $J=66.46$ Hz, CH_2O), 112.28 (2C, d, $J=67.14$ Hz, *m*-ArC-anisole), 131.49 (3C, d, $J=14.29$ Hz, ArC-P & *o*-ArC-anisole), 160.05 (1C, d, $J=2.93$ Hz, *p*-ArC-anisole), Selected IR data (KBr) V/cm^{-1} : 2963(m), 2737(m), 1254 (m), 1021 (s), 643 (s), 543 (s). Mass Spec (ESI): $(2\text{M}+\text{H}_2\text{O})^+$ 577.

(Phenyl-2-aminoethoxy)-4-methoxyphenyl dithiophosphate zwitterion (25)

Lawesson's Reagent (3.0 g, 7.42 mmol) was treated with N-(2-Hydroxyethyl) aniline (1.86 mL, 14.83 mmol) in a clean and dried Schlenk tube containing dried THF (15ml) at room temperature. The reactants were stirred for half an hour until a clear solution was formed and white precipitate resulted. In a case where precipitates are taking longer to form after a clear solution occurred, the solution was

pumped down to dryness and hexane was added to precipitate the compound. The precipitate was filtered under vacuum producing a white free flowing powder (4.22g, 84%). Colourless crystals suitable for X-ray analysis were grown by slow evaporation in a mixture of dichloromethane and methanol solution in the volume ratio 1:1. m.p 159.4°C. $^{31}\text{P-NMR}$ (MeOD): 110.74. $^1\text{H-NMR}$ (MeOD) 3.45(1H,m,NH), 3.66 (2H, d, $J=5.00$ Hz, CH_2N), 3.84 (3H, s, ArOMe), 4.14 (2H, dd, $J=7.56$, 10.13 Hz, OCH_2), 6.90 (2H, d, $J=6.36$, 13.65 Hz, $m\text{-ArH}$), 6.94 (3H, d, $J=6.36$, 11.49 Hz, $p\&o\text{-ArH}$), 7.56 (2H, d, $J=9.45$ Hz, $m\text{-ArH-anisole}$), 8.10 (2H, d, $J=13.65$ Hz, $o\text{-ArH-anisole}$). $^{13}\text{C-NMR}$ (DMSO) 43.35 (1C, d, $J=7.91$ Hz, CH_2N), 55.09 (1C,s,ArOCH₃) 63.02 (1C, d, $J=373.74$ Hz, CH_2O), 112.25 (4C, d, $J=14.13$ Hz, $o\text{-ArC-Ph}$ & $m\text{-ArC-anisole}$), 115.57(2C,s, $m\text{-ArC-Ph}$), 128.82(3C, d, $p\text{-ArC-Ph}$ & ArC-P-anisole), 131.48 (1C, d, $J=12.96$ Hz, $o\text{-ArC-anisole}$), 148.6(1C,s, ArC-N), 159.99 (1C, d, $J=2.93$ Hz, $p\text{-ArC-anisole}$). Selected IR data (KBr) V/cm^{-1} : 2933(m), 2676 (m), 1496(m), 1246 (s), 1060 (s), 643 (s), 541 (s). Mass Spec (ESI): $(\text{M-H})^+$ 338.

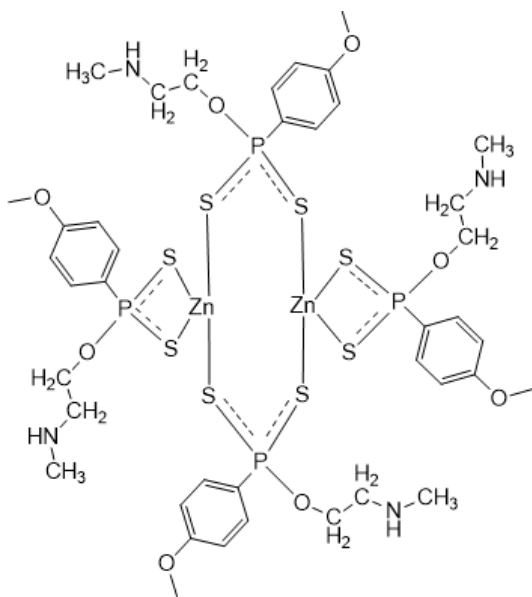
4.3.6 Synthesis of Neutral Ni(II), Cd(II) and Zn(II) Complexes of Zwitterionic Ligand

Bis[(Methyl-2-aminoethoxy)-4-methoxyphenyl dithiophosphonato]Ni (26)

A mixture of NiCl₂·6H₂O (0.21 g, 0.90 mmol) and **24** (0.50 g, 1.80 mmol) in THF (15 ml) was stirred for 3 hours at room temperature. The solvent was removed under reduced pressure and brown sticky solid resulted. Water was added and stirred for few minutes to precipitate the product as free flowing brown solid (0.37

g, 68%). m.p 144^oC. ³¹P-NMR (MeOD):108.39, ¹H-NMR (MeOD) 2.82 (3H, s, CH₃N), 3.34 (2H, d, J=5.00 Hz, CH₂N), 3.90 (3H, s, ArOMe), 4.22 (2H, m, J=8.13, 10.07 Hz, OCH₂), 7.01 (1H, dd, J=8.88, 12.65 Hz, *m*-ArH), 8.13 (1H, dd, J=8.88, 13.65 Hz, *o*-ArH). ¹³C-NMR (DMSO) 33.44(1C, s, CH₃N), 55.63 (1C, s, ArOCH₃), 58.36 (1C,d, J=4.92 Hz CH₂N), 78.91(1C, d,J=14.85Hz, CH₂O), 112.74 (2C, d, J=14.40 Hz, *m*-ArC-anisole), 132.07 (2C, d, J=13.22 Hz, *o*-ArC-anisole), 160.59 (1C, d, J=2.93 Hz, *p*-ArC-anisole). Selected IR data (KBr) *V*/cm⁻¹: 3389(m), 1597(m), 1252 (m), 1019 (s), 646 (s), 536 (s). Mass Spec (ESI): (M)⁺ 609

Bis [(Methyl-2-aminoethoxy)-4-methoxyphenyl dithiophosphonato] Zn (27)



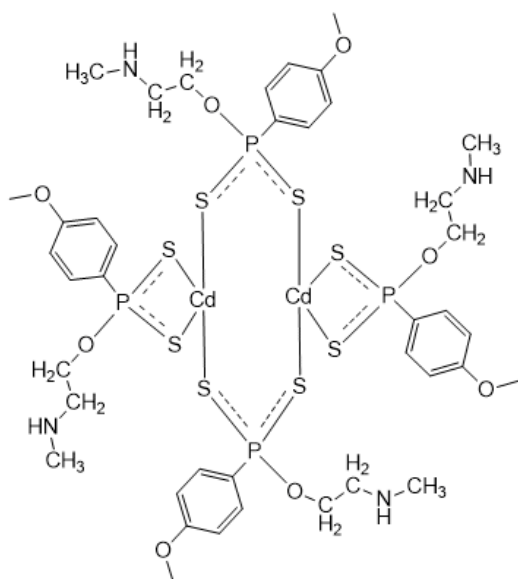
A mixture of anhydrous ZnCl_2 (0.12 g, 0.90 mmol) and **24** (0.50 g, 1.80 mmol) in THF (15 ml) was stirred for 3 hours at room temperature. The solvent from the colourless solution was removed under reduced pressure and white sticky solid resulted. Water was added and stirred for few minutes to precipitate the product, after filtration, as free flowing white solid (0.35 g, 65%). m.p 156°C . ^{31}P -NMR (MeOD): 108.35, ^1H -NMR (MeOD) 2.82 (3H, s, CH_3N), 3.34 (2H, d, $\text{J}=5.00$ Hz, CH_2N), 3.90 (3H, s, ArOMe), 4.22 (2H, m,

$\text{J}=8.13, 10.07$ Hz, OCH_2), 7.01 (1H, dd, $\text{J}=8.88, 14.29$ Hz, *m*-ArH), 8.13 (1H, dd, $\text{J}=8.88, 13.65$ Hz, *o*-ArH).

^{13}C -NMR (DMSO) 33.44(1C, s, CH_3N), 55.13 (1C, s, ArO CH_3), 64.88(1C, s, CH_2N), 78.91(1C, d, $\text{J}=14.85$ Hz, CH_2O), 112.65 (2C, d, $\text{J}=14.85$ Hz, *m*-ArC-anisole), 131.65 (2C, d, $\text{J}=14.29$ Hz, *o*-ArC-anisole), 160 (1C, d, $\text{J}=2.93$ Hz, *p*-ArC-anisole). Selected IR data (KBr) V/cm^{-1} : 3367(m), 2933(m), 1253

(m), 1019 (s), 620 (s), 520 (s). Mass Spec (ESI): $(1/2\text{M}-\text{H})^+$ 617

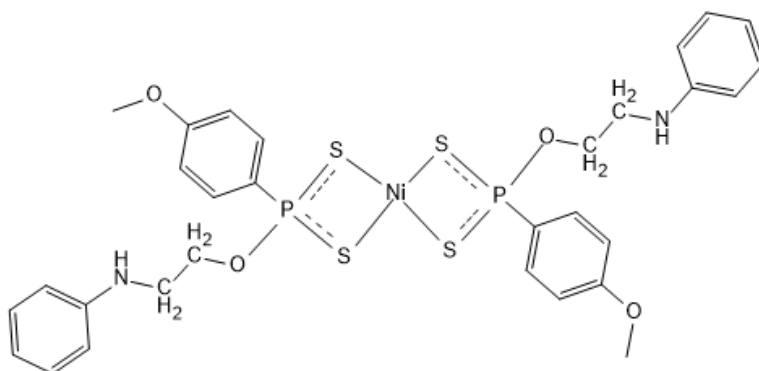
Bis [(Methyl-2-aminoethoxy)-4-methoxyphenyl dithiophosphonato]Cd (28)



A mixture of $\text{CdCl}_2 \cdot \text{H}_2\text{O}$ (0.18g, 0.90 mmol) and **24** (0.50 g, 1.80 mmol) in THF (15 ml) was stirred for 3h at room temperature. The solvent was removed under reduced pressure and white sticky solid resulted. Water was added and stirred for few minutes to precipitate, after filtration, the product as free flowing white solid (0.36 g, 61%). m.p 152° . ^{31}P -NMR (DMSO):106.12, ^1H -NMR (DMSO) 2.57(3H, s, CH_3N), 3.13 (2H, d, $J=10.49$ Hz, CH_2N), 3.76

(3H, s, ArOMe), 4.00 (2H, m, $J=9.73, 10.47$ Hz, OCH_2), 6.89 (2H, dd, $J=8.88, 11.17$ Hz, $m\text{-ArH}$), 7.96 (2H, dd, $J=8.88, 13.37$ Hz, $o\text{-ArH}$). ^{13}C -NMR (DMSO) 33.23(1C, s, CH_3N), 55.75 (1C, s, ArOCH₃), 58.95(1C, s, CH_2N), 61.5(1C, d, $J=14.85$ Hz, CH_2O), 113.64 (2C, d, $J=14.85$, $m\text{-ArC-anisole}$), 132.14 (2C, d, $J=13.32$ Hz, $o\text{-ArC-anisole}$), 161.31 (1C, d, $J=2.93$ Hz, $p\text{-ArC-anisole}$). Selected IR data (KBr) V/cm^{-1} : 3367(m), 2933(m), 1597(m), 1252 (m), 1019 (s), 620 (s), 520 (s). Mass Spec (ESI): $(1/2\text{M-H})^+$ 667

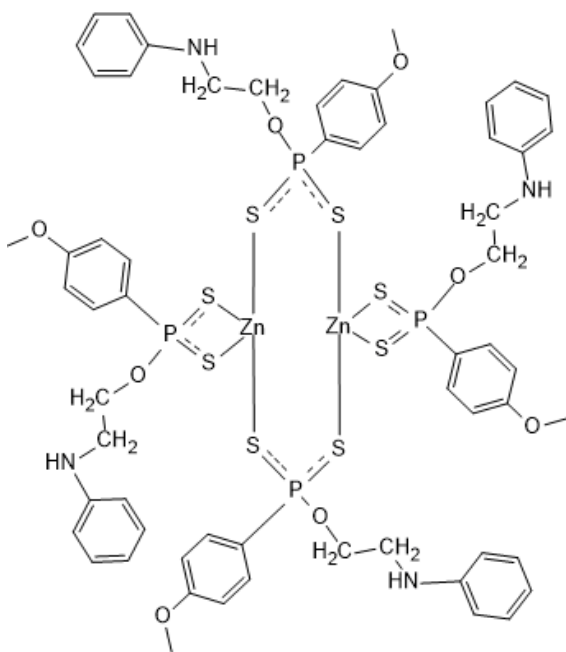
Bis [(Phenyl-2-aminoethoxy)-4-methoxyphenyl dithiophosphonato] Ni (29)



A mixture of $\text{NiCl}_2 \cdot 6\text{H}_2\text{O}$ (0.18 g, 0.74 mmol) and **25** (0.50 g, 1.47 mmol) in THF (15 ml) was stirred for 3h at room temperature. The solvent was removed under reduced pressure

and brown sticky solid resulted. Water was added and stirred for few minutes to precipitate the product as free flowing brown solid (0.36 g, 67%). Purple crystals suitable for X-ray analysis were grown by vapour diffusion of hexane into a dichloromethane solution. m.p 154.6°C . ^{31}P -NMR (CDCl_3) 103.87, ^1H -NMR (CDCl_3) 3.42 (1H,m,NH), 3.58 (2H, t, $J=5.38,10.47$ Hz, CH_2N), 3.89 (1H,s, CH_3) 4.58 (2H, d, $J=5.00$ Hz, OCH_2), 6.70 (2H, m, $J=7.28, 11.17$ Hz, $m\text{-ArH}$), 7.01 (3H, m, $J=7.28, 11.17$ Hz, $p\&o\text{-ArH}$), 7.21 (2H, m, $J=7.70, 11.17$ Hz, $m\text{-ArH-anisole}$), 7.95 (1H, dd, $J=7.70, 13.68\text{Hz}$, $o\text{-ArH-anisole}$). ^{13}C -NMR (CDCl_3) 43.89 (1C, d, $J=7.91$ Hz, CH_2N), 55.53 (1C,s, ArOCH_3) 65.45(1C, d, $J=373.74$ Hz, CH_2O), 114.04 (4C, d, $J=17.08$ Hz, $o\text{-ArC-Ph}$. & $m\text{-ArC-anisole}$), 117.91(2C,s, $m\text{-ArC-Ph}$), 129.36 (3C, d, $p\text{-ArC-Ph}$. & ArC-P), 131.67 (1C,d, $J=15.50$ Hz, $o\text{-ArC-anisole}$), 147.55 (1C,s, $p\text{-ArC-N}$), 163.14 (1C, d, $J=2.93$ Hz, $p\text{-ArC-anisole}$). Selected IR data (KBr) V/cm^{-1} : 3386 (m), 2934(b), 2676 (m), 1593(s), 1253 (s), 1011 (s), 746 (s), 549 (s) Mass Spec (ESI): $(\text{M}+\text{H})^+$ 735

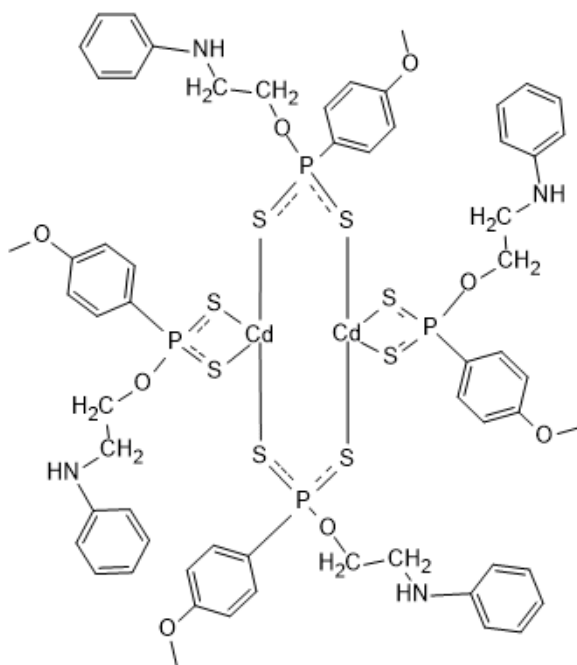
Bis [(Phenyl-2-aminoethoxy)-4-methoxyphenyl dithiophosphonato] Zn (30)



A mixture of anhydrous ZnCl_2 (0.10 g, 0.74 mmol) and **25** (0.50g, 1.47 mmol) in THF (15 ml) was stirred for 3h at room temperature. The solvent was removed under reduced pressure and purple sticky solid resulted. Water was added and stirred for few minutes to precipitate the product as free-flowing purple solid (0.32 g, 59%). m.p 156.2^o. ³¹P-NMR (CDCl_3) 106.07, ¹H-NMR (CDCl_3) 3.58 (2H, t, J=5.38 Hz, CH_2N), 3.89(1H,s, CH_3) 4.58 (2H, d, J=5.00 Hz, OCH_2), 6.70 (2H, m, J=7.88, 11.17 Hz, *m*-ArH), 7.03 (3H, m, J=7.28, 11.17 Hz, *p*&*o*-ArH),

7.21 (2H, m, J=7.70.11.34 Hz, *m*-ArH-anisole), 7.93 (1H, dd, J=7.70, 13.68Hz, *o*-ArH-anisole). ¹³C-NMR (DMSO) 43.35 (1C, d, J=7.91 Hz, CH_2N), 55.09 (1C,s, ArOCH_3) 63.02 (1C, d, J=373.74 Hz, CH_2O), 112.25 (4C, d, J=14.13 Hz, *o*-ArC-Ph. &*m*-ArC-anisole), 115.57 (1C,s,*m*-ArC-Ph), 128.82 (3C, d, *o*-ArC-Ph. & ArC-P- anisole), 131.48 (1C, d, J=12.96 Hz, *o*-ArC-anisole), 148.6(1C,s, ArC-N), 159.99 (1C, d, J=2.93 Hz, *p*-ArC-anisole). Selected IR data (KBr) V/cm^{-1} : 3371(m), 2939(b), 1593(s), 1498(m), 1253 (s), 1019 (s), 748 (s), 539 (s). Mass Spec (ESI): $(1/2\text{M}-\text{H})^+$ 741, $(1/2\text{M}-\text{C}_{15}\text{H}_{18}\text{NO}_2\text{S})^+$ 480

Bis [(Phenyl-2-aminoethoxy)-4-methoxyphenyl dithiophosphonato] Cd (31)



A mixture of $\text{CdCl}_2 \cdot \text{H}_2\text{O}$ (0.15 g, 0.74 mmol) and **1** (0.50 g, 1.47 mmol) in THF (15 ml) was stirred for 3h at room temperature. The solvent was removed under reduced pressure and purple sticky solid resulted. Water was added and stirred for few minutes to precipitate the product as free-flowing purple solid (0.30 g, 64%). m.p 160.3°C . ^{31}P -NMR (CDCl_3) 109.14, ^1H -NMR (CDCl_3) 3.25 (2H, t, $J=5.38$ Hz, CH_2N), 3.79(1H,s, CH_3) 4.17 (2H, d, $J=5.00$ Hz, OCH_2), 6.59 (2H, m, $J=7.28,11.57$ Hz, $m\text{-ArH}$), 6.99 (3H, m, $J=5.36,7.88$, Hz, $p\&o\text{-ArH}$),

7.07 (2H, m, $J=7.70, 16.13$ Hz, $m\text{-ArH-anisole}$), 7.88 (1H, dd, $J=7.70, 14.13$ Hz, $o\text{-ArH-anisole}$). ^{13}C -NMR (DMSO) 43.10(2C, d, $J=8.50$ Hz, CH_2N), 55.26 (1C,s, ArOCH_3) 63.02 (2C,d, $J=7.02$ Hz, CH_2O), 112.25 (4C, d, $J=14.13$ Hz, $o\text{-ArC-Ph. } \& m\text{-ArC-anisole}$), 115.75(1C,s, $o\text{-ArC-Ph}$),128.82(3C, d, $m\text{-ArC-Ph. } \& \text{ArC-P}$), 132.43 (1C, d, $J=11.38$ Hz $o\text{-ArC-anisole}$), 148.87(1C,d, ArC-N), 161.04 (1C, d, $J=2.93$ Hz, $p\text{-ArC-anisole}$). Selected IR data (KBr) V/cm^{-1} : 2943 (b), 1593(s), 1498(m), 1253 (s), 1020 (s), 647 (s), 536 (s). Mass Spec (ESI): $(\text{M}+\text{H})^+ 791(1/2\text{M}-\text{C}_{15}\text{H}_{18}\text{NO}_2\text{S})^+ 530$

4.4 REFERENCES

1. Harrison, P. G.; Begley, M. J.; Kikabhai, T.; Killer, F., *J. Chem.Soc. Dalton Trans.* **1986**, (5), 929-938.
2. Harrison, P. G.; Kikabhai, T., *J. Chem.Soc. Dalton Trans***1987**, (4), 807-814.
3. Shabana, R.; Osman, F. H.; Atrees, S. S., *Tetrahedron* **1994**, 50 (23), 6975-6988.
4. Byrom, C.; Malik, M. A.; O'Brien, P.; White, A. J. P.; Williams, D. J., *Polyhedron* **2000**, 19 (2), 211-215.
5. Aragoni, M. C.; Arca, M.; Devillanova, F. A.; Ferraro, J. R.; Isaia, F.; Lelj, F.; Lippolis, V.; Verani, G., *Can. J. Chem.* **2001**, 79 (10), 1483-1491.
6. Comel, A.; Kirsch, G.; Paquer, D., *Phosphorus, Sulfur, Silicon Relat.Elem.* **1994**, 89 (1-4), 25-29.
7. Karakus, M.; Aydogdu, Y.; Celik, O.; Kuzucu, V.; Ide, S.; Hey-Hawkins, E., *Z.Anorg.Allg.Chem.*2007, 633 (3), 405-410.
8. Van Zyl, W. E., *Comments Inorg. Chem.* **2010**, 31 (1-2), 13-45.
9. Van Zyl, W. E.; Fackler, J. P., *Phosphorus, Sulfur, and Silicon Relat.Elem.* **2000**, 167 (1), 117-132.
10. Gray, I. P.; Slawin, A. M. Z.; Woollins, J. D., *Dalton Trans.* **2004**, (16), 2477-2486.
11. Haiduc, I.; Sowerby, D. B.; Lu, S.-F., *Polyhedron* **1995**, 14 (23-24), 3389-3472.
12. Haiduc, I.; Sowerby, D. B., *Polyhedron* **1996**, 15 (15), 2469-2521.
13. Albano, V. G.; Aragoni, M. C.; Arca, M.; Castellari, C.; Demartin, F.; Devillanova, F. A.; Isaia, F.; Lippolis, V.; Loddo, L.; Verani, G., *Chem. Commun.***2002**, (11), 1170-1171.
14. Karakus, M.; Lönnecke, P.; Yakhvarov, D.; Hey-Hawkins, E., *Z.Anorg.Allg.Chem* **2004**, 630 (10), 1444-1450.

15. Karakus, M.; Lönnecke, P.; Hey-Hawkins, E., *Z. Anorg.Allg.Chem* **2004**, 630 (8-9), 1249-1252.
16. Gray, I. P.; Milton, H. L.; Slawin, A. M. Z.; Woollins, J. D., *Dalton Trans.* **2003**, (17), 3450-3457.
17. Foreman, M. R. S. J.; Slawin, A. M. Z.; Woollins, J. D., *J. Chem.Soc. Dalton Trans.* **1996**, (18), 3653-3657.
18. García-Montalvo, V.; Toscano, R. A.; Badillo-Delgado, A.; Cea-Olivares, R., *Polyhedron* **2001**, 20 (3-4), 203-208.
19. Gryaznov, P. I.; Naumova, O. E.; Alimova, D. R.; Krivolapov, D. B.; Litvinov, I. A.; Al'fonsov, V. A., *Russ. J. General Chem.* **2005**, 75 (11), 1744-1749.
20. Karakus, M.; Lönnecke, P.; Hey-Hawkins, E., *Polyhedron* **2004**, 23 (14), 2281-2284.
21. http://msdssearch.dow.com/PublishedLiteratureDOWCOM/dh_005c/0901b8038005c47e.pdf?filepath=amines/pdfs/noreg/111-01408.pdf&fromPage=GetDoc. (accessed on 2 Dec. 2016).
22. <https://pubchem.ncbi.nlm.nih.gov/compound/N-Methylethanolamine#section=Classification>. (accessed on 2 Dec. 2016).
23. Gray, I. P.; Milton, H. L.; Slawin, A. M. Z.; Woollins, J. D., *Dalton Trans* **2004**, 16. 2477-2486
24. Foreman, M. R. S. J.; Slawin, A. M. Z.; Woollins, J. D., *J Chem. Soc Dalton Trans* **1999**, 7, 1175-1184
25. Aragoni, M. C.; Arca, M.; Demartin, F.; Devillanova, Francesco A.; Graiff, C.; Isaia, F.; Lippolis, V.; Tiripicchio, A.; Verani, G., *Eur. J.Inorg.Chem.* **2000**, 2000 (10), 2239-2244.
26. Çilgi, G. K.; Karakuş, M.; Ak, M., *Synth. Metals* **2013**, 180, 25-31.
27. Qian-Feng, W. X ; *Eur. J.Inorg.Chem* **2011** 30 (3), 380-383

28. Sağlam, E. G.; Erden, S.; Tutsak, Ö.; Eskiköy Bayraktepe, D.; Yazan Durmuş, Z.; Dal, H.; Ebinç, A., *Phosphorus, Sulfur, Silicon .Relat.Elem.* **2017**,119, 322-329
29. Van Zyl, W. E.; Fackler, J. P., *Phosphorus, Sulfur, Silicon Relat Elem* **2000**, 167 , 117-132.
30. Karakus, M.; Lönnecke, P.; Hey-Hawkins, E., *Polyhedron* **2004**, 23, 2281-2284
31. van Zyl, W. E.; Woollins, J. D., *Coord. Chem.Rev.* **2013**, 257 (3–4), 718-731.
32. Pretsch, E.; Buhlmann, P.; Badertscher, M., *Structure Determination of Organic Compounds*. Springer: Springer-Verlag Berlin Heidelberg, **2009**; 4, 120.
33. Lefferts, J.; Molloy, K.; Zuckerman, J.; Haiduc, I.; Curtui, M.; Guta, C.; Ruse, D., *Inorg.Chem.***1980**, 19 (10), 2861-2868.
34. Lai, R., Universita' degli Studi di Cagliari, Doctoral thesis, **2016**.
35. Mantina, M.; Chamberlin, A. C.; Valero, R.; Cramer, C. J.; Truhlar, D. G., *J.Phys.Chem. A* **2009**, 113 (19), 5806-5812.
36. Rudzinski, W.; Behnke, G. T.; Fernando, Q., *Inorg.Chem.***1977**, 16 (5), 1206-1210.
37. Rost, W. D. F., *Fluorescence microscopy*. Cambridge University Press 1992; p 267.
38. Jain, V. K.; Varghese, B., *J.Organomet.Chem.* **1999**, 584 (1), 159-163.
39. Casas, J. S.; García-Tasende, M. S.; Sánchez, A.; Sordo, J.; Vázquez-López, E. M.; Castellano, E. E.; Zukerman-Schpector, J., *Inorg.Chimic. Acta* **1994**, 219 (1), 115-119.
40. Johnson, A.; O'Connell, L. A.; Clarke, M. J., *Inorg.Chimic. Acta* **1993**, 210 (2), 151-157.
41. Gray, I. P.; Milton, H. L.; Slawin, A. M. Z.; Woollins, J. D., *Dalton Trans* **2003**, 17, 3450-3457
42. *Software for the Integration of CCD Detector System Bruker Analytical X-ray Systems, Bruker axs, Madison, WI (2012)*.

43. Sheldrick, G. M., *Acta Cryst.*, (2008) *A64*, 339-341.
44. O.V. Dolomanov and L.J. Bourhis and R.J. Gildea and J.A.K. Howard and H. Puschmann, *J. Appl. Cryst.*, (2009), *42*, 339-341.

CHAPTER 5

DYE SENSITIZED SOLAR CELL APPLICATION OF FERROCENYL DITHIOPHOSPHONATE TRANSITION METAL COMPLEXES

5.1 BACKGROUND

The world's demand for energy is expected to double its current consumption by the year 2050 and triple by the end of the century.¹ A supply of inexhaustible energy is sought for global political, economic and environmental stability. Global warming and environmental pollution caused by the high consumption rate of fossil fuels have led to a greater focus on renewable energy sources and sustainable development. The development of carbon-free sources of energy that are scalable to meet increasing societal demands is, therefore, one of the major scientific challenges of this century. Hence, to replace fast depleting fossil fuels and its hazards arising from increasing global energy demands led to the search for clean alternative energy sources. Solving this challenge has placed solar cells, also called photovoltaic cells, at the center of an ongoing research effort to utilize the clean, cheap and renewable energy.²⁻³

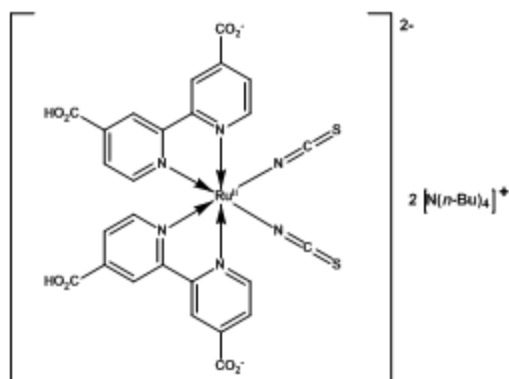
The source of all forms of energy on our planet derives from the sun. The energy radiated by the sun is about 10,000 times the amount currently needed on Earth. Scientific efforts to efficiently trap sunlight and converting it directly into electricity has been a challenge for the last few decades and will be a major breakthrough if achieved. Researchers all over the world are focusing on the development of highly efficient long-term durable solar cells. Recently, organic solar cells and dye-sensitized solar cells gained special attention because of their high photon-to-electricity conversion efficiency, ease of fabrication and low cost involved in mass production compared to the traditional photo-electrochemical cells.⁴⁻⁵

There is an increasing interest in developing metal coordination complexes (MCCs) for photovoltaic performance applications⁶⁻⁷ and the major difficulty in improving the efficiency of photovoltaic energy

conversion lies in the spectral mismatch between the energy distribution of photons in the incident solar spectrum and the bandgap of a semiconductor material⁸.

Co-sensitization is an effective way to improve the device performance through a combination of two or more dyes sensitized by the same semiconductor film together, extending the light harvesting spectrum.^{7,9} To satisfy requirement and with the aim of searching for efficient sensitizers, many new commercial¹⁰⁻¹³ and synthetic dyes (organic compounds and inorganic metal complexes)^{12, 14-17} have emerged and have been studied for spectral sensitization of wide-band-gap semiconductor electrodes. The light-harvesting properties of the homo- and heteroleptic complexes of ferrocenyl dithiocarbamates and their organomercury (II) derivatives have previously been reported.^{12, 17-18} The investigation of ferrocenyl dithiocarbamates as possible systems to be implemented in DSCs was also recently reported.¹⁹ Additionally, other derivatives like hydroxyl, carboxylic, and aldehyde, as well as quinoxaline derivatives of the ferrocenyl systems with different anchors is also found.²⁰ The ferrocenyl-substituted triphenylamine-based donor–acceptor dyes for use in dye-sensitized solar cells was recently reported by Misra et al.²¹

Ferrocenyl systems have been reported to have a characteristic electronic absorption band at around 450 nm²²⁻²³ and therefore it possesses the potential to compensate for weak absorption of N719 dyes in the lower wavelength region. In the quest for new and low-cost DSC materials, we report the first ferrocenyl dithiophosphonate transition-metal complexes as potential high-efficiency co-sensitizers in dye-sensitized solar cells.



N719- dye

5.2 RESULT AND DISCUSSIONS

5.2.1 Optical Properties of the Co-Sensitizers

The optical properties were determined by use of UV-vis absorption experiments carried out on **18–22** in both solution and solid state. All the compounds showed major absorption bands in the region of 450–480 nm with the vibronic structure assignable to π – π^* transition (**Fig 5.1**). The absorption bands of the nickel(II) complex also showed small low-energy absorption bands at around 680 nm which tails to 980 nm. Characteristically, the electronic spectrum of these complexes should show longco-wavelength ligand field (LF) and ligand-metal charge transfer (LMCT) absorptions²⁴ and metal-to-ligand charge-transfer.²⁵ In the LMCT complexes, the transfer of electrons arise from molecular orbitals with metal-like character to those with ligand-like character.²⁵⁻²⁶ For complexes with ligands having low-lying π^* orbitals, transitions will mostly occur at low energy if the metal ion has a low oxidation state, for instance, nickel(II) in our case because its d orbitals are relatively high in energy. In these complexes, the low tailing energy could also be attributed to the availability of low-lying empty 3d orbitals.²⁷ Because the π^* orbitals of the Cp ligand are located at rather high energies, it is essentially a CT donor and hardly a CT acceptor. Low-energy LMCT transitions occur if Cp coordinates to oxidizing metals.²⁸⁻³¹ By inspection, there is a possibility of outer sphere charge transfer (OSCT) excitations which are related to MLCT³⁰ in these complexes. It is known that inter ligand (IL) transitions involving the Cp ligand do not occur at low energies, however, in mixed ligand complexes an additional ligand may provide IL transitions at low energies.^{30, 32-33} It can be argued that low-lying MLCT and ligand-centered (π – π^*) excited states of these complexes are fairly long-lived to participate in electron transfer processes.³⁴ The participation of phosphorus cannot be ignored. Phosphorus accepts electrons from metal π or d orbitals into P–C σ^* anti-bonding orbitals that have π symmetry.³⁵ The P atom bonds to electron-rich metal atoms, the corresponding π -back bonding would be expected to lengthen P–C bonds as P–C σ^* orbitals become populated by electrons.³⁵⁻³⁷ Consequently, the UV-vis absorption is expected to move to a much longer wavelength as observed in this work. In these complexes, the highest occupied molecular orbitals (HOMO) are in the Cp σ -bond while the lowest unoccupied

molecular orbitals (LUMO) are anti-bonding with regard to the P-S-M bond. Hence, The longest wavelength absorption can be assigned to a $d \sigma^*$ transition terminating at the bridging sulfur atoms³⁸.

These compounds have broad absorption spectra with intense LLCT, LMCT and MLCT bands overlapping the solar spectrum, affording suitable photoelectrochemical properties for application in solar cells. The hydroxy groups provide an avenue for strong adsorption of the dye to the TiO_2 surface and the necessary electronic coupling between the charge-transfer excited states (CTES) of the sensitizers and the wave function of the semiconductor conduction band. Consequently, dye excitation with visible light is likely to produce very fast electron transfer through the appended groups to the semiconductor.³¹ The energy band gaps for the complexes was estimated from their UV-vis spectra by use of Tauc plots (**Table 5.1**).

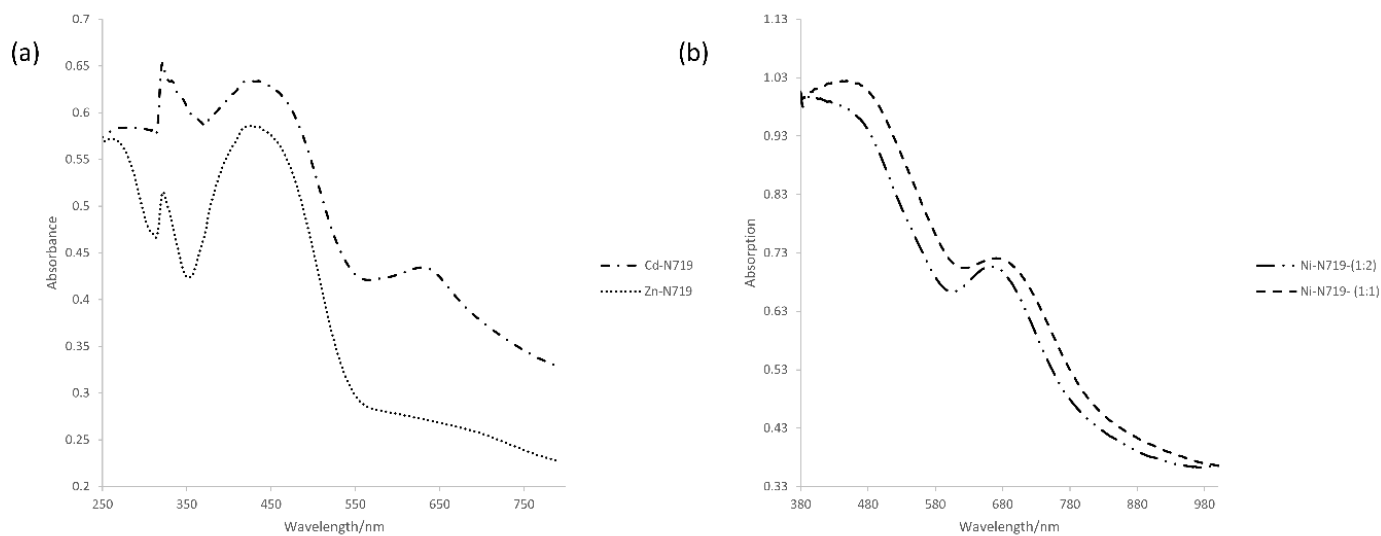


Figure 5.1. Electronic absorption spectra of the co-sensitizers

5.2.2 Electrochemical Properties of Co-Sensitizers

In DSCs, energy matching is of significance and cyclic voltammetry (CV) was employed in this study to determine the highest occupied molecular orbital (HOMO) levels and the lowest unoccupied molecular orbital (LUMO) levels of our new complexes. Experimental data and electrochemical properties of Ni, Zn, and Cd complexes are reported in **Table 5.1**.

Table 5.1. Experimental data and electrochemical properties of Ni, Zn, and Cd complexes

Dye	$\lambda_{\text{abs}}^{\text{a}}$ (nm)	ϵ^{b} ($\text{M}^{-1}\text{cm}^{-1}$)	E_{0-0}^{ci} (eV)	E_{0-0}^{cii} (eV)	$E_{\text{ox}}/\text{Vvs.SCE}^{\text{d}}$	$E_{\text{HOMO}}^{\text{e}}$ (eV)	$E_{\text{LUMO}}^{\text{e}}$ (eV)
Ni (1:1)	462	102050	1.85	2.68	0.35	-4.75	-2.90
Ni (1:2)	406	99620	2.00	3.06	0.53	-4.93	-2.93
Zn	441	58140	2.25	2.82	0.39	-4.79	-2.54
Cd	439	63220	2.15	2.82	0.43	-4.83	-2.68

^a Absorption recorded in a DMSO solution (10^{-5} M) at room temperature. ^b The molar absorptivity calculated from absorption spectra. ^{ci} Optical band gap. ^{cii} Theoretical bandgap. ^d The first oxidation potentials of complexes obtained from CV measurement. ^e The values of E_{HOMO} and E_{LUMO} were calculated with the following formula:³⁹

$$E_{\text{HOMO}} (\text{eV}) = -e (E_{\text{ox}}/\text{Vvs.SCE}^{\text{d}} + 4.4); E_{\text{LUMO}} (\text{eV}) = E_{\text{HOMO}} (\text{eV}) + E_{0-0}^{\text{ci}} (\text{eV})$$

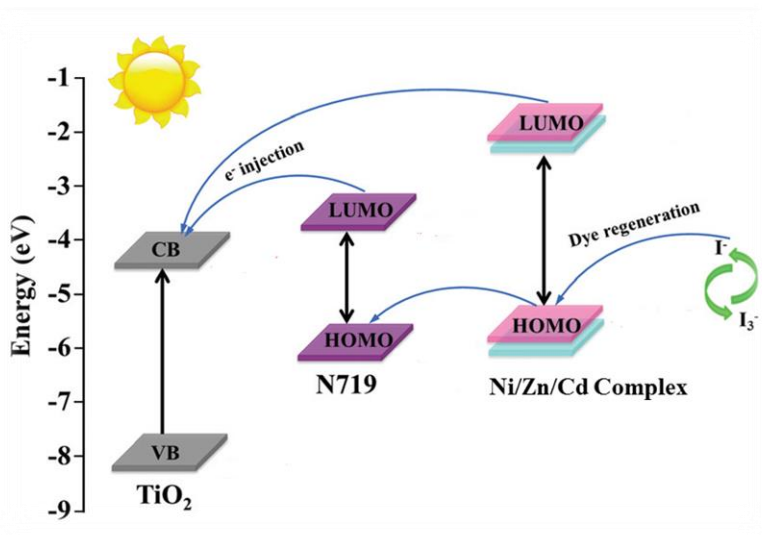


Figure 5.2: Typical schematic energy diagram of HOMO and LUMO levels for the co-sensitizers compared to the energy levels calculated for TiO₂⁷.

The HOMO values for Ni, Zn, and Cd complexes are calculated to be -4.75 , -4.93 , -4.79 and -4.83 eV, while the LUMO levels are calculated to be -2.90 , -2.93 , -2.54 and -2.68 eV.^{7,39} The LUMO level of a sensitizer should be above the conduction band (CB) of the TiO₂ semiconductor (-4.40 eV vs. vacuum) for efficient electron injection, while the HOMO energy level should stay below the energy level of the Γ/I_3^- redox couple (-4.85 eV vs. vacuum) for regeneration⁴⁰ (**Figure 5.2**) which is the case with our experimental data for the prepared complexes, whose LUMO are also higher than that of N719 alone. Therefore, co-sensitizing N719 dye with these complexes will result in a greater combined effect that will improve the electron injection efficiency from the LUMO of the dye to the conduction band of TiO₂.

5.2.3 Photovoltaic Properties

The Ni(II), Zn(II), and Cd(II) complexes were employed as co-sensitizers and co-adsorbents to fabricate metal Complex-N719 photoanodes. The current–voltage characteristics of the DSC devices based on ordinary N719 dye, and the co-sensitized Ni-N719, Zn-N719, and Cd-N719 photoanodes are presented in **Figure 5.3** and the conforming data are summarized in **Table 5.2**. For comparison, the result obtained by the use of N719 dye under the same experimental conditions is included. The cell parameters derived from these curves are also summarized in **Table 5.2**. After overall co-sensitization of the state-of-the-art dye (N719) with the Ni, Zn, and Cd complexes, it was observed that cells containing N719 co-sensitized with zinc and cadmium ferrocenyl dithiophosphonate complexes showed improved performance above the efficiency of conventional N719 dye. The overall conversion efficiency achieved with complex **20**-N719 dye ($\eta=8.30$ %) and complex **22**-N719 dye ($\eta=7.78$ %) showed a better performance compared to that of ordinary N719 dye ($\eta=7.14\%$) under the same experimental conditions. The high efficiencies of this co-sensitized N719 dye with different ferrocenyl dithiophosphonate complexes (Ni, Zn & Cd) may be linked to the electronic properties of ferrocene^{23,20} contained in these complexes. Evaluations were also made on same metal complex formed from two different stoichiometry ratios. Complex **19** contains four ferrocenyl molecules and **18** only have two ferrocenyls. The performances of the cells fabricated by using the Ni complexes **18** and **19** - N719 are lower than that of the state-of-the-art dye N719 alone. However, N719

dye co-sensitized with complex **19** showed a performance that is higher than that of **18**-N719 which may be due largely to the higher number of the ferrocenyl groups associated with the complex. Having observed these photovoltaic parameters, it was evident that the metal complexes were effectively attached to the titania surface and promise to provide an efficient electron injection into the conduction band of the TiO₂ film. Hence, enhancement of electron collection in TiO₂ and reduced recombination of electrons in the conduction band of TiO₂ and oxidized dyes was expected.

Table 5.2: Photovoltaic parameters for the DSCs based on different photoelectrodes.

Photoelectrodes	J_{sc} [mA cm ⁻²]	V_{oc} [V]	FF	η (%)
N719	19.60	0.667	0.55	7.14
Ni/N719 1:1)	17.44	0.680	0.57	6.81
Ni/N719(1:2)	16.70	0.685	0.56	6.28
Zn/N719	21.89	0.665	0.58	8.30
Cd/N719	21.80	0.685	0.57	7.78

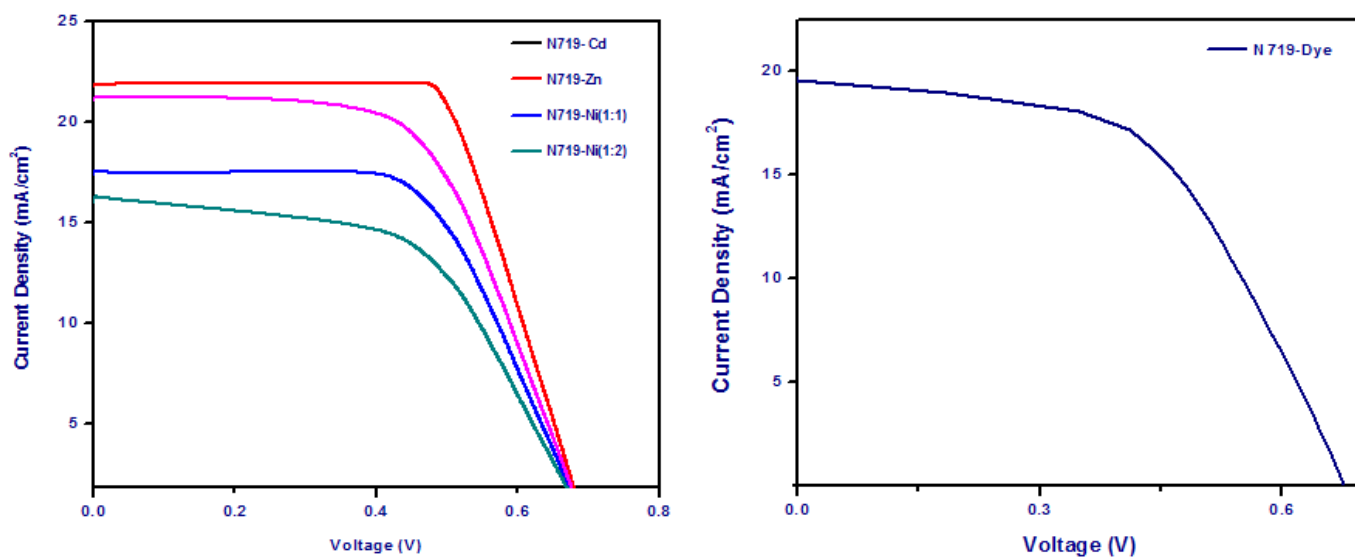


Figure 5.3. J–V curves for DSCs based on N719- co-sensitized with different ferrocenyl dithiophosphonate complexes and N719-sensitized photoelectrodes under irradiation.

5.2.4 Electrochemical impedance spectra analysis

In an effort to further study the dynamics of the electron-transport properties and charge recombination processes in the interfacial regions of the solid/liquid layers involving these complexes, electrochemical impedance spectra (EIS) were acquired. The Nyquist spectra were analysed by fitting varied electrical equivalent circuit elements to obtain the “best-fit” circuit model that represents the investigated system. Four different fits were obtained (**Figure 5.4**). All complexes presented a semicircle associated with the electron/charge transfer at the $\text{TiO}_2/\text{dye}/\text{electrolyte}$ interface⁴¹⁻⁴² for different circuit models. The equivalent circuits represent three different contributions which result in the total resistance of the system. The ohmic resistances of the electrolytes in **22** and **20-N719** complexes, R1 is due to charge transfer, while R2 are attributed to dissociative adsorption on the electrode surface and R3 in **20-N719** interfacial charge diffusion. R1 and R2 have constant phase elements (CPE) in parallel to simulate the distribution of relaxation time in the real system.⁴³⁻⁴⁴ The diameter of semicircles decreases in the order **20-N719** > **22-N719** indicating a decrease in recombination resistance at the $\text{TiO}_2/\text{dye}/\text{electrolyte}$ interface which indicates retardation of charge recombination between injected electrons and I^{3-} ions in the electrolyte, as a result, a rise in open circuit voltage was observed (from 0.665 to 0.685 V). A similar observation was made by Yadav, et al.⁴⁵ who concluded that co-sensitization of the N719 dye with dithiocarbamates' metal complexes favours DSCs performance and our results show a higher efficiency of 8.30 and 7.78% for Zn- and Cd-N719, respectively. The nickel complexes in the metal to ferrocenyl ligand ratio of 1:1 and 1:2 gave different circuit fits. Notably, the **18-N719** (1:2) indicated much higher impedance characteristics compared to **19-N719** (1:1). The **19-N719** (1:1) cell was expected to show higher performance efficiency than observed due to multi ferrocenyl moiety' presence on the co-sensitized complex. But on the contrary, there is more resistance, and thus the impedance increased, which may due largely to the presence of two more nickel centers and extra coordinating THF and water groups. Water is known to increase the resistance of a preparation.⁴⁶ These complexes indicated a higher number of capacitive elements in their corresponding equivalent circuits which indicate a delay between the current and the potential attributed to less efficient

intramolecular charge transfer. The high electrical double layer resistance in **18**-N719 (1:2) indicate poor electron transport.⁴⁷ The consequence was the observed low efficiency at 6.28 and 6.81% for **18**-N719 (1:2) and **19**-N719 (1:1), respectively.

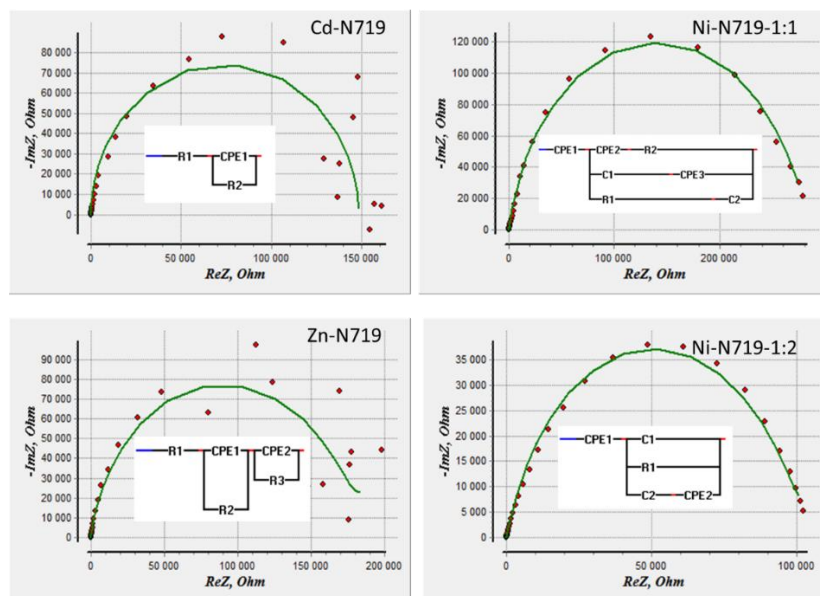


Figure 5.4: Electrochemical impedance measurement fitted data for all complexes

However, their low optical band gap, 1.8 and 2.00 eV indicate the charge accumulation and thus higher open circuit voltage of 0.685 and 0.680 V compared to the N719. This indicated that the percolation of charge was a less efficient process.³⁴ It can be argued that the system is charge conserving and that comparatively, the two systems can be good charge stores.

To further determine electron transport time (τ_d) which is a measure of the rate of an electron injected to the collecting electrode, the electron lifetime was estimated from the peak frequency of the Bode phase plots. The τ_d values were calculated using the expression adopted from Gao, et al.⁴⁸

$$\tau_d = \frac{1}{2\pi f_{peak}}$$

The values were 1.98 and 2.18 ms for Cd- and Zn-N719, respectively and 1.98 and 1.04 ms for Ni-N719 (1:1) and Ni-N719 (1:2), respectively. A shorter time is associated with a higher photocurrent.⁴⁸

The estimated τ_d value for N719 was 2.65 ms which implied that the back charge recombination was suppressed in all investigated systems. The observed difference in the performance these systems is attributed to their structural differences. The insertion of the THF rings in the nickel(II) complexes add π character in the system interspaced with oxygen groups which break the conjugation of π system. Localized electron cloud density in the Cp rings and THF create a charge conserving effect and hence CPE elements observed in the circuit fits and demonstrated by the high barrier to the charge-transfer resistance at the electrode potential⁴⁹ (**Figure 5.4**).

5.3 CONCLUSION

With this study, it can be concluded that the ferrocenyl dithiophosphonate complexes used as co-sensitizers have a positive effect on the efficiency of the DSCs. They are capable of improving J_{sc} as well as V_{oc} . The cells co-sensitized with the d^{10} metal complexes of the ferrocenyl dithiophosphonate show better performance than the DSC fabricated by using the N719 dye alone. Hence, it can be concluded that these ferrocenyl dithiophosphonate complexes are potential co-sensitizer for improving the performances of DSCs. Therefore, solar cells energy researchers should begin to look in this direction.

5.4 EXPERIMENTAL

5.4.1 Material

Titania, platinum electrodes, hot melt gasket, Iodolyte PN-50, a glass cap, seal film and Vac'n'Fill Syringe were purchased from Solaronix SA and the DSC fabrication was carried out in a standard solar cell laboratory. It is critical for the fabrication to be carried out on dried electrodes. Platinum electrodes can be stored away from air and light for future use but will require re-firing prior to assembly. Titania electrodes also might take up water and other pollutants from the air when stored for a long period. It is best to use the electrode right away. If starting with an existing fired titania electrode, it is strongly recommended that electrode is re-fired by putting oven with a relatively high temperature. This ensures that no pollutants are left on the titania surface prior to solar cell assembly.

5.4.2 Method

Ferrocenyl Lawesson's reagent was prepared from literature procedures²² and the complexes were prepared as reported in **Chapter 3**. N719 dye, electrolytes, and all other reagents were used as purchased from Solaronix and used as received. Distilled water was used for the reaction and in all cases where water is required in this work. Dried DCM was obtained and used after distillation over phosphorus(V) pentoxide under a blanket of nitrogen. Ethanol and methanol were either dried over calcium oxide or molecular sieves.

5.4.3 DSC Fabrication

Titania and platinum electrodes were used for both photo- and counter-electrodes. The co-sensitized photoelectrodes were prepared by immersion of the thin nanoporous TiO₂ layers (0.36cm²) into a DCM/Methanol (1:1) solution of the Ni, Zn, or Cd complex (10⁻⁵ M) for 6 h. The electrode with the absorbed complex was washed with DCM/Methanol (1:1) and then DCM. It was blow-dried and finally, the electrodes were dipped into a 10⁻⁵ M ethanol solution of the N719 dye for 12 h. Unabsorbed dye was washed out with anhydrous ethanol. The dye adsorbed TiO₂ electrodes and Pt counter electrodes were assembled in a sealed sandwich-type cell by heating at 110 °C using a hot melt gasket as a sealant and a spacer between the electrodes with the active sides of the anode and the cathode facing each other. Iodolyte PN-50 was used as the electrolyte. The electrolyte solution was introduced into the cell via a hole drilled in the counter electrode and was driven into the cell by vacuum backfilling using Vac'n'Fill Syringe. The hole was sealed by using 0.1 mm thick small glass cap sealed on top of the hole with another piece of sealing film.

5.4.4 Characterization

5.4.4.1 Solar Cell Efficiency

The photoelectrochemical performance characteristics (short circuit current, J_{sc} , open-circuit voltage, V_{oc} , fill factor (FF), and overall conversion efficiency, η) were measured using Sciencetech SF-150 Solar Simulator, Model 201-100 arc lamp housing (150W Xenon lamp) with a beam turning assembly including Air Mass 1.5 Global Filter, Model #AM15G-3 Inch (**Figure 5.5**). Efficiency measurements were carried out with a National Instruments model NI PX1-1033. Each measurement was repeated three times to confirm reproducibility and the average data of all three analyses are reported herein.

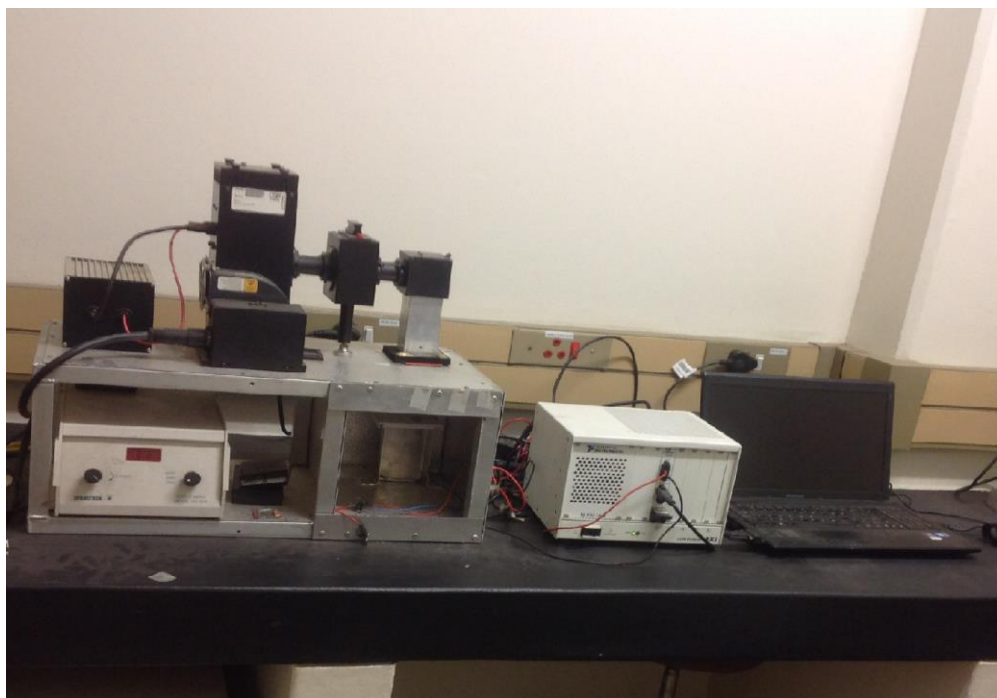


Figure 5.5. Photograph showing the Sciencetech SF-150 Solar Simulator.

5.4.4.2 Electrochemical Impedance Spectroscopy

The electrochemical (impedance and cyclic voltammetry) measurements were carried out using a PGSTAT 12/30/230 potentiostat. A two-electrode configuration was used where the sensitized TiO_2 was connected as the working electrode while the counter electrode (Pt), doubled as the reference electrode. The electrochemical impedance spectrophotometer is shown in **Figure 5.6**

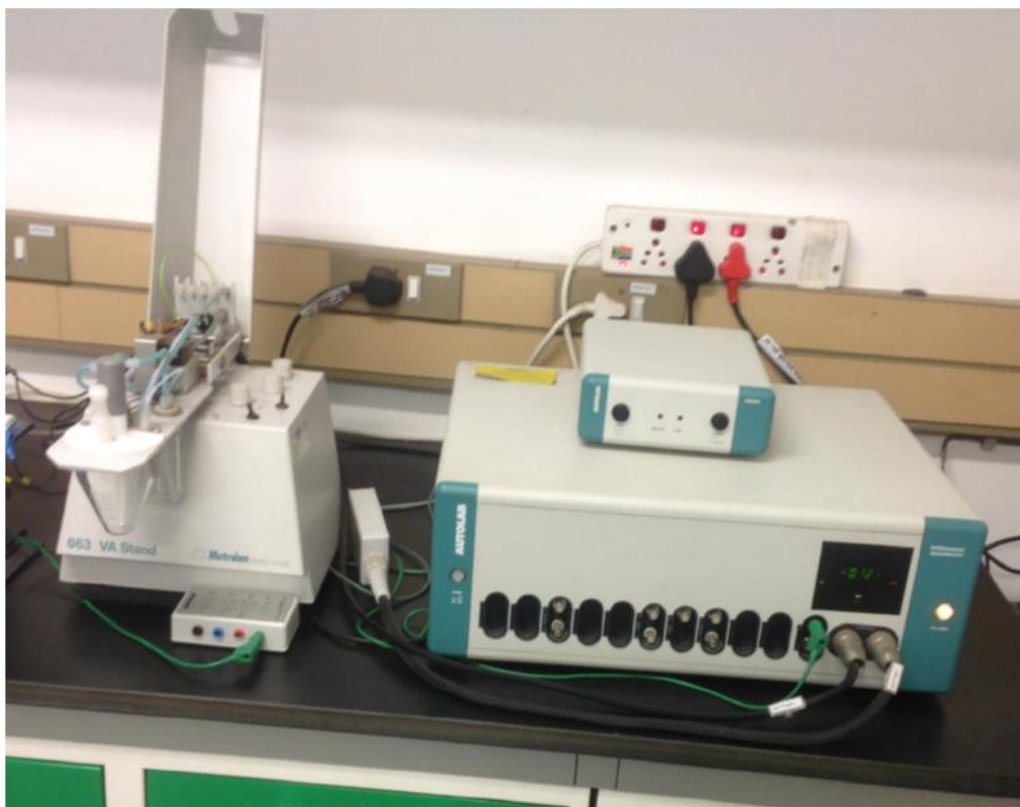


Figure 5.6. Photograph of the electrochemical (impedance and cyclic voltammetry) spectrophotometer

5.5 REFERENCES

1. Lewis, In Basic Research Needs for Solar Energy Utilization, *U.S. Department of Energy*, 2005
2. Editorial, *Nat Mater* **2006**, 5 (3), 159-159.
3. Campbell, C. J., *Population and Environment* 24 (2), 193-207.
4. Chandrasekharam, M.; Rajkumar, G.; Srinivasa Rao, C.; Suresh, T.; Reddy, P. Y.; Soujanya, Y., *J. Chem. Sci.* **2011**, 123 (5), 555-565.
5. Chen, S. G.; Chappel, S.; Diamant, Y.; Zaban, A. *Chem. Mat* **2001**, 13 (12), 4629-4634.
6. Huang, X.; Han, S.; Huang, W.; Liu, X., *Chem. Soc. Rev.* **2013**, 42 (1), 173-201.
7. Gao, S.; Fan, R. Q.; Wang, X. M.; Qiang, L. S.; Wei, L. G.; Wang, P.; Yang, Y. L.; Wang, Y. L., *Dalton Trans.* **2015**, 44 (41), 18187-18195.
8. Falaras, T. S. *Adv. Energy Mater* **2012**, 2, 616-627.
9. Stergiopoulos, T.; Falaras, P., *Adv. Energy Mater.* **2012**, 2 (6), 616-627.
10. Hara, K.; Horiguchi, T.; Kinoshita, T.; Sayama, K.; Sugihara, H.; Arakawa, H., *Solar Energy Materials and Solar Cells* **2000**, 64 (2), 115-134.
11. Hauffe, K.; Bode, U., *Faraday Discuss. Chem. Soc.* **1974**, 58 (0), 281-291.
12. Kumar, A.; Chauhan, R.; Molloy, K. C.; Kociok-Köhn, G.; Bahadur, L.; Singh, N., *Chem. Eur. J.* **2010**, 16 (14), 4307-4314.
13. Kay, A.; Humphry-Baker, R.; Graetzel, M., *J. Phys. Chem.* **1994**, 98 (3), 952-959.
14. Bahadur, L.; Roy, L., *Semiconductor Science and Technology* **1995**, 10 (3), 358.
15. Bahadur, L.; Roy, L., *J. Photochem. Photobiol. A: Chem.* **1995**, 92 (3), 207-212.

16. Nazeeruddin, M. K.; Grätzel, M., *J.Photochem. Photobiol. A: Chem.* **2001**, *145* (1–2), 79-86.
17. Garcia, C. G.; Nakano, A. K.; Kleverlaan, C. J.; Murakami Iha, N. Y., *J.Photochem. Photobiol. A: Chem.* **2002**, *151* (1–3), 165-170.
18. Yadav, R.; Trivedi, M.; Kociok-Köhn, G.; Chauhan, R.; Kumar, A.; Gosavi, S. W., *Eur.J.Inorg.Chem.* **2016**, *2016* (7), 1013-1021.
19. Chauhan, R.; Auvinen, S.; Aditya, A. S.; Trivedi, M.; Prasad, R.; Alatalo, M.; Amalnerkar, D. P.; Kumar, A., *Solar Energy* **2014**, *108*, 560-569.
20. Chauhan, R.; Shahid, M.; Trivedi, M.; Amalnerkar, D. P.; Kumar, A., *Eur.J.Inorg.Chem.* **2015**, *2015* (22), 3700-3707.
21. Misra, R.; Maragani, R.; Patel, K. R.; Sharma, G. D., *RSC Advances* **2014**, *4* (66), 34904-34911.
22. Gray, H. B.; Sohn, Y. S.; Hendrickson, N., *J.Am.Chem.Soc.* **1971**, *93* (15), 3603-3612.
23. Armstrong, A. T.; Smith, F.; Elder, E.; McGlynn, S. P., *J.Chem.Phys.* **1967**, *46* (11), 4321-4328.
24. Kunkely, H.; Vogler, A., *Inorg.Chem.Commun.* **2001**, *4* (12), 692-694.
25. Vicek, A. J., *Coord. Chem. Rev.* **1998**, *177*, 219-256.
26. Atkins, P. J.; Shriver, D. F., *Inorganic Chemistry (3rd ed.)*. W.H. Freeman and Company: New York: 1999.
27. Vogler, A.; Kunkely, H., *Coord. Chem. Rev.* **2000**, *208* (1), 321-329.
28. Vogler, A.; Kunkely, H., *Coord. Chem. Rev.* **2004**, *248* (3-4), 273-278.
29. Yamaguchi, Y.; Ding, W.; Sanderson, C. T.; Borden, M. L.; Morgan, M. J.; Kutal, C., *Coord. Chem. Rev.* **2007**, *251* (3-4), 515-524.
30. Vogler, A.; Kunkely, H., *Coord. Chem. Rev.* **2001**, *211* (1), 223-233.

31. Garcia, C. G.; de Lima, J. F.; Murakami Iha, N. Y., *Coord. Chem. Rev.* **2000**, *196* (1), 219-247.
32. Wagner, B. O.; Ebel, H. F., *Tetrahedron* **1970**, *26* (21), 5155-5167.
33. Ford, W. T., *J.Organomet.Chem.* **1971**, *32* (1), 27-33.
34. Kalyanasundaram, K.; Gra'tzel, M., *Coord. Chem. Rev.* **1998**, *77*, 347-414.
35. Orpen, A. G.; Connelly, N. G., *Organometallics* **1990**, *9* (4), 1206-1210.
36. Maslak, P., *Topics.Curr. Chem.* **1993**, *168*, 1-46.
37. Dunne, B. J.; Morris, R. B.; Orpen, A. G., *J.Chem.Soc. Dalton Trans.* **1991**, (S), 653-661.
38. Kunkely, H.; Arnd, V., *J.Organomet.Chem.* **1998**, *568* 291-293.
39. Cardona, C. M.; Li, W.; Kaifer, A. E.; Stockdale, D.; Bazan, G. C., *Adv. Mat.* **2011**, *23* (20), 2367-2371.
40. Justin Thomas, K. R.; Hsu, Y.-C.; Lin, J. T.; Lee, K.-M.; Ho, K.-C.; Lai, C.-H.; Cheng, Y.-M.; Chou, P.-T., *Chem.Mat.* **008**, *20* (5), 1830-1840.
41. Pinedo, R.; Ruiz de Larramendi, I.; Ortiz-Vitoriano, N.; Gil de Muro, I.; Rojo, T., *J.Pow.Sourc.* **2012**, *201*, 332-339.
42. Guler, Z.; Sarac, A. S., *Expr.Polym.Lett.* **2015**, *10* (2), 96-110.
43. Sacanell, J.; Bellino, M. G.; Lamas, D. G.; Leyva, A. G., *Physica B: Condensed Matter* **2007**, *398* (2), 341-343.
44. Chen, X.; Wang, S.; Yang, Y. L.; Smith, L.; Wu, N. J.; Kim, B. I.; Perry, S. S.; Jacobson, A. J.; Ignatiev, A., *Solid State Ionics* **2002**, *146* (3-4), 405-413.
45. Yadav, R.; Trivedi, M.; Kociok-Köhn, G.; Chauhan, R.; Kumar, A.; Gosavi, S. W., *Eur.J.Inorg.Chem.* **2016**, *2016* (7), 1013-1021.

46. Perini, N.; Prado, A. R.; Sad, C. M. S.; Castro, E. V. R.; Freitas, M. B. J. G., *Fuel* **2012**, *91* (1), 224-228.
47. Maeda, H.; Sakamoto, R.; Nishihara, H., *J Phys Chem Lett* **2015**, *6* (19), 3821-6.
48. Gao, S.; Fan, R. Q.; Wang, X. M.; Qiang, L. S.; Wei, L. G.; Wang, P.; Yang, Y. L.; Wang, Y. L., *Dalton Trans* **2015**, *44* (41), 18187-95.
49. Chang, B. Y.; Park, S. M., *Annual Rev.Analyt.Chem.* **2010**, *3*, 207-229.

CHAPTER 6

ANTIBACTERIAL STUDIES OF THE NEW DITHIOPHOSPHONATE LIGANDS AND THEIR COMPLEXES

6.1 BACKGROUND

Microorganisms have existed on the earth for more than 3.8 billion years and exhibit the greatest genetic and metabolic diversity.¹ Recently, resistance to antimicrobial agents among bacteria, parasites, viruses and other disease-causing organisms has become a public health challenge worldwide.²

A major setback in the development of antibiotics and their application to clinical medicine has been the enhancement of bacterial resistance towards antibacterial drugs. This may be largely due to constant use of antibiotics which in turn increases selective pressure in the bacteria population, thereby permitting the survival of the resistant bacteria and eradication of the susceptible ones.³ Because antimicrobial resistance is fast becoming a global concern with the rapid increase in multidrug-resistant bacteria,⁴ this has led to a continuing search for new antimicrobial compounds. This includes coordination complexes of biologically important molecules⁵⁻⁶ which no doubt make the antimicrobial activities of dithiophosphonate complexes of interest⁷. Although there are many dithiophosphonates, only a few antibacterial activity studies relative to this class of compounds have been reported.⁸⁻¹⁰

In this study focus was therefore directed to the antibacterial activities of some of the new dithiophosphonate compounds on the following bacteria: *Bacillus subtilis*, *Pseudomonas aeruginosa*, *Klebsiella oxytoca*, and *Salmonella* sp, *Methicillin-Resistant Staphylococcus aureus (MRSA)*, *Escherichia coli*, *Staphylococcus aureus*, *Klebsiella pneumoniae*, and *Shigella dysenteriae* which are day to day disease-causing organisms and that has shown resistance to conventional antibiotics.

6.2 RESULT AND DISCUSSIONS

6.2.1 Dithiophosphonate Complexes Synthesized Via Green Route

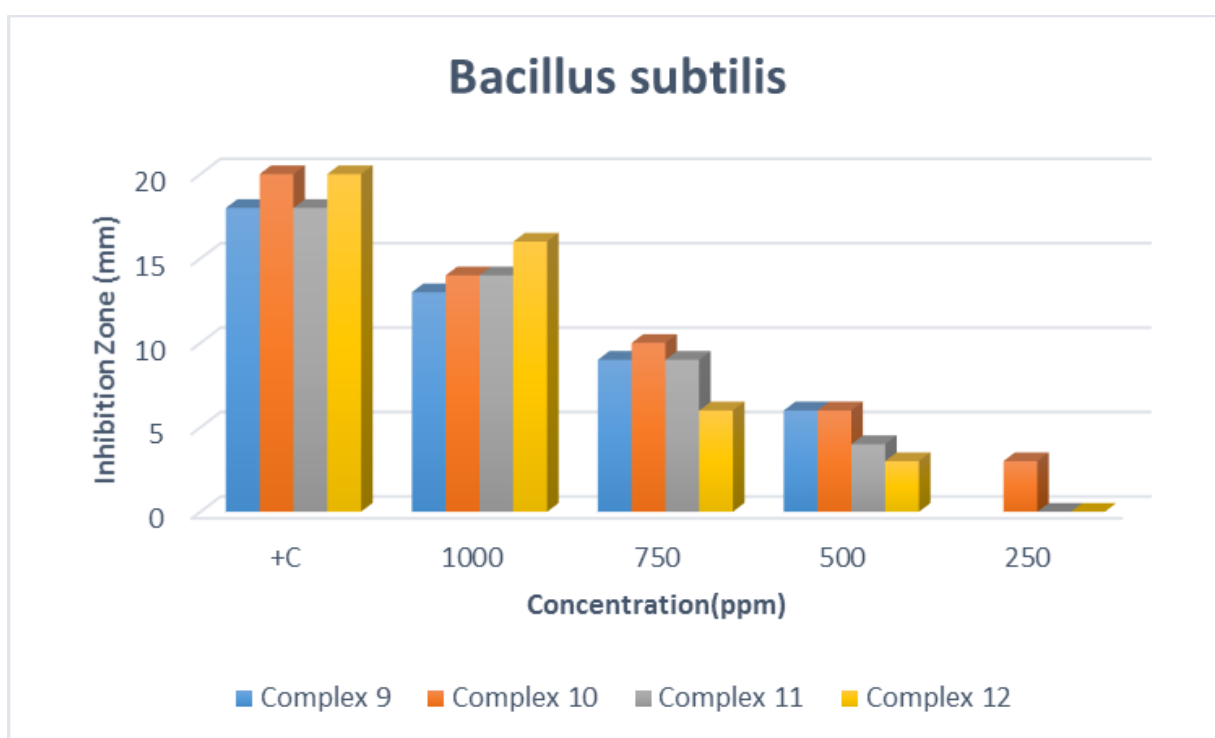
Although there are a number of reported phosphor-1, 1-dithiolates generally, only a few antibacterial activity studies relative to this class of compounds are present in the literature.⁹ Antibacterial susceptibility tests were carried out on compound **1-12** and a summary of the results are presented in **Table 6.1**. Surprisingly, the ligands **1-4** and the nickel complexes **5-8** showed no activity against the test bacteria even at 1000 ppm. The zinc complexes **9-12** did exhibit varying degrees of activity against *Bacillus subtilis*, *Klebsiella oxytoca*, and *Salmonella* sp. Free ligands have been reported to typically be ineffective against some bacterial strains.¹⁴ Metal complexes **9-12** from this work showed considerable antibacterial activity, and just slightly lower to reference antibiotics. Complex **10**, in particular, was effective against *Bacillus subtilis* even at low concentration (250 ppm) (**Figure 6.1**) and it also recorded the most activity against *Klebsiella oxytoca* among all the compounds investigated (**Figure 6.2**).

Antibacterial susceptibility of the compounds was examined using agar-well diffusion method.³ Different concentrations (1000, 750, 500, and 250 ppm) of the compounds was prepared. Mueller Hinton agar (MHA) was prepared and melted to obtain a homogenous solution. The agar was aseptically poured into a sterile petri dish and allowed to solidify. The labeled plates were left on the bench for 2 h after inoculation and 6 mm wells were bored into it. About 100 μ l of test compound were fed into the plates were incubated for 24 h and diameters of zones of inhibition were measured.

Table 6.1: Diameter of Zones of Inhibition (mm) of the Compound against the test Isolates

Compd	Bacillus subtilis					Klebsiella oxytoca					Salmonella sp				
	Concentrations (ppm) of the compound used														
	+C	1000	750	500	250	+C	1000	750	500	250	+C	1000	750	500	250
9	18	13	9	6		18	9	3	-	-	14	10	6	2	-
10	20	14	10	6	3	23	20	16	8	-	-	-	-	-	-
11	18	14	9	4	-	22	12	-	-	-	12	6	4	-	-
12	20	16	6	3	-	14	6	4	2	-	-	-	-	-	-

+C – Positive control (Streptomycin 1000ppm); -ve Control (50% DMSO); Inoculum OD₆₀₀ (0.08 – 0.1); Solvent Used: 50% DMSO

**Figure 6.1.** Graphs showing the comparative result of the antibacterial activity of the compounds *Bacillus subtilis*.

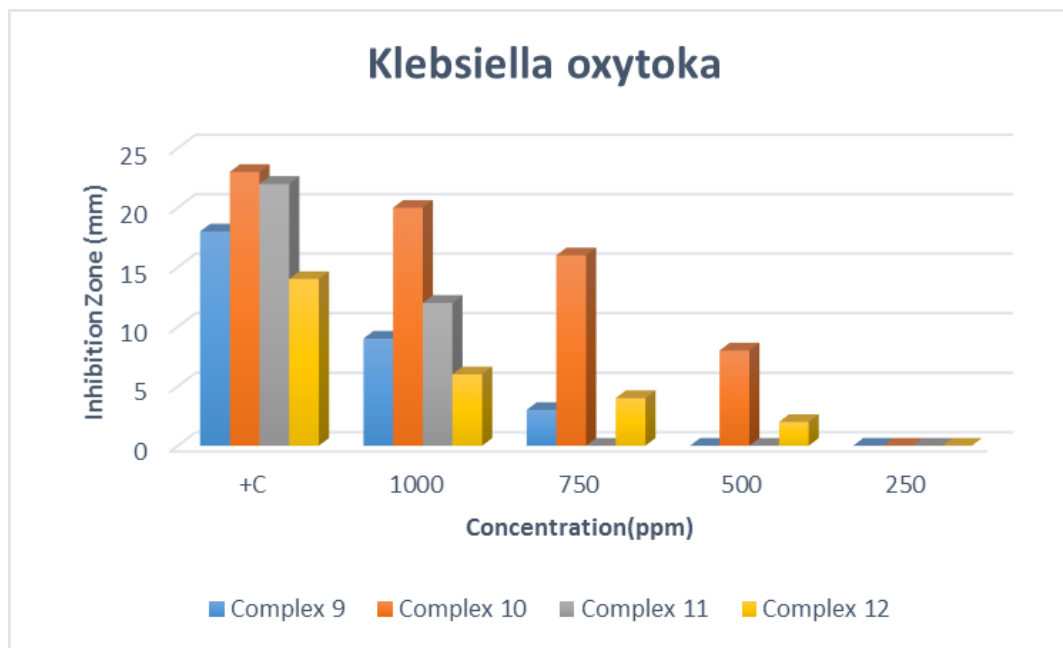


Figure 6.2. Graphs showing the comparative result of the antibacterial activity of our compounds on *Klebsiella oxytoca*.

Compound **9** seems to be the only compound showing activity against *Salmonella* sp (**Figure 6.3**). However, we considered why these bacteria strains were only susceptible to the zinc complex? Antibacterial activity of the zinc precursor salts such as $ZnCl_2$ used in the formation of these complexes was carried out and no noticeable activity resulted compared to susceptibility to their corresponding complexes. This implies that the antibacterial activity derives from a synergetic relation between the ligand and zinc as expounded in complexes **9-12**. Furthermore, we used the same zinc salt for the formation of all our zinc complexes, the different results obtained from the susceptibility test with complexes **9-12** which evidently demonstrate that the activity cannot come from the metal salts alone. Null activities were recorded for some of the zinc complexes in the case of *Salmonella* sp. Nevertheless, bacteria has been reported to be susceptible to zinc (and other transition metals¹¹) and we thus propose that the heightened antibacterial activities of our zinc complexes make the bacteria more susceptible to them.

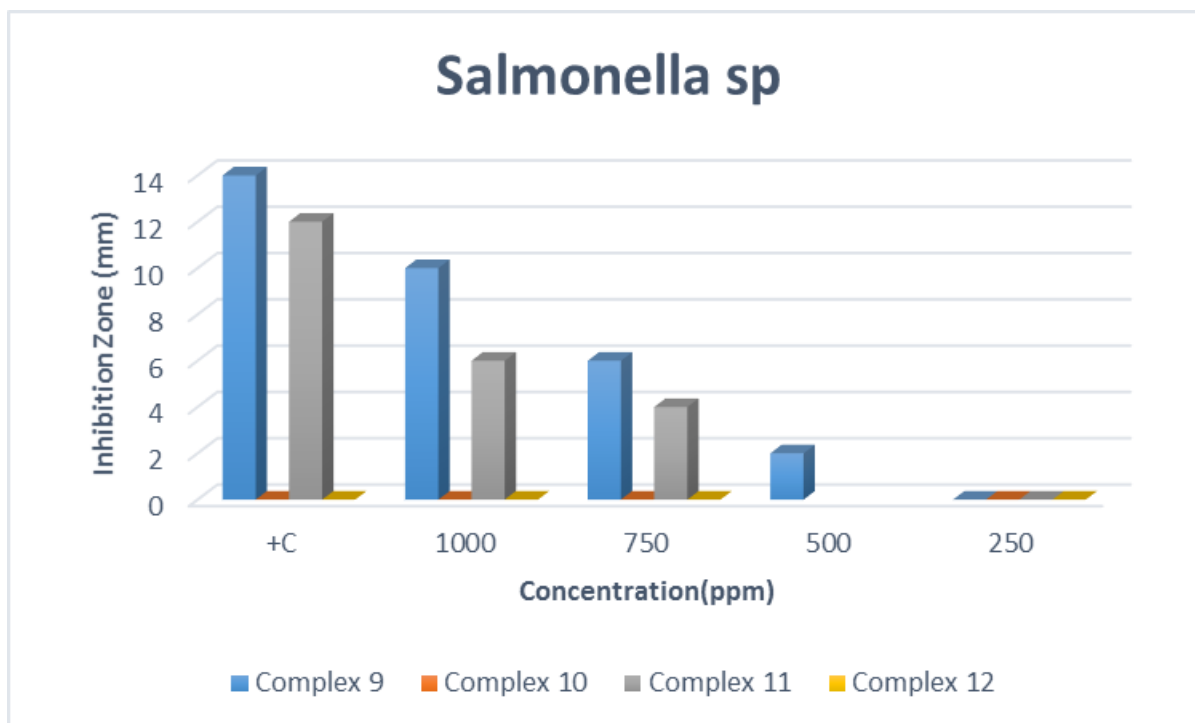


Figure 6.3. Graph showing the comparative result of antibacterial activity our compound on *Salmonella* sp

6.2.2 Zwitterionic Dithiophosphonate Ligands and Their Complexes

In addition to few antibacterial activity studies relative to this class of compounds,¹² we report antibacterial susceptibility tests on compounds **24-31** and the results are summarized in **Table 6.2** and their graphical representation are shown in **Figure 6.4-6.9**. More antibacterial activities were also observed with group 12 metals complexes, compared to other metal groups investigated. The ligands (**24-25**) and the nickel complexes (**26 & 29**) showed less activity against the test bacteria at all level of tested concentration (ppm) while the zinc (**27 & 30**) and the cadmium complexes (**28 & 31**) showed a considerable degree of activity against *Methicillin-Resistant Staphylococcus aureus* (MRSA), *Escherichia coli*, *Staphylococcus aureus*, *Klebsiella pneumoniae*, *Bacillus subtilis*, and *Shigella dysentery*. It is reported that chelation usually makes the ligand act as stronger and effective bactericidal agents, thus showing more antibacterial activity than the ligand.¹³ In a complex, the positive charge of the metal is not fully shared with the ligand's donor atoms and may lead to π -electron delocalization over the whole chelate. This heightens the lipophilic

accomplishment of the metal chelate and fosters its infiltration through the lipid layer of the bacterial membranes. The improved lipophilic performance of these complexes may largely be responsible for their improved potent bacterial susceptibility. There may be other factors responsible for their antimicrobial activity, which are solubility, conductivity, and bond length between the metal and the ligand¹³.

Table 6.2: Diameter of Zones of Inhibition (mm) of the Compound against the test Isolates

Test Isolates	Concentration (ppm)	24	25	26	27	28	29	30	31
<i>Methicillin-Resistant Staphylococcus aureus (MRSA)</i>	+C	-	13	-	4	6	14	15	23
	250	-	-	-	2	5	-	3	4
	500	-	2	-	5	8	-	7	11
	1000	-	7	-	9	14	9	11	17
<i>Escherichia coli</i>	+C	-	10	-	-	15	-	15	15
	250	-	-	-	-	-	-	-	3
	500	-	5	-	-	6	-	5	7
	1000	-	6	-	-	10	-	8	12
<i>Staphylococcus aureus</i>	+C	-	12	-	18	24	-	20	36
	250	-	-	-	-	2	-	3	8
	500	-	4	-	9	8	-	9	19
	1000	-	9	-	15	18	-	15	30
<i>Klebsiella pneumoniae</i>	+C	-	8	12	12	15	11	13	13
	250	-	-	-	-	2	-	-	-
	500	-	5	4	4	6	3	4	3
	1000	-	8	8	9	11	7	9	8
<i>Bacillus subtilis</i>	+C	-	-	-	14	12	-	13	20
	250	-	-	-	-	-	-	-	3
	500	-	-	-	-	-	-	3	6
	1000	-	-	-	10	5	-	8	14
<i>Shigella dysenteriae</i>	+C	5	-	-	12	14	13	15	18
	250	-	-	-	-	-	-	-	3
	500	5	-	-	4	5	3	4	7
	1000	9	-	-	7	8	7	9	12

+C – Positive control (Streptomycin 1000ppm); -ve Control (50% DMSO); Inoculum OD₆₀₀ (0.08 – 0.1); Solvent Used: 50% DMSO

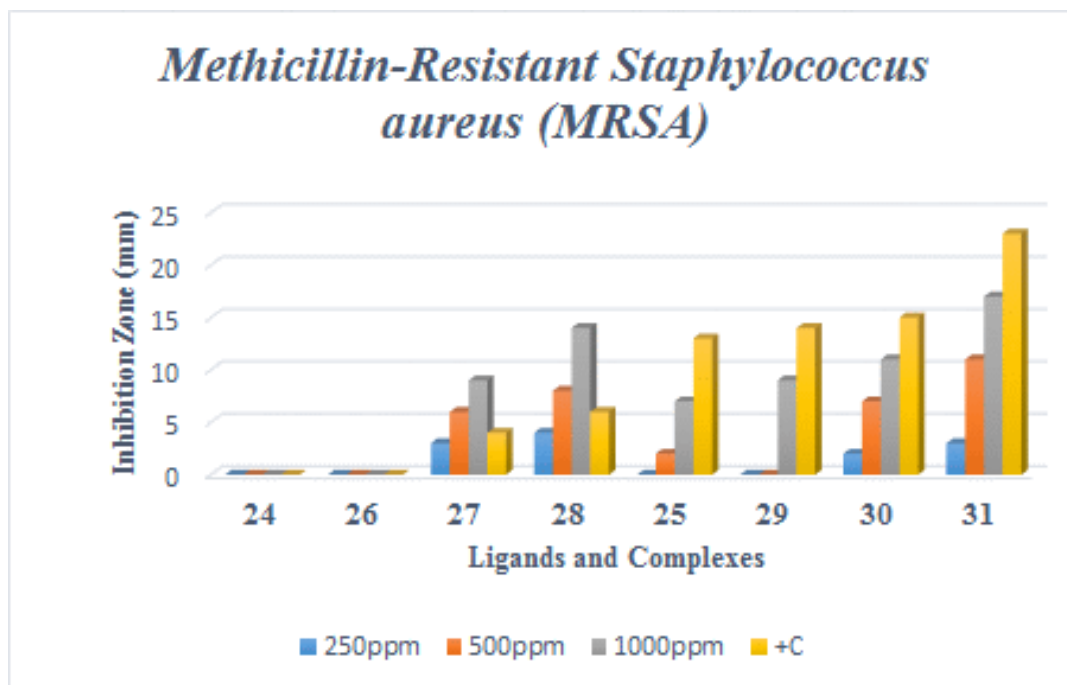


Figure 6.4. Graph showing the comparative result of antibacterial activity of the compounds on *Methicillin-Resistant Staphylococcus aureus (MRSA)*

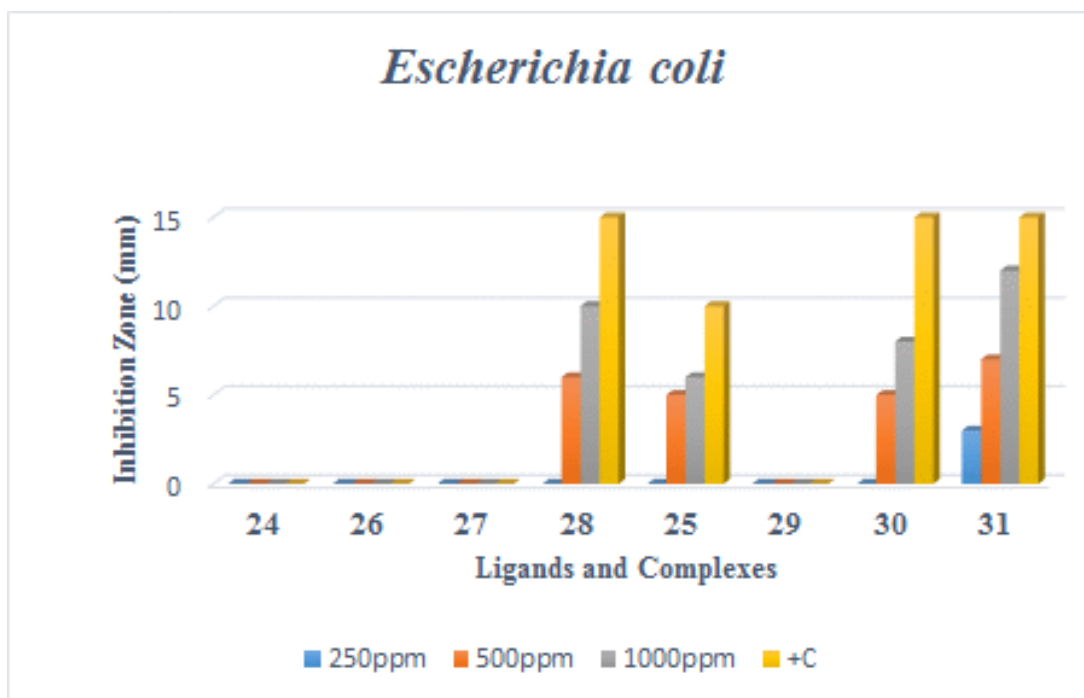


Figure 6.5. Graph showing the comparative result of antibacterial activity of the compounds on *Escherichia coli*

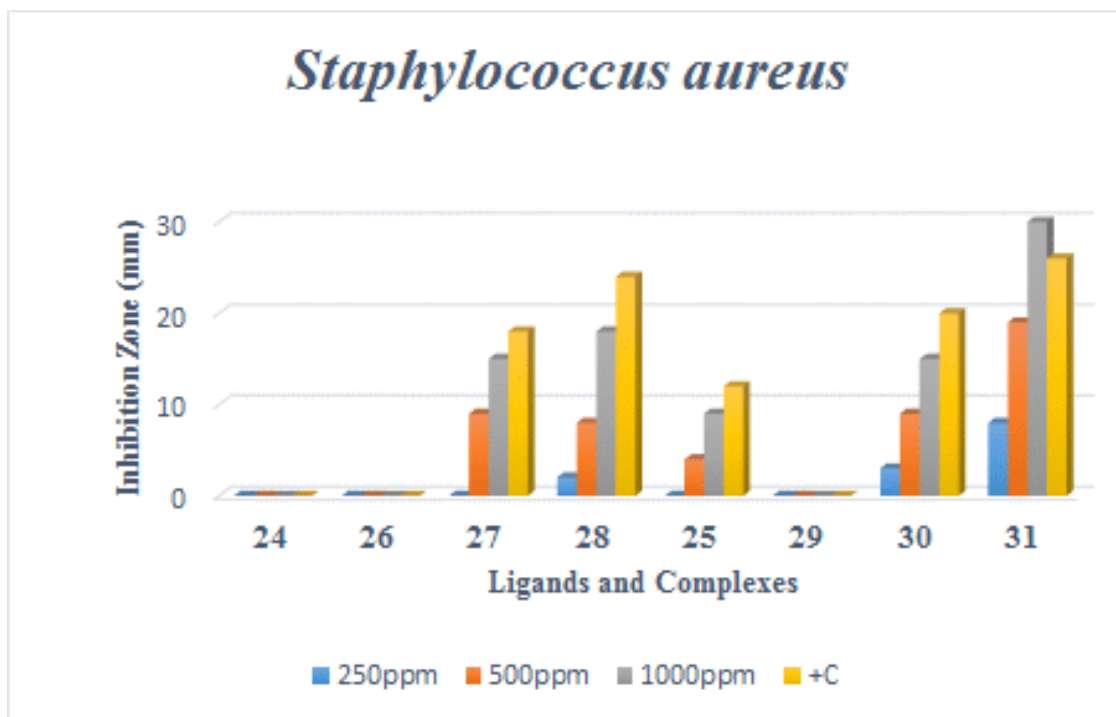


Figure 6.6. Graph showing the comparative result of antibacterial activity of the compounds on *Staphylococcus aureus*

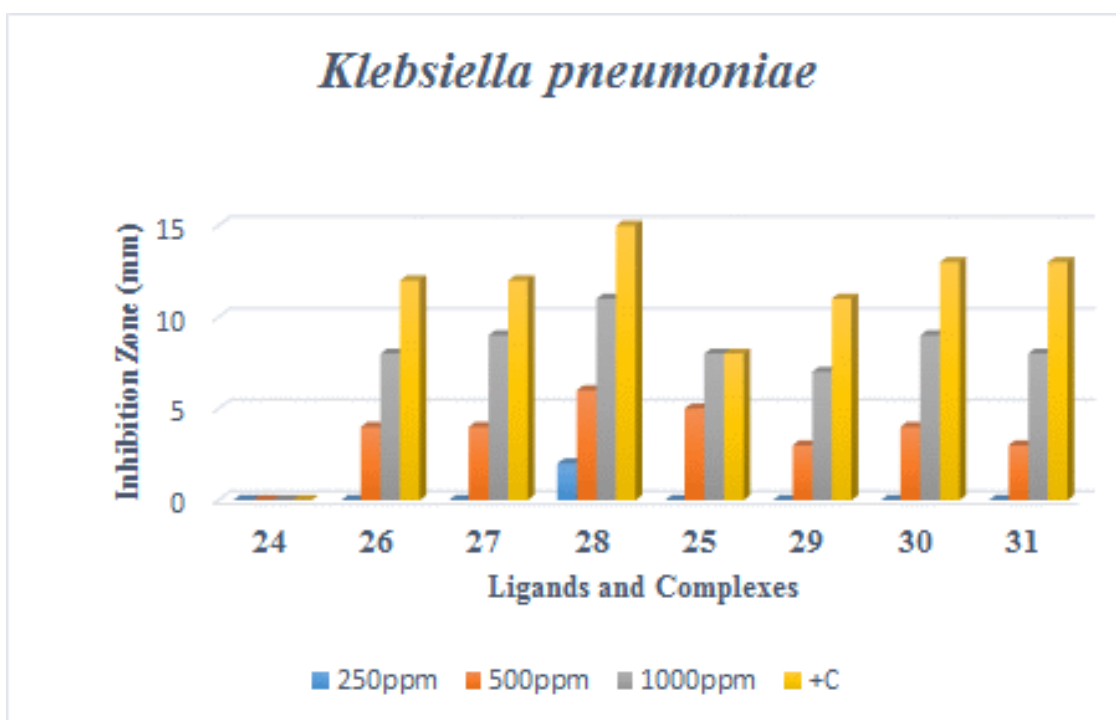


Figure 6.7. Graph showing the comparative result of antibacterial activity of the compounds on *Klebsiella pneumoniae*,

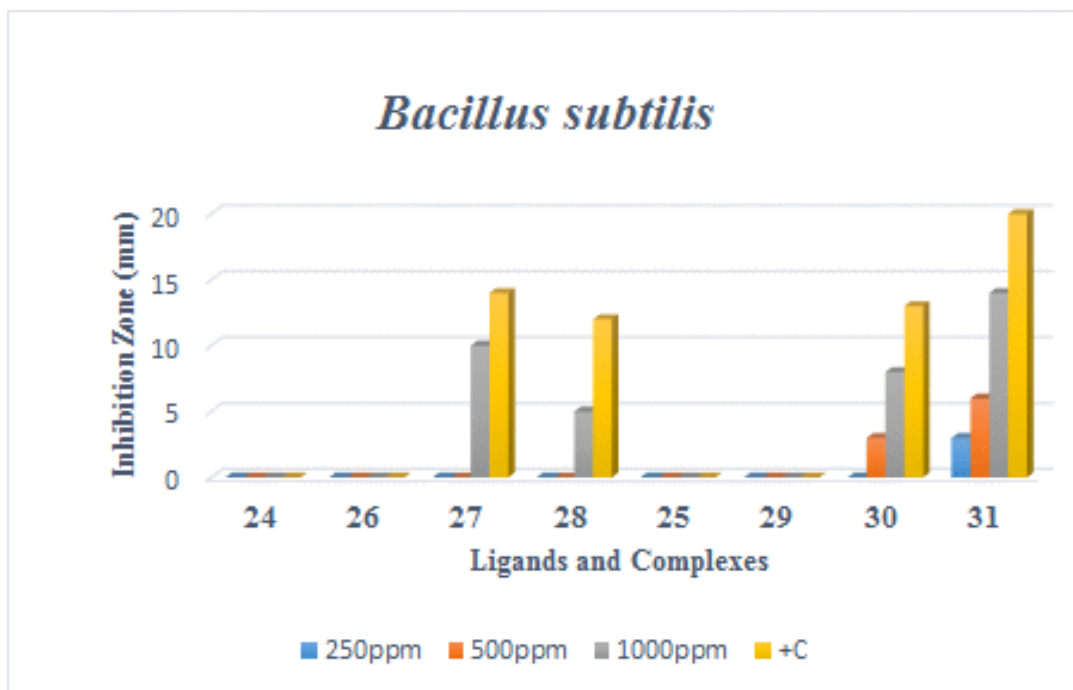


Figure 6.8. Graph showing the comparative result of antibacterial activity of the compounds on *Bacillus subtilis*

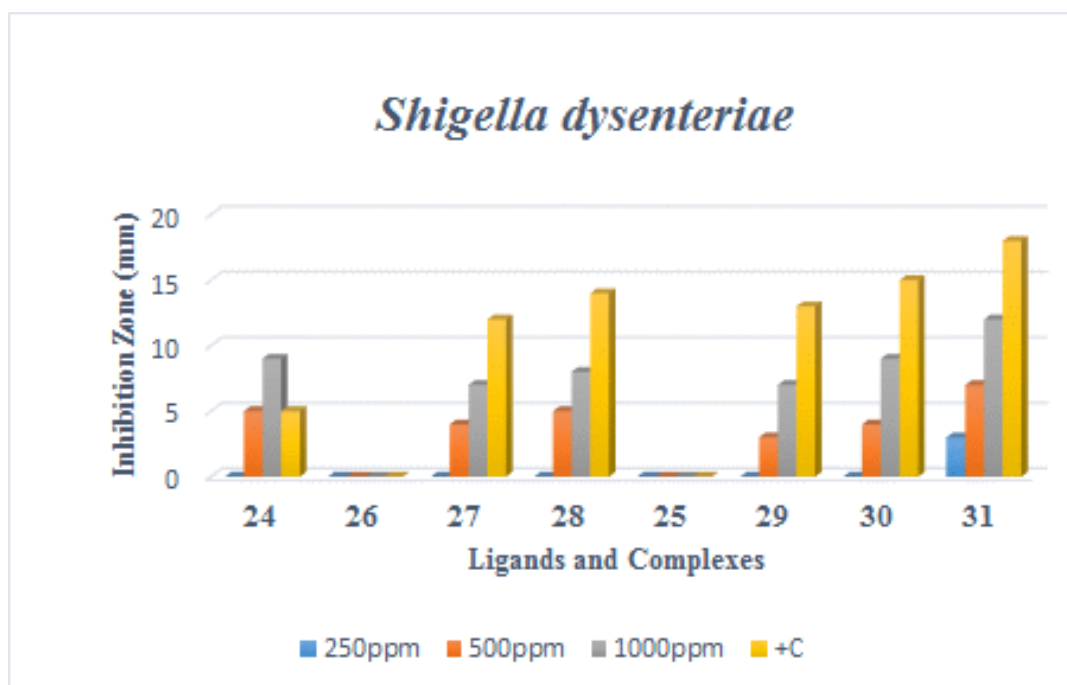


Figure 6.9. Graph showing the comparative result of antibacterial activity of the compounds on *Shigella dysentery*

6.3 CONCLUSION

This study reports on the antibacterial susceptibility tests for the bacteria *Methicillin-Resistant Staphylococcus aureus (MRSA)*, *Escherichia coli*, *Staphylococcus aureus*, *Klebsiella pneumoniae*, *Bacillus subtilis*, and *Shigella dysenteriae*, *Pseudomonas aeruginosa*, *Klebsiella oxytoca*, and *Salmonella sp* using new dithiophosphonate compounds at various concentrations. The obtained result indicated that these compounds showed a range of antibacterial activities from zero to moderate and even significant, and it is evident that the microbial growth inhibition by metal complexes was in most cases higher than that of the free ligands. The result also showed that d^{10} metal dithiophosphonate complexes are better antibacterial compared to the d^8 metal complexes as they displayed much better activity.

6.4 EXPERIMENTAL

6.4.1 Antibacterial susceptibility test Of Dithiophosphonate Complexes Synthesized Via Green Route

Antibacterial susceptibility of the compounds was examined using agar-well diffusion method.³ Different concentrations (1000, 750, 500, and 250 ppm) of the compounds was prepared by weighing out the required quantity and dissolved them in 80% dimethyl sulfoxide (DMSO). Broth culture of the test organisms; *Bacillus subtilis*, *Pseudomonas aeruginosa*, *Klebsiella oxytoca*, and *Salmonella* sp. were standardized (0.01-0.1 at OD₆₀₀ nm) using a spectrophotometer. Mueller Hinton agar (MHA) was prepared according to the manufacturer's specification and melted to obtain a homogenous solution, 20 ml each of the MHA was dispensed into McCartney bottles and autoclaved at 121°C for 15 min and allowed to cool to about 45 °C. The agar was aseptically poured into a sterile petri dish and allowed to solidify. Thereafter, the plates were incubated for 24 h to confirm their sterility. The plates (**Figure 6.10**) were labeled accordingly and inoculated with the test isolates. The plates were left on the bench for 2 h after inoculated for the organism to acclimatize with the agar. With the aid of a sterile cork borer, 6 mm wells were bored into the inoculated plates and the wells were labeled according to the concentration of the test compounds. About 100 µl of test compound were fed into the well and left on the bench for 2 h for the compound to diffuse into the agar, 1000 ppm of conventional antibiotic (streptomycin) was used as positive control and 80% DMSO as the negative control. The plates were incubated for 24 h and diameters of zones of inhibition were measured with the aid of transparent calibrated ruler.



Figure 6.20. The incubated plates showing the diameter of zones of inhibition of the compound against the test isolates

6.4.2 Antibacterial Susceptibility Test Of Zwitterionic Dithiophosphonate Ligand and Their Complexes

Antibacterial susceptibility of the compounds was examined using agar-well diffusion method. Different concentrations (1000, 500, and 250 ppm) of the compounds was prepared by weighing out the required quantity and dissolved them in 50% dimethyl sulfoxide (DMSO). Broth culture of the test organisms; *Methicillin-Resistant Staphylococcus aureus* (MRSA), *Escherichia coli*, *Staphylococcus aureus*, *Klebsiella pneumoniae*, *Bacillus subtilis*, and *Shigella dysenteriae* were standardized (0.01-0.1 at OD₆₀₀ nm) using a spectrophotometer. Mueller Hinton agar (MHA) was prepared according to the manufacturer's specification and melted to obtain a homogenous solution, 20 ml each of the MHA was dispensed into McCartney bottles and autoclaved at 121°C for 15 min and allowed to cool to about 45 °C. The agar was aseptically poured into a sterile petri dish and allowed to solidify. Thereafter, the plates were incubated for 24 h to confirm their sterility. The plates were labeled (**Figure 6.11**) accordingly and inoculated with the test isolates. The plates were left on the bench for 2 h after inoculated for the organism to acclimatize with

the agar. With the aid of a sterile cork-borer, 6 mm wells were bored into the inoculated plates and the wells were labeled according to the concentration of the test compounds. About 100 μ l of test compound were fed into the well and left on the bench for 2 h for the compound to diffuse into the agar, 1000 ppm of conventional antibiotic (streptomycin) was used as positive control and 50% DMSO as the negative control. The plates were incubated for 24 h and diameters of zones of inhibition were measured with the aid of transparent calibrated ruler.

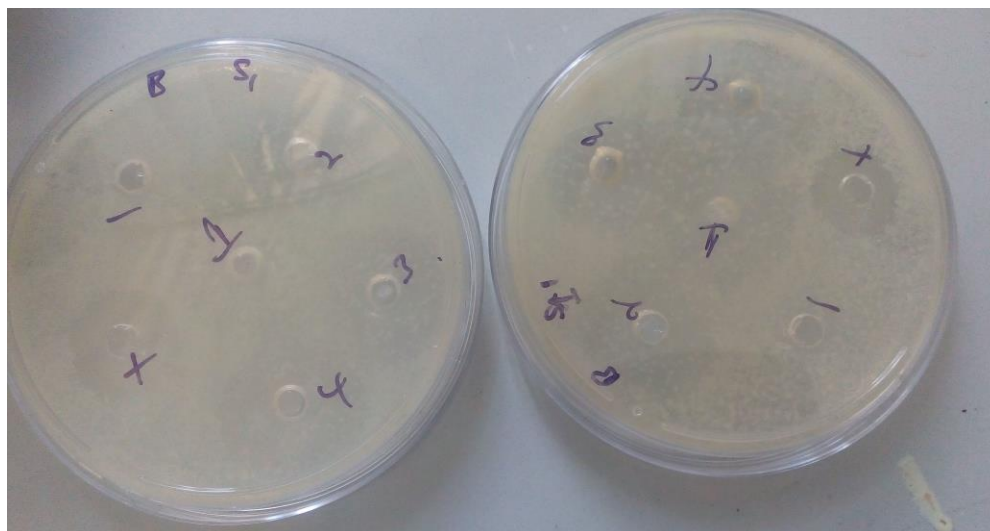


Figure 6.11. The incubated plates showing the diameter of zones of inhibition of the compound against the test isolates

Ethical Consideration

To the best of our knowledge, there is no regulation that requires any ethical consideration for this work.

6.5 REFERENCES

1. Dun, E., *J. Biol. Med.*, **1999**, 72 281–285.
2. Saga, T. Y., K., *JMAJ* **2009**, 52, 103-108.
3. Yanling, J. X., L.; Zhiyuan, L., The antibacterial drug discovery. *InTech*. **2013**, 289-308.
4. Saha, S., Dhanasekaran, D., Chandraleka, S., Thajuddin, N. and Panneerselvam, *Adv.Biol.Res.2010* 4,224-229.
5. Farrell, N., *Compr.Coord.Chem.* **2003**, 9, 809-840.
6. Johari, R., Kumar, G., Kumar, D., and Singh, S., *J.Indi.Chem.Council* **2009**, 26, 23-27.
7. Chauhan, H. P. S.; Singh, U. P.; Shaik, N. M.; Mathur, S.; Huch, V., *Polyhedron* **2006**, 25 (15), 2841-2847.
8. Cherkasov, R. A.; Nizamov, I. S.; Gabdullina, G. T.; Almetkina, L. A.; Shamilov, R. R.; Sofronov, A. V., *Phosphorus, Sulfur, Silicon Relat.Elem.* **2013**, 188 (1-3), 33-35.
9. Aydemir, C.; Solak, S.; Acar Doganlı, G.; Sensoy, T.; Arar, D.; Bozbeyoglu, N.; Mercan Dogan, N.; Lönnecke, P.; Hey-Hawkins, E.; Sekerci, M.; Karakus, M., *Phosphorus, Sulfur, Silicon Relat.Elem.***2015**, 190 (3), 300-309.
10. Karakus, M.; Ikiz, Y.; Kaya, H. I.; Simsek, O., *Chem Central J.***2014**, 8 (1), 18.
12. Aydemir, C.; Solak, S.; Acar Doganlı, G.; Sensoy, T.; Arar, D.; Bozbeyoglu, N.; Mercan Dogan, N.; Lönnecke, P.; Hey-Hawkins, E.; Sekerci, M.; Karakus, M., *Phosphorus, Sulfur, Silicon Relat.Elem.* **2014**, 190 (3), 300-309.
13. Al-Amiery, A. A.; Al-Majedy, Y. K.; Abdulreazak, H.; Abood, H., *Bioinorg. Chem. Appl.***2011**, 2011, 6.

14. Nidhi K., Bhawana G., Savit A., Sandeep K., and Sushil K.P., *Int. J.Inorg. Chem.***2013**,12, 35496.

CHAPTER 7

CONCLUSIONS AND FUTURE WORK

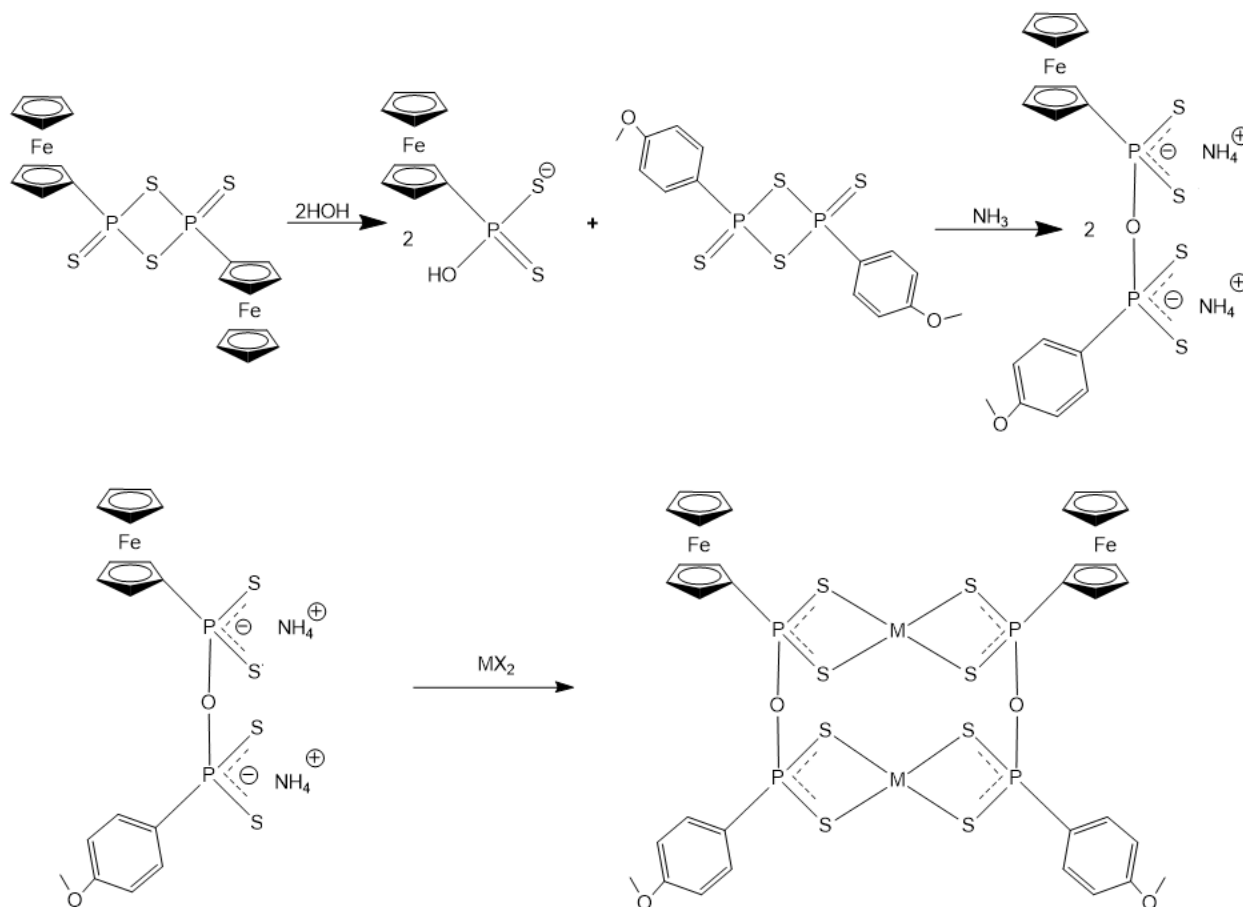
7.1 CONCLUSION

In this study, various new dithiophosphonate ligands were successfully synthesized from the reaction between water, simple aliphatic alcohols (methanol, ethanol & isopropanol), amino alcohols and the phenetole analogue of Lawesson's reagent. The study further prepared a number of new dithiophosphonate complexes of the corresponding ligands. Characterizations of the new compounds establish all our proposed compound and most of the new compounds were confirmed structurally by representative crystal structures. The new ferrocenyl dithiophosphonates synthesized in the study displayed high tendency to be a potential co-sensitizers in dye sensitized solar cells application. Some of the new compounds also showed antibacterial properties in antibacterial susceptibility test. The study, therefore, concludes that dithiophosphonate ligands and complexes were directed into new avenues of research, starting with the report on the green solventless synthetic route to a number of new applications, applying a variety of tools, contained in this thesis.

7.2 FUTURE WORK.

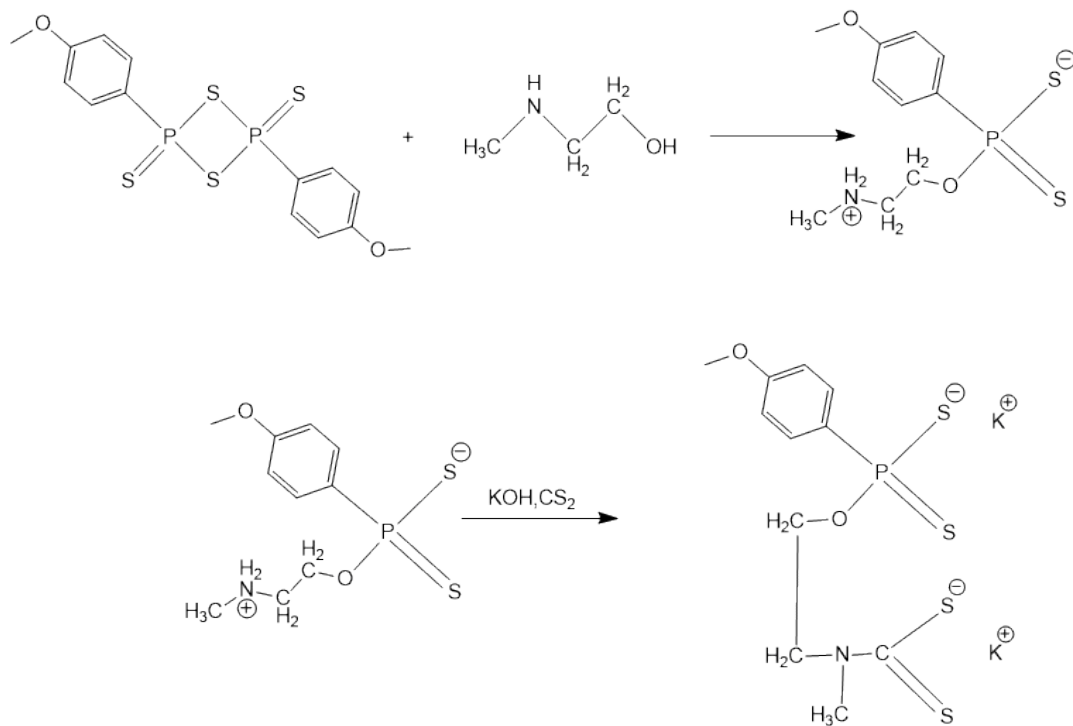
There are a number of possible ways to take this work further, a few are highlighted below:

- ❖ The green synthetic route to the formation of dithiophosphonate ligands and complexes which are established in this work should be extended to other dithio-organophosphorus compound synthesis. This will eventually make green synthesis a preferred synthetic route in this field of research. We only investigated the use of alcohols in the liquid form in this work, it will be beneficial to see solid alcohols being applied in this manner.
- ❖ Polymeric nature of ferrocenyl dithiophosphonate ligand formed in this work should be further explored. A number of coordination polymers can be formed by exploring the multidentate capacity of this ligands and varying the metal to ligand ratio. The reactivity of the hydroxyl group on the ligand/complex could be further engaged through deprotonation, leading to further reactivity in the so-called 'complex of complexes' type reactions. The hydroxyl group can also be treated as P-O-H moiety to see if it can perform the same reactions as that of regular alcohols in the nucleophilic ring opening of Lawesson's reagent dimer and further complex to different transition metals leading to a higher multidentate ligand and forming a multinuclear complexes as shown in **Scheme 9.1** containing different derivatives of Lawesson's reagent on a single complex.



Scheme 7.1. Possible future dithiophosphonate work

- ❖ The zwitterionic ligand promises to be a very exciting multidentate ligand which could act as S,S' chelating ligands towards soft transition metals and concurrently as amino ligands towards hard transition metals, leading to the formation of multinuclear complexes. For example, the primary amine is known to react with CS_2 leading to bi-functional ligands containing both dithiophosphonate and dithiocarbamate entities on the same ligand, see **Scheme 9.2**.



Scheme 7.1. Possible future reactions of zwitterions forming a dual functional dithiophosphonate/dithiocarbamate ligand

APPENDIX

The accompanying CD serves as an Appendix to this dissertation and contains ^{31}P NMR, ^1H NMR, ^{13}C NMR and FTIR spectra, Mass Spectra and X-ray crystallographic data (including cif files).